BMR JOURNAL
OF AUSTRALIAN GEOLOGY & GEOPHYSICS

BMR
S55(94)
AGS.6
C3

VOLUME 10 NUMBER 1

FOR OFFICIAL USE ONLY

BUR. OF MINERAL RESOURCES LIBRARY - 9 MAY 1986 CANBERRA, A.C.T.

BMR JOURNAL

OF AUSTRALIAN GEOLOGY & GEOPHYSICS

VOLUME 10 NUMBER 1

CONTENTS

Front cover: A magnitude 7.0 (ML) earthquake on 10 May 1985 caused extensive landslides to develop in Miocene limestone on the rugged northern slopes of the Nakanai Range, New Britain, in Papua New Guinea. The landslides caused temporary damming in the upper tributaries of the Bairaman River. Geological hazards in the southwest Pacific and southeast Asian region are discussed in this issue in a paper by R.J. Blong & R.W. Johnson. Photograph taken and supplied by Dr P.L. Lowenstein, Volcanological Observatory, Rabaul, Papua New Guinea.

AUSTRALIAN GOVERNMENT PUBLISHING SERVICE CANBERRA 1986

Department of Resources and Energy

Minister: Senator the Hon. Gareth Evans, Q.C.

Secretary: A. J. Woods, A.O.

Bureau of Mineral Resources, Geology and Geophysics

Director: R. W. R. Rutland

Editor, BMR Journal: I. M. Hodgson

The BMR Journal of Australian Geology & Geophysics is a quarterly journal of research. It contains papers and shorter notes by scientists of the BMR or others who are collaborating with BMR. Discussion of papers is invited from anyone.

Subscriptions to the BMR Journal are managed by the Australian Government Publishing Service (Mail Order Sales, GPO Box 84, Canberra, ACT 2601; telephone (062) 95 4485), to which enquiries should be directed.

Other matters concerning the Journal should be sent to the Director, marked for the attention of the Editor, BMR Journal.

©Commonwealth of Australia 1986

Month of issue: March

ISSN 0312-9608

Printed by Graphic Services Pty. Ltd. 516-518 Grand Junction Road, Northfield, S.A. 5085

BMR Journal of Australian Geology & Geophysics, 10, 1-15 ©Commonwealth of Australia 1986

Geological hazards in the southwest Pacific and southeast Asian region: identification, assessment, and impact

R.J. Blong[1] & R.W. Johnson[2]

Geological hazards significantly affect communities in the tectonically active parts of the southwest Pacific and southeast Asian region. Geological hazards include intensive hazards, such as earthquakes, volcanoes, tsunamis, and landslides, and slow-onset hazards, such as subsidence, coastal erosion, and coastal progradation. The ways in which these hazards are perceived differs from one community to the next, and coping strategies can be either traditional or, more often, 'western' in approach. Geological hazards have tended to be treated individually and at the national level, rather than as components of hazard mixtures and at a regional level. Furthermore, information on hazards in the region is widely dispersed; much of it is not readily accessible. A regional data base should be established for the collection, use, and dissemination of data on geological hazards, a comprehensive set of geological-hazard maps should be prepared, and a training scheme in geological-hazard assessment, mitigation, and preparedness should be established.

Introduction

Bush fires and tropical cyclones are the two main phenomena that come to mind in a consideration of natural hazards in Australia. In contrast, geological hazards — that is, those caused by such events as volcanic eruptions, earthquakes, and tsunamis — are generally regarded as being of lesser significance. Yet, geological hazards in the countries neighbouring Australia represent a considerable threat to life, property, and agricultural lands — probably more so than cyclones in some areas, and certainly more than bush fires in most.

We had the opportunity to review the subject of geological hazards in the southwest Pacific and southeast Asian region (excluding Australia and New Zealand) when asked to convene a Working Group that was part of an AGID-ILP* Workshop held during the 7th Australian Geological Convention in Sydney in September 1984 (Johnson & Blong, 1984). The meeting of the Working Group was an occasion when geoscientists concerned with specific aspects of geological hazards presented their views on hazard identification and mitigation in the region, and were able to meet with and hear representatives from emergency-response and aid organisations in Australia. This paper is a summary of our own viewpoints on geological hazards in the southwest Pacific and southeast Asian region, but it has been influenced by the proceedings of the Working Group, and its main recommendations are those which were adopted by the Workshop as General Recommendations (AGID-ILP Workshop, 1985).

The topic of geological hazards in the southwest Pacific and southeast Asian region is clearly a large one, which, in comprehensive treatment, would require a thorough review of past, hazardous, geological events, the cataloguing and analysis of effects, death, casualties, and damage resulting from those events, and a proper assessment of how authorities in the different countries of the region, as well as international aid agencies, perceive and cope with geological hazards. This type of treatment is beyond the scope of the account presented here, largely because of the current unavailability of appropriately compiled data (see below). Nevertheless, an attempt has been made to highlight what we consider to be important aspects of identification and mitigation of geological hazards in the region. The account may be regarded as a first step towards a comprehensive treatment that would be possible if the recommendations made in this paper were put into effect.

[1] School of Earth Sciences
Macquarie University
North Ryde. NSW 2113

[2] Division of Petrology & Geochemistry
Bureau of Mineral Resources
GPO Box 378
Canberra ACT 2601

* Association of Geologists for International Development-International Lithosphere Program

What is a geological hazard?

Nine specific geological or geophysical phenomena (Table 1) are the hazards that we will consider in this paper. They are presented together with a list of the types of study that are required to understand, and to be able to cope with, the range of important aspects of each hazard. The hazards list excludes meteorological and most hydrological events, even though some of these may, in part, have geological controls or be the trigger for geological hazards. For example, flooding is dependent in part on geomorphology and, therefore, on the geology of a flood-prone area; heavy rainfall may induce landslides; and tidal floods are, at least in part, controlled by geophysical forces (gravitational attraction of the moon and sun). Meteorite falls are excluded because, like tidal forces, they are of extraterrestrial origin. We have also eliminated from consideration those hazards resulting from inadequate assessments of engineering work sites — for example, collapse of dams built on unsuitable rock foundations, breaches of river diversions and canals set in geologically inappropriate locations, and damage to the foundations of piers, wharves, and harbours. We do, however, include subsidence as a geological hazard, whether by purely natural causes (earthquakes, volcanic activity, rock solution) or by man-induced activities (for example, underground mining and excessive withdrawal of groundwater from wells). Furthermore, in our assessments of geological hazards given below we draw from the literature on the wider subject of natural hazards in order to illustrate points that are applicable to the narrower field of geological hazards.

Table 1. Geological hazards and some required hazard studies

Hazards:	Earthquakes, volcanoes, tsunamis, landslides, subsidence, expansive soils, coastal erosion, coastal progradation, soil erosion.
Studies:	Prediction and warning systems, physical characteristics of hazards, hazard epidemiology, social and economic consequences, effects on buildings and lifelines, hazard mixture, risk assessment, hazard mitigation.

Exclusion of hydrological, extraterrestrial, and engineering geological hazards helps restrict the limits of our paper, but it does not assist significantly in finding a satisfactory definition of the term 'geological hazards'. The central concept of such a definition, however, embodies the

interaction of a geological or geophysical event with a human community such that significant damage or casualties, or both, are caused (see, for example, Fritz, 1968; Heathcote, 1979). An adequate definition would also recognise that geological hazards span a spectrum — from those such as earthquakes, which are *intensive,* offering no warning and lasting only a few seconds or minutes, to those such as subsidence and coastal progradation, which can be described as *slow-onset,* continuing for decades and creating a slow, progressive alteration of the physical environment. Furthermore, a satisfactory definition would include recognition that human groups differ in their ability to withstand the impact of a geological hazard because of differences in warning systems, leadership, social and economic organisation and development, as well as in building styles and ages, communication infrastructure, and transport networks. There is, therefore, an implication that if a geological event struck a community so well-prepared and protected that no damage or deaths took place, then that event would not be regarded as a geological hazard (see Oliver, 1975).

The meaning of the above phrase 'significant damage or casualties' is an important one. Western attempts at delimiting damage and casualty levels (Table 2) pose numerous difficulties, not least of which is the recognition that the services disrupted in western communities may not exist across large areas of the region with which we are concerned.

Table 2. Some 'western' criteria for the selection of hazard events*

1. Property damage extending to more than 20 families, or economic losses (including loss of income, a halt to production, and costs of emergency actions) in excess of US$50,000.
2. Major disruption of social services, including communications failure and closure of essential facilities or economically important establishments.
3. A sudden, unexpected ('unscheduled') event or series of events which puts excessive strain on essential services (police, fire-service, hospitals, and public utilities) and/or requires the calling in of men, equipment, and funds from other administrative jurisdictions.
4. An event in which 10 or more persons are killed or 50 or more persons are injured.

* After Hewitt & Burton, 1975 (p. 28)

Indeed, some authorities have questioned the 'western' model of disasters outlined above and have proposed a 'Marxist' view, in which '*vulnerability* embraces not merely the risk from extreme phenomena but the endemic conditions inherent in a particular society which may exacerbate the risk' (Westgate & O'Keefe, 1976, p.63). This school of thought recognises the process of *marginalisation,* whereby less-developed countries regress as a result of the control and exploitation of indigenous resources by the governing elite and outside interests. Thus, the poor become more vulnerable as they are forced to seek other sources of livelihood either in more hazardous areas or in alternative resource uses that increase exposure to natural hazards. Marginalisation means that: (i) the forms of exploitation in the underdeveloped countries will increase the frequency of natural disasters as socio-economic conditions and the physical environment deteriorate; (ii) the poorest classes will continue to suffer most losses; (iii) disaster relief aid is designed to maintain the status quo and generally works against the classes who suffered most in disasters and who will suffer again in future disasters; and (iv) disaster mitigation that relies on high technology reinforces the conditions of underdevelopment and increases marginalisation (Susman & others, 1983).

Whether the 'western' view, the 'Marxist' view, or an intermediate view (e.g. Turner, 1979; Hogg, 1982) of natural disaster is correct matters little from our viewpoint. However, geoscientists concerned with hazards in the southwest Pacific and southeast Asian region need to recognise that recipients' views of efforts at hazard reduction may well be different from that of aid donors. In one view, geological hazards are Acts of God and vulnerability can be reduced by scientific and technological efforts. In the other view, geological hazards and hazard vulnerability are induced by socio-economic conditions that can be modified by Man only in the context of integrated development plans (O'Keefe & others, 1976). Lewis (1981), in his government-funded study of natural-disaster vulnerability in Tonga, subscribed to this latter view.

Tectonic framework for geological hazards

Intensive geological hazards in the southwest Pacific and southeast Asian region are determined primarily by a high degree of current tectonic activity caused by the interaction of four of the Earth's major lithospheric plates — Eurasian, Indo-Australian, Pacific, and Philippines (Fig. 1). There are, in addition, minor plates in and to the north of Papua New Guinea that, together with the major plates, make up one of the most tectonically complex and active regions anywhere on Earth. Most of the active plate boundaries are of the convergent or compressional type, representing subduction of one lithospheric plate beneath another along deep ocean trenches. This involves descent of plates into the deep mantle along paths mapped out by inclined seismic, or Wadati-Benioff, zones where earthquakes may reach depths of 500–700 km. The earthquake zones at the surface trace out swirling distribution patterns (Fig. 1) that characterise this complex region of island arcs, back-arc spreading, plate collisions, compressional tectonics, and active volcanism. Most of the active volcanoes of the region are within the seismic zones, and the active plate boundaries and accompanying volcanic belts pass through some of the most heavily populated parts of the region.

Parts of the seismic zones are mountainous, and therefore prone to landslide activity, particularly in areas of high rainfall. Mountains are especially well developed in glacier-capped Irian Jaya, which represents part of a collision zone between the Australian continent (carried on the Indo-Australian plate) and a zone of island arcs and marginal seas to the north. This collision zone stretches from eastern Indonesia eastwards into Papua New Guinea. So-called 'great' earthquakes are comparatively rare in the region. Kanamori (1978) identified the ten largest earthquakes between 1904 and 1976 and showed that only one of these was within the area shown on Figure 1, possibly because of the dominance of 'Marianas-type' compressional plate boundaries in the region (Uyeda & Kanamori, 1979). The great earthquake in the region was an 8.2 surface-wave-magnitude event in 1938 at the western end of New Guinea island, where tectonic style may be closer to that of the 'Chilean-type' of convergent plate boundary identified by Uyeda & Kanamori (1979). Coastal areas and atoll communities in the region are susceptible to earthquake-generated tsunamis, mainly from shocks within the region, but also from the great earthquakes bordering other parts of the Pacific basin. Tsunamis are also generated by collapse of sea-level volcanoes — either caldera-forming events, such as at Krakatau (Indonesia) in 1883, or major avalanches from steep-sided volcanoes, such as Ritter Island (Papua New Guinea) in 1888.

The many active volcanoes of the region include centres of felsic igneous activity capable of producing exceptionally powerful explosive eruptions, the effects of which can be widespread. The explosions result mainly from the rapid vesiculation of basalt, andesite, dacite, and rhyolite magmas containing volatiles derived in part from contact with

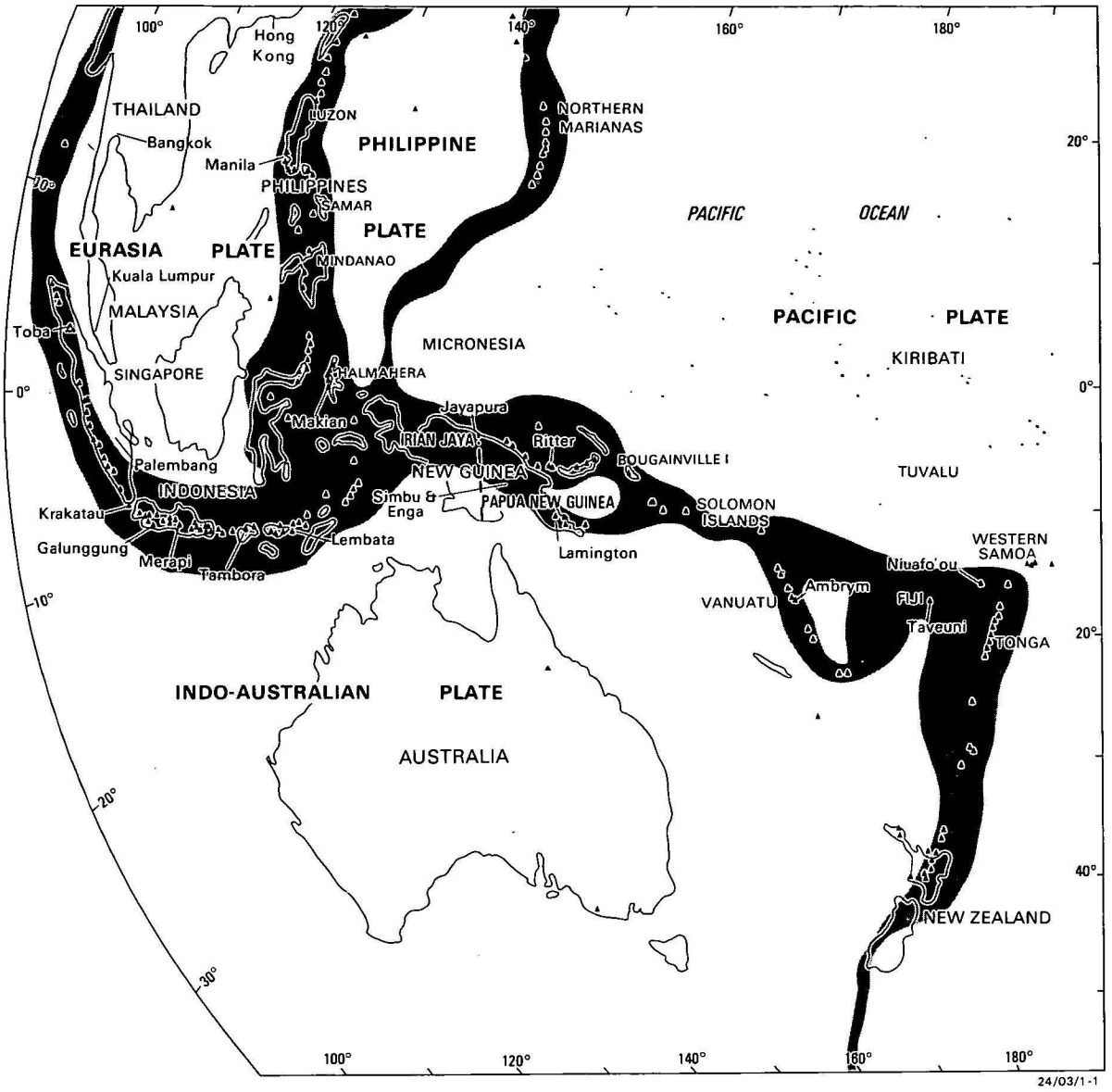

Figure 1. Earthquake zones (stipple) and active volcanoes (filled triangles) of the southwest Pacific and southeast Asian region, showing locations of natural disasters discussed in text.

Adapted from the Plate Tectonic Map of the Circum-Pacific Region (Pacific Basin Sheet) published by the Circum-Pacific Map Project (1984). Lambert Azimuthal Equal Area Projection.

groundwaters and from dehydration reactions in the downgoing slabs of lithosphere that underlies the volcanoes. Well-known historical eruptions in the region include the 1815 Tambora (e.g. Self & others, 1984) and 1883 Krakatau (Simkin & Fiske, 1983) events in Indonesia.

Slow-onset geological hazards in the region are not closely related to the marked tectonic activity that is the cause of the *intensive* hazards discussed above. Nevertheless, beach erosion on small islands, where sands may be a valuable building and resort commodity, coastal progradation in areas that formerly had access to the sea, and ground subsidence, caused, for example, by excessive withdrawal of groundwater, are all geological hazards that significantly affect some communities in the region, including the major cities of Bangkok and Kuala Lumpur, where ground subsidence is a major problem.

Examples of geological hazards in the region

Seventeen examples have been selected to illustrate the following general aspects of geological hazards in the region (Fig. 1): the range of different hazards affecting the region, the ranges in temporal and spatial scales of impact, and the diversity of effects resulting from geological hazards. The first examples relate to life-threatening and social effects on people. Subsequent examples deal with effects on buildings, lifelines, and agriculture. The final examples are concerned with some geological hazard effects that may last for hundreds of years; long time periods may require consideration.

1. The 1815 eruption of Tambora (Fig. 2) was one of the largest in recorded history. It resulted in the deaths of about 92 000 people — more than in any other known eruption. Probably 5000–6000 died in pyroclastic flows, and another

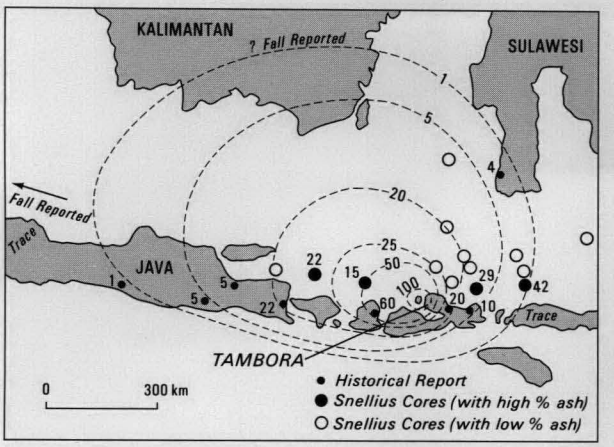

Figure 2. Distal-ash dispersal pattern (isopachs in centimetres) for the 1851 Tambora eruption, Indonesia, as interpreted by Self & others (1984).

Sites of sea-floor samples obtained during the 1929-30 Snellius expedition are also shown, together with thicknesses for 1815 ash that is mixed with as much as 30 per cent sediment.

Figure 3. Damage to this Cotabato City hotel was caused by the 17 August 1976 western Mindanao earthquake in the Philippines.

Street-level supporting posts collapsed during ground liquefaction (personal communication, 1985, from F.B. Limeta, who also supplied the photograph). M2687

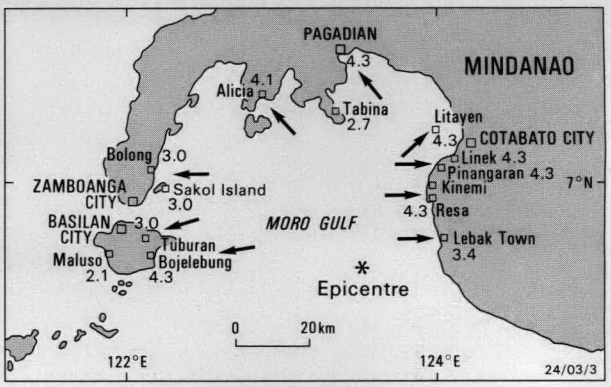

Figure 4. Epicentre, directions of tsunami run-up (arrows), and inundation heights (metres) for the 17 August 1976 western Mindanao earthquake.

Modified after Limeta (1980, fig. 2).

4000-5000 in associated tsunamis. A further 38 000 on Sumbawa and 44 000 on Lombok succumbed to starvation and disease as a result of the destruction of crops by the widespread tephra fall, but despite the large death toll, 65 per cent of the population on Sumbawa and 77 per cent on Lombok survived (Neumann van Padang, 1971). 36 417 people died around Krakatau in 1883. Tephra falls and pyroclastic falls accounted for, perhaps, 3000-4000 of this total, and nearly all of the remainder died in tsunamis. In all, 165 villages were completely destroyed and 132 partly so. In most of the literature, attention is focused on the 37 Dutch who died, with little comment about the 726 Chinese and 35 600 Javan and Sumatran casualties. However, the presence of the Dutch led to effective disaster relief, so that few died from starvation and disease. The effects of the eruption on ports, buildings, railways, roads, and other infrastructure have been well documented by Simkin & Fiske (1983).

The death tolls from these two eruptions of similar style were greater than from any other eruption in the last 1000 years. In each case, the deaths resulted largely from subsequent effects — around Krakatau, a tsunami; around Tambora, starvation and disease — rather than from the eruptions themselves. A significant difference between the two eruptions may have been the disaster relief organised by the Dutch in 1883, which was absent in 1815. Deaths in the aftermath of an eruption or other geological hazard at the present day would be much less because of more organised and rapid disaster-relief responses (see also example 9).

2. A 6 m high tsunami in September 1897, generated by an earthquake of Richter magnitude 8.7, swept through a market on Basilan island in the Sulu Archipelago, Mindanao, southwestern Philippines. The tsunami caused extensive damage and killed or injured scores of people (Berninghausen, 1969; Limeta, 1980). A magnitude 7.8 earthquake in the same region in August 1976 also caused extensive damage and the loss of 400-500 lives in coastal areas of western Mindanao (Fig. 3). More than 80 per cent of the damage and casualties were attributed to a tsunami that, owing to the close proximity of the earthquake epicentre, arrived before warning could be given (Fig. 4). About 12 000 people were made homeless (Acharya, 1978; Stewart & Cohn, 1979; Limeta, 1980).

This example, like the 1883 Krakatau eruption, is of one geological hazard generating another that proved more destructive to life and property than the initial event. Note also that, even though a well-organised tsunami-warning system spans the Pacific, warnings can not necessarily be provided for coastal zones close to tsunamigenic areas.

3. Lava flows from Ambrym, Vanuatu, in June 1929 destroyed three mission stations and the food supplies of about 300 villagers who evacuated by ship. There was one report of inter-tribal warfare breaking out between two groups who accused each other of causing the eruption (*Sydney Morning Herald,* 16-18 July, 1929). Tephra falls again caused evacuations in 1950 and 1951. Some residents left voluntarily, but another 700 were forcibly evacuated by the colonial authorities to the nearby island of Epi, where 48 were killed in a tropical cyclone a few weeks later. Many of the evacuees eventually established a new village on Efate, seat of the capital Vila. Strong links were still maintained 25 years after the evacuation between the evacuees and those still remaining on Ambrym, and many absentees maintained that they would return home some day (Tonkinson, 1979). Similarly, long-lasting evacuation/migration resulted from the Niuafo'ou (Tonga) 1946 eruption and from the threatened activity of Makian (Halmahera arc) during the 1970s (Rogers, 1981; Lucardie, 1979).

Geological hazards may give rise to conflicts between affected populations. Voluntary and forced migrations can result in long absences from ancestral homelands, but strong ties can be maintained for decades with those remaining behind or returning after the immediate adverse effects have dissipated.

4. An earthquake and tsunami took place southeast of San Christobal, Solomon Islands, in October 1931. The tsunami destroyed 18 villages, killing perhaps 20–25 people, and leaving about 700 homeless (*Sydney Morning Herald,* 14, 20 October, 3 November 1931). Overthrust subsea faulting in the 20 July 1975 Bougainville earthquake produced a tsunami that had a maximum amplitude of 2 m around the northern Solomon Islands. Villagers at Torokina (western Bougainville) expected the waves as a result of experiences in 1971 and 1974. Damage was relatively light: several houses were lifted off their stumps (Fig. 5), and petrol drums, canoes, and debris were washed 50 m inland. About half the village chickens and a few dogs disappeared. More extensive damage was caused to the Torokina wharf and Post and Telegraph Station as a result of subsidence following ground liquefaction (Everingham & others, 1977; Fig. 6). Another damaging earthquake (Richter magnitude 7.5) was recorded in the Solomon Islands in February 1984.

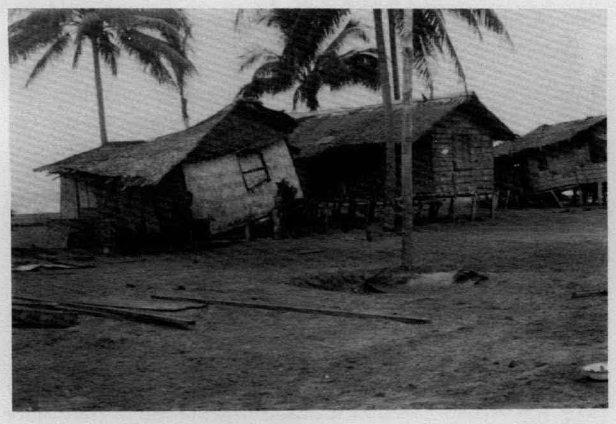

Figure 5. Bush-materials houses along the coast near Torokina, southwestern Bougainville Island were shaken from their stumps by the 20 July 1975 earthquake near Bougainville.
Photograph was taken a few days later by V.F. Dent. M2452.

Figure 6. Old piles from a Second World War wharf at Torokina were extruded by the effects of liquefaction caused by aftershocks from the 20 July 1975 Bougainville earthquake.
The tops of the piles were formerly below ground level, as shown by the grass still growing on them. Photograph by V.F. Dent. M2451.

Earthquakes can induce tsunamis, liquefaction, and ground subsidence, all of which may cause damage. However, local populations may anticipate the occurrence of tsunamis as a result of recent experiences.

5. The 1979 earthquake at Taveuni (220 km northeast of Suva) caused damage estimated at NZ$0.75 million (Paterson & Williams, 1980). An earlier earthquake (MM 7–8) offshore from southeastern Viti Levu damaged Suva on 14 September 1953. Six people died — three were drowned by a tsunami (Fig. 7), two were killed by falling masonry, and one in a landslide — and 40 were injured (eight hospitalised). Structural damage was caused to some buildings in Suva and 40 village houses were destroyed by the tsunami on Kandavu, 90 km to the south. Transport and communication routes were damaged, a section of the wharf subsided, and an inter-island vessel was damaged. The cable station suffered some damage, and the power and telephone systems in Suva took six hours to return to normal; the radio station was off the air for half an hour and the *Fiji Times* missed a day (*Sydney Morning Herald* reports, 15 September to 5 October 1953).

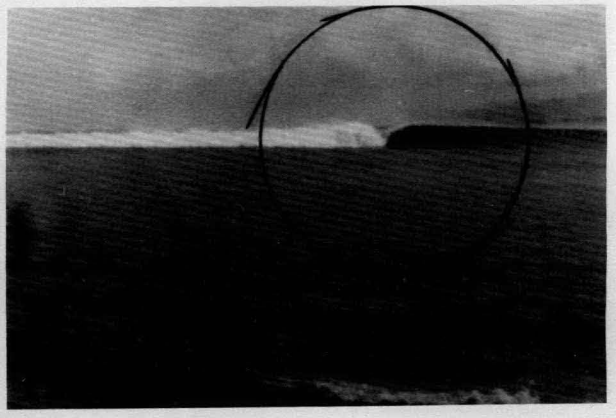

Figure 7. The tsunami generated by the 1953 Suva earthquake breaking over the reef just outside Suva harbour.
Photograph supplied by N.F. Exon. M2687.

Some geological hazards produce a multiplicity of effects. The Suva earthquake killed only 6 people, but there was a number of causes of death. Similarly, a wide range of communication facilities was damaged for different lengths of time.

6. A Richter magnitude 7.2 earthquake in June 1977, 240 km south-southwest of the main Tongan islands of Tongatapu and ʻEua, caused permanent ground movements around wharfs at Nuku'alofa and extensive damage to buildings of concrete block construction (Fig. 8). Campbell & others (1977, p. 208) noted 'The generally low standard of construction, weak materials and the absence of earthquake resistant design contributed to the extent of the damage and it was surprising that no life was lost and that there were few serious injuries. Had the earthquake occurred during the day the damage to the building housing the Prime Minister's offices [Fig. 9] and to the primary school would almost certainly have caused loss of life'. Earthquakes of similar magnitude took place in this area in 1913, 1917, 1943, and 1948 (Campbell & others, 1977).

Recently constructed buildings may suffer severe damage despite knowledge of a long history of damaging earthquakes. The time of day when an earthquake or other intensive geological hazard takes place has little effect on the extent

Figure 8. Collapse of a masonry house on 'Eua caused by the Tonga earthquake of June 1977.
Photograph by G.R. McKay.

Figure 9. Damage to the Prime Minister's building, Nuku'alofa, resulting from the 1977 Tongan earthquake.
Photograph by G.R. McKay.

of damage to buildings, but timing can have a profound effect on the number of casualties.

7. A Richter magnitude 7.3 earthquake in August 1968 in northeastern Luzon claimed at least 322 lives in Manila, 230 km to the southwest. At least 200 buildings in Manila were damaged (Fig. 10), mainly to the north of the Pasig River. Several roads and bridges and Pier 9 in Manila South Harbour suffered minor damage. Most damaged buildings had strong shear fractures or sets of conjugate fissures dipping toward each other at 55–60°. Damage was concentrated along the estuary systems where least-stable foundations are found (Caagusan, 1969a,b).

The damage pattern resulting from this earthquake was influenced by the distribution of palaeochannels in the estuarine sequence. Recent geomorphic history may therefore have a profound influence on both damage and casualty patterns.

8. A typhoon hit Hong Kong on 16–18 June 1972 and generated 185 landslides. The total 3-day rainfall was 662 mm, and the rain had a maximum intensity of 98.7 mm/hr. At San Mau Ping, Kowloon Peninsula, a retaining wall at the foot of a seven-storey resettlement estate collapsed, covering a squatter settlement in 3 m of mud and debris (Fig. 11). This landslide, together with another on the same day, killed 138 people (Lumb, 1975; Kui Che Lam, Chinese University of Hong Kong, personal communication, 1974).

Meteorological hazards often trigger geological hazards that may cause casualties and damage additional to the initiating event. The already disadvantaged suffer most in many cases.

9. A series of explosive eruptions at Galunggung volcano, western Java, began on 5 April 1982, generating tephra fallout and pyroclastic avalanches as well as lahars that flowed down the Cibanjaran and Cikunir river valleys. The lahars caused destruction of farm lands and, eventually, the evacuation of about 35 000 people who had to be provided with emergency shelter, food, and means of support (Katili & Sudradjat, 1984; Fig. 12). Damage was conservatively estimated to exceed the equivalent of US$100 million. The threat of major lahars taking place during the monsoon season at the end of 1982 led to a National Workshop on Mt Galunggung Volcanic Risk Management being held in Bandung in September 1982 (BAKORNAS, 1982), but the threat was ameliorated when rainfall during the wet season was considerably lower than normal. Indonesians were not the only people to be affected by the 1982 explosive eruptions: two Australia-bound 747 aircraft encountered drifting ash clouds from Galunggung at different times in June–July. The jet engines stalled, and the damaged aircraft had to return to Jakarta after the pilots managed to restart the engines at low altitudes.

Although lack of disaster relief following geological hazard impacts in the late 20th century is unlikely to cause many deaths (see also example 1), the aftermath of the 1982 Galunggung eruption illustrates the magnitude of the relief problem. The National Workshop represented a significant, possibly unique, attempt to marshall international resources to assist with a range of different aspects of the problem. The 1982 Galunggung eruption is an illustration of two other points: that seemingly remote travellers, unaware of either the hazard or its source, could suffer fatal consequences; and, again, that the threats produced by secondary hazards may be more severe than those stemming from the initial event.

10. Coastal progradation on the east coast of Sumatra has, according to one viewpoint reported by Chambers & Sobur (1977), changed the status of Palembang from a coastal port in 1000 A.D. to a river port 85 km inland at the present day (Fig. 13). Rates of coastal advance during the last 40 years average only 10–20 m/yr, rather than the 100 m/yr suggested by Palembang's inland position, but there are problems of coastal erosion and sedimentation in planning for a new coastal port. Constant dredging and difficult foundation conditions on the deep soft sediments led to estimated construction costs for the post-Palembang road of $1 million per kilometre. Accretion rates for other areas of the north coast of Sumatra range up to 200 m/yr (Tjia & others, 1968).

Slow-onset hazards such as coastal progradation (and soil erosion and ground subsidence — examples 10 and 11) can produce major costs both for existing infrastructure and development projects.

11. Estimated rates of soil erosion in Simbu Province, Papua New Guinea, are moderate (6–12 t/ha/yr; Humphreys, 1984), but exposed portions of Cretaceous Chim Formation shales, such as road batters, are eroding at rates of 900–1800 t/ha/yr (Blong & Humphreys, 1982). This erosion rate is amongst the highest recorded anywhere in the world, but is equalled in central Taiwan and the Tjatjaban catchment in Java (Li, 1976; van Dijk & Ehrencron, 1949) on similar shale materials.

Soil erosion, like subsidence (example 10), is generally a slow-onset hazard. The erosion rates reported here have profound implications for the continuation of viable agriculture and the maintenance costs of roads, bridges, dams, and other infrastructure.

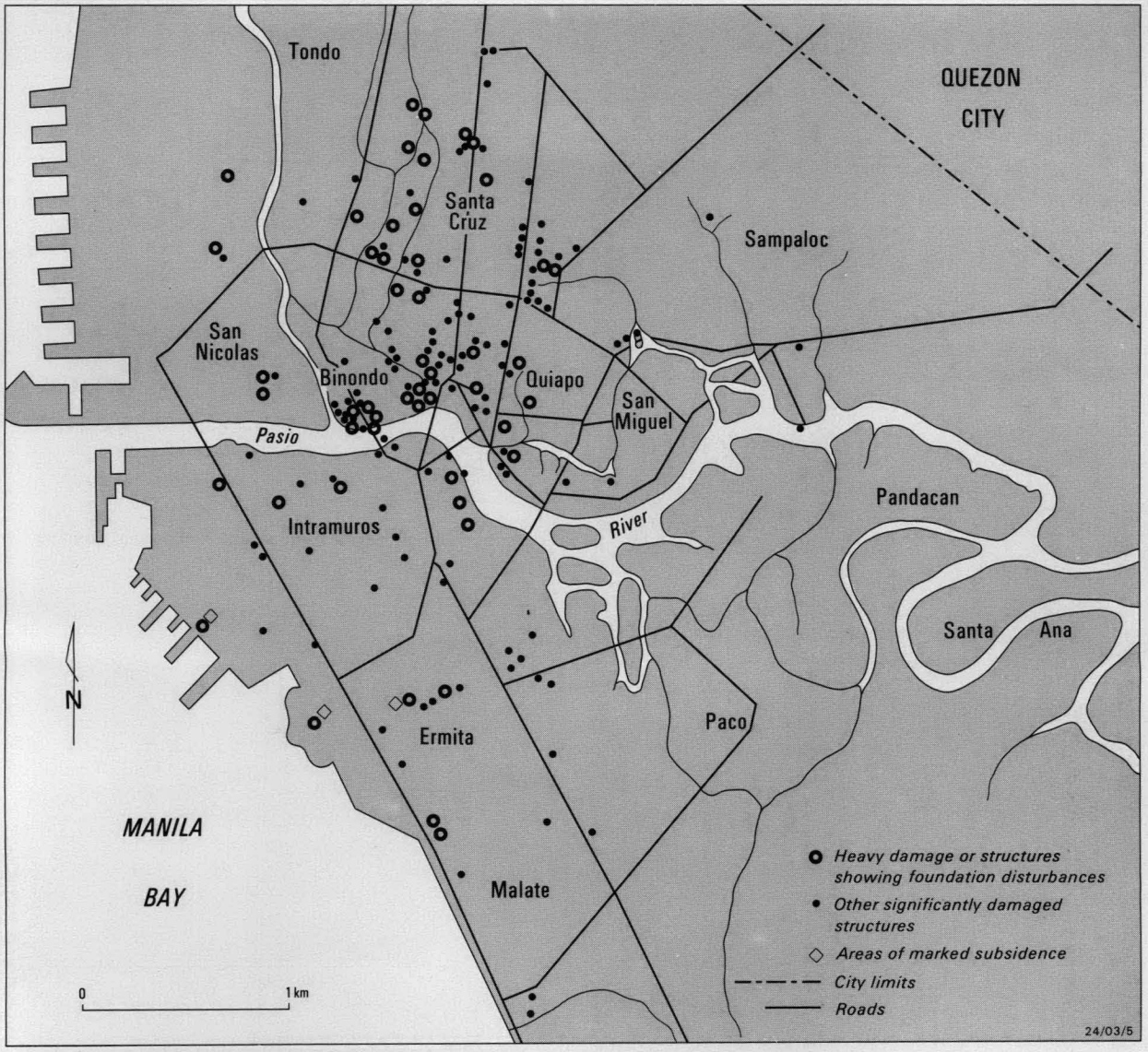

Figure 10. Shoreline and drainage system of the Manila area and the position of buildings damaged in the 2 August 1968 Luzon earthquake.
After Caagusan (1969b, plate V).

Figure 11. This landslide during the Hong Kong typhoon on 17 June 1972 damaged the retaining wall in front of a new seven-storey apartment building at San Mau Ping and buried a squatter settlement and the inhabitants under 3 m of mud and debris.
Photograph by Kin Che Lam. M2689.

12. Large areas of Bangkok are currently subsiding at rates of 2–6 cm/yr (Fig. 14), and some areas have subsided 80 cm in 23 years, largely as a result of groundwater withdrawal from more than 11 000 wells (Fig. 15). Subsidence has made the drainage problem in the Chao Praya River (gradient 1:60 000) and the numerous klongs (canals) more acute. An increase in the frequency of moderate flooding (Fig. 16) by effluent-laden waters creates an increase in health hazards, disruptions to traffic and communications, and damage to buildings, sidewalks, roads and, ironically, well casings and water reticulation pipes. Plans for the further provision of surface water may slow the rate of groundwater pumping, but there is no comprehensive plan to solve Bangkok's subsidence problem (Nutalaya & Rau, 1981; Rau & Nutalaya, 1982).

Like many slow-onset hazards, widespread subsidence in the Bangkok area has resulted in deterioration of a number of community support systems. The effects of slow-onset hazards may have been recognised for years, but rarely are there easy solutions that will reverse these situations.

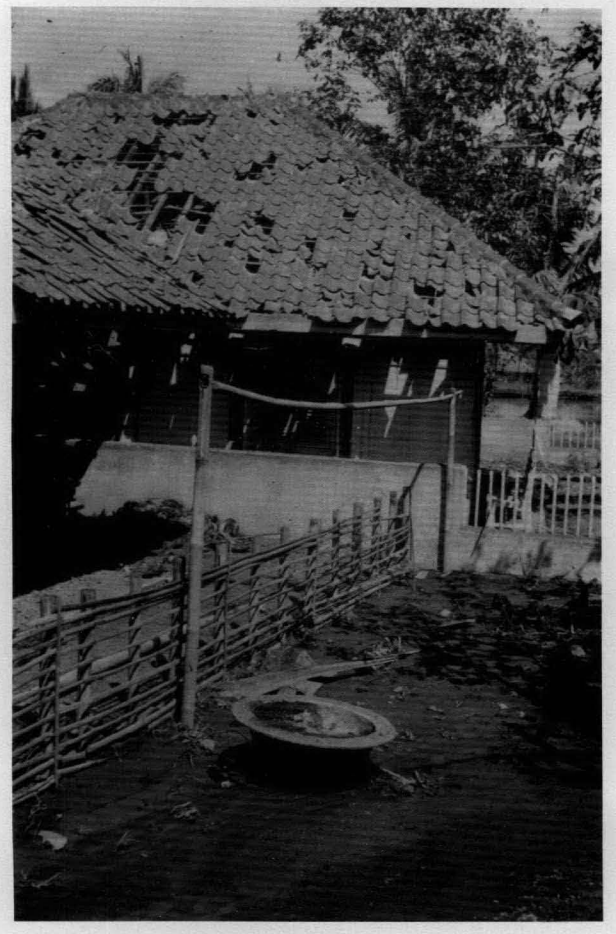

Figure 12. Upper: lahars flood the village of Sinagar on the western flank of Galunggung volcano, Java, following explosive activity at the central crater about 5 km to the west-northwest, in early April 1982. Lower: homes and gardens in the village were also affected by airfall ash and by volcanic bombs, up to several centimetres in diameter, that broke roof tiles.

The village had been evacuated when these photographs were taken (by R.W. Johnson) on 30 May 1982. GB3323 and GB3322.

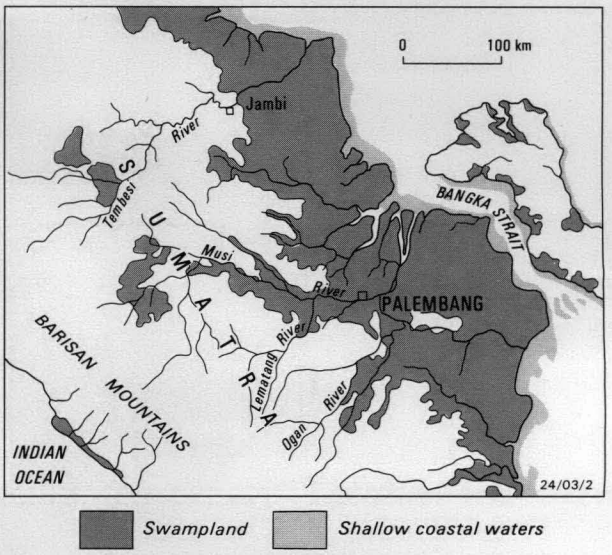

Figure 13. Coastal progradation around Palembang, Sumatra.
Modified after Chambers & Sobur (1977).

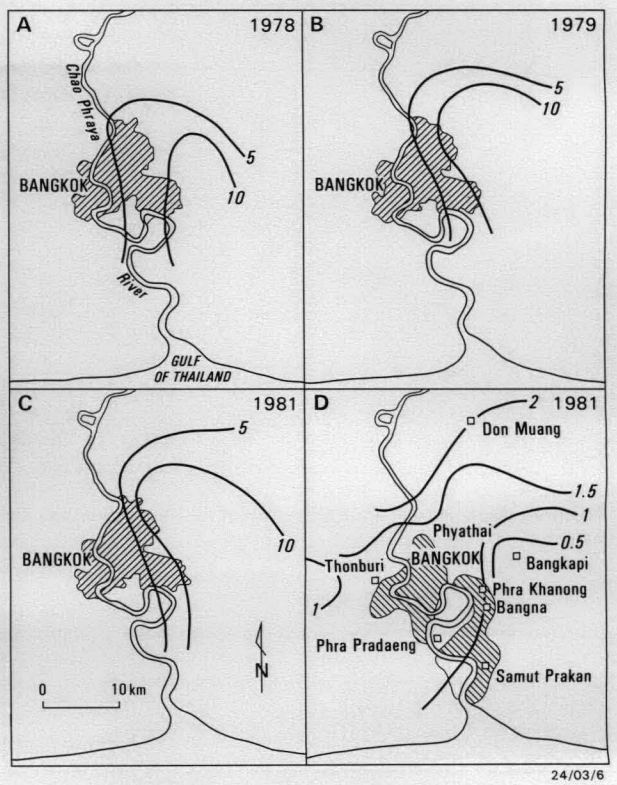

Figure 14. A, B, C: Contours of equal ground subsidence (cm/yr) for the years shown. D: Ground-surface elevations (metres above sea level) and areas having moderate to high concentrations of private wells.
After Nutalaya & Rau (1981, fig. 6).

13. The magnitude 7.1 earthquake that struck the east-central ranges south of Jayapura, Irian Jaya, in June 1976 killed an estimated 420 people, destroying 15 small villages and damaging another 70 or so. Ten seriously injured people required evacuation and 30 more received minor injuries. An average of about 70 per cent of food gardens in the area were destroyed by landslides, and the proportions reached 80–90 per cent around Buire. The affected 7000–8000 local people could readily rebuild their houses, but the staple crop, sweet potato, takes a minimum four months to reach maturity. The United Nations Disaster Relief Organisation estimated that food aid and aircraft for food distribution would be required for about eight months (UNDRO, 1976).

Although the impact period of a geological hazard may be only a few minutes, where agricultural systems are severely damaged, the serious effects may last for months or even

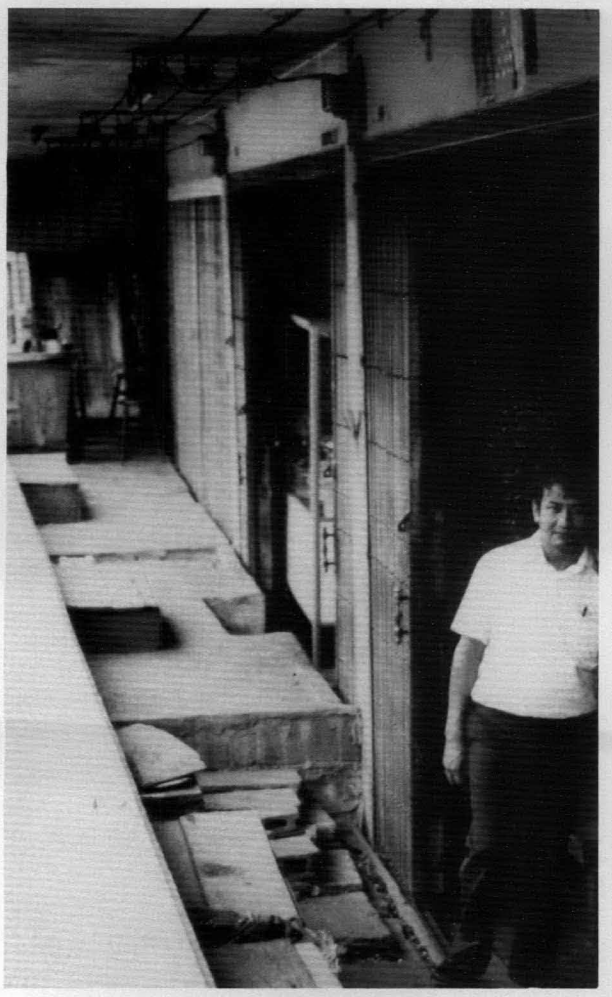

Figure 15. Dramatic evidence of building subsidence in Bangkok as a result of groundwater withdrawal.
Photograph supplied by P. Nutalaya.

years and require long-term assistance from international agencies.

14. Tropical cyclone Wally struck southeastern Viti Levu, Fiji, in April 1980 and initiated hundreds of landslides. Seventy-four landslides (debris flows, debris avalanches, and debris slides) were reported for one 230 ha area, and the average volume of material eroded was over 500 m 3 /ha. These landslides destroyed over 50 per cent of the garden crops, mainly cassava, of Korovou village as well as the village water supply. Roads were also affected (Fig. 17). Villagers supplied evidence that events of a similar magnitude had not taken place during the previous 50 years. However, landslide areas now consist of bedrock or debris (Fig. 18), and cultivation will be difficult or impossible for years to come. Furthermore, decreased slope stability will mean that mass movements are likely to be initiated by rainfalls of lesser magnitude than previously (Crozier & others, 1981).

This geological hazard also resulted from meteorological causes (see also example 8). The threshold for landsliding has been reduced so that meteorological events of lesser magnitude will trigger landslides and cause damage to village gardens, water supplies, and roads in the future. The effects of intensive geological hazards may therefore be experienced for decades after the initial impact.

15. Van Bemmelen (1956) believed a Katmaian-style eruption at Merapi, Java, about 1006 A.D. that followed volcano-

Figure 16. Periods of flooding in Bangkok have become more frequent as a result of ground subsidence.
Photographs taken in 1983 by P. Nutalaya. GB3320.

tectonic collapse of the southwestern sector of the volcano dealt the death blow to the old Hindu-Javanese State of Mataram (and of the monuments of Borobudor). The region did not recover until the foundation in the late sixteenth century of the Mohammedan state of Mataram.

Major geological events less than 1000 years ago may not appear in the historical record; yet, recovery from the impact of such major events may take hundreds of years.

16. A large limestone block, 18 × 25 km, was reported by Wolfe (1977) to have glided 5 km on a 1° slope on Samar island in the Philippines (Fig. 19). This slide, dated at 2000 ± 1000 years ago, shifted the central drainage divide

Figure 17. The main coast road between Suva and Nadi on Viti Levu (Fiji) was cut by landslides during Cyclone Wally in April 1980, and was still impassable when this photograph was taken by M.J. Crozier in May. GB3325.

Figure 18. Many landslides produced by Cyclone Wally along the south coast of Viti Levu stripped soil and regolith from slopes, making cultivation impossible for years to come.
Photograph by M.J. Crozier. GB3324.

to within one kilometre of the west coast, dammed rivers, and formed lakes. It was probably earthquake initiated.

Wolfe (1977) noted that there is no way of controlling a slide of this size, and that some engineering projects could create conditions that would allow such slides to be initiated by an earthquake. He concluded: 'the engineering implication here

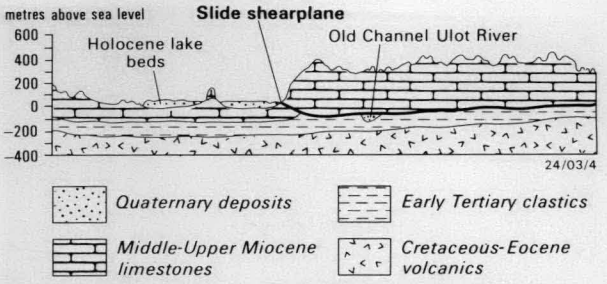

Figure 19. Inferred cross-section through the toe area of the Bagacay landslide, Samar island, Philippines.
Modified after Wolfe (1977, fig. 3).

is that one should look beyond obvious hazards and consider features possibly an order of magnitude larger than those normally dangerous . . .'

17. Three tsunamis in 1979 killed 539–700 people in Waiteba and other villages on Lembata island, Indonesia. The waves evidently washed as much as 500 m inland. Whether the tsunamis were produced by landslide from the slopes of Iliwerung, by an eruption-induced landslide, or by an offshore eruption is not clear (Jeffrey, 1981; Miyoshi, 1979). The afflicted population had evidently migrated to Waiteba about 15 years previously.

Even at the present day, reporting of the effects of many geological hazards is inadequate. In some cases, the precise nature of the hazard has not been identified, let alone the appropriate remedial actions.

Coping strategies and hazard perception

Three principal and somewhat obvious conclusions that can be drawn from the above list of examples are:

(i) all the nations of the region are affected by at least one geological hazard;

(ii) there is a range of hazards, from the intensive (e.g. earthquakes and tsunamis) to slow-onset (coastal progradation, subsidence, soil erosion); and

(iii) hazards affect all facets of national, communal, or individual existence — human deaths and injuries, buildings, transport and communication links, agriculture, tourism, economic activity, and social aspects such as politics, religious beliefs, and migration.

However, not all nations, communities, or individuals are affected equally by geological hazards. For example, there are obvious broad differences in earthquake and volcanic-hazard risk, as illustrated on a gross scale by Figure 1. Similarly, coastal regions suffer from hazards in different ways to hinterland areas.

The above examples also raise other, equally important, but perhaps less appreciated issues — namely, the different ways that geological hazards are *perceived* by the communities affected by them, and the ways in which strategies are formulated in order to cope with the prospect of future hazards once those hazards are recognised as recurrent. For example, coastal and interior communities may have different perceptions of hazard risk. Differences in language and culture, as well as in resource base and physical environment, also influence perception of geological events. Thus, the seventeeth-century tephra fall from Long Island, Papua New

Guinea, is remembered by some language groups as a time of death and famine, whereas others have performed ceremonies to bring about a recurrence of the ashfall (Blong, 1982). Religious and other beliefs at the group and individual level may also influence the coping strategies adopted and the efforts made to reduce future vulnerability as well as death rates. For example, Sims & Baumann (1972) suggested that differing death rates from tornadoes in Illinois and Alabama may be related to differences in fatalism, passivity, and attention to warnings.

The complexity of the relationship between natural phenomena and social systems was also illustrated by Schwimmer (1977) who studied Orokaivan beliefs relating to the 1951 eruption at Mount Lamington. One explanation saw the eruption as the mountain's response to bombing during the war and the subsequent acquisition of rifles. Another saw it as a payback for killing missionaries, a third as God's punishment, and a fourth viewed the eruption in geophysical terms. An individual Orokaivan could evidently hold three or four of these beliefs at once, depending on the context. The significant point is that the Orokaivan response even a decade and more after the eruption (for a summary see Blong, 1984) can only be fully appreciated within the context of these and other beliefs.

Geological hazard impacts may produce long-term changes in some societies. However, Torry (1979) described situations where tribal societies maintain long-term stability in a hazardous environment 'through a battery of institutional safeguards'. Waddell (1975) documented traditional responses to frost hazards amongst the Enga of the Papua New Guinea Highlands, and Firth (1959) and Spillius (1957) reported Tikopian (Solomon Islands) responses to cyclones and drought. Chiefs on Tikopia in the aftermath of these hazards introduced restrictions on many activities, including fishing, dance participation, and marriage and funeral rites, in order to re-establish garden cultivation as quickly as possible. Rappaport (1963) made the suggestion that tsunamis, typhoons, and droughts make food production risky and unstable on small Pacific islands, thus precluding the development of highly stratified social systems such as those found on some high islands that have more intensive agricultural operations.

On the other hand, natural disasters can be identified as one of the forces disrupting social stability and promoting change in some societies (Torry, 1979). The aftermath of the 1951 Mount Lamington eruption mentioned above is one such example. Lessa's (1964) account of the social effects of Typhoon Ophelia on Ulithi atoll (Caroline Islands, Trust Territory of the Pacific Islands) provided another. The cyclone acted as a catalyst in modifications to clothing, housing, diet, urbanisation, and the relaxation of taboos. Increased emphasis on cash cropping opened new avenues of activity for women and a willingness to experiment with introduced improvements in both variety and yield of local plant foods. The younger men who took initiatives gained in economic power, while the power of the traditional leaders was eroded. Churches were amongst the few buildings that survived the cyclone, and, consequently, the place of Christianity was enhanced. Whether the accelerated cultural change and innovation evident in some societies increases or decreases vulnerability to geological hazards is, of course, a moot point (see below).

Perception of geological hazards in the southwest Pacific and southeast Asian region is poorly acknowledged in the general literature on natural hazards. Few general hazard textbooks contain information on the region, despite the evidence of numerous geological and other hazards in the region, illustrated by the above examples. For example, the collection by White (1974) of 26 hazard case studies contained no example from the southwest Pacific and southeast Asia. Similarly, *Cities and geology* (Legget, 1973), which contains a 93-page chapter on 'Geological hazards and cities', contains virtually no information on the region. Indeed, the only references are the following:

p. 398 'Another tremendous natural explosion of recent times was the eruption of Krakatoa in the Strait of Sunda, Indonesia, in 1883.'; and

p. 415 'But the tsunami created by the eruption of Krakatoa in Indonesia in 1883 raced across the Pacific and created heavy seas even as far away as San Francisco'!

Perhaps the best known book on geological hazards is that by Bolt & others, (1975), which contains chapters on earthquakes, volcanoes, tsunamis, landslides, ground subsidence, snow avalanches, and floods. Again, however, there are no references to geological hazards in the southwest Pacific-southeast Asian region, except for a description of the Pacific tsunami-warning system and in the chapter on volcanoes, where G.A. Macdonald referred to at least 11 eruptions and presented case studies of the Krakatau (1883) and Tambora (1815) events. But, little is said, even in these case studies, about the effects of the eruptions, other than to record death tolls.

Similar comments can be made about many of the textbooks on natural hazards. A comparable complaint concerning anthropological literature has been made by Torry (1979). Certainly, there is an underemphasis of the significance of hazards in the region in the general literature on geological and other hazards.

The importance of data files

The brief examples presented above provide some idea of the range of geological hazards in the region and the diversity of their consequences. However, more fundamental data are required in order to answer questions about where hazards will strike, how often impacts will take place, and how big those events will be. The most common approaches to such questions are based on data files listing hazards and, in some cases, their effects.

The Smithsonian Institution Volcano Reference File (Simkin & others, 1981, plus unpublished updates) is an excellent example of a hazard data file. These data are published and computerised so that a range of different types of information can be extracted and analysed. For example, Simkin & Siebert (1981) showed that eruptions in the Halmahera arc have taken place with greater frequency since 1880 per 100 km length than have those in any other volcanic area in the world. Similarly, Blong (1984), using unpublished Volcano Reference File data, showed that in the period 1600–1982, 67.3 per cent (about 161 000) of all deaths in volcanic eruptions were in Indonesia, 1.6 per cent were in the Philippines, and 1.5 per cent in Papua New Guinea. Data can also be extracted from the file for individual volcanoes or even for cause of death. New data are published each month in the *SEAN Bulletin.*

Similar, possibly less comprehensive, data on earthquakes are published in the *SEAN Bulletin,* USGS *Preliminary determination of epicentres,* and the British *Bulletins of the International Seismological Centre.* Regional data are also available in, for example, Hamilton (1974) for Indonesia, and

Masó (1910), Repetti (1946), and Morante (1974) for the Philippines. Hattori (1980) presented seismic-risk maps for much of the region (Fig. 20), using historial data, an attenuation model, and a method of fitting extreme values. Acharya (1980) developed a similar method for a study of the Philippines, concluding that eastern and western coastal areas in the south had the highest seismic risk — a 10 per cent probability of exceeding 0.25–0.30 g ground motion once in 50 years. Catalogues of tsunamis in the area were compiled by Iida & others, (1979), Berninghausen (1969), Everingham (1977), Hatori (1982), and Iida (1983), and Brand (1985) has assembled information on landslides in southeast Asia.

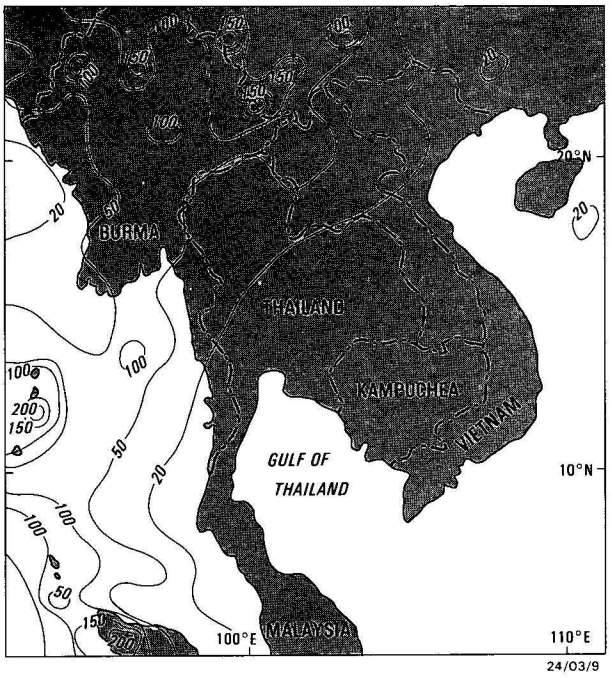

Figure 20. One of the seismic-risk maps produced by Hattori (1980), showing expected acceleration (m/s^2) at the ground surface once every 100 years.

The magnitude and frequency of the physical characteristics of the hazards can be calculated from such data and at least superficial assessments of death and destruction levels can be made. However, several points need to be borne in mind:

(1) Satisfactory data files have not been assembled for landslides, floods, ground subsidence, coastal erosion, expansive soils, or soil erosion, although the Australian Overseas Disaster Response Organisation (AODRO) has maintained a computer file on disasters in the region since 1982.

(2) In some cases, exemplified by example 17, the nature of the hazard impact is not clear and there are conflicting accounts about the extent of casualties and damage. Large discrepancies are common in media reports (see, for example, Blong, 1984, p. 157), and are not unknown in the scientific literature. In example 2 above we report the death toll in the 1976 Moro Gulf (western Mindanao) earthquake and tsunami as 400–500 in coastal areas, with 12 000 left homeless. However, a report stemming from the Honolulu-based (and UNESCO-funded) International Tsunami Information Center puts the death toll from the tsunami at 8000, with 90 000 more homeless (Pararas-Carayannis, 1983, p. 5).

(3) There is a general lack of compiled data such that the hazardousness of any one place is difficult, if not impossible, to assess. For example, Lewis (1982) reported that Tonga experienced 84 hazardous events in the period since 1875 — 41 cyclones, 24 earthquakes of Richter magnitude 7.0 or above, seven periods of drought, nine volcanic eruptions, and three tsunamis. However, we do not know the *relative* magnitudes and impacts of many of these events.

(4) Data files consisting of information only on individual hazards are less useful than those that can lead to assessment of the hazardousness of a place. For example, there may be little point at the local level in increasing the seismic resistance of structures if they remain in flood, storm-surge, or tsunami-prone sites, or in encouraging migration out of one hazard area only to put people at risk in another (see examples 3 & 17).

(5) Most data files include events for far too short a period and therefore provide misleading guides for future risk assessment. For example, according to the Pacific Islands Development Program regional overview (Franco & others, 1982), only 42 lives were lost in Papua New Guinea in the decade beginning 1972 as a result of geological hazards — 27 in earthquakes, 2 in eruptions, and 13 in a landslide — providing a death rate of 4.2 persons per year. Apart from being incomplete (at least 14 others were killed in landslides), extending the period under consideration back to 1950 would increase the death rate to at least 100 per year by including the 1951 Mount Laminton eruption. Comparative assessment of risk is also complicated by different lengths of record. Pararas-Carayannis (1983) noted the tsunami record extends back to 1562 in Chile, 1788 in Alaska, 1821 in Hawaii, but to AD 684 in Japan. Different lengths of record have probably influenced the compilation illustrated in Figure 21 where fluctuations in total deaths in volcanic eruptions per 20-year period are shown from 1600 to the present.

(6) Two other problems are illustrated in Figure 21: (i) the influence of a few large events on the record; and (ii) the general increase in death totals toward the present as a result of increased populations and of more complete (and possibly more accurate) reporting of events and their effects. Even by extending the search to include all written reports of events, volcanic eruptions of the extreme magnitude of that of Toba (circa 25 000 years ago) will remain unrecorded, even though

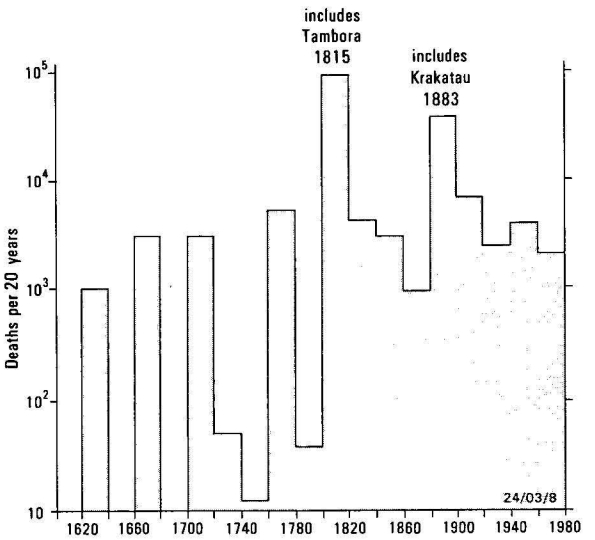

Figure 21. Histogram of known deaths from volcanic eruptions in the southwest Pacific and southeast Asian region for 1600–1980. Data from the Smithsonian Institution Volcano Reference File.

they have a finite annual probability of occurrence. Similarly, no volcanic eruptions have affected the Papua New Guinea Highlands in European times, but legends dated to the seventeenth century (Blong, 1982) include a remarkable range of effects caused by tephra fall. Furthermore, Pain & Blong (1979) showed that this tephra fall was but the most recent from distant sources in a record back at least 30 000 years. The record can be extended by stratigraphic techniques (at least for volcanic eruptions), but stratigraphic procedures will almost certainly miss low-magnitude eruptions, so that the resulting magnitude and frequency distributions are skewed and unreliable.

There is clearly a need to assemble as much high-quality data from as many sources as possible if we are to seriously assess risks from geological hazards, even though every data set will have severe limitations. Clearly, also, the historical record should be extended where possible by geological investigations. *Volcanoes of the World* (Simkin & others, 1981) combines historical and tephrostratigraphic information. The history of landsliding can be determined from sequential photography and historical records (Trustrum & others, 1983). The periodicity of fault movements has been extended by excavation and ^{14}C dating (e.g. Tsukuda & Yamazaki, 1984) and Baker (1982) provided an excellent demonstration of the improvements in flood-risk assessment that can result from the combination of historic (stochastic) and prehistoric (deterministic) flood records.

Hazard vulnerability

Vulnerability takes into account not only an assessment of risk posed by the magnitude and other physical characteristics of a geological hazard, but also the conditions in the threatened society, as discussed above. Conditions requiring consideration include infrastructure — transport and communication networks and building materials, ages, design, and workmanship — and social, economic and political processes. Assessing vulnerability is inherently more difficult than determining risk. Several points need to be recognised:

(1) Vulnerability changes over time, because it depends upon conditions that are continually changing (Lewis, 1982). Repeated exposure to hazard impacts presumably brings cultural adaptation to ameliorate the less desirable effects, but some countries in the southwest Pacific and southeast Asian region may be becoming more vulnerable because of the processes of marginalisation, as discussed above. Certainly, rapid population increases raise the number of people who are vulnerable to natural hazards.

(2) The 'modernisation' characteristic of developing societies may not reduce vulnerability. Heavy and moderate damage to buildings in the 1968 Manila earthquake (Fig. 10; example 7) was concentrated in taller buildings (four and more floors), whereas lower buildings, which were also generally older and constructed of lighter material, suffered little (Caagusan, 1969a,b). Similarly, the 1977 Tongan earthquake (Richter magnitude 7.2) caused extensive damage to buildings (Figs. 8, 9; example 6) constructed from modern material (reinforced concrete, or concrete blocks, or both). Traditional houses, in contrast, suffered little. Campbell & others, (1977, p. 211) concluded:

'In our opinion, significant improvements to the seismic resistance of many structural forms common to Tonga can be achieved with comparative ease and at little expense. But no amount of money will be effective unless the public and building industry are educated in the basic principles that lead to effective earthquake resistant structures.

'Not only is there need for effectively enforced bylaws and construction standards on codes of practice but, and this is equally important, there is a need for education of tradesmen in building construction and housing through a technical institute and by training within government departments'.

At the same time, however, as Lewis (1982, p. 241) noted, any increase in construction standards, 'even if practicable, would impose severe cost burdens on the construction industry which provides significant employment capacity'.

(3) Many countries in the region have only recently become independent. Colonial governments applied exogenous values and solutions in dealing with natural disasters and their aftermaths. New national governments now need to apply indigenous values and solutions, at the same time as coping with largely inherited administrative systems and adjusting priorities for social and economic development.

(4) Development processes, such as the introduction of cash cropping, may also enhance vulnerability by reducing both the time and land available for growing traditional crops. Macdonald (1982) noted that the great drought of the 1870s in the southern Gilbert Islands (Kiribati) was devastating, because for the previous 30 years the population had become accustomed to selling their food surpluses rather than storing them against contingencies. The effects may be exacerbated by allocating the most productive land to cash crops, leaving more marginal sites, which require more space and effort, for the food crops (Lewis, 1982). There is, therefore, in times of crisis, a heavier reliance on food aid than on traditional coping strategies. Waddell (1975) admirably documented this process in relation to frost hazards in the Papua New Guinea Highlands. The desire on the part of local politicians to be seen assisting their constituents resulted in increased calls for food aid and compensation in relation to landslides as well as frost (Blong, in press).

(5) Small countries are more vulnerable to hazard impacts than large countries and small *poor* countries are the most vulnerable of all. Lewis (1982) made the point that the 1977 Andra Pradesh cyclone rendered 2 million people homeless, but that this represented only 4.5 per cent of the State's population and less than one per cent of India's total population. On the other hand, Cyclone Bebe of 1972 created only 120 000 homeless in Fiji, but this represented 22 per cent of the nation's total population. The relative scale of damage may therefore be more important than the absolute magnitude of the disaster.

Conclusions and recommendations

The several issues raised in the foregoing account serve to focus attention on the importance of geological hazard assessment in the southwest Pacific and southeast Asian region. This importance is unlikely to lessen in the future as populations continue to grow and as farming lands extend within and into the areas of significant geological hazard. Individual geological hazards in the region have tended in the past to be treated separately and as problems to be faced at the national rather than regional level. However, the hazardousness of some areas can not be properly treated without considering mixtures of hazards, and hazard types are not restricted by political boundaries. The fact that the general topic of geological hazards in the southwest Pacific and southeast Asia has tended to be overlooked or ignored in textbooks on hazards is probably in part caused by the

dispersed nature of information on the region. For this reason we list the following three proposals as a means of centralising and redistributing basic information on regional geological hazards.

First, we recommend that a data base be established for the collection, use, and dissemination of data on geological hazards in the region with a view to more effective risk and vulnerability assessments. A computer-based system is the most effective way of coming to grips with the compilation and handling of such data, and systems already exist (for example, Simkin & others, 1981) as models for a data base for regional and geological hazards.

Second, we suggest (see also ESCAP, 1984) that a comprehensive set of maps be produced of geological hazards in the region, perhaps under the auspices of the Association of Geologists for International Development. An AGID working group could be established that would manage map production and solicit funds from appropriate governments, industry, and international organisations in support of the cost of data collection and presentation.

Finally, there is a need for training schemes in geological hazard assessment, mitigation, and preparedness in the region (see also ESCAP, 1984). Australian geoscientists could participate in such training courses, perhaps through the Australian Counter Disaster College.

Acknowledgement

We gratefully acknowledge the participation of all those who attended the Working Group meeting on geological hazards held in Sydney in September 1984 (AGID—ILP Workshop, 1985). M.J. Knight, C.G. Newhall, and B.S. Oversby provided valuable reviews of the draft manuscript. We are also indebted to M.J. Crozier, V.F. Dent, N.F. Exon, Kin Che Lam, F.B. Limeta, G.R. McKay, and P. Nutalaya for providing us with photographs of the effects of geological hazards.

References

Acharya, H.K., 1978 — Mindanao earthquake of August 16, 1976: preliminary seismological assessment. *Bulletin of the Seismological Society of America,* 68, 1459-1468.

Acharya, H.E., 1980 — Seismic and tsunamic risk in the Philippines. *Earthquake Engineering, 7th World Conference, Papers and addresses,* 1, 391-393.

AGID-ILP Workshop, 1985 — Geosciences for Development. The Australian Role. *Report of the AGID-ILP Workshop, 7th Australian Geological Convention, Macquarie University, Sydney.*

Baker, V.R., 1982 — Geology, determination and risk assessment. *In* Scientific basis of water resource management. *National Academy Press, Washington D.C.* 109-117.

BAKORNAS, 1982 — Report and recommendations of the National Workshop on Mt Galunggung Volcanic Risk Management held in Bandung, Indonesia, 20-25 September 1982. *Baden Koordinasi Nasional Penanggulangan Bencana Alam, Indonesia.*

Berninghausen, W.H., 1969 — Tsunamis and seismic seiches of southeast Asia. *Bulletin of the Seismological Society of America,* 59, 289-297.

Blong, R.J., 1982 — The time of darkness; local legends and volcanic reality in Papua New Guinea. *Australian National University Press, Canberra.*

Blong, R.J., 1984 — Volcanic hazards, a sourcebook on the effects of eruptions, *Academic Press, Sydney.*

Blong, R.J. (in press) — Natural hazards in the Papua New Guinea highlands. *Mountain Research and Development.*

Blong, R.J., & Humphreys, G.S., 1982 — Erosion of road batters in Chim Shale, Papua New Guinea. *Civil Engineering Transactions, Institution of Engineers, Australia,* CE24, 62-68.

Bolt, B.A., Horn, W.L., Macdonald, G.A., & Scott, R.F., 1975 — Geological hazards. *Springer-Verlag, New York.*

Brand, E.W., 1985 — Landslides in Southeast Asia: A state-of-the-art report. *Proceedings of the 4th International Symposium on Landslides, Toronto,* 1, 17-59.

Caagusan, N.L., 1969a — Geological study of the effects of the August 1968 series of earthquakes. *Philippines Bureau of Mines Report of Investigation* 67, 1-64.

Caagusan, N.L., 1969b — The August, 1968 series of earthquakes and the studies of their effects. *Journal of the Geological Society of the Philippines,* 23, 39-77.

Campbell, M.D., McKay, G.R., & Williams, R.L., 1977 — The Tonga earthquake of 23 June, 1977; some initial observations. *Bulletin of the New Zealand National Society for Earthquake Engineering,* 10, 208-218.

Chambers, M.J.G., & Sobur, S.A., 1977 — Problems in assessing the rates and processes of coastal changes in the province of South Sumatra. *Pusat studi Pengelolaan sumberdaya dan Lingkungran, Centre for Natural Resource Management and Environmental Studies, Bogar Agricultural University. PSPSL Research Report,* 003.

Crozier, M.J., Howorth, R., & Grant, I.J., 1981 — Landslide activity during cyclone Wally, Fiji: a case study of Wainitubatolu catchment. *Pacific Viewpoint,* 22, 69-88.

ESCAP, 1984 — Urban geology: building with the natural environment. *United Nations Economic and Social Council, Economic and Social Commission for Asia and the Pacific, Committee on Natural Resources, E/ESCAP/NR.* 11/33, October 1984.

Everingham, I.B., 1977 — Preliminary catalogue of tsunamis for the New Guinea/ Solomon Islands region, 1768-1972. *Bureau of Mineral Resources, Australia, Report* 180; *BMR Microform* MF14.

Everingham, I.B., Gaull, B., & Dent, V.F., 1977 — Effects of a major earthquake near Bougainville, 20 July 1975. *BMR Journal of Australian Geology & Geophysics,* 2, 305-310.

Firth, R., 1959 — Social change in Tikopia. *George Allen & Unwin, London.*

Franco, A.B., Hamnett, M.P., & Makasiale, J., 1982 — Disaster preparedness and disaster experience in the South Pacific. *Pacific Islands Development Programme, East-West Center, Honolulu.*

Fritz, C.E., 1968 — Disasters. *International Encyclopedia of the Social Sciences,* 4, 202-207.

Hamilton, W., 1974 — Earthquake map of the Indonesian region. *U.S. Geological Survey Map* I-875-C.

Hatori, T., 1982 — Philippine, Solomon and New Hebrides Islands. Tsunamis observed along the coast of Japan, 1971-1980. *Bulletin of the Earthquake Research Institute,* 57, 221-237.

Hattori, S., 1980 — Seismic risk maps in Asian countries — China, Philippines, Indonesia and others. *7th World Earthquake Engineering Conference, Papers and Addresses,* 1, 383-386.

Hewitt, K., & Burton, I., 1975 — The hazardousness of a place: a regional ecology of damaging events. *University of Toronto Press, Toronto.*

Heathcote, R.L., 1979 — The threat from natural hazards in Australia. *In* Heathcote, R.L., & Thom, B.G., (editors), Natural hazards in Australia. *Australian Academy of Science, Canberra.*

Hogg, R., 1982 — Destitution and development: the Turkana of northwest Kenya. *Disasters,* 6, 164-168.

Humphreys, G.S., 1984 — The environment and soils of Chimbu Province, Papua New Guinea with particular reference to soil erosion. *Department of Primary Industry, Papua New Guinea, Research Bulletin* 35.

Iida, K., 1983 — Some remarks on the occurrence of tsunamigenic earthquakes around the Pacific. *In* Iida, K., & Iwasaki, T., (editors), Tsunamis — their science and engineering. *Terra Scientific Publishing Company, Tokyo.* 61-76.

Iida, K., Cox, D.C., & Pararas-Carayannis, G., 1967 — Preliminary catalog of tsunamis occurring in the Pacific Ocean. *Hawaii Institute of Geophysics, Data Report* 5, 1-270.

Jeffery, S.E., 1981 — Our usual landslide: ubiquitous hazard and socioeconomic causes of natural disaster in Indonesia. *Natural Hazard Research, Working Paper* 40, *Institute of Behavioural Science, University of Colorado.*

Johnson, R.W., & Blong, R.J., 1984 — Geological hazards: assessment, mitigation, and disaster/emergency responses in the Southwest-Pacific/ Southeast-Asia region. *Geological Society of Australia Abstracts,* 12, 285.

Kanamori, H., 1978 — Quantification of earthquakes. *Nature,* 271, 411-414.

Katili, J.A., & Sudradjat, A., 1984 — Galunggung. The 1982-1983 eruption. *Volcanological Survey of Indonesia, Bandung.*

Leggett, R.F., 1973 — Cities and geology, *McGraw Hill, New York.*

Lessa, W.A., 1964 — The social effects of Typhoon Ophelia (1960) on Ulithi. *Micronesia, Journal of the College of Guam,* 1, 1-47.

Lewis, J., 1981 — Some perspectives on natural disaster vulnerability in Tonga. *Pacific Viewpoint,* 22, 145-162.

Lewis, J., 1982 — Natural disaster mitigation: environmental approaches in Tonga and Algeria. *The Environmentalist,* 2, 233-246.

Li, Y.-H, 1976 — Denudation of Taiwan Island since the Pliocene Epoch. *Geology,* 4, 105-107.

Limeta, F.B., 1980 — Earthquake damage in Mindanao and its relation to structural design. *Bulletin of the International Institute of Siesmology and Earthquake Engineering,* 18, 137-150.

Lucardie, G.R.E., 1979 — The Makianese — preliminary remarks on the anthropological study of a migration-oriented people in the Moluccas. *In* Masinambao, E.K.M., (editor), Halmahere dan Raja Ampat. Konsep dan Strategi Penelitian. *Leknas-Lipi, Jakarta.* 347-373.

Lumb, P., 1975 — Slope failures in Hong Kong. *Quarterly Journal of Engineering Geology,* 8, 31-65.

Macdonald, B., 1982 — Cinderellas of the Empire — towards a history of Kiribati and Tuvalu. *Australian National University Press, Canberra.*

Maso, M.S., 1910 — Catalogue of violent and destructive earthquakes in the Philippines, 1599-1909. *Weather Bureau, Manila.* 1-25.

Miyoshi, H., 1979 — The sea walls on the sand. *In* Braddock, R.D. (editor), Proceedings of Tsunami Symposium, Canberra, Australia, December 1979, *Griffith University and Intergovernmental Oceanographic Commission,* 103-115.

Morante, E.M., 1974 — The Ragay Gulf earthquake of March 17, 1973, southern Luzon, Philippines. *Journal of the Geological Society of the Philippines,* 28(2), 1-31.

Neumann van Padang, M., 1971 — Two catastrophic eruptions in Indonesia, comparable with the Plinian outburst of the volcano of Thera (Santorini) in Minoan time. *Acta Ist International Scientific Congress on the Volcano of Thera, Greece, 15-23 September, 1969, Archaeological Services of Greece, Athens,* 51-63.

Nutalaya, P., & Rau, J.L., 1981 — Bangkok: the sinking metropolis. *Episodes,* 4, 3-8.

Oliver, J., 1975 — The geographer's concern with natural hazard studies. *Geological Education,* 2, 339-348.

O'Keefe, P., Westgate, K., & Wisner, B., 1976 — Taking the naturalness out of natural disasters. *Nature,* 260, 566-567.

Pain, C.F., & Blong, R.J., 1979 — The distribution of tephras in the Papua New Guinea Highlands. *Search,* 10, 228-230.

Pararas-Carayannis, G., 1983 — The tsunami impact on society. *In* Iida, K., & Iwasaki, T., (editors), Tsunamis — their science and engineering. *Terra Scientific Publishing Company, Tokyo.* 3-8.

Paterson, A.W., & Williams, R.L., 1980 — The Taveuni earthquake, Fiji, on 17 November 1979. *Bulletin of the New Zealand National Society for Earthquake Engineering,* 13, 194-201.

Rappaport, R.A., 1963 — Aspects of man's influence upon island ecosytems: alteration and control. *In* Fosberg, F.R.,(editor), Man's place in the island ecosystem, a symposium. *Bishop Museum Press, Honolulu.* 155-170.

Rau, J.L., & Nutalaya, P., 1982 — Geomorphology and land subsidence in Bangkok, Thailand. *In* Craig, R.G., & Craft, J.F., (editors), Applied geomorphology. *George Allen & Unwin, Boston.* 181-201.

Repetti, W.C., 1946 — Catalogue of Philippine earthquakes, 1589-1899. *Bulletin of the Seismological Society of America,* 36, 133-322.

Rogers, G., 1981 — The evacuations of Niuafo'ou; an outlier in the Kingdom of Tonga. *Journal of Pacific History,* 16, 149-163.

Schwimmer, E.C., 1977 — What did the eruption mean? *In* Leiber, M.D., (editor), Exiles and migrants in Oceania. *University of Hawaii Press, Honolulu.* 296-341.

Self, S., Rampino, M.R., Newton, M.S., & Wolff, J.A., 1984 — Volcanological study of the great Tamboro eruption of 1815. *Geology,* 12, 659-663.

Simkin, T., & Fiske, R.S., 1983 — Krakatau 1883, The volcanic eruption and its effects. *Smithsonian Institution Press, Washington D.C.*

Simkin, T., Siebert, L., McClelland, L., Bridge, D., Newhall, C., & Latter, J.H., 1981 — Volcanoes of the World. *Hutchinson Ross, Stroudsburg, Pennsylvania.*

Simkin, T., & Siebert, L., 1981 — Arc volcanism in space and time: A look at the global historical record. *International Association for Volcanology and Chemistry of the Earth's Interior, Conference Abstracts, Tokyo,* 342.

Sims, J.H., & Baumann, D.D., 1972 — The tornado threat: coping styles of the north and south. *Science,* 176, 1386-1392.

Spillius, J., 1957 — Natural disaster and political crisis in a Polynesian society. *Human Relations,* 10, 3-27.

Stewart, G.S., & Cohn, S.N., 1979 — The 1976 August 16, Mindanao, Philippine earthquake (MS = 7.8) — evidence for a subduction zone south of Mindanao. *Geophysical Journal of the Royal Astronomical Society,* 57, 51-65.

Susman, P., O'Keefe, P., & Wisner, B., 1983 — Global disasters, a radical interpretation. *In* Hewitt, K., (editor), Interpretations of calamity from the viewpoint of human ecology. *Allen & Unwin, Massachusetts,* 181-201.

Tjia, H.D., Asikin, S., & Atmadja, R.S., 1968 — Coastal accretion in western Indonesia. *Bulletin of National Institute of Geology and Mining, Bandung,* 1, 15-45.

Tonkinson, R., 1979 — The paradox of permanency in a resettled New Hebridean community. *Mass Emergencies,* 4, 105-116.

Torry, W.I., 1979 — Anthropological studies in hazardous environments: past trends and new horizons. *Current Anthropology,* 20, 517-540.

Trustrum, N.A., Lambert, M.G., & Thomas, V.J., 1983 — The impact of slip erosion on hill country pasture production in New Zealand. *Second International Conference on Soil Erosion and Conservation, Honolulu, January 1983, Paper* 113.

Tsukuda, E., & Yamazaki, H., 1984 — Excavation survey of active faults for earthquake prediction in Japan — with special reference to the Ukihashi Central Fault and the Atera Fault. *Geological Survey of Japan, Report* 263, 349-361.

Turner, B.A., 1979 — The social aetiology of disasters. *Disasters,* 3, 53-59.

UNDRO, 1976 — Report of the United Nations Disaster Relief Coordinator on the Earthquakes in Irian Jaya and Bali, Indonesia, June-July, 1976. *UNDRO Case Report,* 002.

Uyeda, S., & Kanamori, H., 1979 — Back-arc opening and the mode of subduction. *Journal of Geophysical Research,* 84, 1049-1061.

van Bemmelen, R.W., 1956 — The influence of geologic events on human history. *Verhandelingen Geologisch Mijnbouwkundig Genootschap voor Nederland en Kolonen Geologisch,* 16, 20-36.

van Dijk, J.W., & Ehrencron, V.K.R., 1949 — The different rate of erosion within two adjacent basins in Java. *Mededelingen van het Algemeen Proefstation voor den Landbouw,* 84, 1-10.

Waddell, E., 1975 — How the Enga cope with frost: responses to climate perturbations in the Central Highlands of New Guinea. *Human Ecology,* 3, 249-273.

Westgate, K., & O'Keefe, P., 1976 — Some definitions of disaster. *Bradford University, Disaster Research Unit, Occasional Paper* 4.

White, G.F., (editor), 1974 — Natural hazards — local, national, global. *Oxford University Press, New York.*

Wolfe, J.A., 1977 — Large, Holocene, low-angle landslide, Samar Island, Philippines. *Geological Society of America Reviews in Engineering Geology,* 3, 149-153.

BMR Journal of Australian Geology & Geophysics, 10, 17-22 ©Commonwealth of Australia 1986

Global sea-level change as a method of correlating the Late Permian coal measures in the Sydney, Gunnedah, and Bowen Basins, eastern Australia

A.T. Brakel[1]

Eustatic changes in sea level can be used to correlate sequences in widely separated areas. Thick terrestrial sequences with marine intercalations are especially suitable, provided the marine beds are not the result of tectonic subsidence. The method has been used to correlate Late Permian coal measures in the Sydney, Gunnedah, and Bowen Basins. The Dempsey Formation and its equivalents in the Sydney Basin, an unnamed correlative in the Gunnedah Basin, and the Black Alley Shale and MacMillan Formation in the Bowen Basin have been identified as being deposited during the same eustatic highstand, a result consistent with palynological conclusions. The Kulnura Marine Tongue (Sydney Basin) and the lower Burngrove Formation (Bowen Basin), on the other hand, owe their origin to tectonism. The correlations indicate that deposition of Late Permian coal measures began in the Bowen Basin later than in the Sydney and Gunnedah Basins, a conclusion that appears to be supported by marine macrofossil studies.

Introduction

Fundamental to any regional appreciation of the sedimentary and tectonic evolution of the coal basins of eastern Australia is reliable correlation of the sequences they contain. Without an accurate knowledge of the correspondence of geological events in one basin with those in other basins, it would be difficult to get more than a blurred overview of the regional pattern of sedimentation, basin subsidence, and tectonism, and therefore of how the basins originated and developed. This in turn is relevant to the location, depth, quality, type, and rank of coal in poorly known areas.

This paper aims to correlate the Late Permian coal measures of the Sydney, Gunnedah, and Bowen Basins (Fig. 1) in sufficient detail to enable elucidation of the effects of tectonic and eustatic sea-level changes, and to lay the foundation for other regional studies, such as the construction of structure-contour and isopach maps for sub-units of the coal measure sequence.

The Late Permian coal measures in the Sydney Basin include the Tomago Coal Measures and Newcastle Coal Measures of the lower Hunter Valley, the Singleton Supergroup of the upper Hunter Valley, and the Illawarra Coal Measures of the southern and western parts of the basin. The Black Jack Formation is the equivalent of these in the Gunnedah Basin north of the Hunter Valley. In the Bowen Basin, the Late Permian coal measures embrace the entire sequence from the base of the German Creek Formation to the top of the Rangal Coal Measures, as well as lateral coal-bearing equivalents (the Baralaba, Bandanna, and Tinowon formations). They therefore comprise both the Group III and Group IV coals of Goscombe & others (1976), which are distinguished by being respectively below or above the marine to brackish incursion in the Burngrove Formation.

A broad correlation of the coal measures across the three basins can be made on the basis that all the units lie above the base of the Fauna IV biozone and are therefore Late Permian. More detailed correlation of individual formations between the Sydney and Bowen Basins has not previously been published, because there was very little firmly based information on which to correlate these largely terrestial sequences. Normal correlation tools were inadequate for the task: marine macrofaunas cannot, of course, be used for terrestial sequences, and the marine to brackish incursions present are usually devoid of body fossils, except for rare individuals of no value for the degree of stratigraphic resolution required here. The coal measures interval in the Bowen Basin has not yet been examined for foraminifera, except for the top portion of the MacMillan Formation, which proved barren (V. Palmieri, 1981, personal communication); nor have plant megafossils been researched in sufficient detail for it to be known if they would be useful on the time scale of the upper coal measures. Almost no isotopic dating has been carried out so far.

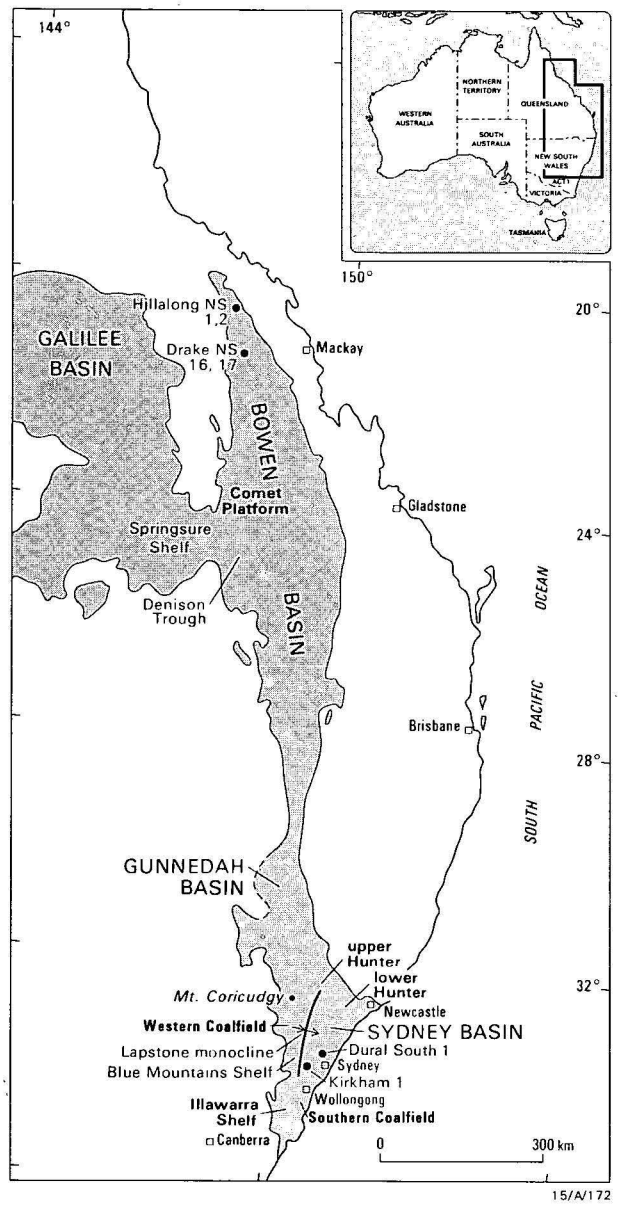

Figure 1. Localities

[1] Division of Continental Geology,
Bureau of Mineral Resources
GPO Box 378, Canberra, ACT 2601

When this study commenced, palynology did not appear to have a fine enough time resolution, and a question mark hung over whether palynozones were influenced by periglacial climatic zones and hence were diachronous (Brakel, 1982a,b). These doubts have now been allayed by recognition of the significance of the hiatus near the start of Late Permian time (Price, 1983), and by work on the microfloras of the Sydney and Gunnedah Basins (McMinn, 1980, 1982). In the meantime, another correlation method, using the concept of global sea-level cycles, appeared promising, was investigated, and has provided useful results.

The concept of sea-level changes

Global sea-level cycles were first recognised by petroleum exploration geologists from seismic traverses across various continental shelves around the world, where it was found that unconformities and sedimentary sequences deposited during highstands and lowstands of sea level occurred in the same respective stratigraphic positions (Vail & others, 1977). Extension of the work onshore showed that cycles of fluctuations a couple of hundred metres either side of present sea level had been operative at least since the Cambrian (Fig. 2a). The broad cycles have been described in greater detail from the Triassic onwards, as, for example, in the sea-level curve for the Tertiary (Fig. 2b). The effect of local tectonism can modify the general pattern, but the global cycles can usually still be identified from field evidence and comparison with other regions. As well as being applied to correlation on continental shelves world-wide, the detailed cycles have been used successfully in Australia for correlation in the Mesozoic of the Surat Basin (Exon & Burger, 1981) and for correlating the New Zealand Tertiary stages with the international ones (Loutit & Kennett, 1981).

Such detail has not yet been published for the Permian, but if short duration global highstands occurred then, as they did in later periods, and if corresponding incursions could be identified within coal measure separated by great distances, then the sequences could be correlated. Mörner (1981) has argued that sea-level cycles are not global in effect, but are caused by changes in the shape of the geoid and migrate with time as large latitudinal waves 50-60° wide. If this is correct, it will not invalidate the technique for correlation between the Permian of the Sydney and Bowen Basins, because the latitudinal difference involved is only 15° and any time difference between sea-level highstands in the two regions will be less than 5 Ma, which is below the threshold of time resolution currently possible.

To qualify for consideration as an unambiguous eustatic change suitable for correlation purposes, a marine incursion should be of wide areal extent. As well, there should have

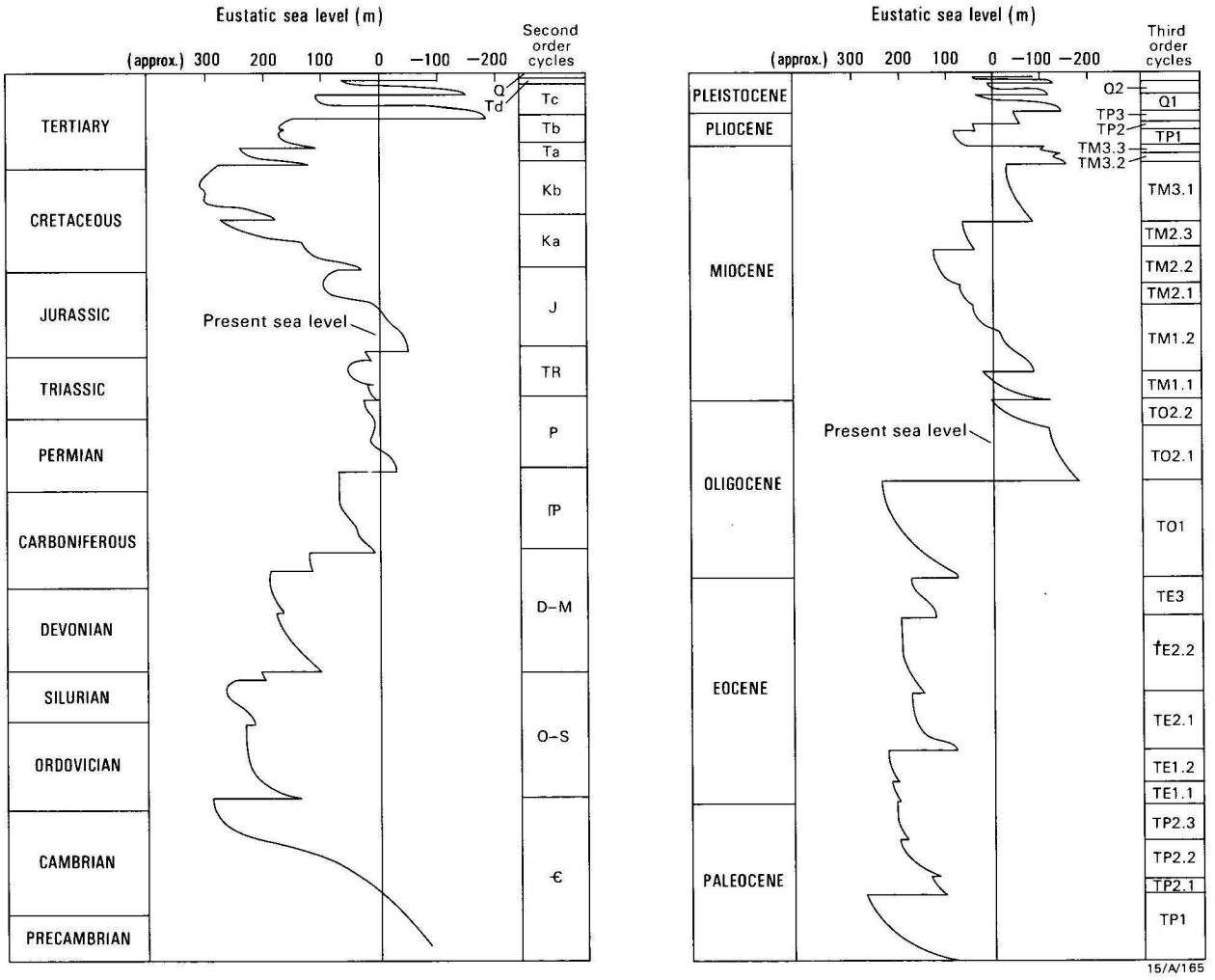

Figure 2a (left). Generalised (second order) global sea-level changes for Phanerozoic time.
After Vail & others (1977). Horizontal scale after Loutit & Kennett (1981).
2b (right). Detailed (third order) sea-level changes for the Mesozoic and Cainozoic.
After Vail & others (1977)

been no significant contemporaneous tectonism, or the effects of the two processes could be confused. For example, the Collinsville Coal Measures of the Bowen Basin and the Greta Coal Measures of the Sydney Basin cannot be interpreted as necessarily representing the same eustatic lowstand, because both units record contemporary tectonism in the form of many thick, extensive alluvial fan conglomerates (palaeontological evidence shows that the two units are in fact not contemporaneous).

A marine or brackish incursion can usually be recognised by the presence of sporadic body fossils and abundant burrowing. Burrows are most common in marine or paralic environments, but are not confined to them (Heckel, 1972), so that if marine macrofauna are absent, other evidence, such as mud flasers, lenticular bedding, acritarchs, and foraminifera, is required to confirm tidal activity or saline conditions.

Sydney–Gunnedah correlation

Examination of the Late Permian coal measures sequences of the Sydney, Gunnedah, and Bowen Basins shows that there were two widespread incursions in each basin. In the Sydney Basin these are the Kulnura and Dempsey incursions, represented respectively by (1) the Kulnura Marine Tongue and its lateral equivalents, the Bulga and Archerfield Formations (upper Hunter Valley), and Erins Vale Formation (South Coast), and (2) the Dempsey Formation and its equivalents, the Denman Formation (upper Hunter Valley), Baal Bone Formation (Western Coalfield), and Bargo Claystone (South Coast).

The deposits of the Kulnura incursion, with a shelly fauna and abundant burrowing, are overlain in most places by a coal seam that contains a distinctive section of dull coal (the Bayswater and Woonona Coal Members). This characteristic couplet of marine to brackish sediments overlain by dull coal can be readily recognised in the Gunnedah Basin as the Arkarula Sandstone Member and Hoskissons Coal Member (Brakel, 1982a,b; Weber & others, 1982; Beckett & others, 1983).

The deposits of the Dempsey incursion, higher in the sequence, usually underlie a marker sandstone unit (the Waratah Sandstone and equivalents). No marine macrofossils are present, but the unit contains acritarchs and a marine microfauna (McMinn, 1982a), and is extensively burrowed. The Dempsey incursion is represented in the Gunnedah region by a burrowed unit in the interval below the Goran Conglomerate Member, but it is much thinner (5m or less) than the Sydney Basin equivalents (Beckett & others, 1983), and in some bores may be absent.

These correlations between the Sydney and Gunnedah Basins are supported by palynological evidence. The Kulnura-Arkarula incursion contains the first appearance of *Dulhuntyspora parvithola,* which marks the boundary between lower stage 5 and upper stage 5 (McMinn, 1980, 1982b). The Dempsey incursion is a little later than the first appearance of *Microreticulatisporites bitriangularis,* which marks the base of the *M. bitriangularis* subzone (upper stage 5c) (McMinn, 1980, 1982b).

Sydney–Bowen correlation

The most needed correlation in the Late Permian is between the Sydney-Gunnedah and Bowen Basins, the exposed parts of which are separated by thick Mesozoic cover overlying poorly known Permian.

Like their counterparts in the Sydney and Gunnedah Basins, the Late Permian coal measures of the Bowen Basin also display evidence of two widespread marine to brackish incursions. These are the MacMillan and Burngrove incursions, represented respectively by (1) the MacMillan Formation and its lateral equivalent, the Black Alley Shale, and (2) the lower, intensely burrowed portion of the Burngrove Formation. The MacMillan Formation and Black Alley Shale contain burrowing and rare shelly fossils, and the latter also contains the P3c acritarch zone. Interpretation of the lower Burngrove Formation is based on the intense burrowing and minor lenticular bedding. Both incursions are widespread, but they appear not to have reached the far north of the Bowen Basin. A marine to brackish interval equivalent to the Burngrove incursion within the Bandanna Formation of the Denison Trough has not been well established, but an interval with some burrowing and bioturbation has been noted in the formation on the adjacent Springsure Shelf by Brakel (1983) and Anderson (1976).

The most obvious and simplest model correlating the Sydney and Bowen sequences equates the Kulnura incursion with the MacMillan incursion, and the Dempsey incursion with the Burngrove incursion (Fig. 3). It has the added attraction of having deposition of upper coal measures start at about the same time in both basins, which can be readily explained by a global drop in sea level initiating deltaic progradation along the eastern seaboard. Consequently, it was the model favoured earlier (Brakel, 1982a,b), but there are now two reasons against it.

The first is evidence that the Kulnura incursion in the Sydney and Gunnedah Basins and the Burngrove incursion in the Bowen Basin were probably caused by tectonism. The lateral equivalent of the Kulnura Marine Tongue in the Western Coalfield of the Sydney Basin is the non-marine Marrangaroo Conglomerate. It underlies the Bayswater Coal Member-equivalent, the Lithgow Coal, and extends along the western basin margin for about 200 km as an alluvial fan apron. This deposit is not what would be expected in response to lower relief resulting from a eustatic sea-level rise. The conglomerate could only be consistent with a eustatic rise if it represents a basal transgressive deposit overlain by a marine interval wherever lower energy marine conditions existed. But no such relationship is known. Furthermore, the Marrangaroo Conglomerate records fluvial rather than nearshore marine deposition (Bradley, 1980; Bembrick, 1983). The Kulnura Marine Tongue and Marrangaroo Conglomerate occur together in the AOG Kirkham 1 well, where a poorly sorted sandy, silty unit (unit Km 26 of Raine, 1969, at 1003-1058 m), containing mud flasers and bioturbation, coarsening upward from sandy siltstone to medium sandstone and topped by a thin coal, is overlain by a conglomeratic unit (unit Km 25 of Raine, 1969, at 979-1003 m). This is the reverse of what would be produced by a eustatic rise in sea level and must therefore be a response to tectonism.

A similar sequence exists in Shell Dural South 1 (1178-1372 m), where a dominantly siltstone sequence is overlain by sandstone (units D11 and D10 of Hawkins & Ozimic, 1967). The siltstone contains arenaceous foraminifera and probable burrowings, and, given its stratigraphic level, it can be correlated confidently with the Kulnura Marine Tongue. The overlying medium-grained sandstone contains some pebble layers and could represent either the distal fan delta of the Marrangaroo Conglomerate or a beach-zone facies. Minor coal in the sandstone could have been deposited in coastal swamps fringing the fan delta or in back-beach marshes. Rare patches of anhydrite may record short-lived, local evaporitic conditions. The Kirkham 1 sequence, and possibly that in

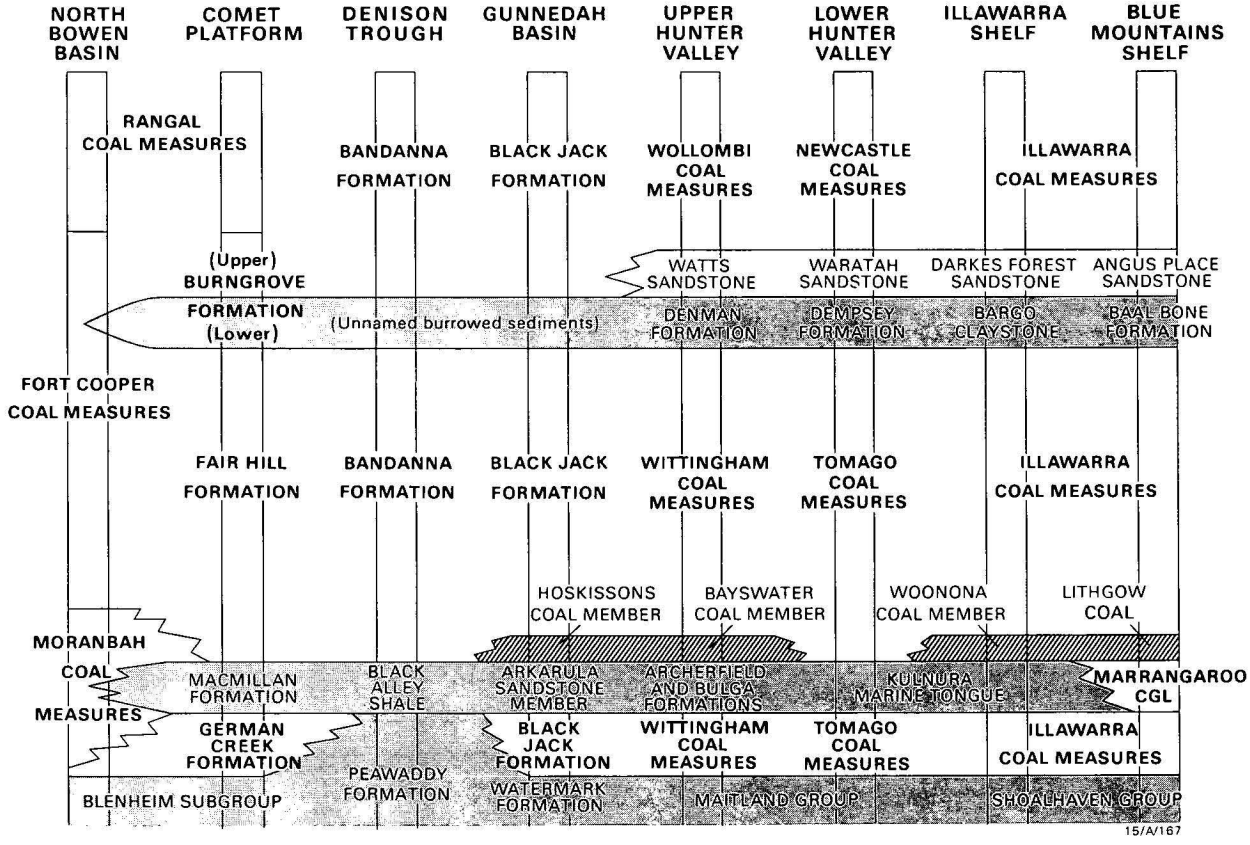

Figure 3. Correlation model equating the Kulnura, Arkarula, and MacMillan incursions in the Sydney, Gunnedah, and Bowen Basins, respectively.

Major marine units are stippled, minor local marine intercalations are not shown.

Dural South 1, records the Kulnura marine incursion being overridden by a prograding fan delta of Marrangaroo Conglomerate. Recently, Havord & others (1984) have reported finding the Marrangaroo Conglomerate overlying the Kulnura Marine Tongue over much of the western and southern Sydney Basin, thus confirming the interpretation of the Kirkham 1 and Dural South 1 sequences.

The absence of the Kulnura Marine Tongue west of the Lapstone Monocline strongly suggests that the Lapstone basement fault (Harrington & Brakel, 1981) was active at the time, the central and eastern parts of the Sydney Basin being downthrown. The subsidence allowed the sea to cover the basin up to the Lapstone line, while on the emergent Blue Mountains Shelf the drop in base level caused the alluvial fan of the Marrangaroo Conglomerate to form in response. The fan eventually reached the sea as a fan delta at Kirkham 1. Farther north, in the Mount Coricudgy area, bioturbation and marine influence have been observed in the Marrangaroo Conglomerate (G.M. Bradley, personal communication) near a hinge-line and Landsat lineament west of the Lapstone line, indicating that the sea reached further west in this area and that tectonic activity occurred on more than one basement fault.

Deposition of the Burngrove Formation in the Bowen Basin was also accompanied by substantial tectonic activity. Tuffs from contemporaneous volcanism are abundant, and, in the far north of the basin, conglomerates are common in the upper part of the Fort Cooper Coal Measures, which is equivalent to the Burngrove Formation. The conglomerates have been intersected in GSQ Hillalong NS 1 and 2 bores; they were laid down in alluvial fans advancing towards the southeast, parallel to the basin axis, and some contain clasts of cobble size (Koppe, 1973). Conglomerate also occurs at the same level in GSQ Drake NS 16 and 17 (Koppe, 1976). It seems likely then that the Burngrove incursion also had a tectonic cause.

A second line of evidence against a Kulnura-MacMillan correlation is provided by palynology. The base of the Black Alley Shale, equivalent to the MacMillan Formation (Brakel, 1983), marks the first appearance of *Microreticulatisporites bitriangularis* and the beginning of the upper stage 5c palynozone (Rigby & Hekel, 1977). This same species first appears in the Sydney and Gunnedah Basins a little below the Dempsey Formation (McMinn, 1980, 1982). If diachroneity of palynozones between the Sydney and Bowen Basins is no longer a tenable hypothesis, then the MacMillan and Dempsey incursions are contemporaneous.

The result is an alternative Sydney-Bowen correlation model (Fig. 4), which equates the MacMillan incursion with the Dempsey incursion, has the Kulnura incursion equivalent to part of the Blenheim Subgroup time (Peawaddy and Maria Formations), and places the Burngrove incursion at a level within the interval corresponding to the Newcastle Coal Measures. Coal measure deposition in the Sydney Basin began markedly earlier than in the Bowen Basin. The only global sea-level rise that can now be unambiguously identified in upper coal measures time is the MacMillan–Dempsey incursion, which is the only marine transgression to affect the whole region simultaneously and not be accompanied by significant tectonic activity. There are no conglomerates or volcanogenic rocks associated with the Dempsey Formation in the Sydney and Gunnedah Basins, nor are there conglomerates in the MacMillan Formation in the Bowen Basin, but the Black Alley Shale and MacMillan Formation

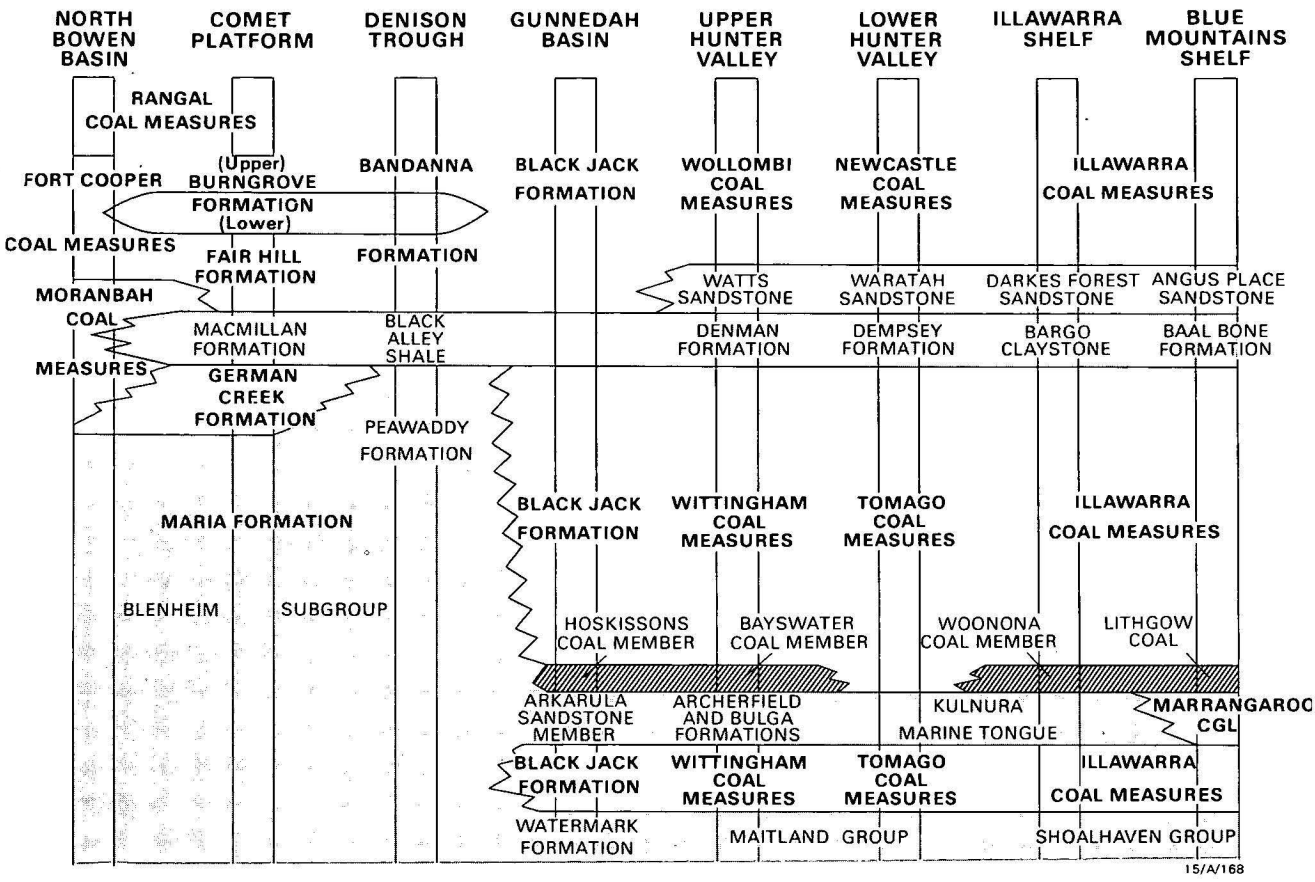

Figure 4. Correlation submitted in this paper between the Sydney, Gunnedah, and Bowen Basins, equating the Dempsey and MacMillan incursions.

Major marine units are stippled, minor local marine intercalations are not shown.

do contain some tuff, though not as much as in the overlying formations.

The longer persistence of marine conditions in the Bowen Basin suggests that a possible check on the model would be the examination of macrofaunal assemblages from the MacMillan Formation and the top of the Maria and Peawaddy Formations to see if they show any indication of being younger than assemblages at the top of the Maitland Group or in the Kulnura Marine Tongue (No shelly fossils are known from the Dempsey Formation or its equivalents in the Sydney-Gunnedah region). An investigation of the fossil assemblages by Dickins (1983) found that the upper Blenheim Subgroup, including the MacMillan Formation and Black Alley Shale, contains Fauna IV fossils, but that they belong to a distinctive faunal subdivision at the top of Fauna IV, termed the *M. havilensis* zone, which is not known from the Sydney Basin. The implication is that the top of Fauna IV could well be younger in the Bowen Basin than in the Sydney Basin, consistent with the favoured correlation model (Fig. 4). Runnegar (1967) has also suggested that the upper part of Fauna IV may be younger in the Bowen Basin.

Concluding discussion

The identification of marine incursions in the Late Permian coal measures of the Sydney, Gunnedah, and Bowen Basins has enabled these sequences to be correlated over a distance of 1400 km in more detail than previously. In particular, the Dempsey, Denman, and Baal Bone Formations, and the Bargo Claystone (Sydney Basin), an unnamed marine to brackish unit below the Goran Conglomerate Member of the Black Jack Formation (Gunnedah Basin), and the Black Alley Shale and MacMillan Formation (Bowen Basin) can be seen as recording the same global highstand in sea level. Late Permian coal measure deposition began later in the Bowen Basin than in the Sydney and Gunnedah Basins, so that the German Creek Formation is equivalent only to part of the upper Tomago Coal Measures. The limited palaeontological and palynological data available are consistent with these observations.

The Kulnura Marine Tongue and Marrangaroo Conglomerate of the Sydney Basin are, by contrast, the result of tectonic subsidence of the eastern half of the basin, so that the Kulnura incursion cannot be used for correlation outside the affected Sydney-Gunnedah region. It is equivalent to a level in the Peawaddy Formation in the Bowen Basin. The marine to brackish incursion of the lower portion of the Burngrove Formation, confined to the Bowen Basin in Newcastle Coal Measures time, also appears to have a tectonic cause.

Eustatic changes in sea level can therefore be used to correlate between widely separated areas. Although the method has previously been used for sequences in geological periods for which global sea-level curves have been published, this study has shown that it may also be applied to older sequences for which no published curves are available, if eustatic highstands (or lowstands) can be recognised. Thick terrestrial sequences, which are usually difficult to date precisely by normal correlation methods, are especially suitable for this technique if they contain marine intercalations that are demonstrably not the result of tectonically induced subsidence.

Acknowledgements

I would like to thank H.J. Harrington, J.W. Hunt, J.M. Dickins, A. McMinn, J. Beckett, D.S. Hamilton, G.M. Bradley, C. Herbert, J. Draper, and P.L. Price for useful discussions on various aspects of correlation problems, but responsibility for the views expressed is mine. I also thank H.J. Harrington and J.M. Dickins for reviewing the manuscript, and the Geological Surveys of New South Wales and Queensland for kindly allowing access to their core libraries. M.R. Moffat drafted the diagrams. The work was funded by a NERDDC grant for Project 78/2617 on the Permian Coals of Eastern Australia.

References

Anderson, J.C., 1976 — Coal evaluation of the Bandanna Formation, western Springsure Shelf. *Queensland Government Mining Journal*, 77, 201-203.

Beckett, J., Hamilton, D.S., & Weber, C.R., 1983 — Permian and Triassic stratigraphy and sedimentation in the Gunnedah-Narrabri-Coonabarabran region. *Geological Survey of New South Wales, Quarterly Notes* 51, 1-16.

Bembrick, C.S., 1983 — Stratigraphy and sedimentation of the Late Permian Illawarra Coal Measures in the Western Coalfield, Sydney Basin, New South Wales. *Journal and Proceedings of the Royal Society of New South Wales*, 116, 105-117.

Bradley, G.M., 1980 — Notes on the stratigraphy of the Illawarra Coal Measures in the Western Coalfields. *Geological Survey of New South Wales, Report* GS 1980/180.

Brakel, A.T., 1982a — Stratigraphic correlation of the upper coal measures of the Sydney Basin with their equivalents in the Bowen Basin. *16th symposium on advances in the study of the Sydney Basin, Abstracts*, 32-34. *University of Newcastle, New South Wales.*

Brakel, A.T., 1982b — Stratigraphic correlation of the upper coal measures of the Sydney Basin with their equivalents in the Bowen Basin (Abstract). *BMR Journal of Australian Geology & Geophysics*, 7, 147.

Brakel, A.T., 1983 — Correlation between the Comet Platform and the Denison Trough, Bowen Basin. *Proceedings of the symposium on the Permian geology of Queensland*, 295-302. *Geological Society of Australia, Queensland Division, Brisbane.*

Dickins, J.M., 1983 — The Permian Blenheim Subgroup of the Bowen Basin and its time relationships. *Proceedings of the symposium on the Permian geology of Queensland*, 269-274. *Geological Society of Australia, Queensland Division, Brisbane.*

Exon, N.F., & Burger, D., 1981 — Sedimentary cycles in the Surat Basin and global changes in sea level. *BMR Journal of Australian Geology & Geophysics*, 6, 153-159.

Goscome, P.W., Koppe, W.H., & Moelle, K.H.R., 1976 — Permian coal geology — eastern Australia. *25th International Geological Congress, Sydney, Excursion Guide* 10A.

Harrington, H.J., & Brakel, A.T., 1981 — The Lapstone basement fault and the development of the western section of the Sydney Basin. *Western Coalfield Symposium, Abstracts*, p. 10. *Coal Geology Specialist Group, Geological Society of Australia, Sydney.*

Havord, P., Herbert, C., Conaghan, P.J., Hunt, J.W., & Royce, K., 1984 — Marrangaroo Conglomerate — its distribution and origin in the Sydney Basin. *Seventh Australian Geological Convention, Sydney.* Geoscience in the development of natural resources. *Geological Society of Australia, Abstracts* 12, 221-223.

Hawkins, P.J., & Ozimic, S., 1967 — Petrological study of the Dural South (Shell) No. 1 Well, Sydney Basin, New South Wales. *Bureau of Mineral Resources, Australia, Record* 1967/160.

Heckel, P.H., 1972 — Recognition of ancient shallow marine environments. *In* Rigby, J.K., & Hamblin, W.K., (editors), Recognition of ancient sedimentary environments. *Society of Economic Paleontologists and Mineralogists, Special Publication* 16, 226-286.

Koppe, W.H., 1973 — Departmental drilling, Exmoor and Hail Creek East, north Bowen Basin. *Geological Survey of Queensland, Record* 1973/6.

Koppe, W.H., 1976 — Departmental reconnaissance drilling northwest Bowen Basin. *Geological Survey of Queensland, Record* 1976/7.

Loutit, T.S., & Kennett, J.P., 1981 — New Zealand and Australian Cenozoic sedimentary cycles and global sea level changes. *AAPG Bulletin*, 65, 1586-1601.

McMinn, A., 1980 — Palynology of the Browns Gap section, Lithgow. *Unpublished Palynological Report* 1980/11, *Geological Survey of New South Wales, Report* GS 1980/159.

McMinn, A., 1982a — Late Permian acritarchs from the northern Sydney Basin. *Journal and Proceedings of the Royal Society of New South Wales*, 115, 79-86.

McMinn, A., 1982b — Palynology of DM Doona DDH1, southern Gunnedah Basin. *Unpublished Palynological Report* 1982/1, *Geological Survey of New South Wales, Report* GS 1982/009.

Price, P.L., 1983 — A Permian palynostratigraphy for Queensland. *Proceedings of the symposium on the Permian geology of Queensland*, 155-221. *Geological Society of Australia, Queensland Division, Brisbane.*

Raine, I., 1969 — Petrological study of Kirkham (A.O.G.) No. 1 Well, Sydney Basin. *Bureau of Mineral Resources, Australia, Record* 1969/61.

Rigby, J.F., & Hekel, H., 1977 — Palynology of the Permian sequence in the Springsure Anticline, central Queensland. *Geological Survey of Queensland, Palaeontological Paper* 37, *Publication* 363, 1-76.

Runnegar, B., 1967 — Preliminary faunal zonation of the eastern Australian Permian. *Queensland Government Mining Journal*, 68, 552-556.

Vail, P.R., Mitchum, R.M., & Thompson, S., 1977 — Seismic stratigraphy and global changes in sea level. Part 4: Global cycles of relative changes of sea level. *In* Rayton, C.E. (editor), Seismic stratigraphy — applications to hydrocarbon exploration. *American Association of Petroleum Geologists, Memoir* 26, 83-97.

Weber, C.R., Beckett, J., & Hamilton, D.S., 1982 — Recent exploration in the Gunnedah Basin by the Department of Mineral Resources. *16th symposium on advances in the study of the Sydney Basin, Abstracts*, 36-37. *University of Newcastle, New South Wales.*

BMR Journal of Australian Geology & Geophysics, 10, 23-37 © Commonwealth of Australia 1986

Lithospheric velocity beneath the Adavale Basin, Queensland, and the character of deep crustal reflections

D. M. Finlayson[1] & C. D. N. Collins[1]

Along a traverse across the main depression of the Devonian Adavale Basin in western Queensland, lateral variations in lithospheric velocity are predominantly displayed in the upper 15 km of the crust. In this region, Devonian sediments (up to 7 km thick) underlie the Jurassic-Cretaceous Eromanga sequence (up to 2 km thick) with only minor pockets of intervening Permo-Triassic sediments of the Cooper and Galilee Basins. P-wave velocity in the sediments ranges from 2.0 to 5.5 km/s. Underlying the Devonian sediments is a 2-3 km thick basement transition zone of highly folded, faulted, and sheared rocks, where metamorphic grade increases and weathering decreases with depth, and velocity increases from 5.6 to 5.85 km/s. Upper crustal basement extends to 24-25 km with velocity increasing from 5.9 km/s below the basement transition zone to 6.4 km/s above a mid-crustal horizon. Multiply refracted phases suggest the velocity gradient of 0.02-0.03 km/s/km in the upper crustal basement is fairly uniform along the traverse. The increase in mid-crustal velocity from 6.4 to 6.6-6.7 km/s is a prominent feature of the lithosphere. It marks the upper boundary of the lower crustal reflection zone evident from continuous reflection profiling. Within this zone, the velocity increases to 6.8-7.1 km/s at the top of the crust/mantle transition zone at a depth of about 35 km. Neither the mid-crustal velocity horizon nor the Moho varies greatly in depth. The upper mantle velocity of 8.15 km/s is reached at 38-40 km depth, the same as that measured on an east-west cross traverse. The preferred interpretation of the lower crustal velocity gradient and reflections is that they arise from extensive lower crustal magma intrusion during the formation of quasi-continental crust and that subsequent thermal events have enabled isostatic readjustment and basin formation in a compressive regime.

Introduction

The Devonian Adavale Basin in southern Queensland represents the most extensive remnant of a Palaeozoic tectonic episode after which the region was effectively part of the wider Australian craton (Veevers & others, 1982). During 1981, basement to the Adavale Basin was the target of a deep seismic refraction/wide- angle reflection study to determine the deep crustal velocity structure. This study formed part of a more extensive seismic investigation of the central Eromanga Basin region, using seismic reflection and refraction profiling methods (Finlayson & others, 1984; Wake-Dyster & others, 1983; Collins & Lock, 1983; Mathur, 1983).

Adavale Basin–geological summary

The north-south, deep-seismic, refraction profile extends from the Maneroo Platform in the north, across the main depression of the Adavale Basin and the Quilpie Trough, to the Thargomindah Shelf in the south. These features are part of a number of Palaeozoic and Mesozoic intracratonic basins that overlie Early Palaeozoic rocks in southwestern Queensland. The structural development of the Adavale Basin has been described by Passmore & Sexton (1984) and this paper contains only a summary of their description relevant to the deep structure of the region.

A simplified structure of the basin is contained in Figure 1, together with the location of BMR seismic reflection and refraction/wide-angle reflection profiles. The Adavale Basin has a main depression and several peripheral troughs separated from it by faults and upthrown basement blocks. The basin is overlain by Carboniferous-Triassic sediments of the Cooper and Galilee Basins and the whole region is blanketed by the Jurassic-Cretaceous sediments of the Eromanga Basin (Fig. 2).

On the Yaraka Shelf (Fig. 1) good reflection horizons have been identified with basement (pre-Devonian) rocks, but in the main depression the velocity contrasts in the lowest part of the Devonian sequence are not great and, consequently, basement is not well identified. Basement depth can be inferred only from the termination of overlying reflectors. Figure 3, derived from Passmore & Sexton (1984), illustrates the detailed structural information available. The depth to pre-Devonian basement along the refraction profile across the main depression is 5.5 km at most and under the Quilpie Trough does not exceed 5 km (Collins & Lock, 1983; Passmore & Sexton, 1984). However, in the Cooladdi Trough the sediment thickness may exceed 8.0 km; this affects some interpretations described later. The thickness of sediment on the sides of uplifted blocks suggests that up to 8.5 km of Devonian sediment may have been removed during the Carboniferous.

The Adavale Basin is described by Passmore & Sexton (1984) as an Early Devonian foreland basin lying west of a volcanic arc-trench system developed during the Palaeozoic. Deposition in the Early Devonian was followed by a period of active subsidence, mobility of basement rocks, volcanism, and rapid facies changes. In the Late Devonian the basin was blanketed by a thick red-bed sequence. The few wells to penetrate pre-Devonian basement have encountered low-grade metamorphic, volcanic, plutonic, and strongly folded clastic rocks, generally with Ordovician-Silurian ages (Murray & Kirkegaard, 1978).

The whole region was reactivated during the deposition of sediments in the Galilee and Cooper Basins in the Late Carboniferous-Triassic and again during the deposition of Eromanga Basin sediments in the Jurassic-Cretaceous. East of the Canaway Ridge, the thickness of these sequences is 1-2 km. The morphological relief on post-Devonian sediments is considerably less than that on the Adavale Basin sediments.

Field survey

Shots were fired at five locations, Thargomindah, Toompine, Adavale, Blackall, and Barcaldine (Fig. 1). Shot sizes varied between 0.9 t and 3.4 t; all explosive was dispersed in shot-hole patterns drilled to about 40 m depth. Recording was conducted in two stages, the first between Toompine and Adavale, the second between Adavale and Blackall. Station spacing was about 7.5 km. Records were made on 21 BMR portable seismic tape-recording systems. Each comprised a single vertical-component seismometer with output amplified and recorded on a slow-speed FM tape recorder at two gain levels together with the Telecom VNG radio time signal and an internal, time-coded, clock signal (Finlayson &

[1]Division of Geophysics, Bureau of Mineral Resources, GPO Box 378, Canberra, ACT 2601.

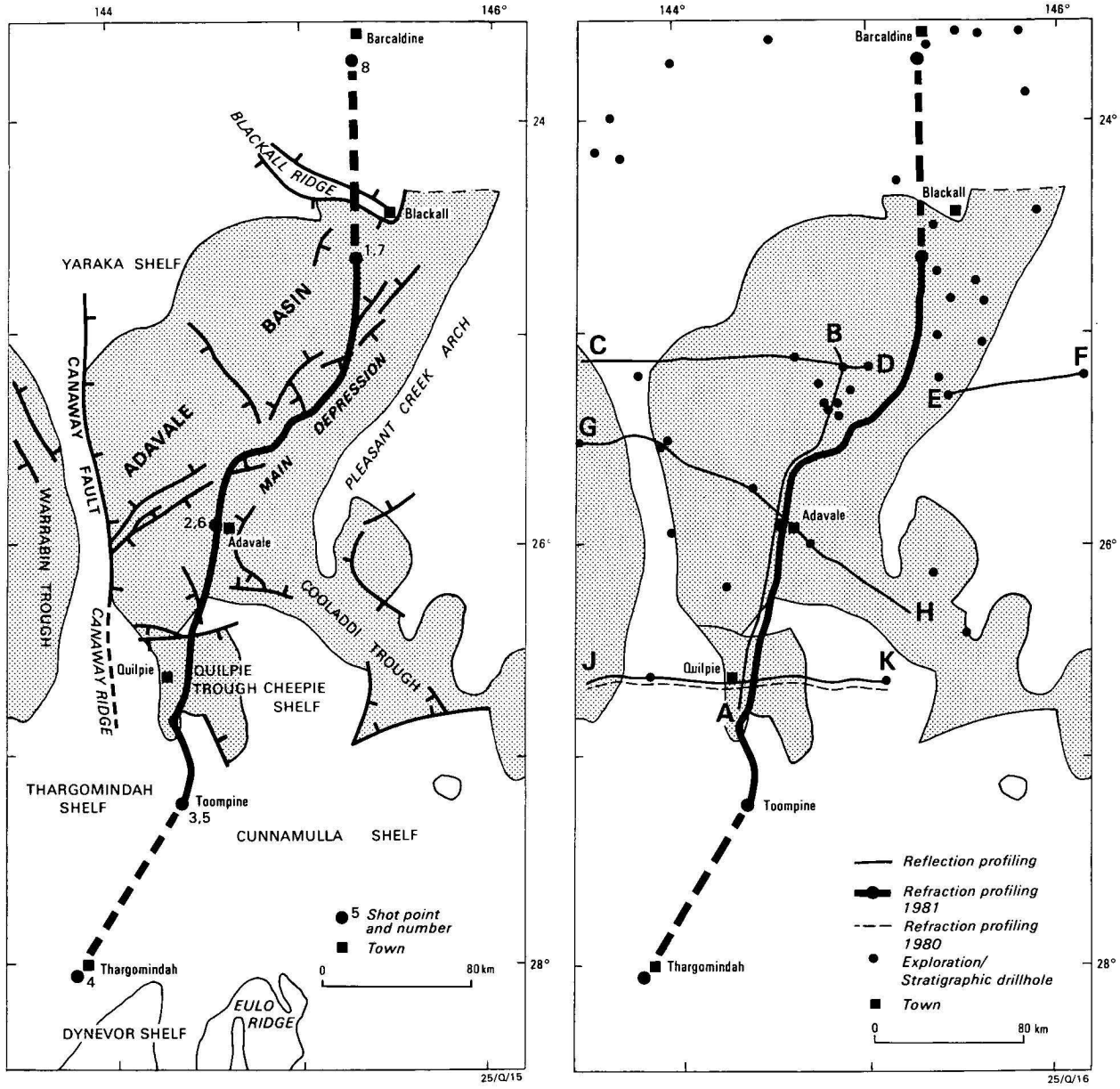

Figure 1. (Left) Simplified structure of the Adavale Basin and location of the wide-angle reflection/refraction seismic traverse. (Right) Location of exploration and stratigraphic drillholes, and BMR seismic profiling traverses.

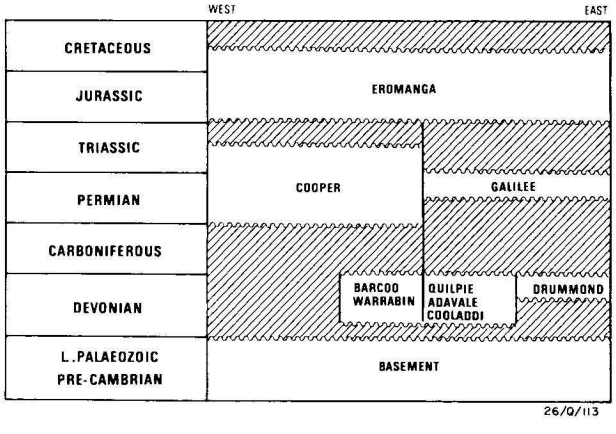

Figure 2. Stratigraphic setting of the Adavale Basin.

Collins,1980). Records were subsequently digitised and displayed on a BMR-designed playback system (Liu & Seers, 1982).

Sedimentary basin structure

The basin structure has been extensively evaluated by seismic reflection profiling, including regional seismic lines shot by BMR in the period 1980-82 using 6-fold CDP methods (Fig. 1). Figure 3 shows a summary of the basin structure as interpreted by Passmore & Sexton (1984): the numbers indicate prominent reflecting horizons tied to exploration well data. The unconformity at the top of the Devonian (6) is at a depth of 1.0–2.4 km and is overlain by sporadic occurrences of Permian (5), and the Eromanga Basin sequences (1,2,3). The Adavale Basin region, therefore, largely escaped the major Permo-Triassic subsidence phases that created the Cooper Basin to the west and the Galilee Basin to the east.

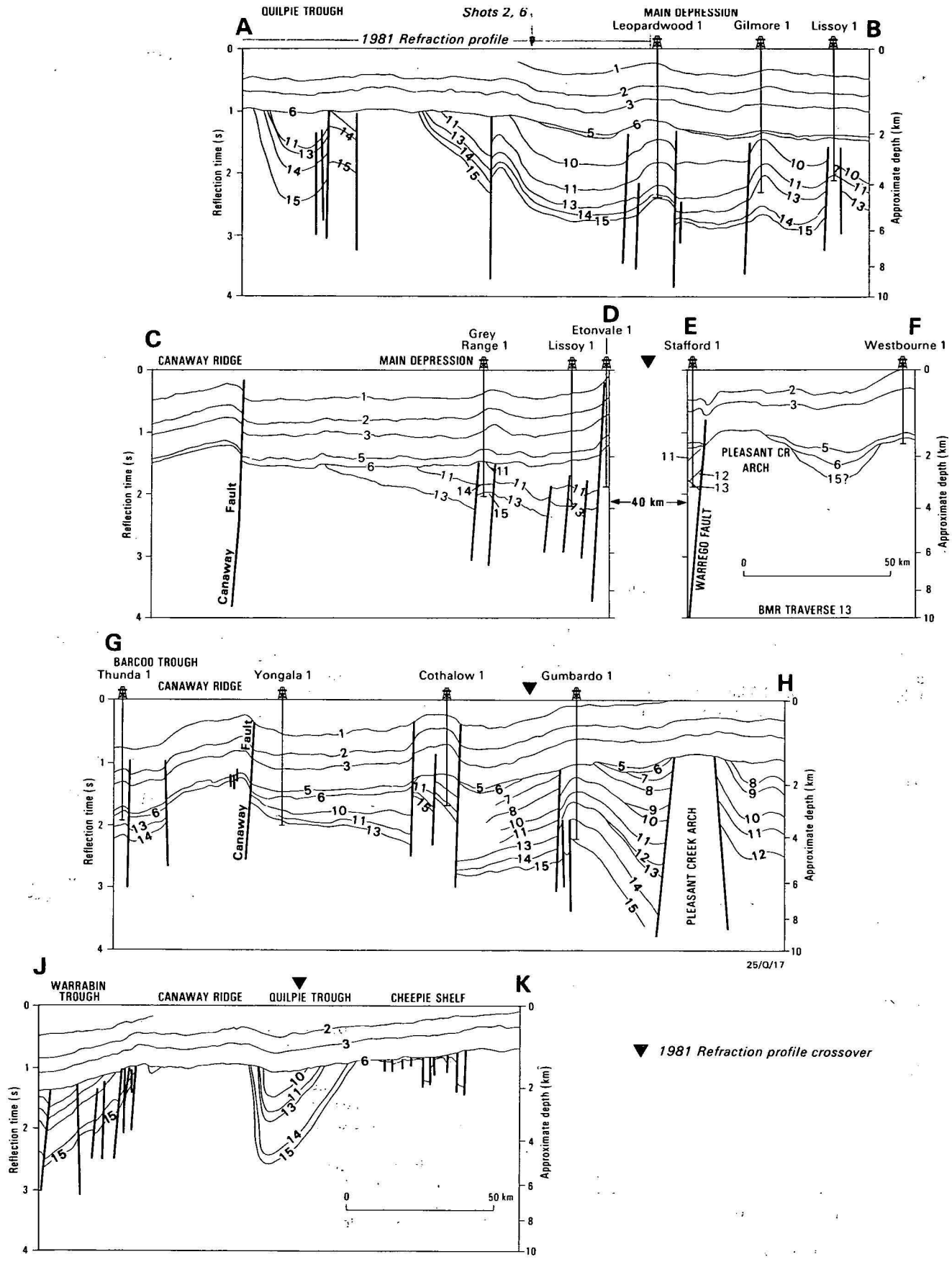

Figure 3. Interpreted BMR shallow reflection profiles (located in Fig. 1). 1 — Winton Formation coal measures; 2 — Toolebuc Formation; 3 — Cadna-Owie Formation; 5 — top Permian; 6 — top Devonian unconformity; 7-10 — within Buckabie Formation; 11 — Etonvale Formation; 12 — Boree Salt; 13 — Cooladdi Dolomite/Bury Limestone; 14 — base of Log Creek Formation; 15 — basement or base of Gumbardo Volcanics: (from Passmore & Sexton, 1984). Vertical exaggeration ×10.

Major faults in the Adavale Basin are indicated in Figures 2 and 3. Passmore & Sexton (1984) indicated that the main deformation occurred in the Late Devonian, when severe faulting was accompanied by uplift of basement blocks followed by peneplanation. They found no evidence within basement that would indicate the attitude of faulting below the Devonian rocks.

Collins & Lock (1983) and Lock & Collins (1983) interpreted closely spaced, wide-angle reflection/refraction data on an east-west traverse that intersects the profile interpreted in this paper near Quilpie (Fig. 1). Together with the move-out velocities derived for the reflection profiling data, these interpretations provide information on the velocity structure within the sedimentary sequences and uppermost basement. However, it is recognised that, at the upper limit of the frequencies recorded by the portable seismic systems (20 Hz), detailed lithologic boundaries within the sedimentary section, such as those seen on sonic velocity logs in boreholes, cannot be identified.

Generally, the Eromanga Basin sequence is characterised by velocities of 2.0–2.3 km/s at the surface, 3.6–3.8 km/s at about 1 km depth, and about 4.9 km/s at 2 km depth. The transition to basement is not characterised by a sharp velocity discontinuity west of the Canaway Ridge. Rather, a continuing velocity increase is observed until velocity of about 5.8–5.9 km/s is reached at 5 km depth. Within the Devonian sequencies of the Quilpie Trough, Collins & Lock (1983) interpreted velocity ranging from 4.0 km/s at the top to 5.5 km/s at their deepest (5 km). Lock & Collins (1983) indicated that the high-angle faulting seen in the sedimentary section at 2 km depth continues to be evident in the velocity structure to at least 5 km depth. Under the Eromanga Basin sequence across the Canaway Ridge there is a sharper increase in velocity to about 4.1–4.5 km/s, and across the Cheepie Shelf the velocity increases to 4.8–5.0 km/s. The immediate basement velocity, therefore, seems to be higher under the Cheepie Shelf than under the Canaway Ridge.

These refraction velocity estimates in the upper 6–7 km, together with the structure from the reflection profiling, have been incorporated directly in the 2-dimensional seismic-modelling process to derive the structure in the deeper crust from the wide-angle reflection/refraction data.

Interpretation methods

Previous interpretations of deep seismic refraction/wide-angle reflection data from the Eromanga Basin region (Finlayson & others, 1984; Finlayson, 1983) have employed methods of modelling the kinematic (travel-time) and dynamic (amplitude) features of the seismic record sections that simplify deep structures into one-dimensional velocity/depth models. This has enabled the broad features of crustal and upper mantle velocity inhomogeneities to be determined, but has limited the extent to which the lateral inhomogeneities in basin and basement structure could be incorporated in models. In the interpretation presented in this paper the 1-D approximation was used in the initial stages to derive starting velocity/depth models for more detailed 2-D models.

The ability to interpret two-dimensional laterally varying velocity structures has been greatly improved by the developments of Cerveny (1979) and McMechan & Mooney (1980). They have applied zero-order, asymptotic ray theoretical methods to calculate the amplitude of emergent rays traversing a two-dimensional velocity model.

The RAYAL/RAYAMP computer programs applied in this paper are those described by McMechan & Mooney (1980). The travel-times and amplitudes of first arrivals, single and multiple refractions, and wide-angle reflections were modelled, although, for reasons of space, not all models are presented in this paper. The additional constraints placed on the models by multiple reflections from the low-velocity (about 2.0 km/s) near-surface sediments provided very useful information on upper crustal velocities. Only those phases that were consistently identified and correlated on the record sections have been used in the interpretation. On some sections, isolated events can be seen, but no attempt has been made to interpret these.

The seismic P-waves used in this interpretation are as follows:

P—Refractions through the sedimentary layers (apparent velocity less than 5 km/s);
PP—Refractions through the sedimentary layers twice (reflected at the surface);
PPP—Refractions through the sedimentary layers three times (reflected at the surface twice);
P_1—Refractions through the uppermost basement (apparent velocity less than 5.8 km/s);
P_1P_1—Refractions through the uppermost basement twice (reflected at the surface);
Pg—Refractions through the upper crustal basement (apparent velocity 5.8–6.4 km/s);
P-bar—Refractions through the upper crustal basement twice (reflected either at the surface or some boundary near the base of the sedimentary sequence);
Pc—Reflections from a horizon at mid-crustal depths (maximum apparent velocity about 6.6–6.7 km/s);
Pg'—Refractions through the lower crust (apparent velocity about 6.7–7.0 km/s);
Pg''—Refractions through the crust/upper mantle transition zone;
PmP—Reflections from the crust/mantle transition zone (Moho);
Pn—Refractions through the upper mantle (apparent velocity about 8.1–8.2 km/s);

The interpretation of many phases to determine crustal structure is regarded as important. Different seismic phases illuminate different regions of the crust and upper mantle, and the composite interpretation is enhanced by satisfying the travel-time and amplitude data from a number of phases. However, as with other geophysical methods, the solutions presented are not unique; the interpretation presented here is the authors' preferred interpretation. Figure 4 illustrates results from program RAYAL/RAYAMP using a simple layered model that approximates the structure south from Blackall and Barcaldine. In particular, the relative arrival times and amplitudes of the Pn, PmP, Pg', Pg'' and P-bar phases should be noted together with the distance ranges over which they are observed.

In this model, the amplitude of the Pn phase is about the same as that of the later P-bar phase. This is contrary to observed data, in which the Pn phase is smaller, indicating that a lower velocity gradient in the upper mantle should be preferred. Lateral variations in velocity will change the smoothly varying amplitudes illustrated.

The resultant interpretation should not be considered as a continuous structure, but as a series of velocity features that, taken together, give the broad-scale velocity structure.

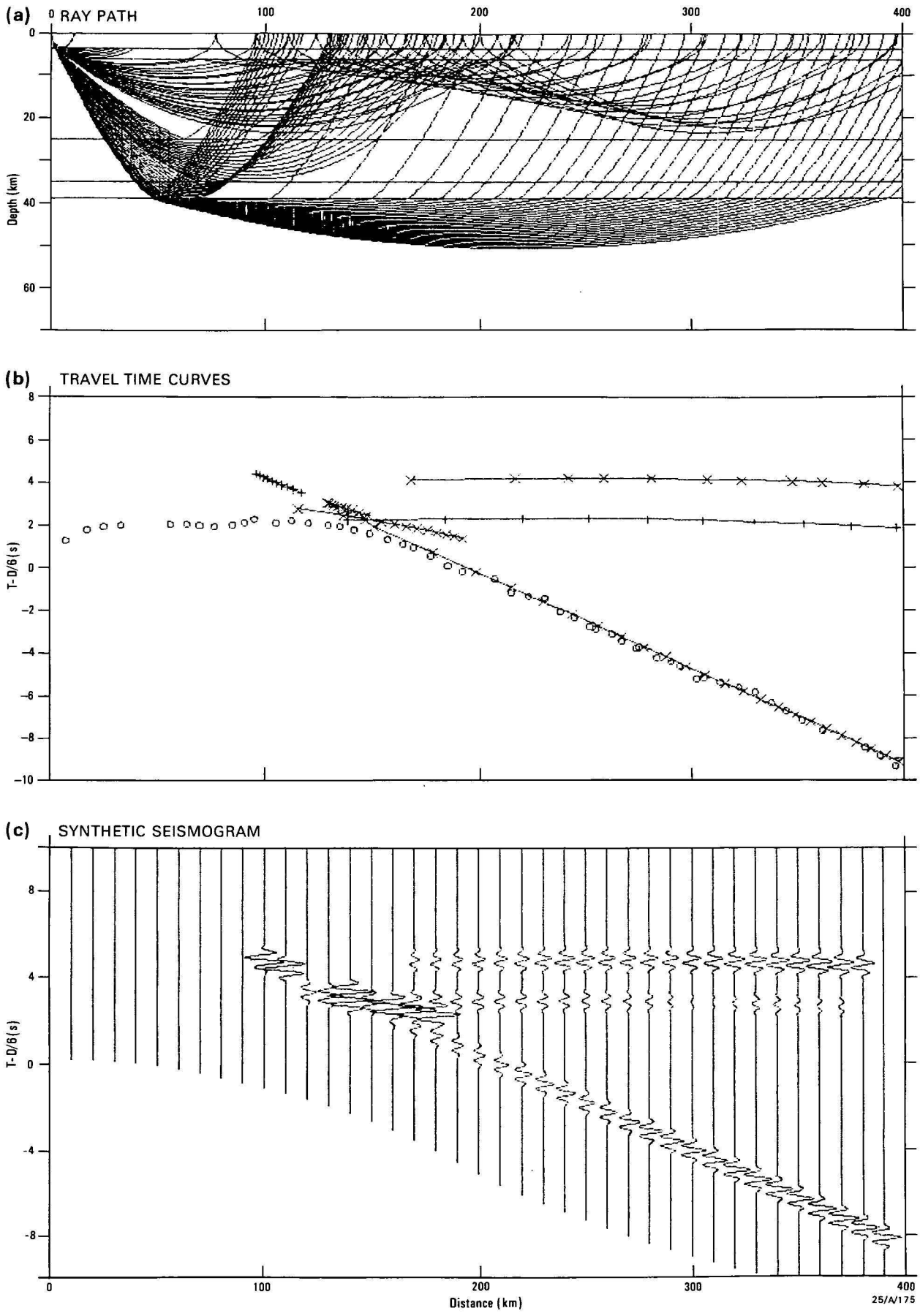

Figure 4. Example of seismic modelling using RAYAL/RAYAMP through a simple velocity model based on Blackall and Barcaldine data: a) ray paths through the model for Pn, PmP, Pg′, Pg″ and P-bar phases; b) travel-time curves; c) amplitudes, normalised for distance (D) by a factor 1/D.

Adavale–Blackall

The shotpoint near Adavale, in the centre of the recording line, serves to define the upper crustal structure within the main part of the Adavale Basin. One-dimensional velocity/depth models for the region have been derived already by Finlayson (1983), and these served as a starting point for the two- dimensional models that include Devonian basin structure.

The record section for the 150 km between Adavale and Blackall and the interpreted seismic phases are shown in Figure 5. For clarity of presentation, the traces on record sections in this paper have been normalised to have equal maximum amplitude. The majority of records have been filtered in the bandpass 4–14 Hz. The travel-time curves for the seismic phases derived from the preferred velocity model are also shown.

The velocity structure and gradients in the sedimentary sequence are well constrained by the P, PP, and PPP phases, any travel-time errors being evident from the multiple path lengths and corrected. Below the Devonian sediments, there is, what is termed here, a transition zone to basement rocks. It is identified with continuing velocity gradients below the depth of identified reflectors on the continuous profiling

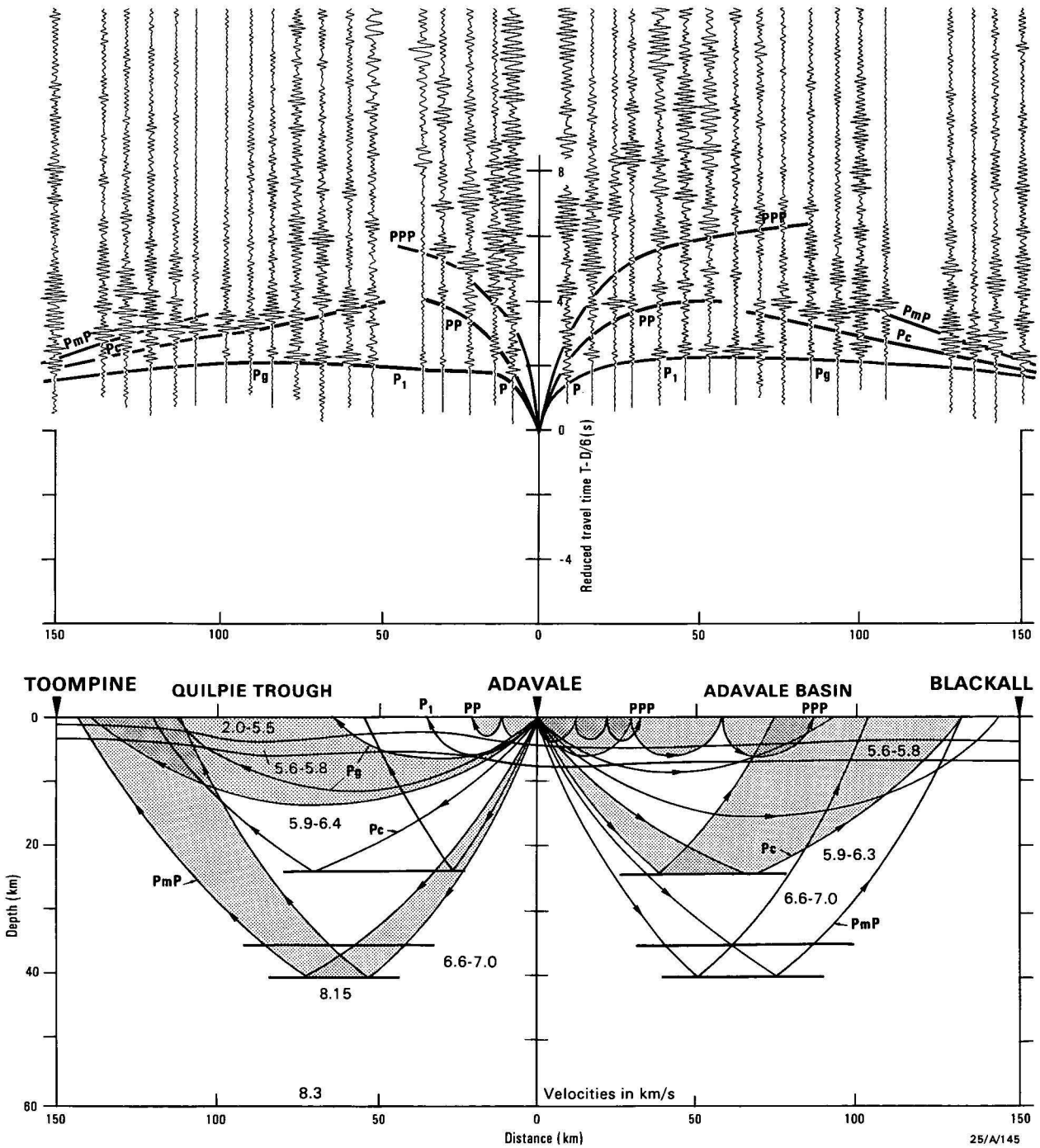

Figure 5. a) Seismic record sections for shots fired at Adavale and recorded south to Toompine and north to Blackall, together with travel-time curves for ray paths shown in Fig. 5b. b) Seismic ray paths and velocity models derived using recordings made north and south of the Adavale shotpoint.

(CDP) records. The velocity gradient (0.07 km/s/km) is less than that encountered in the sedimentary sequences (average 0.77 km/s/km), but greater than that within basement, here identified as having a velocity greater than 5.9 km/s. The geological interpretation of the transition zone is considered later in this paper.

The Pg phase is identified clearly as a prominent first arrival out to 150 km from Blackall. The amplitude of this event suggests that a velocity gradient exists within the upper crustal basement so that refracted energy continues to be returned to the surface at larger distances. The velocity is in the range 5.9-6.3 km/s (gradient 0.02 km/s/km).

The most prominent phase after Pg at distances beyond 60 km is the Pc phase identified with reflected energy from a boundary at 24-25 km depth, here termed the mid-crustal velocity horizon. The data are consistent with a velocity increase from about 6.3 km/s to 6.6-6.7 km/s across this horizon, which has been described by Finlayson (1983). This horizon is interpreted here as being the boundary between the upper and lower crust.

Arriving later than the Pc phase, the PmP reflected energy is observed beyond 80 km from the shot point and interpreted as being from a crust/mantle boundary at a depth of 39-40 km. The velocity gradient within the lower crust and velocity contrast across the Moho are better determined from observations at greater distances, described later in this paper. It will be shown later that the transition to the upper mantle extends over a depth range of about 4 km.

Adavale–Toompine

South from Adavale towards Toompine, the recording line crosses the Quilpie Trough and goes on to the Thargomindah Shelf. There is a basement high between the shot point and the Quilpie Trough. The prominent seismic phases seen on the record section (Fig. 5) are P, PP, P_1, Pg, Pc, and, to a lesser extent, PmP.

The velocity within the transition zone ranges from 5.6 to 5.8 km/s. The velocity within basement ranges between 5.9 and 6.3-6.4 km/s between depths of 6.5-8.0 km and 24.0-24.5 km respectively. The mid-crustal velocity horizon is evident from the prominent Pc phases seen at distances between 60 and 150 km. The velocities above and below this horizon are 6.3-6.4 km/s and 6.6-6.7 km/s respectively. At distances beyond 100 km the PmP phase is only poorly recorded and does not effectively constrain the velocity model.

Blackall–Toompine

Recordings of shots fired at Blackall were made out to 300 km and, therefore, the Pn phase through the upper mantle can be clearly identified as well as P-bar phases and Pg' phases through the upper and lower crust respectively. Figure 6 shows the principal phases identified on the record section, and illustrates the ray paths through the preferred seismic model, together with the travel-time curves for these seismic phases.

The model structure midway between Blackall and Toompine is constrained by the interpretations of data recorded north and south of Adavale, discussed above. Beneath the sediments a transition zone is interpreted to a depth of 6.6 km, below which basement velocities are observed. The mid-crustal velocity horizon is interpreted at 24.0 km.

Below the crust/mantle boundary the velocity increases to 8.15 km/s (after spherical earth corrections have been applied). Initially, the crust/mantle boundary was modelled as a first-order velocity increase at 36 km depth. This, however, would produce large amplitude PmP phases, which are not observed in practice. The preferred model incorporates a crust/mantle transition zone over the depth range 35-39 km, below which the upper mantle velocity is reached (Table 1). This interpretation is in accord with the cross-traverse interpretation of Finlayson & others (1984) and the two-way time of the base of the lower crustal reflection zone determined from seismic profiling (about 14.0 s), discussed later in this paper. The deviations of the Pn arrivals from a linear fit are accounted for by the sedimentary structure in and around the Quilpie Trough.

Table 1. Seismic velocity/depth values at shotpoints 1—Thargomindah, 2—Toompine, 3—Adavale, 4—Blackall, 5—Barcaldine.

1		2		3		4		5	
0.0	2.0	0.0	2.0	0.0	2.1	0.0	2.0	0.0	2.0
1.5	5.5	1.5	4.8	4.7	5.5	3.6	5.5	3.6	5.5
1.6	5.6	1.6	4.9	4.8	5.6	3.7	5.6	3.7	5.6
3.2	5.85	3.2	5.85	7.7	5.8	6.6	5.85	6.6	5.85
3.3	5.9	3.3	5.9	7.8	5.9	6.7	5.95	6.7	5.9
25.0	6.3	29.0	6.45	24.3	6.3	24.0	6.3	24.0	6.3
25.1	6.6	29.1	6.5	24.4	6.6	24.1	6.6	24.1	6.6
35.0	7.0	35.0	6.9	35.5	7.0	35.0	7.0	35.0	7.0
35.1	7.1	35.1	7.0	35.6	7.1	35.1	7.1	35.1	7.1
39.0	7.8	39.0	7.8	39.5	7.8	39.0	7.8	38.0	7.9
39.1	8.15	39.1	8.15	39.6	8.15	39.1	8.15	38.1	8.15
70.0	8.35	70.0	8.35	70.0	8.35	70.0	8.35	70.0	8.35

Barcaldine–Toompine

A shot near Barcaldine (Fig. 1) was recorded between Adavale and Toompine at distances between 250 and 410 km. The first arrivals are the Pn phase from beneath a crust/mantle transition zone in the depth range 35-40 km, below which the upper mantle velocity is reached. As with the Pn data from Blackall shots, travel-time variations are modelled using the known sediment thickness variations in and around the Quilpie Trough (Fig. 7).

The other seismic phase clearly evident in Figure 7 is the P-bar phase, which has an apparent velocity of 6-7 km/s. The travel-times of these and later seismic arrivals can be modelled successfully by seismic energy traversing the upper and lower crust as refracted waves and being reflected at a depths no greater than the base of the transition zone. Reflections at the surface produce the arrivals at later travel-times and explain the considerable energy at reduced times of 2-7 s (Fig. 7). These arrivals place strong constraints on the velocity gradients in the upper and lower crust and add weight to interpreted velocity structure determined using other seismic phases.

Toompine–Blackall

The seismic record section for shots fired at Toompine is shown in Figure 8 together with an indication of the seismic phases used in the interpretation. The travel-times of P1 and Pg phases are influenced by the Quilpie Trough structure. Near-surface velocities range from 2.0 km/s at the surface to 4.8 km/s at 1.5 km depth. Below this the velocity increases from 4.9 km/s to 5.35 km/s at 3.2 km depth (the transition zone). Basement velocities above 5.9 km/s are observed below this. Multiple refractions are observed about 1 s after the first arrivals out to 50 km. These place quite severe constraints on the velocity gradients within the upper 7 km.

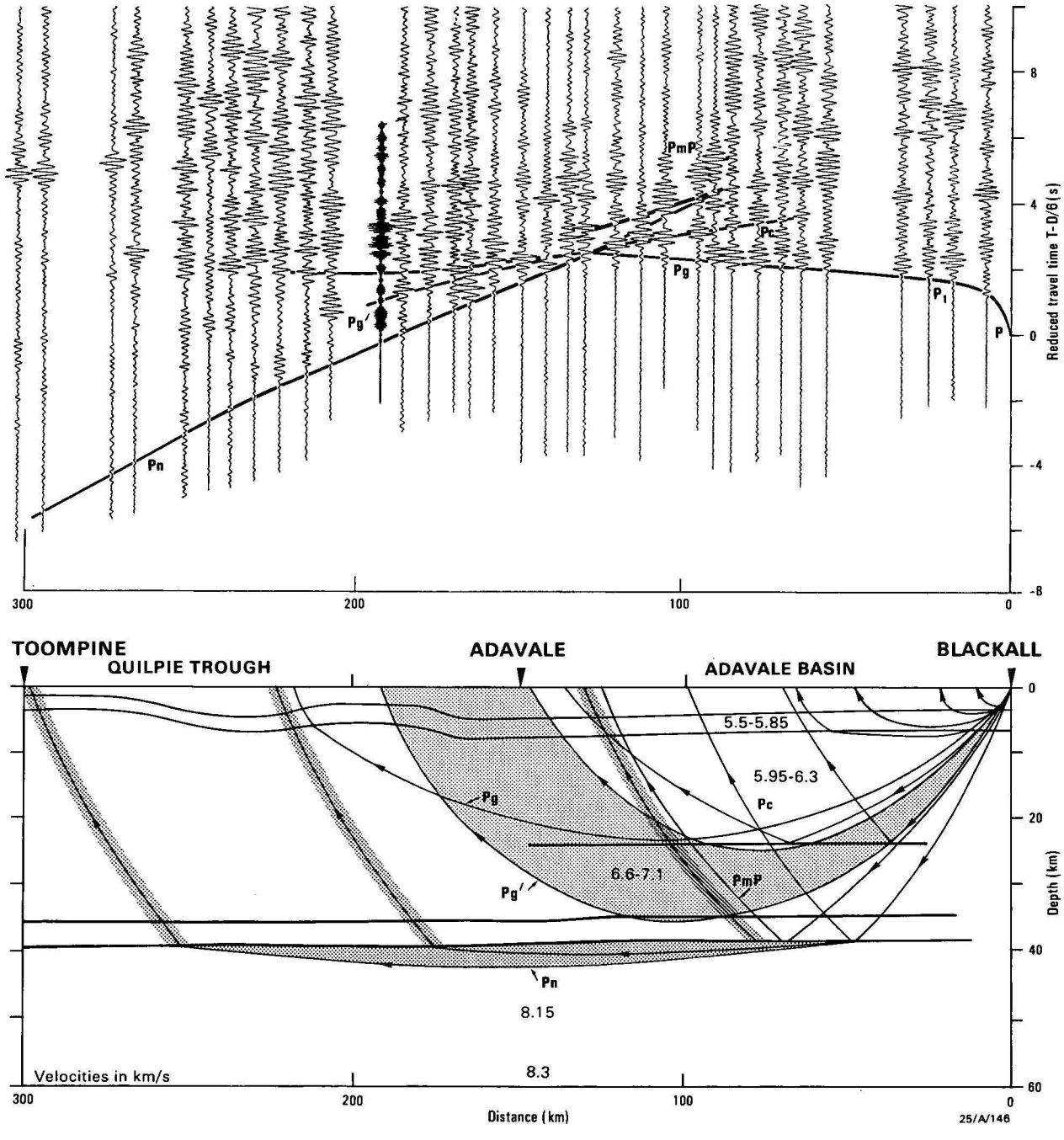

Figure 6. a) Seismic record section for shots fired at Blackall and recorded south to Toompine, together with travel-time curves for the ray paths shown in Fig. 6b. b) Seismic ray paths and velocity model derived using recordings of shots at Blackall.

In the distance range 90-150 km the first arrivals are smaller in amplitude compared with the secondary arrivals (Fig. 8). The second arrivals are interpreted as being super critical reflections from a horizon at depths of about 29 km. This depth is greater than that for the mid-crustal velocity horizon interpreted from the Adavale shots and may be associated with Canaway Ridge crustal structures described by Finlayson & others (1984).

Beyond 160 km the first arrivals are refracted waves through the upper mantle (Pn). A notable feature of these arrivals is the delayed arrivals in the range 180-200 km and the high apparent velocity beyond (about 8.5 km/s). Various velocity models were tried to account for this feature, consistent with data from other shot points. It is concluded that this feature is caused by the change in direction of the recording line north of Adavale (Fig. 1), causing ray paths to traverse progressively deeper parts of the Adavale Basin. These ray paths are different from those of the Blackall and Barcaldine shots. Hence the apparent inconsistency in basin depth between Figures 6 and 8.

The preferred model in Figure 8 has a 9 km sedimentary sequence in the deepest part of the basin, slightly deeper than the 8.5 km from BMR reflection profiling (Passmore & Sexton, 1984).

Arriving after the Pn phase are prominent Pg' arrivals. The waves are modelled with a velocity in the lower crust of 6.7 to 6.8-6.9 km/s in the depth range 25-35 km. Stronger

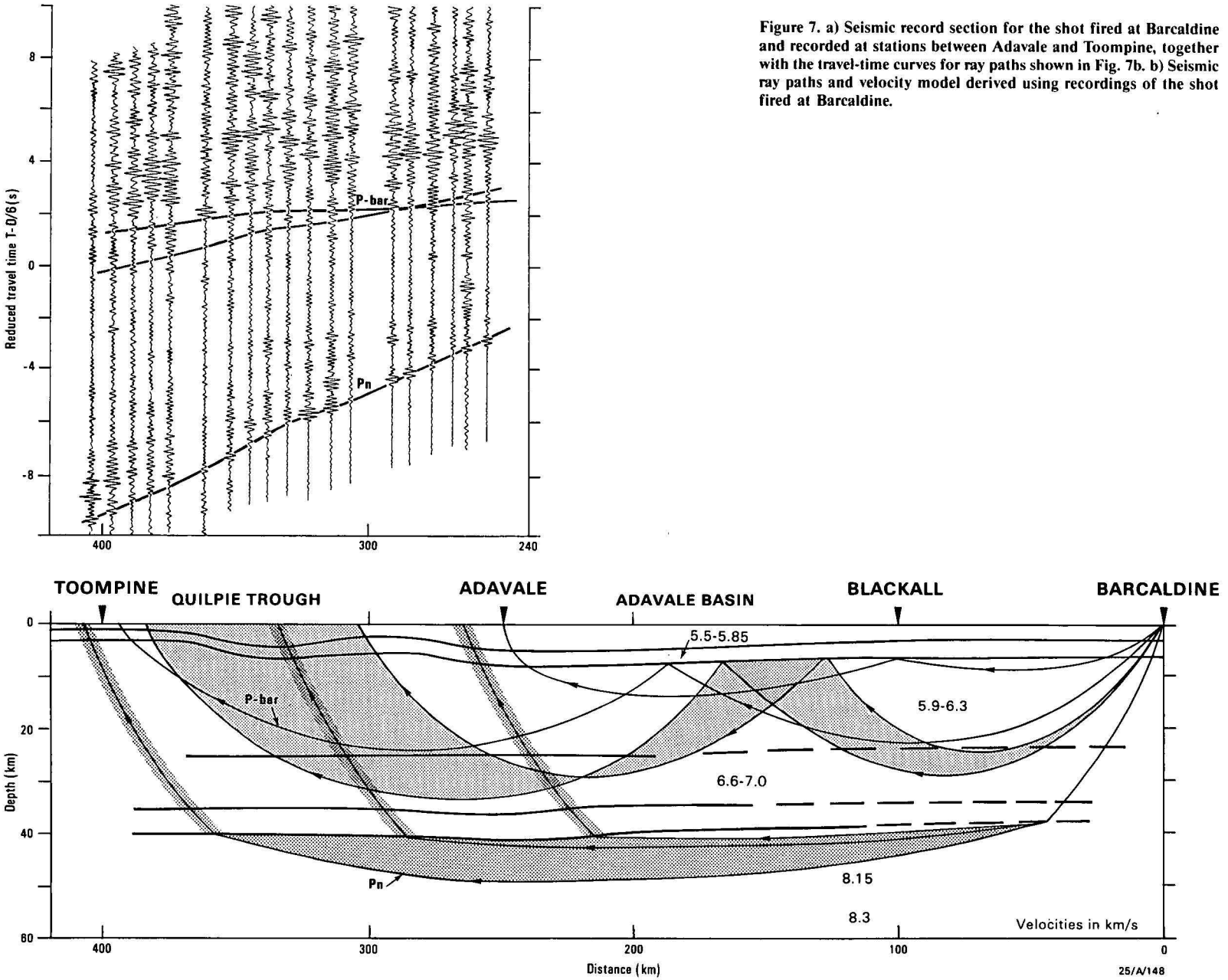

Figure 7. a) Seismic record section for the shot fired at Barcaldine and recorded at stations between Adavale and Toompine, together with the travel-time curves for ray paths shown in Fig. 7b. b) Seismic ray paths and velocity model derived using recordings of the shot fired at Barcaldine.

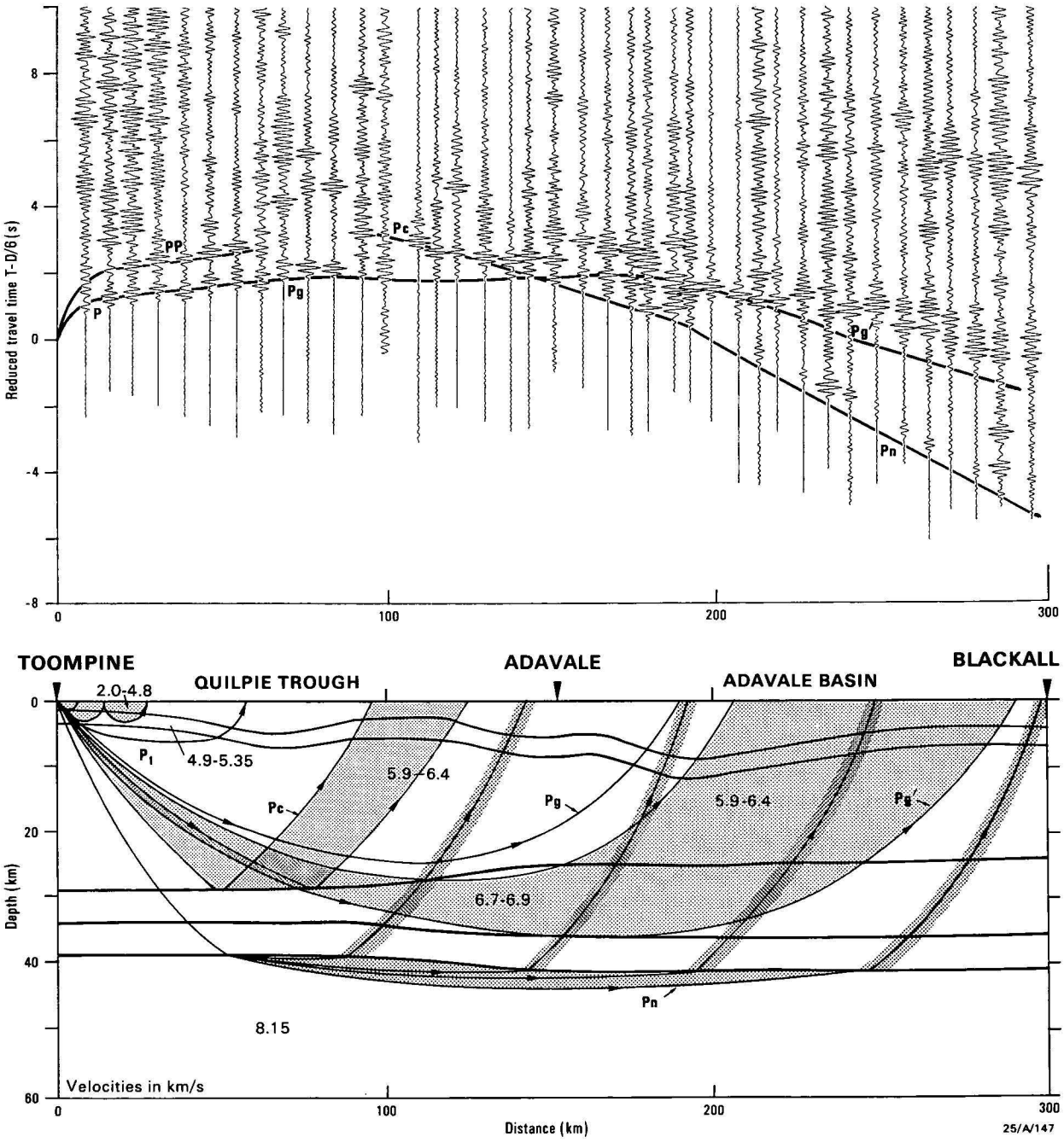

Figure 8. a) Seismic record section for the shots fired at Toompine and recorded northward towards Blackall, together with travel-time curves for ray paths shown in Fig. 8b. b) Seismic ray-paths and velocity model derived using recordings of the shots at Toompine.

gradients do not allow energy to be refracted to the observed distances of about 300 km. Below this is the transition to the upper mantle at a depth of 39-40 km, interpreted from the Pn arrivals. As with the reverse profile from Blackall, the PmP phase is not strongly recorded, further emphasising the interpretation of a velocity gradient at the crust/mantle interface.

Thargomindah–Blackall

The shot at Thargomindah, 100 km south of Toompine (Fig. 1), was recorded between Adavale and Blackall at distances of 250-400 km. The first arrivals in this distance range were of the Pn phase (Fig. 9). The late Pn arrivals in the distance range 280-300 km correspond well with the interpretation of late Pn arrivals from the Toompine shot, namely, being due to a 9 km sedimentary sequence in the main depression of the Adavale Basin.

The P-bar arrivals at 2-6 s reduced travel-time are interpreted, as with similar arrivals from the shot at Barcaldine, as energy multiply refracted through the upper and lower crust and reflected from interfaces at various depths from the surface down to the bottom of the transition zone above basement.

Adavale Basin deep structure

The major features of the crustal velocity structure of the Adavale Basin are summarised in Figure 10. The velocity/depth profiles are derived from the 2-dimensional

Figure 9. a) Seismic record section for the shot fired at Thargomindah and recorded between Adavale and Blackall, together with the travel-time curves for ray paths shown in Fig. 9b. b) Seismic ray paths and velocity model derived using recordings of the shot fired at Thargomindah.

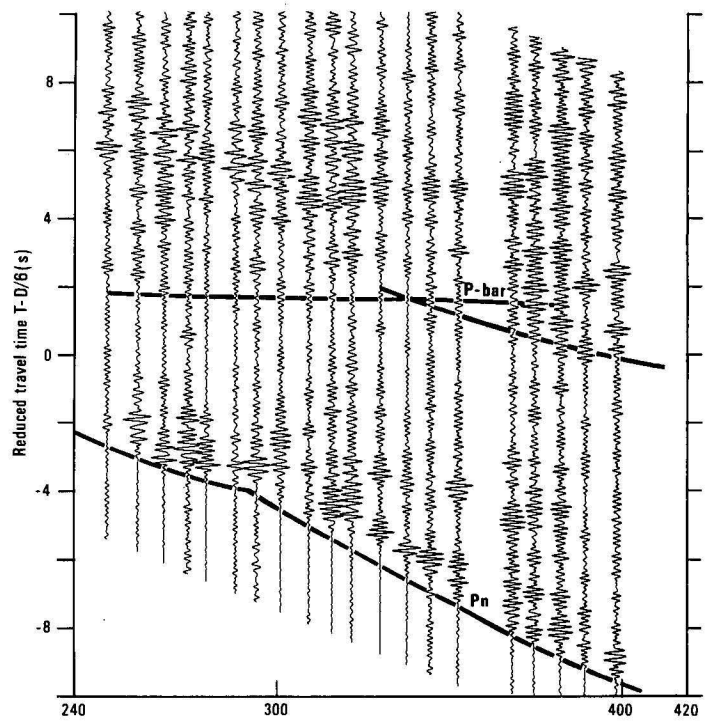

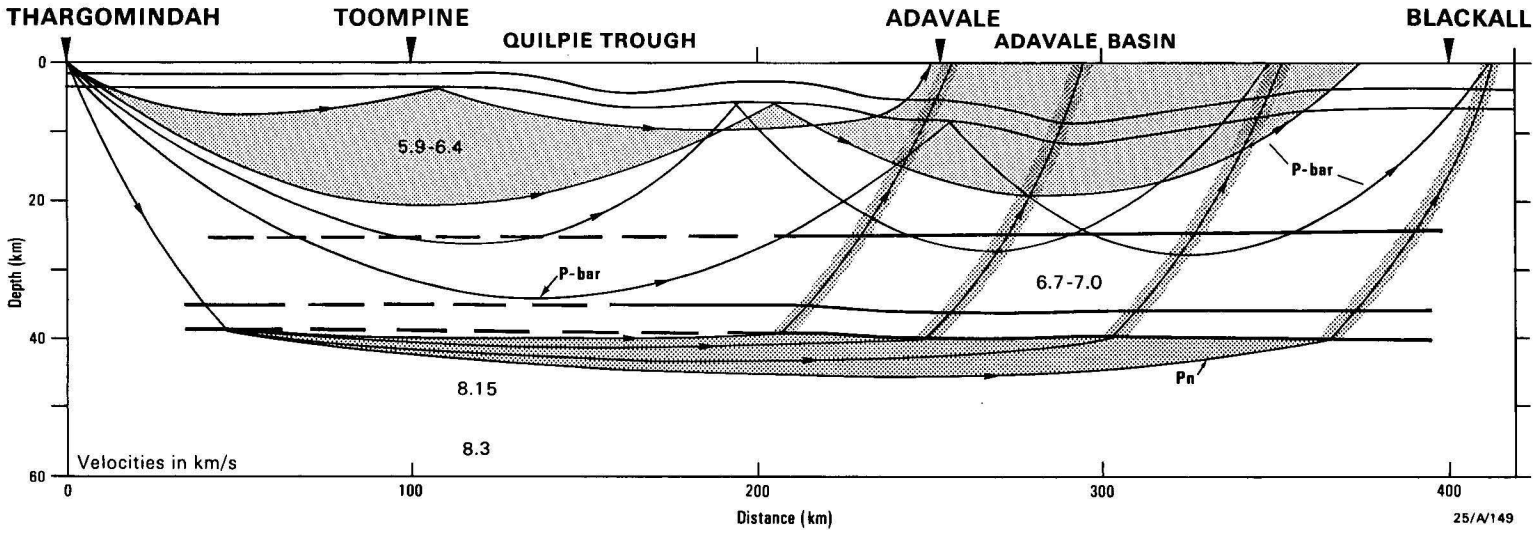

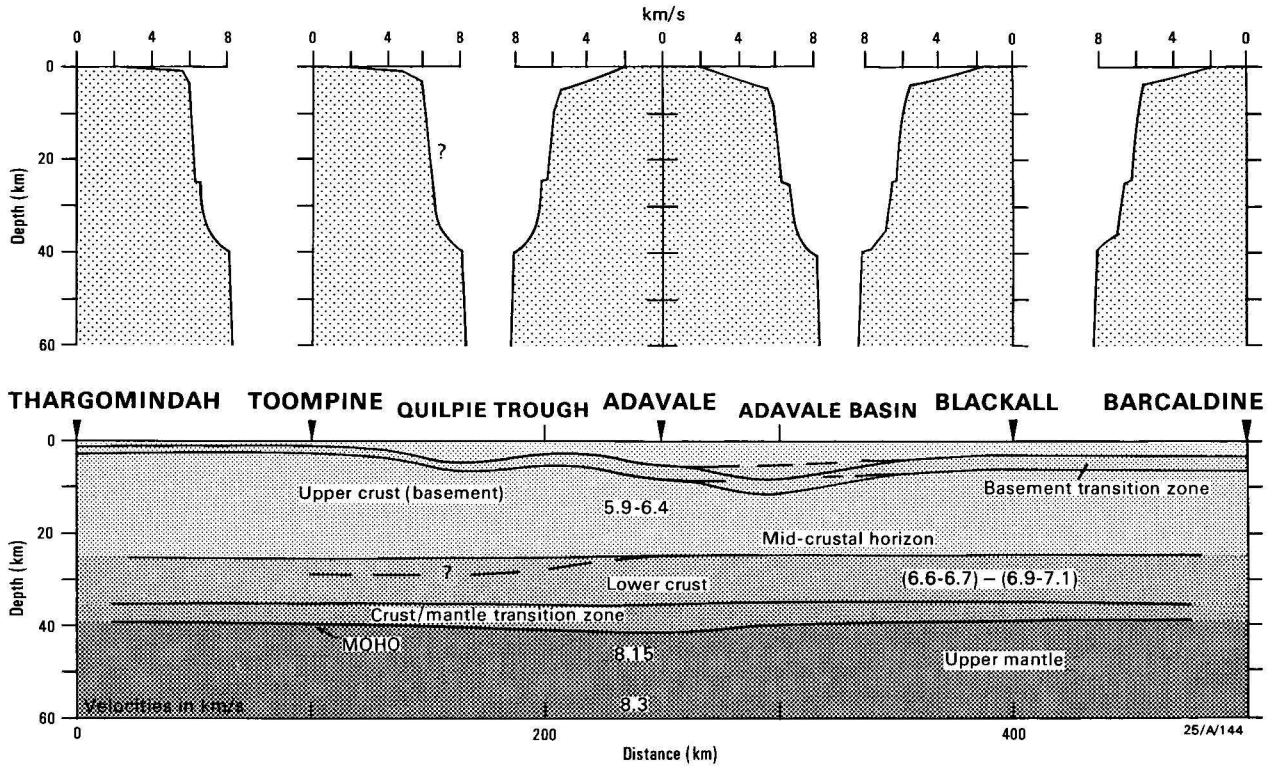

Figure 10. a) Velocity/depth profiles appropriate for the five shot locations between Thargomindah and Barcaldine. b) Crustal-upper mantle velocity model for the traverse across the Adavale Basin from Thagomindah to Barcaldine.

seismic modelling and have a spherical earth correction applied. The velocity/depth values are listed in Table 1.

The major lateral variations in velocity structure are above the mid-crustal velocity horizon. The morphology of the basin sediments and basement transition zone below is a major contributor to variations in the travel-time curves. The transition zone is a feature of the region as a whole. Lock & Collins (1983) and Collins & Lock (1983) have discussed the evidence for this zone based on detailed shallow refraction work. Their velocity gradients in the Eromanga Basin sedimentary section identified from reflection profiling were typically 1.2-1.4 km/s/km. Within the underlying Devonian sediments the gradient is typically about 0.4 km/s/km, and within the transition zone it is about 0.1-0.3 km/s/km. From the data interpreted in this paper the velocity gradient in the basement transition zone is typically about 0.1 km/s/km. Within basement the velocity gradient decreases considerably to about 0.02-0.03 km/s/ km with velocities between about 5.9 and 6.4 km/s over the depth range 4-8 to 24-25 km.

The geological nature of the basement is difficult to determine uniquely. There are very few reflections evident on continuous profiling records from below the Devonian sequences at two-way times of 2-8 s (Mathur, 1983), indicating that the geological structure is either very uniform (plutonic rock?) or that it consists of rocks that are sheared, folded, and faulted at high angles so that they are transparent to reflection profiling methods. Spence & Finlayson (1983), using magnetotelluric data, have drawn attention to intermediate conductivity rock (1000-2000 ohm-m) to depths of at least 20 km, underlying the high conductivity sedimentary sequence. Their interpretation favoured a sheared, folded, and faulted zone into which water could penetrate, as opposed to a uniform plutonic upper crust. This is in accord with the few drill holes that have penetrated basement into low-grade metasediments, volcanics, and plutonic rocks.

The conductivity, seismic reflections, and seismic velocity gradient data are consistent with the basement consisting of highly deformed, folded, and sheared rocks. It seems likely that the transition zone represents a 2-3 km gradual change in metamorphic grade or a thick weathered layer in pre-Devonian rocks.

The upper crustal basement with velocity of 5.9-6.4 km/s is indistinguishable from upper continental crust of many other regions. If there is a notable characteristic of the upper crustal basement it is the consistency of the velocity gradient that produces the well-developed P-bar phases both along the traverse interpreted in this paper and on the east—west traverse described by Finlayson & others (1984). The P-bar phases in some other Australian regions, e.g. McArthur Basin (Collins, 1983), are not well developed, but there is evidence for such phases in the Lachlan Fold Belt (Finlayson & others, 1979).

The upper crustal basement extends to 24-25 km depth, where there is an increase in seismic velocity identified by the Pc phase. This intra-crustal velocity horizon is a prominent feature of the region (Finlayson, 1983; Finlayson & others, 1984) and coincides with the top of a zone of lower crustal reflections (Mathur, 1983). Figure 11 illustrates the characteristics of deep crustal reflections near Adavale along a north-south reflection profiling line coincident with the refraction/wide-angle reflection traverse. On this particular traverse the reflection zone is at 7-14 s two-way time. Reflection segments are continuous over distances of 2-3 km (exceptionally 6 km). The velocity in the lower crust from the refraction recording ranges from 6.6-6.7 km/s at 24-25 km depth to 6.8-7.1 km/s at 35-36 km depth, below which there is a velocity gradient to the upper mantle velocity of 8.15 km/s at 38-40 km depth. The marked section (Fig. 11) indicates the two-way times of the horizons determined from the refraction interpretation.

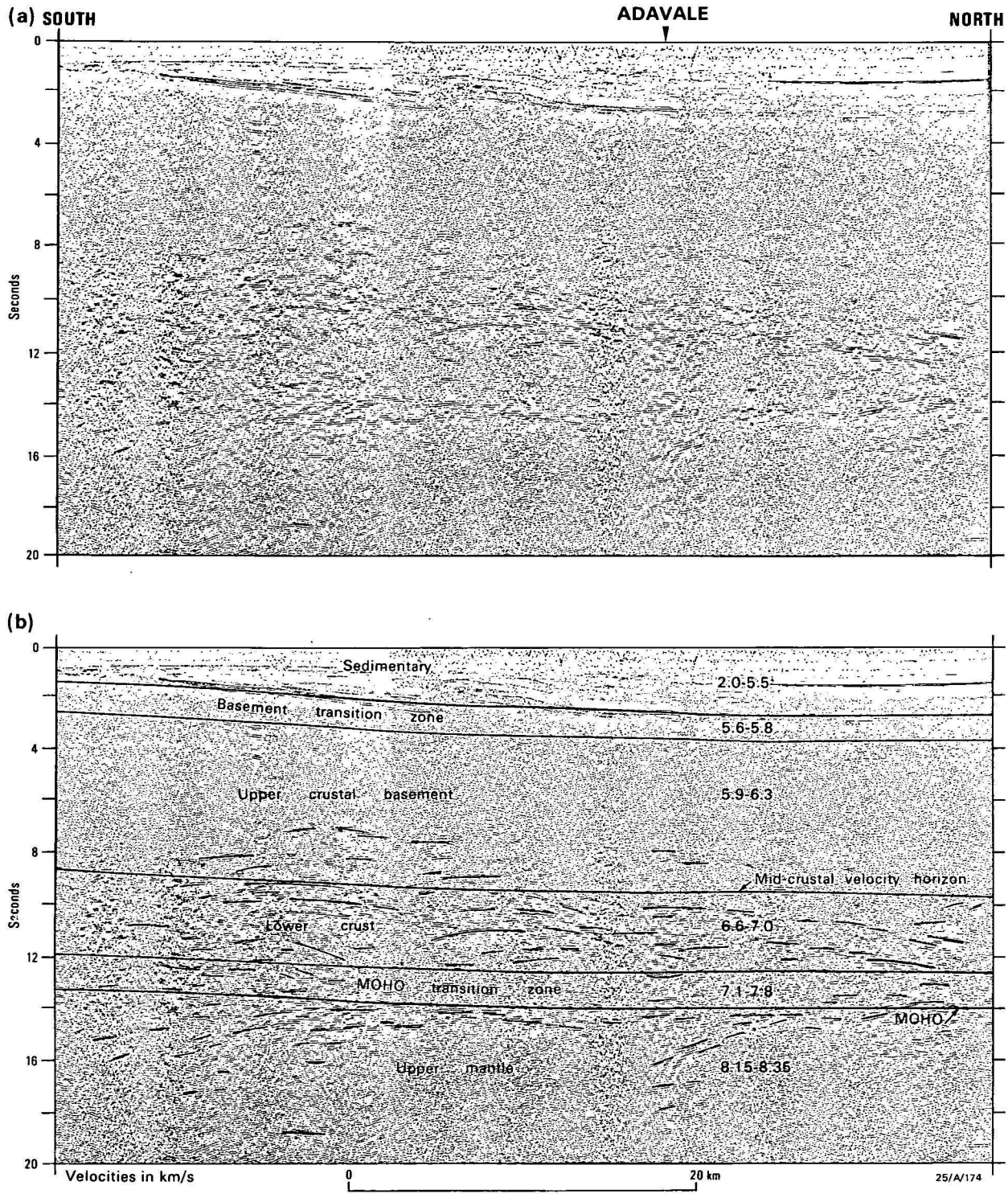

Figure 11. BMR deep reflection record section in the vicinity of the Adavale shot point; a) unmarked section, 6-fold CDP with time-varying filter and coherency scaling after stack; b) section marked with prominent events and the velocity boundaries derived from the wide-angle reflection/refraction profiling.

The ubiquitous reflections in the lower crust and the mid-crustal velocity horizon strongly suggest that different processes predominated in the formation of the upper and lower crust. The present temperature in the lower crust is 600-700°C (Cull & Conley, 1983) and during orogenic episodes there must have been higher average temperature and magmatic activity. If shearing/ faulting in the cooler, brittle upper crust is not evident, it seems likely that lower crustal reflections result, not from faulting and shearing, but from magmatic activity and ductile flow in the lower crust on a massive scale. This need not be an exclusive process and does not preclude metamorphic effects caused by deep burial of near-surface rocks at convergent plate boundaries. Such processes could quite easily cause felsic-mafic layering, seen in deep seismic profiling records as discontinuous sub-horizontal reflections. Magmatic activity involving the mantle

could also cause a mass excess in the crust, which would contribute to isostatic readjustments during later episodes of elevated lithospheric temperature.

Below the crust/mantle transition zone, the P-wave velocity increases to 8.15 km/s. There is, therefore, no observable difference in upper mantle velocity from the east-west value determined by Finlayson & others (1984). However, in the data interpreted in this paper through the Adavale Basin there is no conclusive evidence for energy arriving at velocities higher than 8.15 km/s from a horizon deeper in the mantle, as interpreted by Finlayson & others (1984). A velocity gradient of less than 0.01 km/s/km is interpreted in the upper mantle under the Adavale Basin. At two-way times greater than 14 s on the deep profiling records (Fig. 11) there are few, if any, reflection events that cannot be interpreted as diffractions. Hence, a homogeneous character can be attributed to the upper mantle at seismic wavelengths of about 2 km or less. This does not preclude broad-scale geochemical zonation with increasing depth, which would not be seen by profiling methods unless some major impedance contrast was maintained by structure, as, for example, within the upper mantle north of Scotland (Brewer & others, 1983).

Comment

The principal features of the deep structure in the lithosphere under the Adavale Basin are similar to those determined from an east-west traverse in the same region, interpreted by Finlayson & others (1984). The main lateral velocity variations are contained in the upper crust and the deepest part of the Devonian basin is identified at 8-9 km depth in the main depression, adjacent to the Pleasant Creek Arch. The velocity gradients in the upper crust, taken together with the conductivity interpretation of Spence & Finlayson (1983) and the character of deep reflection profiling records, suggest that the pre- Devonian crust was quasi-continental in nature. The geological record suggests that the upper crust, at least, consists of tightly folded, faulted, and sheared metasediments, volcanics, and plutonic rocks, the product of major compressional events.

Further deformation during the Carboniferous, contemporaneous with the Kanimblan Orogeny in the Lachlan Fold Belt and possibly accompanied by basin-wide compression and/or transcurrent movement, resulted in the current morphology of basement to the Devonian sediments. Powell (1984) has suggested this event was the result of 100-150 km of crustal shortening throughout central and eastern Australia with associated transcurrent movements.

The velocity range (6.7-7.1 km/s), the character of deep reflections in the lower crust, and the series of sedimentary episodes suggest that a quasi-continental crust has been modified by an intrusive process originating in the mantle. Finlayson & Mathur (1984) have pointed out that the crust is thicker under the outcropping igneous, metamorphic, and fold belt provinces than under the intracratonic basins, and attribute this to underplating during episodes of high thermal flux from the mantle. It seems probable that a similar process applied to the early Palaeozoic quasi-continental crust of the Adavale region, resulting in a crust about 40 km thick.

The tectonic processes prevailing up to the Carboniferous seem to have been compressional and, possibly, trancurrent events with intrusion or underplating operating in the lower crust. However, the mechanism of the episode that led to the Devonian sedimentary deposition is still not clear. The later Permo-Triassic and Cretaceous events that led to the Cooper-Galilee and Eromanga sequences appear to have resulted from simple depression of the whole Adavale region, owing to mild compression or isostatic response to a mass excess, or both, during episodes of high geothermal flux. Shallow seismic profiling data have not yet revealed convincing evidence for crustal extension (Wake-Dyster & others, 1983). The Eromanga Basin and its infrabasins differ from current models of, for example, the North Sea Basin, which include thin crust (20-30 km), listric faulting, and lack a mid-crustal velocity horizon (Barton & Wood, 1984, Ziegler, 1982).

There are, however, some similarities with basins on the edge of Precambrian cratons in North America, e.g. Mississippi Embayment (Mooney & others, 1983), Williston Basin (Hajnal & others, 1984), which have thick crust (38-40 km and 38-50 km respectively) and prominent intracrustal velocity horizons. In the Keweenawan Rift in North America, Serpa & others (1984) described the character of deep reflections from COCORP seismic profiling in terms very similar to those used in this paper for the Eromanga Basin. They indicated that a boundary deep within basement 'separates an overlying section containing relatively few continuous or strong seismic events from an underlying zone of numerous reflections and diffractions.' The transparent character of the upper crust is attributed to highly deformed rocks and intrusive complexes. The lower crustal events are attributed by Brown & others (1983) to gneissic banding, interlayering of granite and restites related to anatexis, mafic intrusions, and the juxtaposition of amphibolites and granulites derived from both igneous and sedimentary sources. Reflections are rare at two-way times greater than 14-15 s; some events at greater times are attributed to structure within the crust laterally displaced at least 60 km away from the profiling line. However, a detailed comparative study is beyond the scope of this paper and will be the subject of further work.

Acknowledgements

The authors wish to thank all those who took part in field recording, in particular Jo Lock, John Williams, and Jim Whatman, and the BMR crews responsible for drilling and shot loading. Jane Rogers is thanked for data processing assistance, and the diagrams were drafted by Jill Clarke and C. Fitzgerald. Surendra Mathur is thanked for making available the processed seismic profiling record from near Adavale.

References

Barton, P., & Wood, R., 1984 — Tectonic evolution of the North Sea basin: crustal stretching and subsidence. *Geophysical Journal of the Royal Astronomical Society,* 79, 987-1022.

Brewer, J.A, Matthews, D.H., Warner, M.R., Hall, J., Smythe, D.K., & Whittington, R.J., 1983 — BIRPS deep seismic reflection studies of the British Caledonides. *Nature,* 305, 206-210.

Brown, L., Serpa, L., Setzer, T., Oliver, J., Kaufman, S., Lillie, R., Steiner, D., & Steeples, D., 1983 — Intra-crustal complexity in the U.S. midcontinent: preliminary results from COCORP surveys in N.E. Kansas. *Geology,* 11, 25-30.

Cerveny, V., 1979 — Ray theoretical seismograms for laterally inhomogeneous structures. *Journal of Geophysics,* 46, 335-342.

Collins, C.D.N., 1983 — Crustal structure of the southern McArthur Basin, northern Australia, from deep seismic sounding. *BMR Journal of Australian Geology & Geophysics,* 8, 19-34.

Collins, C.D.N., & Lock, J., 1983 — A seismic refraction study of the Quilpie Trough and adjacent basement highs, Eromanga Basin, eastern Australia. *Tectonophysics,* 100, 185-198.

Cull, J.P., & Conley, D., 1983 — Geothermal gradients and heat flow in Australian sedimentary basins. *BMR Journal of Australian Geology & Geophysics,* 8, 329-337.

Finlayson, D.M., 1983 — The mid-crustal horizon under the Eromanga Basin, eastern Australia. *Tectonophysics,* 100, 199-214.

Finlayson, D.M., Prodehl, C., & Collins, C.D.N., 1979 — Explosion seismic profiles, and implications for crustal evolution, in southeastern Australia. *BMR Journal of Australian Geology & Geophysics,* 4, 243-252.

Finlayson, D.M., & Collins, C.D.N., 1980 — A brief description of BMR portable seismic tape recording systems. *Bulletin of the Australian Society of Exploration Geophysicists,* 11, 75-77.

Finlayson, D.M., Collins, C.D.N., & Lock, J., 1984 — P-wave velocity features of the lithosphere under the Eromanga Basin, eastern Australia, including a prominent mid-crustal (Conrad?) discontinuity. *Tectonophysics,* 101, 267-291.

Finlayson, D.M., & Mathur, S.P., 1984 — Seismic refraction and reflection features of the lithosphere in northern and eastern Australia, and continental growth. *Annales Geophysicae,* 2(6), 711-722.

Hajnal, Z., Fowler, C.M.R, Mereu, R.F., Kanasewich, E.R., Cumming, G.L., Green, A.G., & Mair, A., 1984 — An initial analysis of the earth's crust under the Williston Basin: 1979 COCRUST experiment. *Journal of Geophysical Research,* 89, 9381-9400.

Liu, Y.S.B. & Seers, K.J., 1982 — A playback system for portable seismic recorders. *Bulletin of the Australian Society of Exploration Geophysicists,* 13, 77-81.

Lock, J., & Collins, C.D.N., 1983 — Velocity/depth modelling using reflection and refraction data recorded in the central Eromanga Basin, Queensland, Australia. *Tectonophysics,* 100, 175-184.

Mathur, S.P., 1983 — Deep crustal reflection results from the central Eromanga Basin, Australia. *Tectonophysics,* 100, 163-173.

McMechan, G.A., & Mooney, W.D., 1980 — Asymptotic ray theory and synthetic seismograms for lateral varying structures: theory and application to the Imperial Valley, California. *Bulletin of the Seismological Society of America,* 70, 2021-2035.

Mooney, W.D., Andrews, M.C., Ginzburg, A., Peters, D.A., & Hamilton, R.M., 1983 — Crustal structure of the northern Mississippi Embayment and a comparison with other continental rift zones. *Tectonophysics,* 94, 327-348.

Murray, C.G., & Kirkegaard, A.G., 1978 — The Thomson Orogen of the Tasman Orogenic Zone. *Tectonophysics,* 48, 299-325.

Passmore, V.L., & Sexton, M.J., 1984 — The structural development and hydrocarbon potential of Palaeozoic source rocks in the Adavale Basin region. *APEA Journal,* 24(1), 393-411.

Powell, C.McA., 1984 — Terminal fold-belt deformation: relationship of mid- Carboniferous megakinks in the Tasman fold belt to coeval thrusts in cratonic Australia. *Geology,* 12, 546-549.

Serpa, L., Setzer, T., Farmer, H., Brown, L., Oliver, J., Kaufman, S., & Sharp, J., 1984 — Structure of the southern Keweenawan Rift from COCORP surveys across the Midcontinental Geophysical Anomaly in northern Kansas. *Tectonics,* 3, 367-384.

Spence, A.G., & Finlayson, D.M., 1983 — The resistivity structure of the crust and upper mantle in the central Eromanga Basin, Queensland using magnetotelluric techniques. *Journal of the Geological Society of Australia,* 30, 1-16.

Veevers, J.J., Jones, J.G., & Powell, C.McA., 1982 — Tectonic framework of Australia's sedimentary basins. *APEA Journal,* 22, 283-300.

Wake-Dyster, K.D., Moss, F.J., & Sexton, M.J., 1983 — New seismic reflection results in the central Eromanga Basin, Queensland: the key to understanding its tectonic evolution. *Tectonophysics,* 100, 147-162.

Ziegler, P.A., 1982 — Thoughts on mechanisms of basin subsidence *In* Ziegler, P.A., (editor), Geological atlas of western and centra Europe. *Shell International Petroleum & Elsevier,* 100-106.

BMR Journal of Australian Geology & Geophysics, 10, 39-51 ©Commonwealth of Australia 1986

Geology and offshore petroleum prospects of the eastern New Ireland Basin, northeastern Papua New Guinea

N.F. Exon[1], W.D. Stewart[2], M.J. Sandy[2] & D.L. Tiffin[3]

The eastern part of the New Ireland Basin of Papua New Guinea is about 600 km long by 150 km wide and mostly offshore, northeast of New Hanover and New Ireland. Basin geology and petroleum prospects have been interpreted from onshore geology integrated with offshore seismic reflection data and limited geological sampling. Most of the basin is a structurally simple downwarp that formed as a fore-arc basin between an Eocene-early Miocene volcanic arc in the southwest and an outer-arc high in the northeast. The basin contains up to 5 km of strata interpreted as early Miocene and possibly Oligocene volcaniclastics, early-late Miocene shelf carbonates, late Miocene and Pliocene bathyal chalks and volcaniclastics, and Pleistocene-Recent sediments ranging from terrestrial conglomerates to hemipelagic oozes. In the east, Plio-Pleistocene volcanism has formed islands and greatly disturbed the older strata. Petroleum prospects offshore appear to be moderate. Early-late Miocene clastic and carbonate source rocks are thought to be present, and presumed reefal bodies may form traps within a thick and deeply buried early-late Miocene platform carbonate sequence, similar to the widespread Lelet Limestone exposed on New Ireland.

Introduction

This paper integrates onshore and offshore geological and geophysical data in the eastern part of the New Ireland Basin in northeastern Papua New Guinea, in order to better comprehend its regional geology and petroleum prospects. The basin is an arcuate feature extending 900 km northwestward from the Feni Islands in the east to Manus Island in the west (Figs 1 & 2). It is bounded by the 6000 m deep Manus-Kilinailau Trench* in the north, and the 2500 m deep Manus Basin in the south. The eastern part of the basin (Fig. 2) is up to 150 km wide and includes both New Ireland and New Hanover.

The basin slopes gently to the northeast, with axial water depths increasing from about 1500 m in the northwest to 3000 m in the southeast. It is truncated in the southwest by a series of major southeast-trending onshore and offshore faults with overall vertical displacement of more than 2000 m (e.g. Connelly, 1976); these are related to the Pliocene-Recent formation of the Manus Basin, a spreading marginal basin (Taylor, 1979).

The New Ireland Basin was shown by Exon & Tiffin (1984) to be a relatively simple downwarp with up to 5 km of Oligocene and younger sedimentary fill. It was a fore-arc basin to the Manus-Kilinailau Trench in Eocene and Oligocene times. Two outer-arc highs to the north, the Emirau-Feni Ridge and the Nuguria Ridge (new names), limit much of the depositional basin. Evidence from Mussau indicates recent uplift of that part of the Emirau-Feni Ridge. Eocene to early Miocene arc volcanics form basement to the basin, and there were further periods of volcanism in the early Miocene, Pliocene, and Pleistocene. The pre-middle Miocene, Pliocene, and younger volcanics of the Tabar to Feni groups of islands (Wallace & others, 1983) have cut through the southeastern part of the basin, destroying its simple structure.

A thick sequence of Miocene reefal carbonates on New Ireland (Hohnen, 1978), and possibly offshore (Exon & Tiffin, 1984) has focussed attention on the petroleum prospects of the New Ireland Basin. The Geological Survey of Papua New Guinea is carrying out detailed stratigraphic studies of the sequence on New Ireland, and a multichannel seismic cruise of the R.V. *S.P. Lee,* carried out in mid 1984 under an Australian, New Zealand, and United States of America aid program for the South Pacific region, under the auspices of CCOP/SOPAC, Suva, will be reported on when fully interpreted.

The present report relies on seismic reflection surveys carried out by the Committee for Coordination of Joint Prospecting for Mineral Resources in South Pacific Offshore Areas (CCOP/SOPAC) (Exon, 1981; Tiffin, 1981), the IFP-CEPM-ORSTOM group (de Broin & others, 1977), and Gulf Research and Development Company (1973), and continues the study started by Exon & Tiffin (1984). The bathymetric map (Fig. 2A) was prepared from all available data, but the structure contour and isopach maps (Figs. 2B & C) are based only on the Gulf lines, of which there are 25 in the area. The assessment of the petroleum potential makes no use of the *S.P. Lee* results.

Because there are no drill holes and few offshore samples in the New Ireland Basin, it is difficult to control our seismic interpretation, which perforce relies heavily on the offshore extrapolation of onshore geology and on seismic reflection character. Drilling on New Ireland, such as that proposed by the Working Group on Island Drilling at the late 1984 CCOP/SOPAC-IOC STAR meeting in Samoa, would resolve many questions related to regional geology and petroleum source and reservoir rocks.

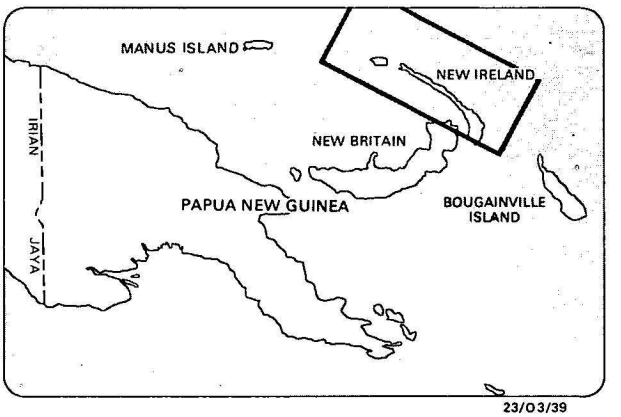

Figure 1. Location of eastern New Ireland Basin.
Boxed area is that studied.

[1] Division of Marine Geosciences & Petroleum Geology, Bureau of Mineral Resources, GPO Box 378, Canberra, ACT 2601.
[2] Geological Survey of Papua New Guinea, Box 778, Port Moresby, Papua New Guinea
[3] CCOP/SOPAC, C/- Mineral Resources Department, Suva, Fiji

* This paper follows the nomenclature of the latest published bathymetric map (Kroenke & others, 1983).

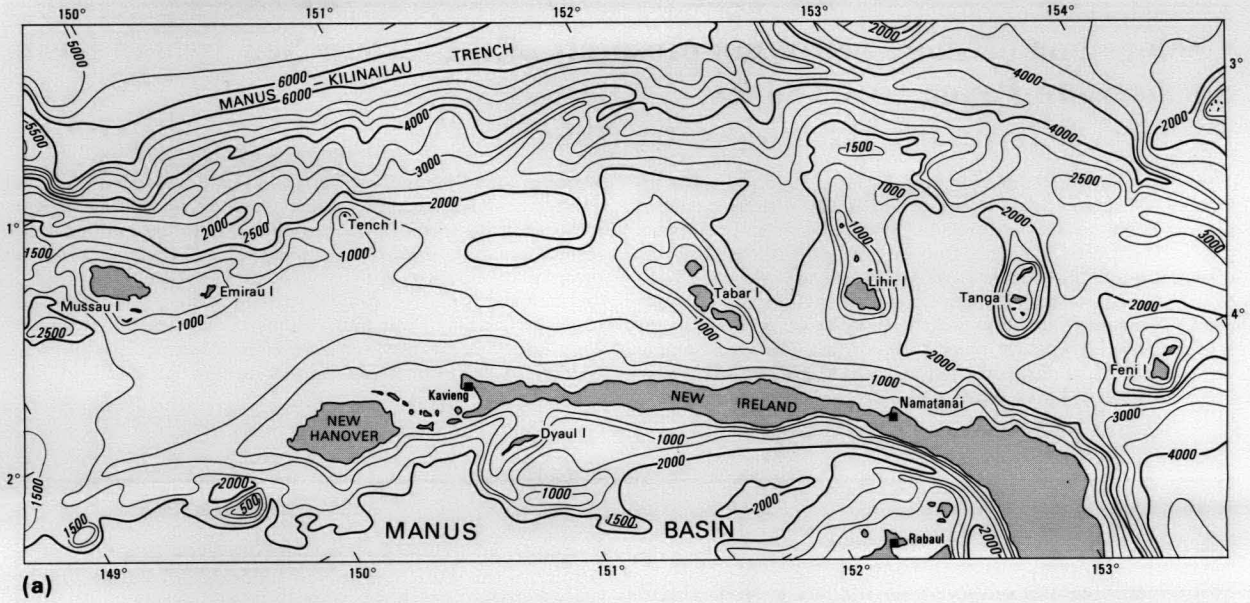
MANUS TRENCH
KILINAILAU TRENCH
Tench I
Emirau I
Mussau I
Tabar I
Lihir I
Tanga I
Feni I
Kavieng
NEW IRELAND
Namatanai
NEW HANOVER
Dyaul I
MANUS BASIN
Rabaul
(a)

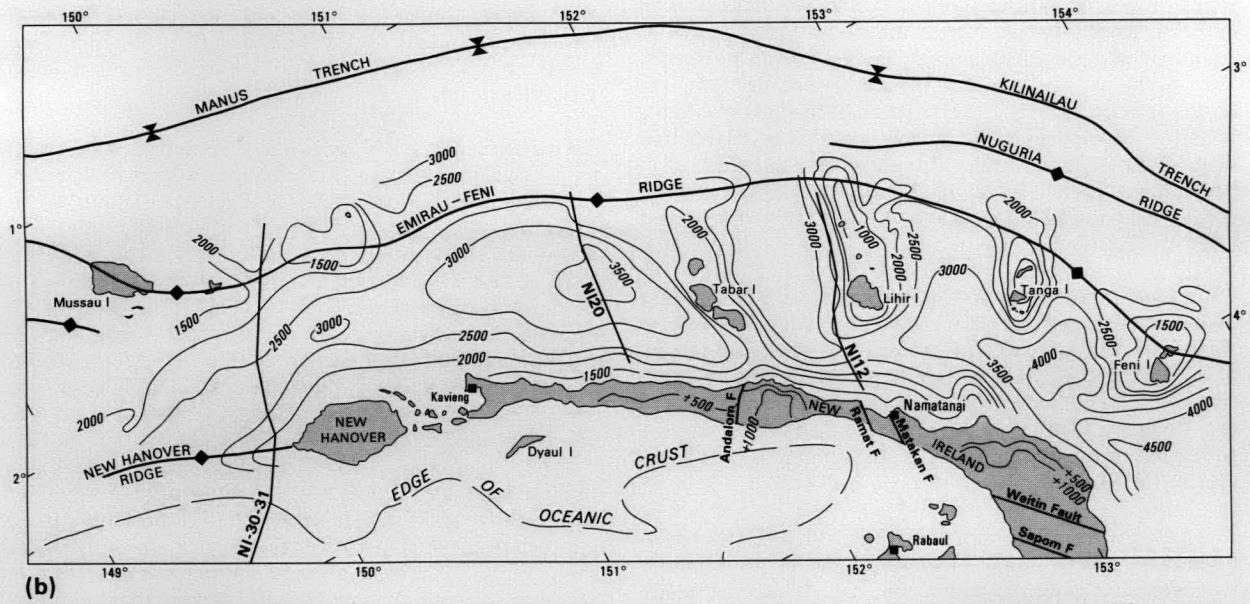
MANUS TRENCH
KILINAILAU TRENCH
NUGURIA RIDGE
EMIRAU – FENI RIDGE
NI20
NI12
NI-30-31
Mussau I
Tabar I
Lihir I
Tanga I
Feni I
Kavieng
NEW IRELAND
Namatanai
NEW HANOVER
NEW HANOVER RIDGE
Dyaul I
Andaiom F
Ramat F
Matakan F
Weitin Fault
Sapom F
EDGE OF OCEANIC CRUST
Rabaul
(b)

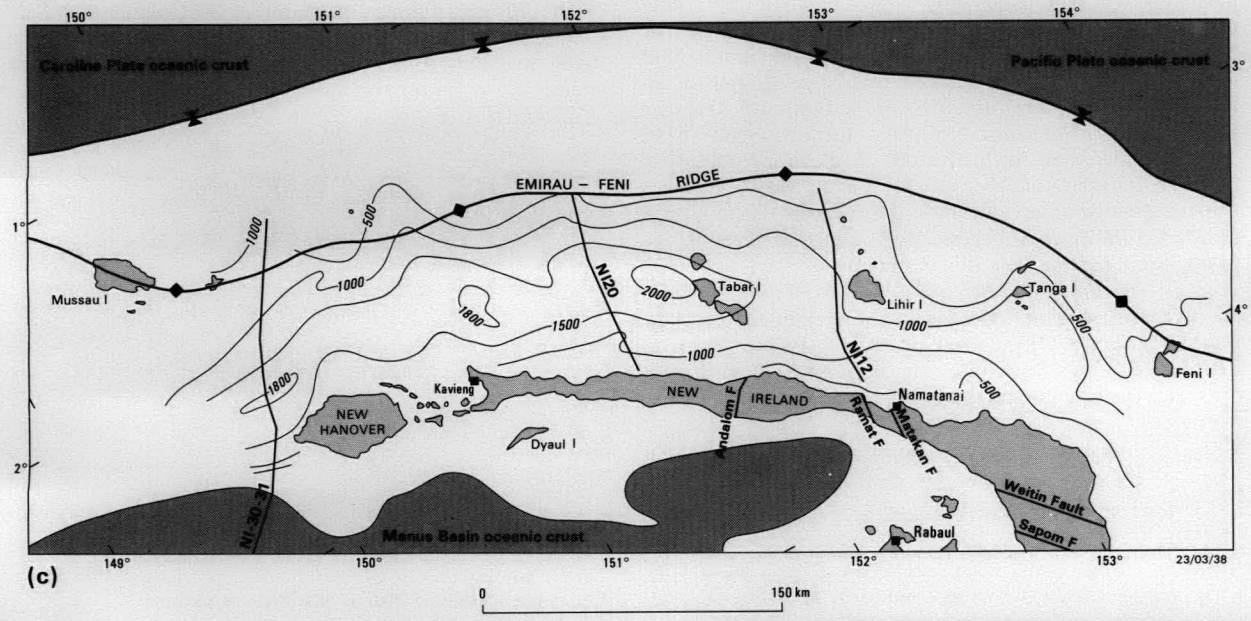
Caroline Plate oceanic crust
Pacific Plate oceanic crust
EMIRAU – FENI RIDGE
NI20
NI12
NI-30-31
Mussau I
Tabar I
Lihir I
Tanga I
Feni I
Kavieng
NEW IRELAND
Namatanai
NEW HANOVER
Dyaul I
Andaiom F
Ramat F
Matakan F
Weitin Fault
Sapom F
Manus Basin oceanic crust
Rabaul
23/03/38
(c)
0
150 km

Regional tectonics

The tectonics of the New Ireland Basin have been discussed by several authors, including Taylor (1979), Wallace & others, (1983), Falvey & Pritchard (1984), Exon & Tiffin (1984), and Kroenke (in press). Palaeomagnetic data in conjunction with other information suggest that New Britain, Manus Island, New Hanover, and New Ireland were all part of a northwest-facing volcanic arc in the Eocene-early Oligocene (Falvey & Pritchard, 1984). By late Oligocene times the arc had rotated to face northeast, perhaps as the result of formation of the Solomon Sea back-arc basin. Volcanism related to this arc ceased in the early Miocene, and there followed a long period of quiescence, during which limestones were widely deposited on the arc. After a short period of southwest-facing arc activity, probably involving the New Britain Trench, development of the Manus Basin started in the mid Pliocene, and this led to the relative movement of New Britain southeastward past New Hanover and New Ireland. A hot and light mantle anomaly associated with the opening of the Manus Basin may have caused the uplift of the southwestern side of the New Ireland Basin by as much as 2000 m (Johnson & others, 1979).

Onshore geology

Exon & Tiffin (1984) hypothesised that the offshore sedimentary sequence northeast of New Ireland was laid down in environments similar to those of the succession exposed onshore. Plio-Pleistocene uplift of the present-day onshore area has since greatly changed relative elevations. This section discusses the stratigraphy of the onshore sequence shown in Figure 3. The descriptions that follow are based partly on stratigraphic work by Hohnen (1978) on New Ireland and by Brown (1982) on New Hanover, but also incorporate new data from onshore stratigraphic studies being carried out by the Geological Survey of Papua New Guinea. Only those sequences which have relevance to the offshore geology are discussed in any detail.

The oldest rocks exposed on New Ireland and New Hanover are the middle Eocene to early Miocene Jaulu Volcanics, typical island-arc volcanics estimated to be 2000 m thick (Fig. 3). Similar rocks are present on Mussau, and more alkaline types on the Tabar Islands (Fig. 2). The dominant lithologies are porphyritic andesite, lapilli tuff, and agglomerate. Subordinate welded tuff, amygdaloidal and pillow lava, and limestone also occur.

The precise age of the Jaulu Volcanics is difficult to establish. Hohnen (1978) reported a single K-Ar date of 30.7 ± 1.0 Ma (earliest late Oligocene). Early Oligocene forams (Tertiary letter stage Tc) have been recovered from one limestone lens. Similar basement rocks (Tinniwi Volcanics) on Manus Island, which initially formed as part of the same island-arc complex, have been dated at 47.8 ± 5.0 Ma (middle Eocene) to 20.2 ± 0.8 Ma (early Miocene) (Jaques, 1980).

In central and southern New Ireland, the Jaulu Volcanics are intruded by the Lemau Intrusive Complex — stocks and dykes of basic, dioritic and granodioritic composition — dated as late Oligocene to middle Miocene.

A small inlier of bedded Oligocene calcilutite was found on Ambitle, in the Feni islands, apparently carried up by the Plio-Pleistocene volcanics. It consists largely of planktonic foraminifera identified by D.J. Belford as middle-late Oligocene (Wallace & others, 1983).

A period of bathyal clastic and neritic carbonate sedimentation followed the cessation of island-arc volcanism, continuing until the earliest middle Miocene in the area of northwestern New Ireland, and until late middle or late Miocene in the area of the remainder of the island (Fig. 3). In deeper water areas, the Lossuk River beds accumulated at upper bathyal depths (150–500 m), and in shallower areas the Lelet Limestone accumulated contemporanously as a carbonate shelf.

The Lossuk River beds were originally named by Hohnen (1978). Here the term is restricted to massive bedded, medium to dark grey, tuffaceous calcareous siltstone and very fine-grained sandstone of earliest middle Miocene (N8) age and older. They contain visible carbonaceous and woody material, and have yielded some high values of total organic carbon (M. Glikson, personal communication). Neritic limestone olistoliths of probable early Miocene (upper Te) age occur at one locality, and there are thin interbeds of agglomerate at the top of the unit. The overall thickness of the Lossuk River beds cannot be determined accurately because of poor exposure, but the exposed portion is estimated to be some 100–200m thick.

The Lelet Limestone consists of thick to massive bedded reefal, backreef, and forereef limestones, which accumulated under stable conditions on a steadily subsiding substrate. Most of the unit appears to have been deposited in an inner to mid-neritic environment (water depths of less than about 50 m), with part in an outer neritic facies environment. Algal-foraminiferal biomicrite is the most common lithology, but in-situ coral and algal biohermal reef material was identified by Hohnen (1978). Common faunal constituents include gastropods, bryozoa, echinoids, pelecypods, encrusting forams, corals, benthic foraminifera, and coralline and calcareous algae. Some algal limestones have surprisingly high values of total organic carbon (M. Glikson, personal communication).

The overall thickness of the Lelet Limestone cannot be determined with confidence, owing to extensive faulting and the absence of complete sections. It was probably deposited on a rugged substrate, and its thickness may vary considerably. In northwestern New Ireland, where carbonate deposition terminated early, thickness is probably about 400–500 m. Thicker sections are present in the Lelet Plateau area and in the northern Hans-Meyer Range, where the unit may reach 1000 m.

Precise dating of the limestone sequence is hampered by a general lack of short-lived foraminifera. The lowermost part of the succession is early Miocene (upper Te). Some beds have yielded specific late early to middle Miocene (lower Tf) ages and two samples gave possible late Middle to late Miocene (upper Tf) ages.

Figure 2. Eastern New Ireland Basin.

A — Bathymetric map, showing 500 m contours, derived from all available bathymetric and seismic profiles. Triangles are dredge samples from *Machias* cruise PN-79(1) (Eade, 1979, & Table 3). Circles are cores from *Vema* cruise 24 (Table 4).

B — Structure contour map on the top of the C horizon, which is believed to correspond to the top of the Miocene carbonate sequence. Offshore contours (500 m intervals) derived from 25 Gulf profiles only; onshore contours on top of Miocene limestones after Hohnen (1978). Key profiles NI12, NI20 & NI30-31 are illustrated in Figs 4, 5 & 6. Velocity assumed to be 1500 m/s in water and 2000 m/s in sedimentary section.

C — Isopach map of the seabed—C sequence assuming a velocity of 2000 m/s. Oceanic crust stippled.

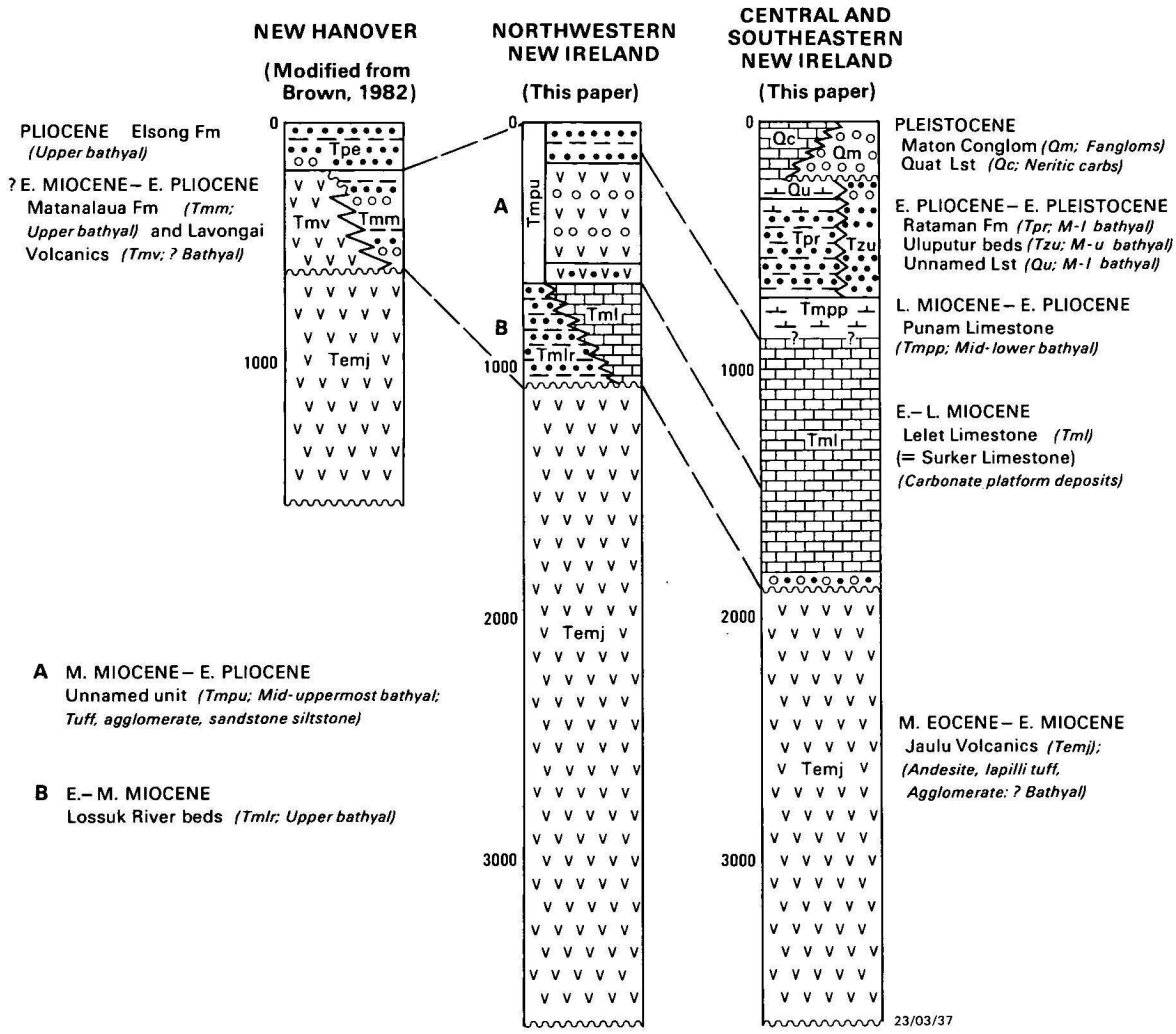

Figure 3. Generalised stratigraphic columns on land.
After Brown (1982) and recent Papua New Guinea Geological Survey stratigraphic studies in New Ireland.

In northwestern New Ireland, both the Lossuk River beds and the Lelet Limestone are conformably overlain by an unnamed succession of middle Miocene to early Pliocene pyroclastic and epiclastic rocks, the product of a renewed phase of volcanism commencing in the earliest middle Miocene. The volcanism ended carbonate deposition nearby, and coincided with a general period of subsidence. The unnamed succession is probably between 550 and 650 m thick in outcrop, and is divisible into three distinct units (Fig. 3). A lower, 70 m thick unit, of early middle Miocene age (probably about N9), is dominantly tuff with minor interbedded agglomerate. A middle unit, of mid middle Miocene age (probably about N10-N12), consists of about 350-450 m of agglomerate, volcanic conglomerate and subordinate tuff. An upper, 150 m thick unit, of late middle Miocene to possibly earliest Pliocene age (about N12 to upper N17 or N18), consists of tuff, tuffaceous sandstone, and tuffaceous siltstone. Preliminary palaeobathymetric determinations by D.W. Haig (formerly University of Papua New Guinea) suggest that the sequence was deposited in middle to uppermost bathyal depths.

In areas of central and southeastern New Ireland, far removed from this volcanic activity, platform carbonate deposition apparently continued unabated until latest middle Miocene or late Miocene (upper Tf) time. Hohnen (1978) mapped two limestone units over this area: the Lelet Limestone in central New Ireland, and the Surker Limestone in southeastern New Ireland. The term Surker Limestone is now considered redundant by the Geological Survey of Papua New Guinea, and the name Lelet Limestone is preferred.

On Simberi, the northernmost of the Tabar Islands, at least 160 m of southward-dipping limestone, with a maximum elevation of 180 m, rests on pre- middle Miocene volcanics. The limestone is typically massive, and contains limestone clasts and the fragmentary remains of corals, algae and molluscs (Wallace & others, 1983). Foraminiferal identifications on four samples (D.J. Belford in Wallace & others, 1983) gave early Miocene to Pliocene ages. Much of this sequence is inferred to be of fore reef origin, indicating the presence of reefs well to the north of New Ireland, and at least partly contemporaneous with the Lelet Limestone. Marine seismic data indicate that the Tabar Islands are horsts (Wallace & others, 1983).

Reconnaissance mapping of Mussau (C.M. Brown, personal communication) revealed early Miocene shelf limestone, pebbles of early Miocene planktonic foraminiferal limestone in a conglomerate, and Pliocene planktonic foraminiferal limestone. Determinations by D.J. Belford and G.C. Chaproniere include upper Te, upper Te or possibly lower Tf, and N19-20. A series of raised limestone terraces indicate marked recent uplift on the island.

The next youngest unit exposed in central and southern New Ireland is the late Miocene to early Pliocene Punam Limestone (Fig. 3), which crops out extensively along the east coast of the island in faulted contact with the Lelet Limestone. The stratigraphic relationship between the Punam and Lelet Limestone is unclear, as the two units have been observed only in faulted contact. The Punam Limestone typically consists of soft, foraminiferal biomicrite, which accumulated at mid to lower bathyal depths (500–4000 m) as a *Globigerina* ooze. In central New Ireland, only the upper 20–30 m is exposed; it is early Pliocene (N18-low N19/20) in age. Similar rocks, probably part of the Punam Limestone, are extensively exposed at Cape St. George at the southeastern tip of New Ireland. McGowran (*in* Mitchell & Weiss, 1982) tentatively dated part of this succession as late Miocene (N16). If these sediments are included, the Punam Limestone could be as thick as 150–200 m.

The Punam Limestone is sharply but conformably overlain by volcaniclastic sediments of the early Pliocene to early Pleistocene Rataman Formation (Fig. 3), which is exposed in the narrow central part of New Ireland, in fault-bounded blocks southeastward along both coasts, and on Dyaul Island to the northwest (Fig. 2). The Rataman Formation represents a short-lived phase of volcanism that affected the whole of the New Ireland area and lasted about 2 million years from mid Pliocene to earliest Pleistocene (N19/20 to high N21).

The Rataman Formation is largely andesitic and dacitic crystal lithic tuff interbedded with slightly to non-calcareous volcanogenic lutite. Foraminiferal assemblages indicate deposition in mid-lower bathyal depths, and abundant sedimentary structures indicate deposition by turbidity currents. Tuffaceous units become thinner and less numerous upward, and foraminiferal biomicrites predominate towards the top of the formation. Equivalent rocks on Dyaul Island were apparently situated nearer to eruptive centres, as they contain interbedded andesitic lava flows. Thickness estimates of the Rataman Formation are complicated by extensive mesoscale faulting; thickness is probably about 400 m.

In central New Ireland, the Rataman Formation grades upward into an unnamed limestone unit similar in lithology to the Punam Limestone. Only about 15 m is exposed, and foraminiferal assemblages indicate deposition at mid to lower bathyal depths. In parts of central and southern New Ireland there are shallower water time equivalents of the Rataman Formation and the upper unnamed limestone, the Uluputur beds (Fig. 3). The unit is largely well-bedded silty sandstone, with some poorly sorted cobble and boulder conglomerate in its upper part. Foraminiferal assemblages indicate that the Uluputur beds were deposited mainly at mid to upper bathyal depths, and that their age ranges from mid Pliocene to early Pleistocene (N19/20-low N22). The youngest clastic sediments in southwestern New Ireland belong to the Maton Conglomerate, a sequence of poorly sorted cobble and boulder conglomerate, pebbly sandstone, and minor coal.

The stratigraphic sequence on New Hanover has been described by Brown (1982). There, Miocene platform limestones are absent and the Jaulu Volcanics are overlain by the early Miocene to early Pliocene Lavongai Volcanics, a predominantly pyroclastic succession probably related to a short-lived southwest-facing volcanic arc involving the New Britain Trench. The Lavongai Volcanics are inferred to be partly laterally equivalent to and partly unconformably overlain by the Matanalaua Formation, which consists of up to 400 m of tuffaceous clastics and rare lignite. The Matanalaua Formation is succeeded by calcareous tuffaceous clastics of the Pliocene Elsong Formation, estimated to be 200 m thick.

Micropalaeontological samples from the Matanalaua and Elsong Formations (D.W. Haig, personal communication) indicate that both were deposited, at least in part, in upper bathyal depths. Foraminiferal assemblages from the upper Matanalaua Formation suggest a late Miocene to early Pliocene (upper N17–N18) age, indicating equivalence to the Punam Limestone. Micropalaeontological control is very sparse, and the formation probably ranges downward in age into the middle Miocene and possibly older (Lelet Limestone equivalent). Samples from the basal Elsong Formation have yielded early to mid Pliocene (N18–N19/20) ages. Equivalents of this unit are not exposed in northwestern New Ireland, but are the uppermost Punam Limestone in central New Ireland.

Onshore structural geology

According to Brown (1982), both New Ireland and New Hanover are dissected by a series of northwesterly trending, northeasterly tilted fault blocks bounded by high-angle normal faults; this fault pattern is complicated by a 'rectilinear pattern of northeasterly, north-northwesterly and easterly trending tensional and conjugate fractures as illustrated by the regular sawtooth pattern of the southern coastline of New Hanover and New Ireland.' Brown (1982) concluded that the main fracture sets probably formed during development and uplift of the volcanic arc in the mid-Tertiary, and that differential subsidence of the fault blocks bounded by these fractures accompanied limestone deposition during the Miocene. Major adjustments were inferred to have occurred during the Pliocene to Recent uplift that formed the present-day islands.

In southeastern New Ireland, Hohnen (1978) mapped two prominent northwest- trending fault systems, the Weitin and Sapom Faults (Fig. 2B). Taylor (1979) noted that these faults are probably part of the surface expression of a major transform fault system trending N60°W southwest of New Ireland. According to Johnson (1979), earthquake focal-mechanism solutions and the general trend of this feature are consistent with left-lateral strike-slip motion.

The onshore geology of New Ireland indicates that extensive uplift has occurred since the various sedimentary sequences were deposited. The presence of early Pleistocene (low N22) sediment of mid-lower bathyal origin (500–4000m water depth) in central and southeastern New Ireland suggests that much of the uplift has occurred in the last 1.5 Ma. The unnamed Pleistocene limestone is now found at elevations as much as 200 m above sea level, and has therefore experienced a minimum vertical displacement of 700 m at an average rate of 470 m/Ma. Even greater uplift is indicated in the case of fault blocks in southeastern New Ireland, where the Lelet Limestone occurs as much as 1900 m above sea level (see contours in Fig. 2B). The Lelet Limestone must have been downfaulted to considerable depths during the late Miocene, and was overlain by an unknown thickness of younger sediments. Hence the indicated 1900 m of uplift (about 1300 m/Ma, assuming uplift started 1.5 Ma ago) represents only a minimum, and the actual amount was probably much greater. Similar calculations involving the sedimentary sequences in central and northwestern New Ireland and New Hanover suggest that the amount and rate of uplift decline in a northwesterly direction.

Offshore geology

Seafloor samples have been recovered by Eade (1979), and on Lamont-Doherty Geological Observatory cruises Vema

24, Vema 33, and Robert Conrad 10. Dredge material from the Eade (1979) cruise (Table 2) has been supplied to us by CCOP/SOPAC, and unpublished descriptions of Quaternary (probably Holocene) cores have been provided by Lamont-Doherty Geological Observatory (Table 3). A preliminary investigation of the dredge material has provided foraminiferal ages ranging from late Pliocene (N21) to Recent (D.J. Belford, BMR, personal communication).

The New Ireland Basin samples (Tables 2 & 3) suggest that, in the Quaternary, deposition of foram-rich ooze and chalk predominated in shallower water (less than 3000 m), with foram-bearing mud, sand, and ash being laid down in deeper water. In Holocene cores from the Manus Basin south of New Ireland, volcanic ash is more abundant.

The locations of all the seismic lines used in this study are shown in Exon & Tiffin (1984). For the purposes of this paper, three seismic lines, NI30-31, NI20, and NI12, are taken as typical (Figs 2, 4, 5, & 6). Seismic reflection character varies but little in the western part of the basin, which is the area with thicker sediment and, hence, greater petroleum prospects. East of the Tabar Islands the sequence is not only thinner, but in deeper water, where it is faulted and cut by volcanic intrusions and extrusions.

The overall character of the major seismic sequences is shown in Figures 4 & 5, and summarised in Table 1. The discussion refers largely to the area west of the Tabar Islands, where multichannel seismic data are concentrated, and where there is less structural complexity to obscure seismic character.

Correlation of seismic sequences with the onshore sequences is hampered by a gap of about 5 km between the shoreline and the seismic profiles. It therefore depends on interpretation of seismic character, interval velocities, and relative thickness of onshore and offshore sequences. There is little change in seismic character of the various sequences over the very large part of the basin extending west-northwestward for about 270 km from Tabar Island to south of Mussau, and north-northeastward for about 100 km from New Ireland to the Emirau-Feni Ridge. Because New Ireland and New Hanover were integral parts of the depositional basin until their uplift in the Pliocene, it is reasonable to suggest that the older parts of the sequence should be similar onshore and offshore.

Table 1. Seismic sequences

Sequence Velocity* Thickness	Character	Interpretation
SB-A 1800 m/s 200-300 m	Semi-transparent well-bedded sequence immediately beneath sea bed (SB). Conformably overlies high-frequency reflector (A), which is unconformable on underlying sequence in places	Pleistocene to Recent hemipelagic oozes.
A-B 2000 m/s 500-1000 m	Well-bedded sequence with interbedding of strong reflectors and semi-transparent intervals. Progrades north-eastward. Conformably overlies shallowest continuous low-frequency reflector (B) that is conformable on underlying sequence	Pliocene volcaniclastic turbidites resulting from volcanism, possibly triggered by subduction at the New Britain Trench just before and during the initial opening of the Manus Basin, interbedded with marls and chalks. Equivalent to the Rataman Formation on New Ireland.
B-C 2300 m/s 200-500 m	Well-bedded sequence like A-B. Progrades northeastward and is unconformable on regular underlying low-frequency reflector (C)	Late Miocene to earliest Pliocene chalks and marls, which accumulated as *Globigerina* oozes, interbedded with volcaniclastic turbidites. Equivalent to Punam Limestone on New Ireland.
C-D 3600 m/s 1000- 2500 m	Mixed seismic character. Weak to strong parallel reflectors, dipping reflectors, and buildups. Unconformably overlies continuous low-frequency reflector (D), which is generally conformable on underlying sequence	Early to late Miocene platform and upper slope limestones equivalent to thick Lelet Limestone of New Ireland. Potential petroleum source and reservoir rocks.
D-E 3000 m/s 1000 m	Well-bedded variably reflecting sequence, locally containing dipping reflectors, channels, and buildups. Unconformably overlies strong low-frequency reflector (E)	Early Miocene outer shelf and slope sediments, largely volcaniclastic, with some channels and possible carbonate banks. Equivalent to Lossuk River beds on New Ireland; potential petroleum source rocks.
E-V velocity unknown 1000 m	Well-bedded variably reflecting, poorly defined sequence at limit of acoustic penetration. Unconformably overlies strong, diffracting irregular surface	Probably Eocene to early Miocene volcanics and volcaniclastics equivalent to Jaulu Volcanics on islands. Diffracting surface beneath may either be oceanic basement or lie within Jaulu Volcanics.

* 'Velocity' is average seismic interval velocity for Gulf line NI20, derived from the normal moveout velocities used for stacking.

Table 2. Dredge hauls from the New Ireland region (Eade, 1979)

Station	Location	Latitude	Longitude	Water depth (m)	Description
14	E Emirau	1°40.0'S	150°27.0'E	537-830	Pleistocene-Recent white chalk, gravel, pebbles
15	W New Hanover	2°21.2'S	149°49.7'E	483-492	Altered volcanics, pumice
16	E Emirau	1°44.7'S	150°24.3'E	825	Late Pliocene-early Pleistocene (N21) white chalk; quartz vein rock, pumice
17	NW Tabar	2°32.9'S	141°50.7'E	344-1084	Limestone
22	NE Lihir	2°43.6'S	152°50.8'E	1000-1100	Late Pliocene-early Pleistocene (N21) foram-bearing limestone, sandstone, siltstone; foram sand.

Table 3. Cores from the New Ireland region (Lamont-Doherty Geological Observatory)

Station	Location	Latitude	Longitude	Depth (m)	Recovery (cm)	Description
V24-152	NE Tanga	3°18'S	153°32'E	2410	343	Foram chalk
V24-153	S Feni	4°30'S	153°28'E	4103	198	Foram-bearing clay', interbedded ash
V33-116	Manus Basin	2°54.5'S	148°35'E	2363	309	Foram-rich mud and sand; some ash
V33-117	Manus Basin	3°47'S	151°0'E	2340	10	Volcanic ash
RC10-138	E Feni	4°05'S	154°34'E	3563	523	Pelagic mud,interbedded foram-rich sand.

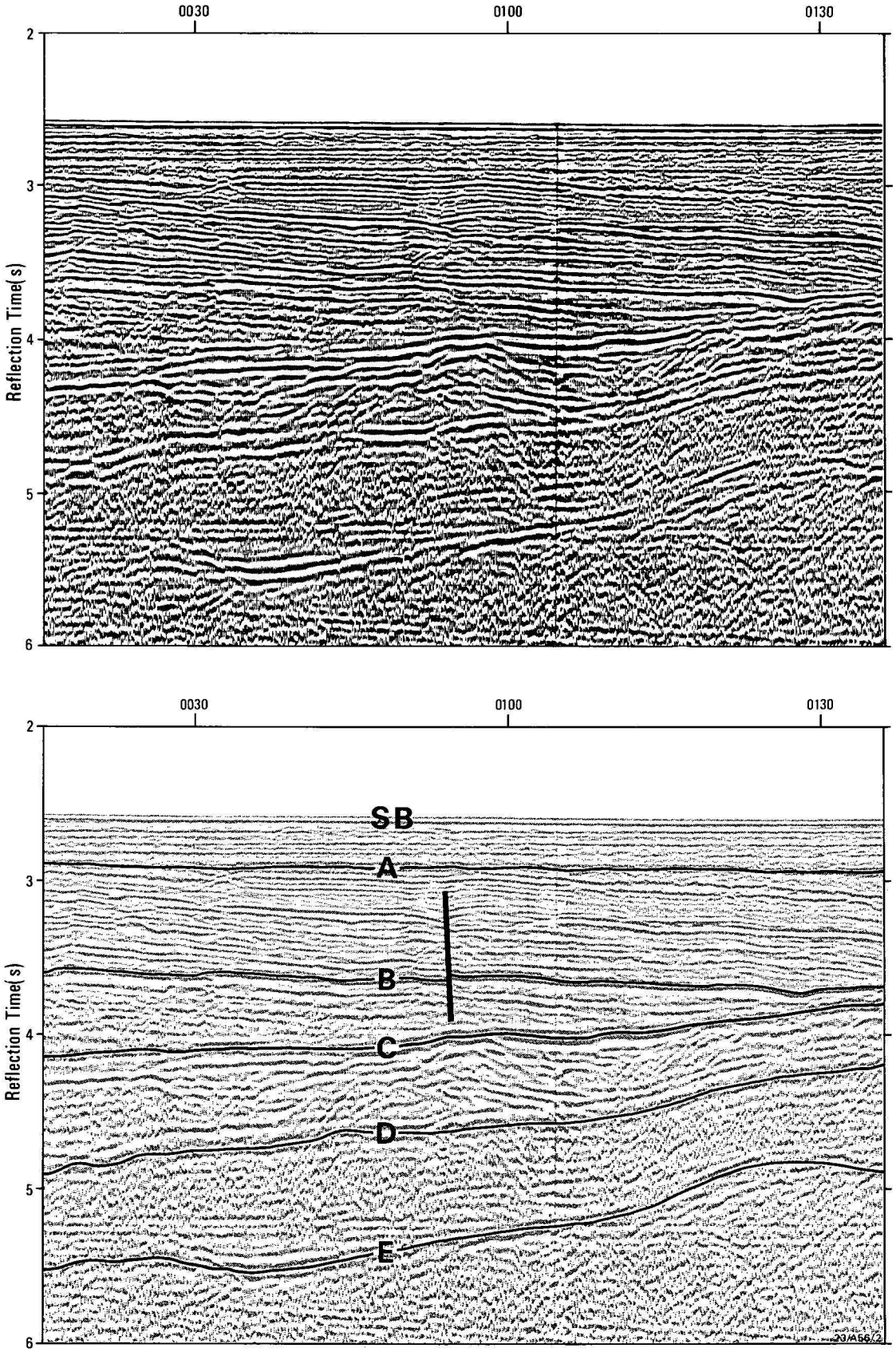

Figure 4. Part of multichannel Gulf seismic profile NI20 showing intepretation.
Profile location shown in Fig. 2, and location within profile shown in Fig. 6. Sequence nomenclature given in Table 1. Note especially the complex character of sequence C–D, believed to consist of shelf carbonates, including reefs.

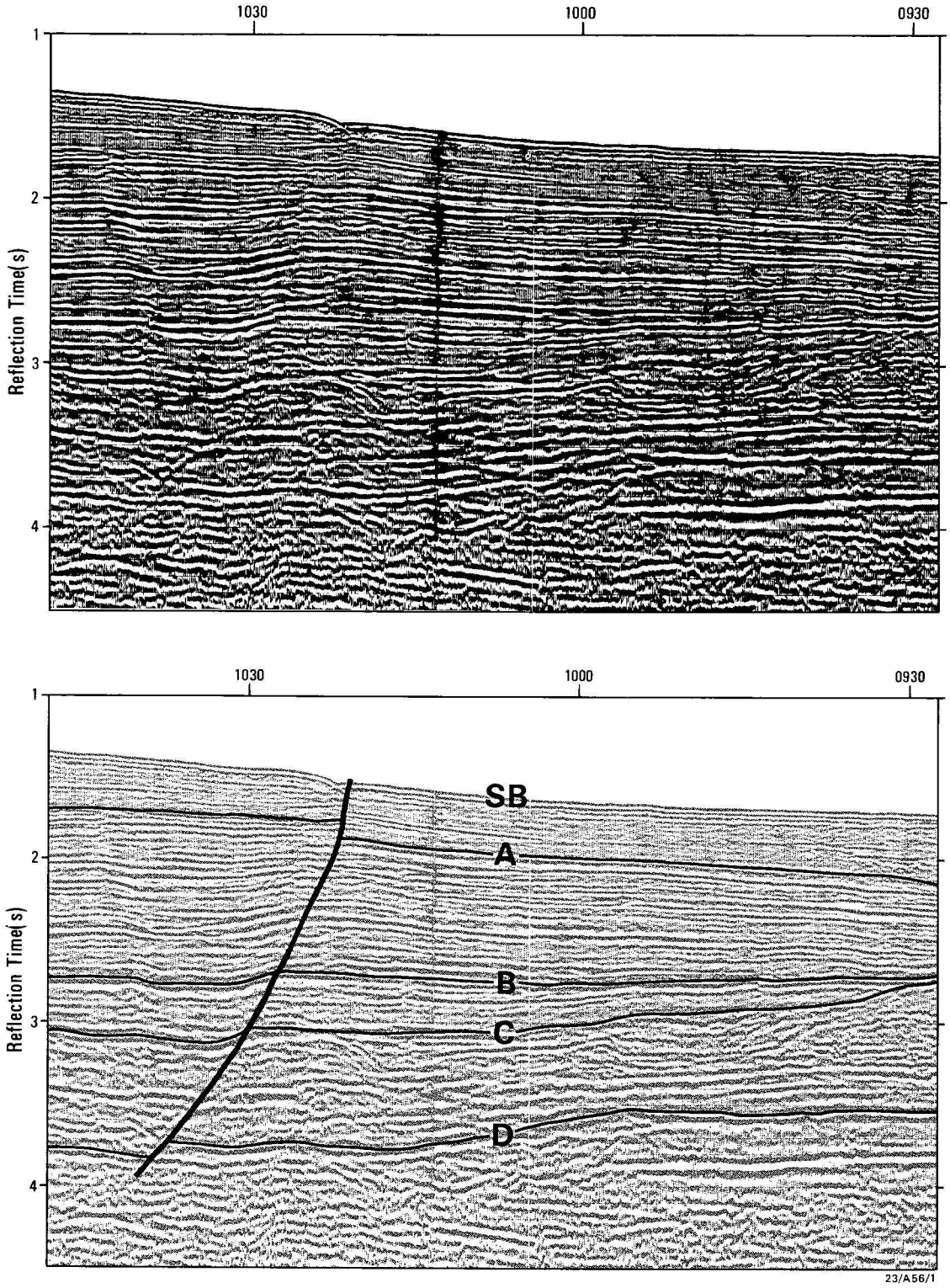

Figure 5. Part of multichannel Gulf seismic profile NI30, showing interpretation.
Profile location shown in Fig. 2, and location within profile shown in Fig. 6. Sequence nomenclature given in Table 1. Note the complex character of sequence C–D, and the fault extending throughout the column, with normal movement apparent at depth and reverse movement near the surface. Should the C–D sequence just to the right of the fault be a reef, the apparently large normal movement on D would be an artifact of 'velocity pull-up'.

By far the most distinctive seismic sequence is C–D, which has a high interval velocity (derived from seismic stacking velocities) of about 3600 m/s (Exon & Tiffin, 1984) and structures reminiscent of a shelfal carbonate sequence, or flows or sills (Figs 4 & 5). Because it is very widespread, retains its character very well, and varies relatively little in thickness, we assume it is a carbonate rather than an igneous sequence. A correlation with the similarly thick Miocene Lelet Limestone on New Ireland appears obvious, especially as shelfal limestone of similar age occurs on uplifted offshore islands such as Mussau. If that correlation is accepted, then correlation of the other seismic sequences becomes more sound.

The seismically transparent SB–A sequence, assumed to be Pleistocene–Recent ooze, maintains its character and

thickness widely. The A-B and B-C sequences generally prograde northeastward from New Ireland and New Hanover, and hence thin in that direction. These sequences are assumed to consist largely of late Miocene to Pliocene volcaniclastic turbidites, marls, and chalks; the more strongly bedded A-B sequence may be predominantly volcaniclastics equivalent to the Rataman Formation, and the less strongly bedded B-C sequence may be predominantly chalks and marls equivalent to the Punam Limestone.

The C-D sequence, with the overall character and interval velocity of a carbonate platform sequence, is taken to be the equivalent of the early to late Miocene Lelet Limestone of New Ireland. In both NI20 and NI30 (Figs 4 & 5), buildups, dipping beds, and flat-lying strata can be seen, and these are present in places throughout the basin. They could correspond to reefs, fore-reef rubble and general back-reef and platform deposits. Buildups are more common in this sequence than the others, but can also be seen in both higher and lower sequences in a few areas.

The D-E sequence is the lowest clearly recognisable sedimentary sequence, and probably corresponds in part to the Lossuk River beds of New Ireland; it may contain rocks as old as the Oligocene limestone of Ambitle. Its composition is not known with any confidence.

The line drawings of the parallel basin-crossing profiles NI30-31, NI20, and NI12 show the change in basin character along its length (Fig. 6). Profile NI20 was taken by Exon & Tiffin (1984) as typical of the basin. The profile shows the gentle slope down from New Ireland and an overall thickening toward the basin axis, followed by overall thinning toward the Emirau-Feni Ridge to the north. The generally prograding nature of the A-B and B-C sequences is clear, as are the buildups in the C-D sequence, especially near the structurally high ends of the lines. Faulting and erosion have removed some of the section near the Emirau-Feni Ridge.

Profile NI30-31 is generally similar to NI20, but shows the southern part of the section, which could not be recorded on NI20 because of the existence of the New Ireland landmass. This profile runs just west of New Hanover, and illustrates the major fault system on which the southern side of the basin steps down to the young 2000 m deep Manus Basin (see steep slope on Fig. 2). The oceanic crust of the Manus Basin is shown by reflector V on the extreme left of the profile. The profile indicates that the fault movements occurred very late in the history of the New Ireland Basin, in agreement with the onshore geology, and perhaps caused by initial rifting associated with seafloor spreading in the Manus Basin, which started some 3.5 Ma ago (Taylor, 1979).

Profile NI12 lies in the eastern part of the basin through which the Plio-Pleistocene volcanics of the Tabar-Feni group of islands have made their way to the surface. Although correlation is uncertain across the faults bounding Lihir Island, it is clear that there has been a considerable amount of uplift of the older sequences by the intrusive and volcanic activity. This agrees with the presence of upthrown Miocene carbonates in the Tabar Islands (see **Onshore geology**).

Turning from the seismic profiles to the maps constructed from them and from bathymetric information (Fig. 2), the close inter-relationship of all three maps is clear. The structure contour map of the C horizon (Fig. 2B) — the top of the presumed shelf carbonates — shows highs around the islands formed largely of Miocene and older rocks, such as Mussau, New Hanover, and New Ireland, and around those consisting of younger igneous rocks punched through the older basinal sediments in the Tabar-Feni group. Our interpretation of the seismic profiles (e.g. Fig. 6) indicates that the C structure generally reflects deeper structure. The Emirau-Feni Ridge and older outer-arc high bounding the Manus-Kilinailau Trench are quite apparent. The major structural depression between the Emirau-Feni Ridge and the land areas to the south is well defined in the west, but much disturbed around the volcanic islands in the east.

Assuming that the top of the C horizon corresponds to the top of the Lelet Limestone on land, the maximum relief between the structural high of New Ireland and the structural low offshore is some 5000 m, west of Tabar (Fig. 2B). In the area near Tanga and Feni the maximum relief is even more at 5500 m. Over all, the offshore basin deepens southeastward at the C horizon.

The isopach of the seabed—C interval (Fig. 2C) clearly shows the thick and thin sedimentary sequences that have developed since the early late Miocene. Deposition has been least on the highs, on the margins of the structural basin near New Hanover and New Ireland, and along the Emirau-Feni and Nuguria Ridges — and also on the slope down into the trench system. A major depocentre extends from west of New Hanover to the Tabar Islands, and contains 1500-2000 m of sediment. It persists eastward from Tabar, but sediment thickness decreases by at least 500 m. Despite the detrital influx from the volcanic islands, the controlling influence on sedimentation appears to have been sediment eroded from the flanking structural highs. Both this and the volcanic detritus were superimposed on the pelagic rain, which must have been roughly the same throughout the offshore area. The displacement of the depocentre south of the structural low (cf. Figs 2B & 2C) shows the importance of material derived from and deposited near the southern landmasses. The relative thinness in the east is probably due to downslope removal of sediment into the structural low south of Feni and into the trench system, especially before the growth of the volcanic islands from Pliocene times onward accentuated the Emirau-Feni Ridge.

The bathymetry of the area (Fig. 2A) clearly reflects the deep structure, and illustrates the continuing importance of the Emirau-Feni and Nuguria Ridges. The position of the present bathymetric basin, well north of the structural low on the C horizon of Figure 2B, emphasises the effect of the increased deposition in the south (Fig. 2C). Both the structural and bathymetric maps suggest that the north to northwest fault trends on land are present offshore as controlling and bounding faults under and near the Tabar, Lihir and Tanga Island groups, all of which are elongate northward.

As pointed out by Exon & Tiffin (1984), most offshore faults have formed fairly recently and are probably still active, although some are long-lived growth faults on which movement directions have changed through time. The most spectacular fault system trends northwestward and forms the southern flanks of New Hanover and New Ireland. Onshore, this fault system is extensively developed on both islands (Brown, 1982; Hohnen, 1978), perhaps most clearly in the Weitin and Sapom Faults (Fig. 2), but also in the high-angle faults, downthrown to the south, on New Hanover (Brown, 1982). Offshore, it is clearly shown on Profile NI31 (Fig. 6). This fault system separates the arc crust of the New Ireland Basin from the oceanic crust of the Manus Basin (Taylor, 1979), and is almost certainly a transform fault system (Curtis, 1973; Connelly, 1976) along which New Britain moved southeastward relative to New Ireland (Taylor, 1979; Johnson & others, 1979; Falvey & Pritchard, 1984). Movement on the system has varied from fault to fault, with both

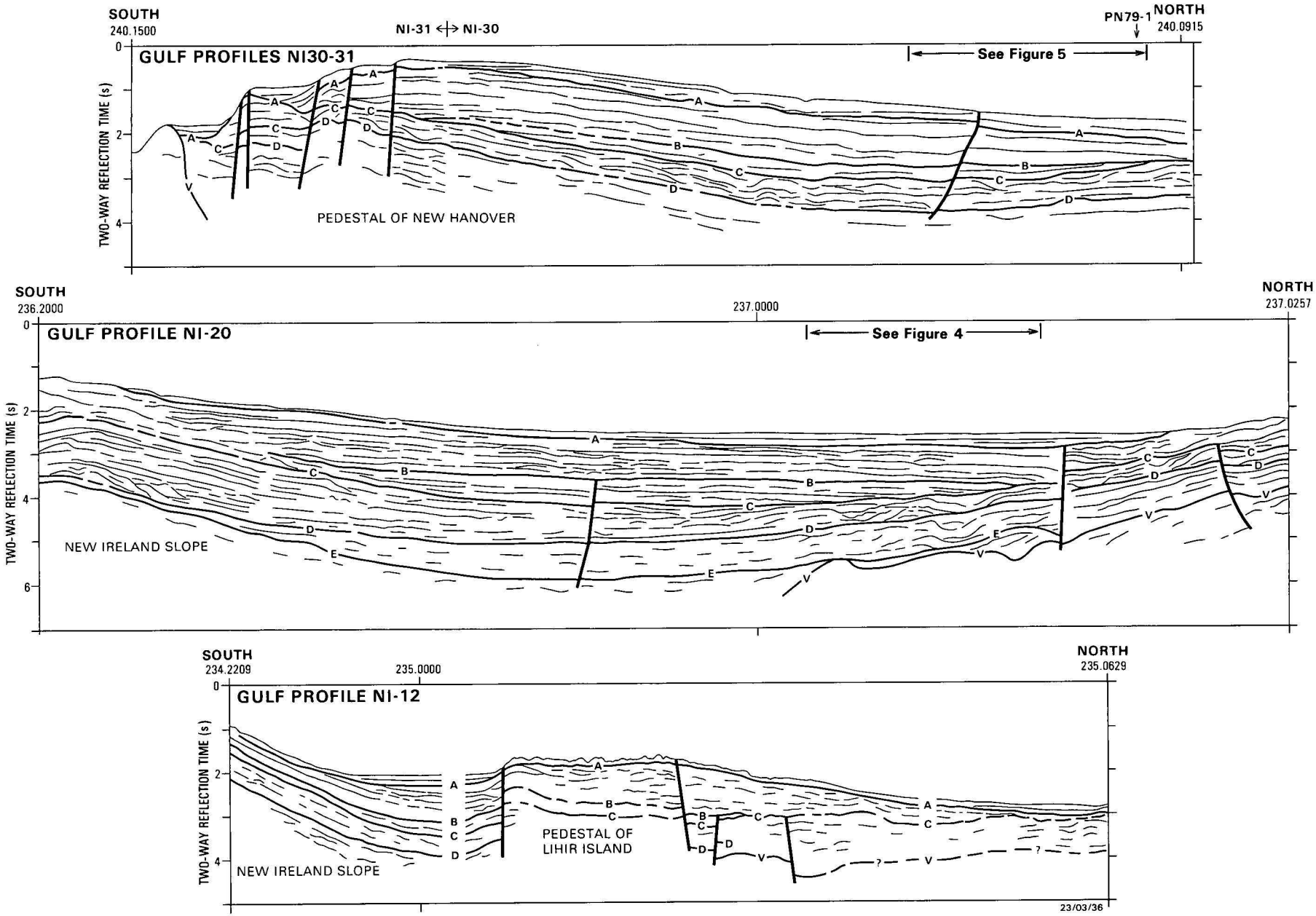

Figure 6. Line drawings of Gulf seismic profiles NI30–31, NI20, and NI12.

Parts of NI30 and NI20 are shown in Figs 4 & 5. Sequence nomenclature is given in Table 1. Note the over-all thickening into the basin, the prograding nature of the A–B and B–C sequences in NI30–31 and NI20, the youth of the faults, and the upthrowing of the older sequences in NI12 on the Lihir Island horst, probably caused by the eruption of the Plio-Pleistocene volcanics.

transcurrent and vertical movements being important. A lesser, parallel set of normal faults occurs further north, on land and offshore. These seem to have formed as simple adjustments to differential loading in the basin and, especially, to post-Pliocene tilting of the basin.

Summary of the geological history

The New Ireland area first came into existence during the Eocene, as a northwest-facing volcanic arc with the oceanic crust to the north being subducted southeastward at the Manus and Kilinailau Trenches. Island-arc volcanics built up from older sea floor to form the Jaulu Volcanics in the New Ireland–New Hanover area and its lateral equivalents on Mussau and Manus Islands (E-V sequence). By the late Oligocene, the arc had rotated to face northeast, owing to seafloor spreading in the Solomon Sea (Falvey & Pritchard, 1984). During the early Miocene, subduction and volcanism ceased, but younger phases of the Lemau Intrusive Complex continued to intrude the Jaulu Volcanics and overlying sedimentary cover until at least middle Miocene time.

The main phase of island arc volcanism ceased during the early Miocene, but volcaniclastic sedimentation continued in the forearc basin between the relative highs formed by the Jaulu Volcanics and the Emirau-Feni Ridge. More than 1000 m of these sediments is present in places (D-E sequence). Lateral equivalents of at least part of this succession are exposed onshore as turbidites of the Lossuk River beds. A carbonate platform developed directly on the volcanic substrate in shallow-water areas, and prograded outward over deeper water sediments from early Miocene time to form the Lelet Limestone and its lateral equivalents offshore (C-D sequence). Central and southern New Ireland and adjacent areas offshore were free from Miocene volcanic activity, and carbonate deposition persisted until at least latest middle Miocene or late Miocene time. The resultant, laterally extensive carbonate succession may be thicker than 2000 m in parts of the present-day offshore area.

Over the equivalent period, the present-day New Hanover area was the site of persistent volcanism, as represented by the Lavongai Volcanics. Nearby areas, such as northwestern New Ireland and offshore from New Hanover, were not initially affected, and the Lossuk River beds and lower Lelet Limestone were laid down during the mid-early Miocene to earliest middle Miocene. A subsequent resurgence of volcanism terminated carbonate deposition in the northwest and led to a phase of subsidence and pyroclastic deposition that lasted until the late middle Miocene. Pyroclastic and epiclastic deposition continued in the northwest until the latest Miocene or early Pliocene, and carbonate deposition was not re-established. This middle to late Miocene sequence is probably only of local extent, and has not been specifically recognised in the offshore seismic sections.

Elsewhere in the New Ireland Basin, the early late Miocene appears to have been marked by rapid regional subsidence to bathyal depths. This event may have coincided with reversal of the island arc and its transferral to the Pacific Plate, which is thought by Falvey & Pritchard (1984) to have occurred at about that time. Initially, pelagic deposition prevailed, with the accumulation of the chalks and marls of the Punam Limestone and its offshore equivalents (B-C sequence), until early Pliocene time. A resurgence of regional volcanism followed until the earliest Pleistocene, resulting in the deposition of volcaniclastic turbidites and tuffs of the Rataman Formation and its equivalents offshore (A-B sequence). The volcanism may have been triggered by subduction at the New Britain Trench while New Ireland was still part of the newly formed southwest-facing arc, just prior to the opening of the Manus Basin about 3.5 Ma ago. The volcanic activity was short-lived, lasting only about 2 Ma. Pelagic carbonate deposition gradually returned to the area by the early Pleistocene. However, New Hanover and New Ireland had already commenced movement to the northwest, relative to New Britain, along a transform fault system, as the Manus Basin opened. Rapid uplift accompanied the strike-slip movement, and over 1.5 Ma present-day New Ireland emerged from the sea. The uplift, which probably exceeded 1900 m in southeastern New Ireland, but decreased greatly to the northwest, may have been associated with the thermal anomaly of the spreading centre and heating along the transform faults. Fanglomerate deposits of the Maton Conglomerate were subsequently laid down against the newly emergent mountain chain adjacent to the fault scarps, and various terrestrial and shelfal detrital deposits and coastal limestones were laid down elsewhere on New Ireland, and on New Hanover and Mussau. During the same period, subsidence continued in the offshore areas to the northeast, where pelagic deposition has continued to the present day (SB-A sequence).

Plio-Pleistocene alkali volcanism in the central part of the basin formed the Tabar-Feni group of islands, in an area where there had been similar pre-middle Miocene volcanism. Much of the faulting in these areas appears to be associated with related tectonism.

Petroleum potential

Elements that must be considered in any petroleum assessment are thickness of the sediments, the palaeo-heat flow, the existence of potential source rocks, reservoirs, and traps, and the geological timing of events. As no wells have been drilled in the area, little control exists over the major part of the basin to assist in the evaluation of these factors. Hence, this preliminary assessment of petroleum potential relies heavily on extrapolation offshore of existing onshore information, on the seismic character of the various sequences identified in the sections, and on comparisons with other basins in similar tectonic settings.

The New Ireland Basin, with about 5 km of sedimentary section visible in the seismic sections, is clearly deep enough to have generated hydrocarbons. No data are available, however, to assess palaeo-temperatures or even modern heat flow. Recent studies in the intra-arc New Georgia Basin in the Solomon Islands (Free & others, 1982) have shown that the present heat flow there is rather low, and that petroleum is only likely to have been generated where overburden exceeds 2000 m in thickness. If the New Ireland Basin has similar heat flow, only the Miocene sequence offshore is likely to contain mature potential source rocks (C-D and D-E sequences in Table 1). This stratigraphic interval is inferred to contain equivalents of the Lelet Limestone and Lossuk River beds identified onshore.

A comprehensive onshore study of New Ireland source rocks is currently being carried out by M. Glikson (Australian National University), but only preliminary results were available at the time of writing. Volcaniclastic sediments generally contain only small quantities of organic carbon, as has been shown by recent onshore and offshore studies in Tonga, Vanuatu, Fiji, and the Solomon Islands (Buchbinder & Halley, in press; Exon & Herzer, in press; Exon & others, 1984). The Lossuk River beds contain abundant plant remains and total organic carbon is high (M. Glikson, personal communication). However, the organic particles have

low hydrogen indices and the rocks themselves are at a thermally immature stage for hydrocarbon generation. These onshore exposures may not be representative of the equivalent sequence offshore. In more distal parts of the fore-arc basin, organic matter of marine origin might be more prevalent. Also, the seismic sections suggest much deeper burial in the offshore area than is indicated for the Lossuk River beds exposed onshore. The possibility exists, therefore, that better quality and mature source rocks might be present in the D-E seismic sequence offshore.

In southeastern New Ireland, highly carbonaceous shale of probable lagoonal origin has been found in the Lelet Limestone at one locality. Owing to poor exposure and structural complications, its stratigraphic position and vertical extent are unknown. Initial geochemical results indicate the presence of material similar to cannel coal (M. Glikson, personal communication). Such material could be highly productive for hydrocarbon generation under the right burial conditions.

Onshore exposures of the Lelet Limestone are known to contain abundant algal material in some facies. Concentrations of relatively fresh, translucent, brown algal organic matter have been identified in thin section, and total organic carbon values are high in some cases (M. Glikson, personal communication). This suggests that the inferred offshore equivalent of the Lelet Limestone, the C-D sequence, could contain petroleum source rocks similar to those documented by Hatley & Harry (1980) in the Miocene carbonate succession off Palawan in the Philippines. The C-D sequence appears to be buried by up to 2000 m of overburden in places, and may itself be up to 2500 m thick, suggesting that sufficient burial has probably taken place to induce hydrocarbon generation.

The most attractive reservoir rocks in the New Ireland Basin are inferred reef and reef-related carbonate sediments in the offshore C-D seismic sequence. Probable similar strata examined onshore in the Lelet Plateau area display up to 25% primary porosity. It is not known whether primary porosity is preserved at depth or secondary porosity is developed.

Younger volcanigenic sediments such as the Rataman Formation are unlikely to contain thick, good quality reservoirs, except in cases where reworking has enhanced porosity and permeability. In general, the offshore equivalents of this unit and the underlying Punam Limestone (B-C and A-B sequences) are more likely to act as seals above the C-D sequence.

Both structural and stratigraphic traps are possible in the New Ireland Basin. Structural traps are most likely to occur where there has been extensive fault movement, such as on the basin margins in the southwest (Profile NI31), or on the Emirau-Feni Ridge in the northeast (Profile NI20; Fig. 6), or around the volcanic Tabar-Feni islands. Stratigraphic traps, on the other hand, probably exist over a wider area in the C-D sequence, in the form of porous and permeable reef or fore-reef carbonates. These would be sealed laterally by impermeable carbonates and vertically by impermeable carbonates or volcaniclastic sediments. Such traps are common in the Miocene sequences of Irian Jaya and Palawan. Traps in the C-D sequence would have been little affected by the Plio-Pleistocene tilting of the basin.

In summary, the New Ireland Basin does have petroleum potential, with the prime reservoir target being reefs in the C-D sequence. Organic-rich shale, siltstone, and limestone within and below this sequence would provide potential source rocks. Trapping would be most likely stratigraphic, but structural traps could also be present near the basin margins. The most prospective areas in water shallower than 1000 m lie north and west of New Hanover and northwestern New Ireland, where a thick sedimentary section and stratigraphic traps may exist, and perhaps on the Emirau-Feni Ridge between Mussau and Emirau Islands, where structural targets may be found. Other prospective areas lie in deeper water.

Acknowledgements

We are most grateful to Lamont-Doherty Geological Laboratory for their provision of unpublished core data. The interpretation of the onshore geology relies heavily on the foraminiferal studies of Dr D. Haig of the University of Papua New Guinea, and the foraminiferal dating of the offshore dredge material was carried out by Dr D.J. Belford of BMR. Drafts of this paper were substantially improved in the light of comments by J.B. Colwell, C.M. Brown and R.W. Johnson (BMR), and M. Marlow (USGS).

References

Brown, C.M., 1982 — Kavieng, Papua New Guinea — 1:250 000 Geological Series. *Geological Survey of Papua New Guinea, Explanatory Notes* SA/56-9.

Buchbinder, B., & Halley, R.B., in press — Source rock evaluation of outcrop and borehole samples from Tongatapu and Eua Islands, Tonga, and from Viti Levu and Vanua Levu Islands, Fiji. *In* Scholl, D., & Vallier, T., (editors), Geology and offshore resources of Pacific island arcs — Tonga region. *Circum-Pacific Energy and Mineral Resource Council, Earth Science Series,* 2.

Connelly, J.B., 1976 — Tectonic development of the Bismarck Sea based on gravity and magnetic modelling. *Geophysical Journal of the Royal Astronomical Society,* 46, 23-40.

Curtis, J.W., 1973 — Plate tectonics and the Papua New Guinea Solomon Islands region. *Journal of the Geological Society of Australia,* 20, 21-36.

De Broin, C.E., Aubertin, F., & Ravenne, C., 1977 — Structure and history of the Solomon-New Ireland region. *In* International symposium on geodynamics in south-west Pacific, Noumea, 1976. *Edition Technip, Paris.* 37-50.

Eade, J.V., 1979 — Papua New Guinea offshore survey, Cruise SI-79(1). *CCOP/SOPAC Cruise Report* 24 (unpublished).

Exon, N.F., 1981 — Papua New Guinea geophysical survey: Hydrocarbons. Cruise PN-81(1). *Committee for Coordination of Joint Prospecting for Mineral Resources in South Pacific Offshore Areas, Cruise Report* 52 (unpublished).

Exon, N.F., & Tiffin, D.L., 1984 — Geology and petroleum prospects of offshore New Ireland Basin in northern Papua New Guinea. *In* Watson, S.T., (editor), *Transactions of the Third Circum-Pacific Energy and Mineral Resources Conference,* 623-630.

Exon, N.F., Colwell, J.B., & Bolton, B., 1984 — Sedimentology of Quaternary cores from the Solomon Islands offshore region. *Committee for Coordination of Joint Prospecting for Mineral Resources in South Pacific Offshore Areas Technical Report,* 34, 209-243.

Exon, N.F., & Herzer, R.H., in press — Mixed volcaniclastic and pelagic sedimentary rocks from the Cenozoic Tonga Platform, and their implications for petroleum potential. *Circum-Pacific Energy and Mineral Resource Council Earth Science Series,* 2.

Falvey, D.A., & Pritchard, T., 1984 — Preliminary paleomagnetic results from northern Papua New Guinea : evidence for large microplate rotations. *In* Watson, S.T., (editor), *Transactions of the Third Circum-Pacific Energy and Mineral Resources Conference.* 593-599.

Free, E.R., Weissel, J.K., & Hobart, M.A., 1982 — Geothermal surveys in the Solomons Island arc. *EOS,* 63(45), 1120 (abstract).

Gulf Research and Development Company, 1973 — Regional marine geophysical reconnaissance of Papua New Guinea, 1973. (unpublished profiles available from BMR Division of Marine Geosciences & Petroleum Geology, Canberra).

Hatley, A.G., & Harry, R.Y., 1980 — Exploration and development of the Nido Reef Compex oil discovery, Philippines. *Committee for Coordination of Joint Prospecting for Mineral Resources in South Pacific Offshore Areas, Technical Bulletin,* 3, 253-260.

Hohnen, P.D., 1978 — Geology of New Ireland, Papua New Guinea. *Bureau of Mineral Resources, Australia, Bulletin* 194.

Johnson, R.W., 1979 — Geotectonics and volcanism in Papua New Guinea: a review of the late Cenozoic. *BMR Journal of Australian Geology & Geophysics,* 4, 181-207.

Johnson, R.W., Mutter, J.C. & Arculus, R.J., 1979 — Origin of the Willaumez- Manus Rise, Papua New Guinea. *Earth and Planetary Science Letters,* 44, 247-260.

Kroenke, L.W., in press — Cainozoic tectonic development of the southwest Pacific. *Committee for Coordination of Joint Prospecting for Mineral Resources in South Pacific Offshore Areas, Technical Bulletin,* 6.

Kroenke, L.W., Jouannic, C., & Woodward, P., 1983 — Bathymetry of the southwest Pacific. Map, scale 1:6 442 192. *Committee for Coordination of Joint Prospecting for Mineral Resources in South Pacific Offshore Areas, Suva, Fiji.*

Marlow, M., Exon, N.F., & shipboard party, 1984 — Initial report on 1984 R.V. S.P. Lee Cruise L7-84-SP in northern Papua New Guinea. *Committee for Coordination of Joint Prospecting for Mineral Resources in South Pacific Offshore Areas, Cruise Report* 95 (unpublished).

Mitchell, P.A., & Weiss, T.V., 1982 — Prospecting Authority 465, New Ireland, Papua New Guinea. Final report. *Esso Papua New Guinea Inc. Report, Geological Survey of Papua New Guinea open file* (unpublished).

Taylor, B., 1979 — Bismarck Sea : evolution of a back-arc basin. *Geology,* 7, 171-174.

Tiffin, D.L., 1981 — Papua New Guinea offshore hydrocarbon and phosphate survey, Cruise PN-81(2). *Committee for Coordination of Joint Prospecting for Mineral Resources in South Pacific Offshore Areas, Cruise Report* 53 (unpublished).

Wallace, D.A., Chappell, B.W., Arculus, R.J., Johnson, R.W., Perfit, M.R., Crick, I.H., Taylor, G.A.M., & Taylor, S.R., 1983 — Cainozoic volcanism in the Tabar, Lihir, Tanga and Feni islands, Papua New Guinea : geology, whole-rock analyses, and rock-forming mineral composition. *Bureau of Mineral Resources. Australia, Report* 243; *BMR Microform* MF 197.

BMR Journal of Australian Geology & Geophysics, 10, 53-63 ©Commonwealth of Australia 1986

Stratigraphy and sedimentology of Late Palaeozoic glaciomarine sediments beneath the Murray Basin, and their palaeogeographic and palaeoclimatic significance

P. E. O'Brien[1]

Sediments of the Late Palaeozoic Urana Formation in infrabasins beneath the Cainozoic Murray Basin include glaciomarine diamictite, fine-grained sediment, sandstone, and conglomerate facies. The facies assemblage is dominated by paratillites, formed by ice-rafting, and fine-grained sediments with a small ice-rafted component. Rhythmically bedded siltstone and claystone, sediment gravity-flow diamictites, traction-current deposits, and, possibly, subglacial tillites are also present. Interpretation of the facies indicates that grounded-ice deposits are absent from the glaciomarine sequence over large areas of the basin and has enabled estimation of the likely limits of grounded ice. Palaeontological and sedimentological evidence suggests that these rocks were deposited towards the end of the major Late Palaeozoic glaciation of southeastern Australia.

Introduction

Late Palaeozoic sediments across southeastern Australia clearly bear the marks of glacial processes. Striated bedrock surfaces and faceted and striated clasts are abundant in diamictites and dropstone laminites in outcrops in South Australia, Victoria, and Tasmania (Crowell & Frakes, 1972a,b). Infrabasins beneath the Cainozoic Murray Basin contain an array of similar, poorly sorted, pebbly facies, but they also contain, in places, marine fossils. Though these fossiliferous sediments are the same age as the glacial sediments, they have been largely ignored in studies of the Late Palaeozoic palaeogeography of southeastern Australia (e.g. Crowell & Frakes, 1971a,b). This paper reappraises data gathered by exploration companies and government geological surveys, and presents new sedimentological data and considers the light they shed on the palaeogeography and palaeoclimatic history of southeastern Australia during the major Late Palaeozoic glaciation.

The Late Palaeozoic sediments beneath the Murray Basin have been loosely described as glaciomarine in character (Thornton, 1974), but have never been the subject of lithofacies analysis. The lithofacies include diamictite, mudstone, sandstone, and conglomerate deposited in a glaciomarine setting. Lithofacies assemblages in some infrabasins suggest that grounded glacial ice never reached some areas, and so provide an estimate of the limits of the Late Palaeozoic ice sheets in southeastern Australia. Vertical changes in lithofacies assemblages also enable dating of the final retreat of the Late Palaeozoic ice mass from the region.

Geological setting

Tertiary and Quaternary sediments of the Murray Basin form a continuous blanket, up to 600 m thick, over at least nine infrabasins containing Late Palaeozoic and Mesozoic (Devonian to Cretaceous) sediments (Fig. 1, Table 1). Both the Murray Basin and infrabasin sediments rest on Early to Mid-Palaeozoic metasediments and granite. Geophysical evidence suggests that the infrabasins contain up to 6 km of sediment and are bounded by normal faults, although, as yet, drilling has penetrated only 2100 m of pre-Tertiary sediments (Thornton, 1974) and there are areas in which Late Palaeozoic and Mesozoic sediments overlap the boundary faults. Late Palaeozoic sediments are present in all but the Bundy Trough (O'Brien, 1981). The greatest thickness yet penetrated is in the Ovens Graben, where up to 70 m of Late Permian coal measures overlies 887 m of Early Permian sediments (Wright & Stuntz, 1963; Yoo, 1983).

Late Palaeozoic sediments beneath the Murray Basin consist of two units, the Late Permian Coorabin Coal Measures and an older unit, herein named the Urana Formation (see Appendix 1 for full definition). The Urana Formation contains Stage 2 and Stage 3 microfloras of Kemp & others (1977) and is, therefore, Late Carboniferous to Permian in age: Kemp & others (1977) regard Stage 2 as latest Carboniferous and Stage 3 as earliest Permian, whereas Archbold (1982) regards both stages as Early Permian (Table 2).

Table 1. Stratigraphy of infrabasins beneath the Murray Basin. Thicknesses in metres

Infrabasin	Reference well	Cainozoic	Mesozoic	Permo-Carb	Devonian
Renmark	North Renmark No. 1	548	440	>235	
Paringa Embayment	Nadda No. 1	449	179	395	0
Tararra Trough	Tararra No. 1	440	90	323	>1022
Blantyre Trough	Blantyre No. 1	184	0	169	>1883
Wentworth Trough	Wentworth No. 1	329	101	>145	
Ivanhoe Trough	Ivanhoe No. 1	107	39	285	> 178
Bundy Trough	Killendoo No. 1	357	0	0	> 398
Ovens Graben	Jerilderie No. 1	362	202	957	0
Numurkah Trough	Katunga No. 1	158	0	>64	

[1]Division of Continental Geology,
Bureau of Mineral Resources,
GPO Box 378,
Canberra, ACT 2601

Facies descriptions

The Urana Formation contains four groups of facies: diamictite, fine-grained sediment (mostly siltstone and claystone), sandstone, and conglomerate facies (Table 3).

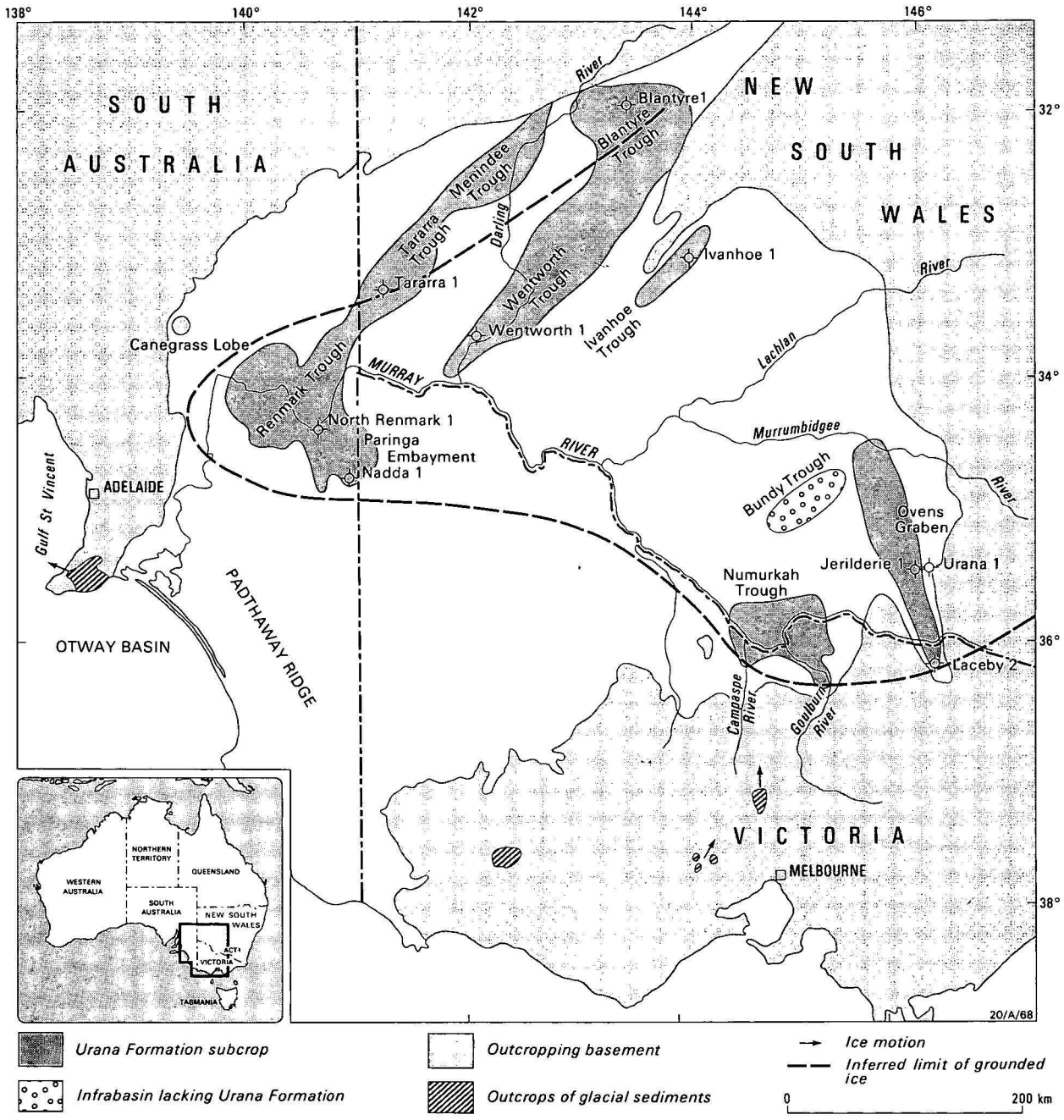

Figure 1. Infrabasins beneath the Murray Basin, distribution of the Urana Formation, and inferred limit of grounded ice during the Late Palaeozoic glaciation of southeastern Australia.

Table 2. Alternative correlations of Late Palaeozoic microfloras in eastern Australia (Kemp & others, 1977; Archbold, 1982).

Microfloral stage	Permo-Carboniferous boundary	
	Kemp & others (1977)	Archbold (1982)
Stage 3	Early Permian	
Stage 2	Late Carboniferous	Early Permian
Stage 1		Late Carboniferous

Diamictites

Diamictites in the Urana Formation are of three types, which have different proportions of pebbles and sand, and different bedding characteristics.

Facies D_1 is fine-grained with a clayey and fine sandy silt matrix surrounding medium to coarse sand and scattered pebbles (Fig. 2). It forms massive to faintly laminated beds from a few centimetres to over 20 cm thick. Many beds have gradational upper and lower boundaries.

Facies D_2 has a similar grain-size distribution to that of some silty subglacial tillites in central Victoria (O'Brien, 1981). It contains more medium to coarse sand and pebbles than facies D_1. Beds range from 5 cm to over 20 cm thick and are massive (Fig. 3). Contacts with other facies are sharp and irregular, with small flame structures along the contact. Fragments of mudstone and diamictite from other facies are present in some cores.

Table 3. Facies of the Urana Formation

Facies	Lithology	Interpretation
D_1	Fine diamictite; gradational bed boundaries.	Compound paratillite.
D_2	Diamictite; sharp bed boundaries; mud clasts.	Sediment gravity-flow deposits or subglacial tillite.
D_3	Fine diamictite; claystone matrix; thin, gradational bedding.	Compound paratillite.
M_1	Massive to poorly laminated mudstone.	Settling of suspended mud.
M_2	Graded siltstone–claystone couplets 2mm to 5 cm thick.	Deposition from episodic, waning currents.
M_3	Interbedded mudstone and fine sandstone.	Alternating deposition by currents and settling of suspended mud.
S_1	Poorly sorted, silty coarse sandstone. Massive to faintly laminated.	Rapid deposition by currents, possibly high density turbidity currents.
S_2	Massive medium sandstone.	Current deposition.
S_3	Parallel laminated to ripple cross-laminated fine sandstone.	Current deposition.
Conglomerate	Coarse sandy conglomerate.	Deposition from high energy currents in deltas, sub-aqueous outwash fans and beaches.

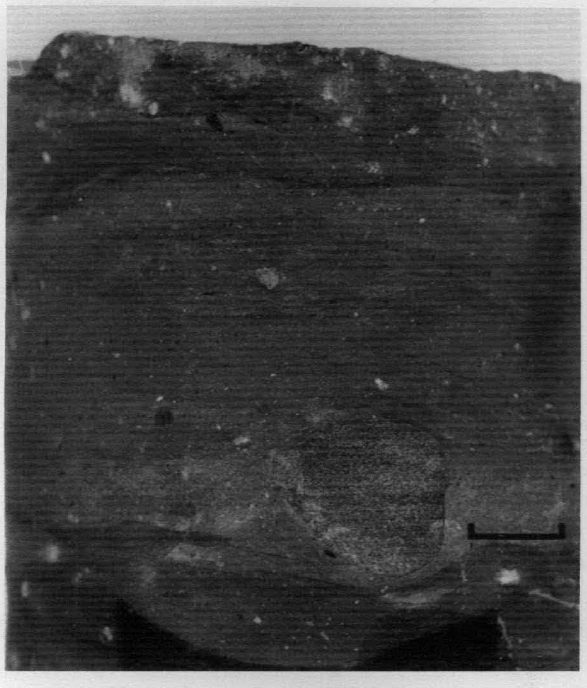

Figure 2. Facies D_1. Faintly laminated silty diamictite deposited by ice-rafting.
Core from Jerilderie No. 1. Scale bar = 1 cm.

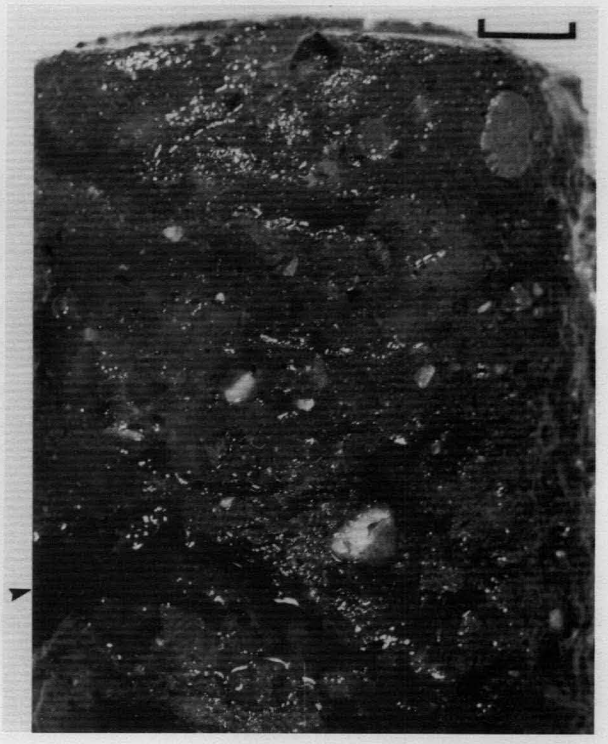

Figure 3. Facies D_2. Massive, tillite-like diamictite. Arrow indicates mud clast.
Core from Jerilderie No. 1. Scale bar = 1 cm.

Facies D_3 is poorly laminated claystone with abundant coarse sand grains and scattered pebbles (Fig. 4). Many pebbles are oversized compared to the laminae in which they rest. Beds are up to 5 cm thick and have gradational boundaries with overlying and underlying beds of mudstone facies and facies D_1.

Fine-grained sediment

Three facies consisting mostly of siltstone and claystone are common in the Urana Formation.

Facies M_1 is massive to poorly laminated mudstone with minor fine sand and rare pebbles. Beds range from 10 cm to over 30 cm thick. Most cores are massive, but a few from Jerilderie No. 1 show faint and discontinuous horizontal laminae and burrowed horizons. Arenaceous foraminifera of the genera *Ammodiscus* and *Hyperammina* are present in some cores. Common features of this facies are red-brown ferruginous patches and concretions.

Facies M_2 consists of graded siltstone and claystone couplets from 2 mm to 5 cm thick (Fig. 5). The base of each unit is sharp and the lower siltstone grades continuously into the overlying claystone. Some cores contain scattered coarse sand grains, most commonly in the claystone part of the graded units, and some contain clasts of a medium sand framework in a mud matrix. These clasts have indistinct boundaries with the surrounding sediment. Facies M_2 is commonly deformed, either by clay beds intruding the bottom of the siltstones and breaking them into boudins or by mixing of the interbeds accompanied by small recumbent folds. This mixing and folding may affect over 40 cm thickness of sediments and tends to destroy the well-bedded structure of the facies (Fig. 6).

Facies M_3 consists of thin mudstone, graded and ungraded fine sandstone beds, and rare sandstone beds consisting of single ripple cross-sets. The beds are mostly less than 1 cm thick.

Sandstone

Sandstone beds are common in some parts of the Urana Formation. The few cores cut in sandstone consist of three facies.

Figure 4. Facies D_3. Diamictite formed by ice-rafting of sand and gravel into clay.
Core from Wentworth No. 1. Scale bar = 1 cm.

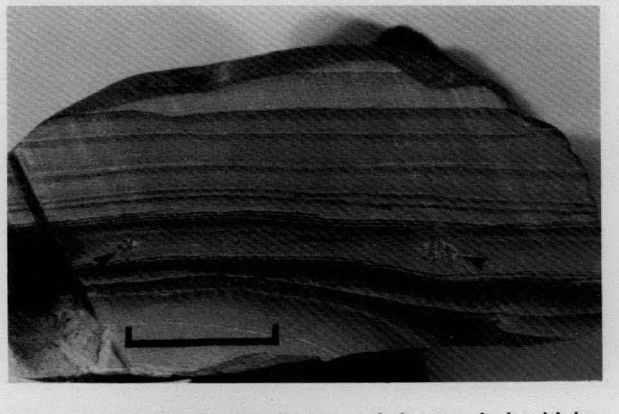

Figure 5. Facies M_2. Graded siltstone and claystone beds with ice-rafted till pellets indicated by arrows.
Scale bar = 1 cm.

Facies S_1 is poorly sorted, silty coarse sandstone with rare pebbles and mud clasts. It forms beds from 1.5 cm thick (Fig. 7) to over 30 cm thick. The facies is massive in most cores, though some contain faint horizontal laminae, and the thin bed in Figure 7 is normally graded over the upper 0.5 cm.

Facies S_2 is white, massive, well-sorted medium sandstone, commonly with a carbonate cement.

Facies S_3 is yellow fine sandstone showing parallel laminae or ripple cross-bedding. Some cores contain fine fragments of organic matter scattered along laminae. Beds range from 1 cm to over 5 cm thick.

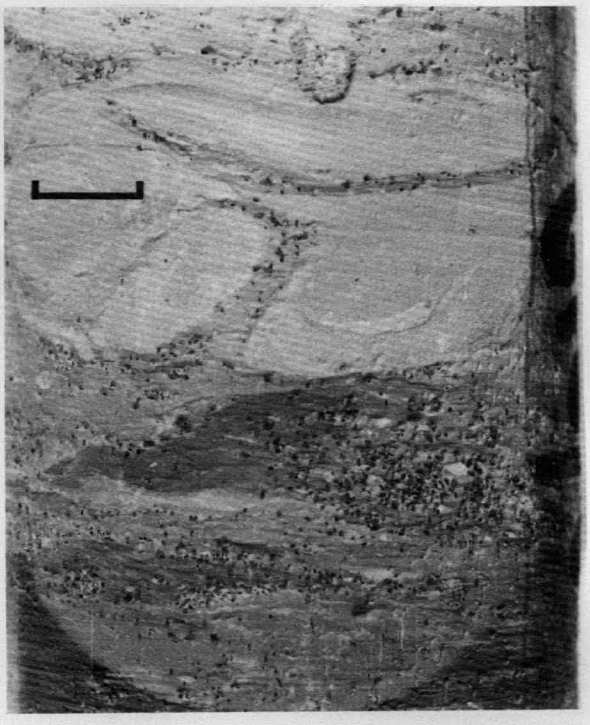

Figure 6. Facies M_2 that has suffered soft-sediment deformation.
The light grey siltstone forms load casts separated by flames of underlying claystone. The darker claystone contains abundant ice-rafted coarse sand. Scale bar = 1 cm.

Figure 7. A normally graded bed of facies S_1 interbedded with facies M_1.
Scale bar = 1 cm.

Conglomerate

A few wells penetrate sandy, boulder conglomerate. This facies is clast supported, with up to 20 per cent coarse sand

Table 4. Facies assemblages and microfloras from various sequences in the Urana Formation.

Section	D_1	D_2	D_3	M_1	M_2	M_3	S_1	S_2	S_3	Cong	Microflora
Nadda-1	2	—	—	—	2	—	2	—	—	—	Stage 2
North Renmark-1	—	—	—	—	2	2	—	—	—	2	Stage 2
Wentworth-1	—	—	2	—	2	—	1	—	—	1	Stage 2
Tararra-1	—	2	—	2	—	—	—	—	2?	—	Stage 2
Blantyre-1	—	2	—	—	—	—	—	—	—	—	—
Laceby-2	2	2	—	1	—	—	2	—	1	1	—
Numurkah Trough	2	2	—	2	—	—	—	—	—	—	Stages 2 & 3
Jerilderie-1	2	1	—	2	—	—	2	2	2	—	Stage 3

2 indicates major constituent of the section, 1 indicates a minor constituent. Palynology from Ludbrook (1962, 1963), Derrington & Anderson (1970), Boyd & Heibler (1967), McLeod (1977, 1978, 1979) and Morgan (1975b).

matrix, and framework clasts up to 15 cm across. One core has interbeds of coarse sandstone up to 5 cm thick in the conglomerate.

Well sequences

From cores, cuttings, and geophysical logs, it is possible to draw tentative conclusions on the assemblage of facies in various parts of the Urana Formation (Table 4, Figs 8-15).

The most abundant facies in the Urana Formation appear to be D_1, M_1, and M_2. Tillite-like facies D_2 is abundant in Tarrara No. 1, Blantyre No. 1, Laceby No. 2, and part of the Numurkah Trough. In the other wells it is rare or absent. Conglomerate is a major part of the North Renmark No. 1 section (Fig. 8), but is only a minor part of the Urana Formation in Wentworth No. 1 and Laceby No. 2, and is not present in any other well. Blantyre No. 1 intersected a thick conglomerate, which Campe & Cundill (1965) correlated with Early Carboniferous sediments that crop out elsewhere in eastern Australia and which, therefore, is not part of the Urana Formation. Sandstone facies generally form relatively thin beds, but are abundant in parts of Nadda No. 1 and Jerilderie No. 1, and may constitute a major component of Tarrara No. 1, though it is not clear from core or cuttings what the intervals of negative S.P. response represent (Fig. 11).

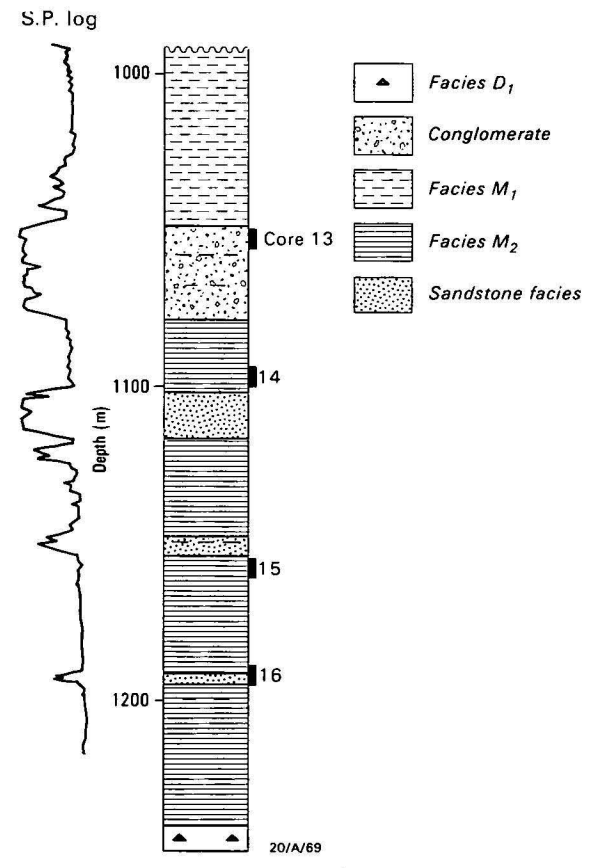

Figure 8. Interpreted lithological log of the Urana Formation in A.O.C. North Renmark No. 1.

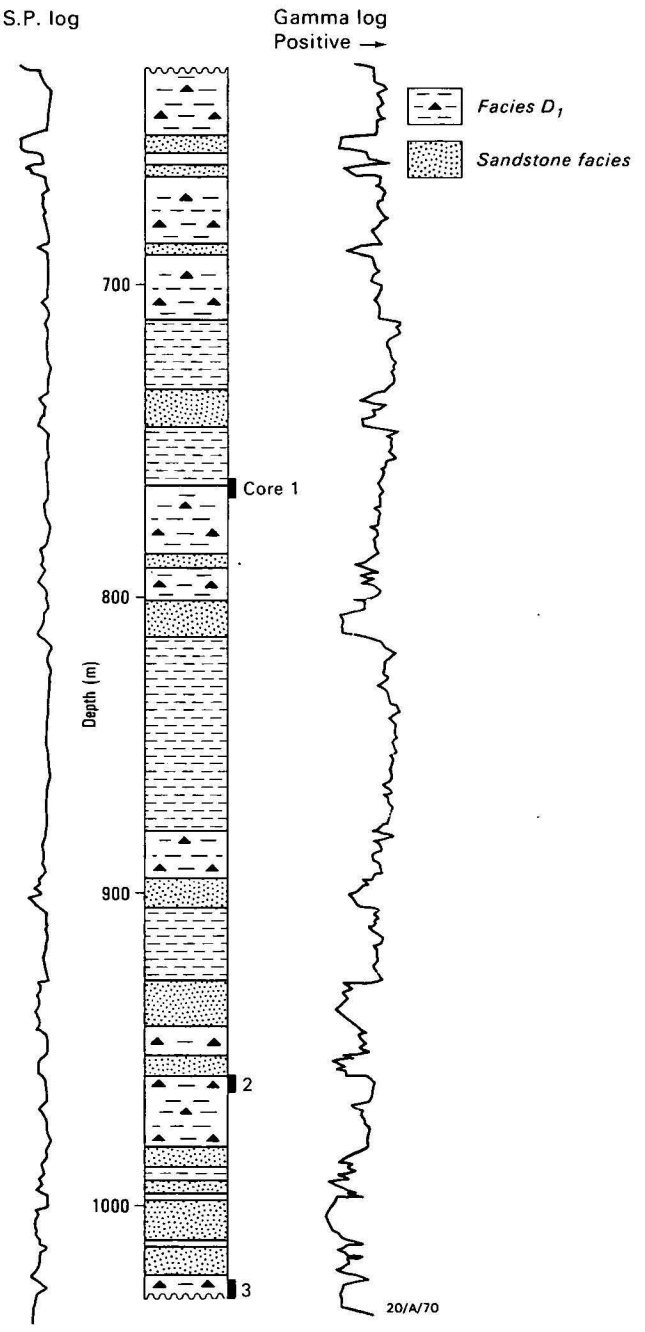

Figure 9. Interpreted lithological log of the Urana Formation in A.A.O. Nadda No. 1.

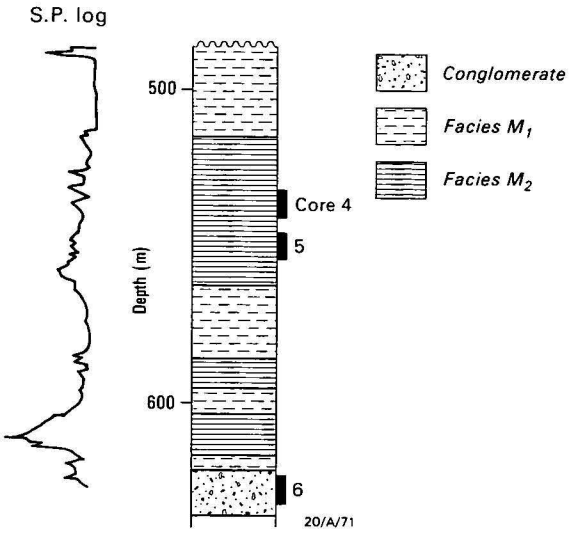

Figure 10. Interpreted lithological log of the Urana Formation in A.O.G. Wentworth No. 1.

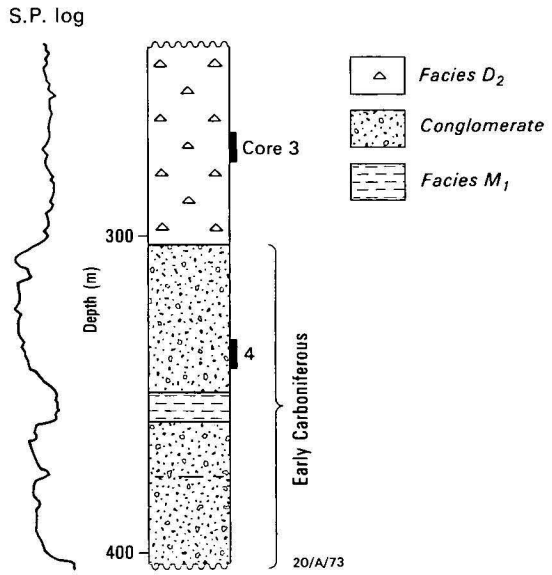

Figure 12. Interpreted lithological log of the Urana Formation and underlying Early Carboniferous sediments in Mid-East Oil Blantyre No. 1.

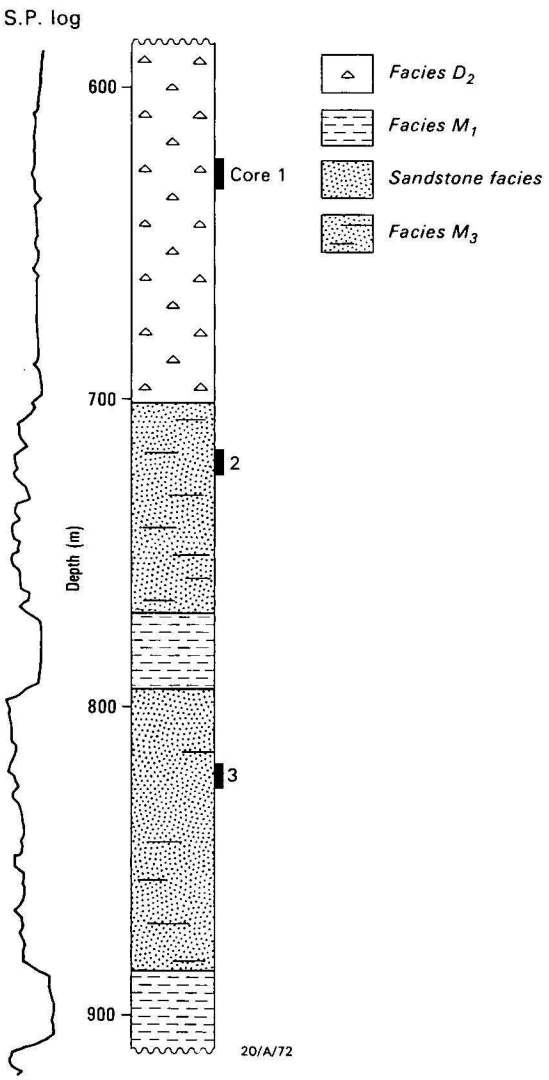

Figure 11. Interpreted lithological log of the Urana Formation in A.O.G. Tararra No. 1.

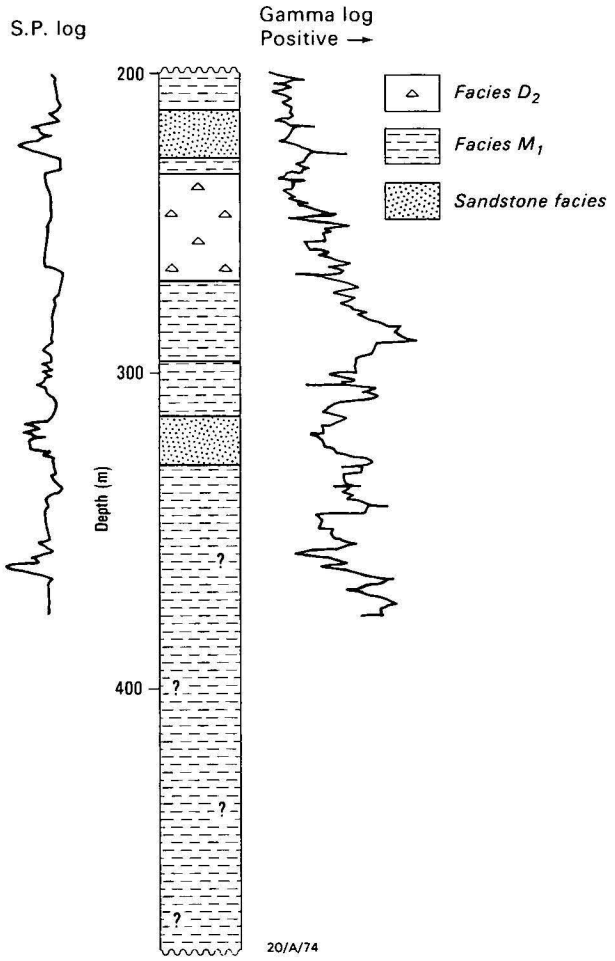

Figure 13. Interpreted lithological log of the Urana Formation in North Star Oil Ivanhoe No. 1.

The Numurkah Trough sequence and Jerilderie No. 1 show a vertical change in facies. In the Numurkah Trough, the subcrop around the southern margin consists mostly of facies D_2 and D_1, and contains a Stage 2 microflora. Further from

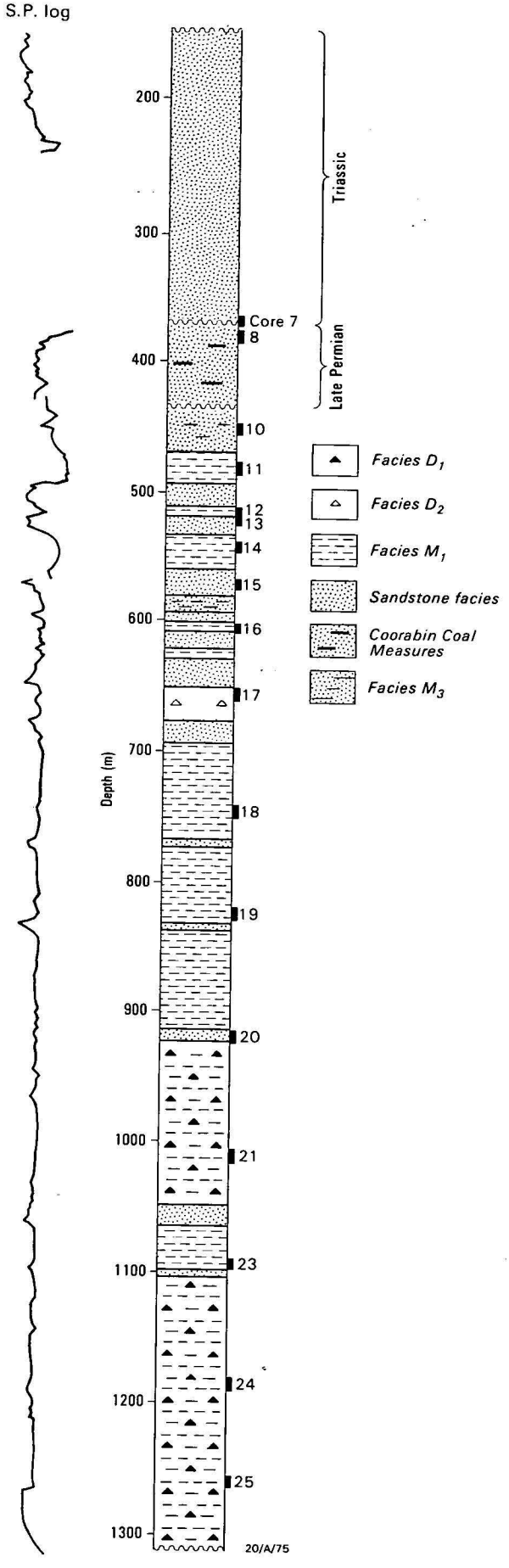

Figure 14. Interpreted lithological log of the Urana Formation in A.O.G. Jerilderie No. 1.

the margin, the predominant facies is M_1, which contains a Stage 3 microflora (Fig. 15; McLeod, 1977, 1978, 1979). In Jerilderie No. 1, the proportion of facies D_1 decreases up the sequence, with M_1 and S_1 becoming the most abundant facies (Fig. 14). The S.P. log of Jerilderie No. 1 suggests a sandstone sequence, coarsening upwards, over the upper part of the Urana Formation (Fig. 14).

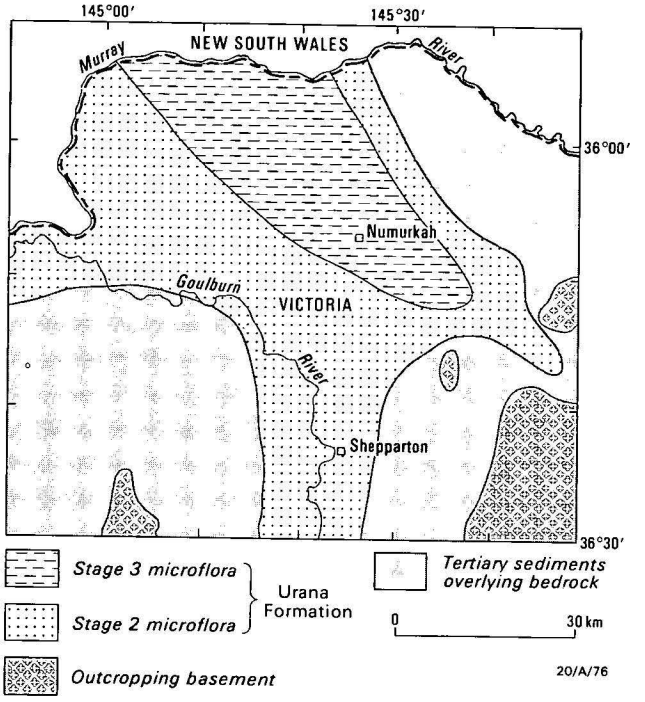

Figure 15. Subcrop of the Urana Formation in the Numurkah Trough. Sediments containing a Stage 2 microflora are mostly facies D_2 and those containing a Stage 3 microflora are mostly facies M_1.

Facies interpretation

Chronostratigraphic framework

Stratigraphically, the most important microfossils in the Urana Formation are palynomorphs that provide correlations between the various infrabasins and other sequences in Australia. According to the Late Palaeozoic palynozones defined by Kemp & others (1977), Stage 2 microfloras are present in the Renmark and Wentworth Troughs and the Paringa Embayment; Stage 2 and Stage 3 microfloras are present in the Numurkah Trough; and in the Ovens Graben the Urana Formation contains a Stage 3 microflora.

Kemp & others (1977) showed that these microfloras provide good correlations between Late Palaeozoic sequences in Australia, and therefore tie the Urana Formation into its regional context. Stage 2 microfloras are present in Late Palaeozoic sediments around the Murray Basin. In central Victoria and South Australia, these sediments contain abundant evidence of glacial activity, in the form of striated bedrock pavements, grooved pavements within the successions, streamlined erosion features, facetted and striated clasts, and imbricated boulder clusters (Crowell & Frakes, 1972a,b; Bowen & Thomas, 1976; Foster, 1974). In South Australia, diamictites associated with striated pavements are conformably overlain by sediments, similar to facies D_1 and

M_1, that contain the same genera of arenaceous foraminifera as the Urana Formation (Foster, 1974; Ludbrook, 1967). Therefore, the Urana Formation is probably the marine equivalent of the Late Palaeozoic glacial sediments that crop out in southeastern Australia, and it is reasonable to interpret the facies of the Urana Formation in terms of glacial and glaciomarine depositional processes.

Diamictite facies

In glaciomarine environments, three different sorts of diamictite may be present (Kurtz & Anderson, 1979; Anderson & others, 1980; Clarke & others, 1980; Drewry & Cooper, 1981; Gravenor & others, 1984; Eyles & Eyles, 1983).

1. **Paratillites** — diamictites formed by ice-rafting of sediment (Harland & others, 1966).

2. **Subglacial tillites** — diamictites deposited beneath glacial ice that grounds on the sea floor. Two types of subglacial tillite may be present in a glaciomarine depositional setting: lodgement tillite, deposited directly beneath the sole of active ice (Boulton & Deynoux, 1981), and undermelt tillite, deposited beneath glacial ice near the grounding line as a slurry by continuous basal melting (Gravenor & others, 1984).

3. **Sediment gravity-flow deposits** — diamictites formed by slumping of paratillites, subglacial tillites, or other sediments Kurtz & Anderson, 1979).

Paratillites are characterised by a range of sorting. Clarke & others (1980) recognised *compound* paratillites, consisting of a coarse component transported to the depositional site by floating ice and a hemipelagic component of normal suspended sediment brought in by the water mass, and *residual* paratillites, representing ice-rafted sediment from which the finer fractions have been removed by currents. Compound paratillites are distinctly bimodal, whereas residual paratillites are depleted in clay compared to equivalent unmodified subglacial tillites. Other features of paratillites are gradational bedding contacts, lateral and vertical variations in sorting, and sheet-like geometry. They may display horizontal laminae, and contain stones that depress bedding beneath them and are larger than the beds in which they rest. Also, Overshine (1970) described pellets of compressed till that, when released from floating glacial ice, resist disaggregation by waves and currents. Clarke & others (1980) reported such till pellets in abyssal plain sediments of the Arctic Ocean. Overshine (1970) also described carapace structures, which are piles of ice-rafted stones deposited when icebergs roll over.

Facies D_3 displays a bimodal size distribution, gradational bedding, and oversized stones, and is therefore probably a compound paratillite formed by rafting of the coarse fraction into an area of clay deposition. Facies D_1 is also a compound paratillite, resulting from rafting of sand and pebbles into silts. It probably represents higher rates of ice-rafted sediment deposition than D_3 because the sand fraction is much more abundant in facies D_1.

Massive, tillite-like facies D_2, however, has two possible origins: it may be sediment gravity-flow deposits or subglacial tillites deposited by ice advance into the basin. Subglacial tillites may be present along the southern margins of the Numurkah Trough and the Ovens Graben and in Tararra No. 1 and Blantyre No. 1, but the cores of facies D_2 recovered from the other petroleum wells are probably sediment gravity flows because they are thin and contain mudclasts ripped up from mud over which the flows moved.

Fine-grained sediment facies

Settling of fine particles from suspension produced the massive facies M_1 and the claystone parts of M_2 and M_3, but the graded siltstone parts of M_2 and the siltstone and sandstone laminae of M_3 indicate deposition by currents. Facies M_2 exhibits grading without clear separation of silt and clay parts of the graded beds. This sort of grading is typical of rhythmites deposited in marine environments where clay minerals flocculate and settle with part of the silt fraction (Duff & others, 1967).

Currents of three possible origins may have deposited the graded beds. Either density currents produced by meltwater inflow moving as underflows or overflows (Keunen, 1951), or turbidity currents generated by slumping of the sea floor (Carey & Ahmad, 1961), or currents generated by katabatic winds flowing off a large ice mass (Gilbert & Shaw, 1981) might have deposited the graded beds of facies M_2. The scattered coarse grains in facies M_1, M_2, and M_3 were probably ice-rafted into place.

In facies M_2, the development of flame structures and soft-sediment boudins, is the result of loading of the clays by rapid deposition of silts, causing clay-into-silt intrusion, but the complex mixing of siltstones and claystones with recumbent folding of laminae possibly results from slumping of the sea floor.

Sandstone facies

The sandstone facies are difficult to interpret with any certainty because of the small cores available. The poor sorting of facies S_1 suggests rapid deposition from currents carrying a wide range of particle sizes (Stewart & La Marche, 1967), such as high-density turbidity currents (Lowe, 1981). These currents were powerful enough to erode mud clasts from underlying sediment. The other two sandstone facies are finer and better sorted than S_1, suggesting more consistent currents. In a glaciomarine setting, sandstone might be deposited as part of subaqueous outwash fans or deltas (Banerjee & McDonald, 1975), by tidal or wind-generated currents sorting the sea bed, or by slump-generated turbidity currents. Sandstone facies in the upper part of Jerilderie No. 1 give an S.P. log signature that suggests an upward coarsening, deltaic sequence (Fig. 14), but elsewhere in the basin, evidence for the origin of the sandstones present is lacking.

Conglomerate facies

The small size of the cores taken in the conglomerates makes it difficult to draw any conclusions on the origin of this facies, other than that high-energy conditions prevailed during deposition. Likely depositional settings for conglomerate in glaciomarine environments are deltas, subaqueous outwash fans, and beaches.

Discussion

Correlations within the Urana Formation

The microfloras within the Urana Formation suggest possible correlations between well sections (Fig. 16). Nadda No. 1, Wentworth No. 1, and North Renmark No. 1 contain Stage 2 microfloras (Derrington & Anderson, 1970; Ludbrook, 1962, 1963). Paten & Price (*in* Derrington & Anderson, 1970) considered that the microfloras of Wentworth No. 1 and North Renmark No. 1 are more diverse and, hence, slightly younger than that of Nadda No. 1. Morgan (1975) listed a Stage 3 microflora from low in the Jerilderie No. 1 section,

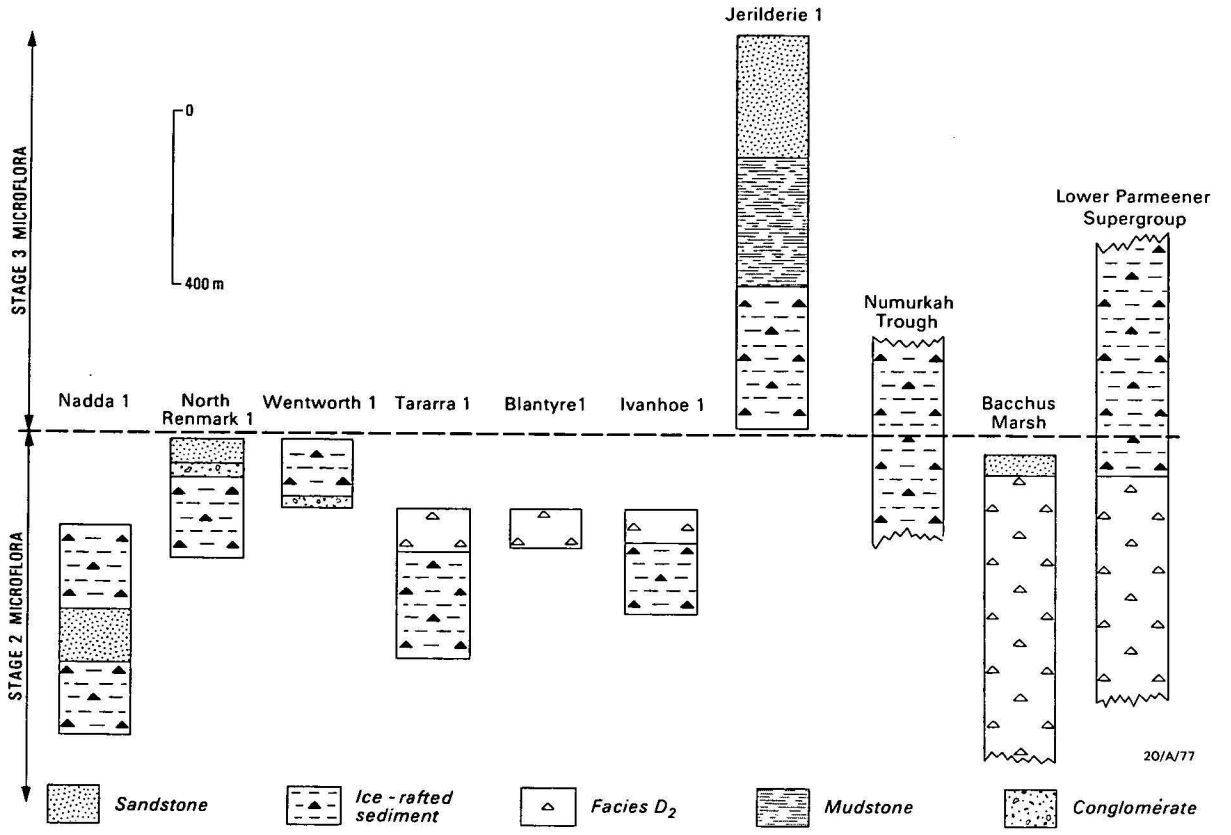

Figure 16. Correlation of Urana Formation sections with each other and with the Late Palaeozoic sequences in central Victoria (Bacchus Marsh) and Tasmania (Lower Parmeener Supergroup).

implying that Nadda No. 1, North Renmark No. 1, and Wentworth No. 1, and Jerilderie No. 1 were deposited approximately consecutively. The palynological zones are too coarse to identify gaps or overlap between these sections (Fig. 16).

The Numurkah Trough sequence ranges from Stage 2 to Stage 3 (McLeod, 1977, 1978, 1979). Of the other petroleum wells, Tararra No. 1 yielded a Stage 2 microflora (Boyd & Heibler, 1967; Evans, 1977), but Blantyre No. 1 and Ivanhoe No. 1 did not produce an identifiable microflora. In Figure 16, Blantyre No. 1 and Ivanhoe No. 1 are tentatively correlated with holes containing Stage 2 microflora because the sediments and the settings of these two well sequences are broadly similar to Tararra No. 1.

Palaeogeography

Depositional environment. The most abundant facies in the Urana Formation beneath the Murray Basin are paratillites and mudstone, with sandstone, mass-flow diamictites, and tillites less abundant. Some of the sandstones and conglomerates may be deltaic deposits. This facies assemblage suggests that the Murray Basin area was a shallow marine basin with ice masses encroaching on its edges at times and deltas prograding into it.

The nature of the ice that deposited the paratillites in the Urana Formation remains a problem. The till pellets found in the formation (Fig. 5) imply floating glacial ice (Overshine, 1970), but whether this was in the form of ice shelves or icebergs is impossible to determine from the available data.

Position of the ice margin. The Nadda No. 1 sequence is the oldest Urana Formation section (Derrington & Anderson, 1970), and consists of compound paratillite, sandstone, and mudstone, whereas the slightly younger North Renmark No. 1 and Wentworth No. 1 sequences contain less ice-rafted detritus and more facies resembling density-current deposits, and include beds of conglomerate. These facies assemblages suggest that grounded glacial ice did not extend to the Paringa Embayment, Renmark Trough, and Wentworth Trough during the period represented by these three sections. It is unlikely that grounding of the ice would leave no trace, because the ice was probably wet-based and, upon retreating, it would leave a blanket of tillite deposited at the grounding line (Carey & Ahmad, 1961). Striated pavements and other indicators of ice motion in the Late Palaeozoic outcrop areas of Victoria show ice movement from south to north (Bowen & Thomas, 1976). Therefore, the grounded ice probably did not extend as far north as the southern edge of the Paringa Embayment on the southwestern side of the Murray Basin (Fig. 1).

Tararra No. 1 and Blantyre No. 1 contain relatively large proportions of facies D_2, suggesting that glaciers may have covered parts of the Tararra and Blantyre Troughs. Such ice would have come from a landmass to the northwest, because these areas lie north of the Renmark and Wentworth Troughs, which ice from the south is unlikely to have crossed, and because debris was fed by ice into other basins to the north and northwest (Crowell & Frakes, 1971a,b).

The Numurkah Trough and Ovens Graben may have tillites along their southern margins. The few cores of Numurkah Trough sediments along its southern margin contain massive tillite-like facies D_2. These diamictites pass up into mudstone facies, suggesting that the ice retreated at some time close to the change from Stage 2 to Stage 3 microfloras. The southern end of the Ovens Graben is surrounded by patchy outcrops of tillite (M. Craig, personal communication, 1981)

and the sequence in Laceby No. 2 may include tillites, so that this part of the graben was possibly covered by grounded ice. In Jerilderie No. 1, however, there is no evidence for grounded ice during deposition, probably because the graben was not active until after the ice had retreated. This is inferred from the Stage 3 microflora found near the base of the sequence (Morgan, 1975), in which case the tillites at the southern end of the graben must have been deposited close to the edge of an ice mass or be remnants of a more extensive blanket of tillite eroded from the area of the northern part of the Ovens Graben before the graben formed. Craig & Brown (1984) presented evidence that suggests small glaciers developed around the southern end of the Ovens Graben, so it seems likely that major ice sheets did not reach the central part of the Ovens Graben.

Thus, from the evidence offered by the Urana Formation, the maximum extent of grounded ice in this area is as shown in Figure 1. This estimate is tentative because of the widely spaced data points and coarse biostratigraphic control.

Climatic change during deposition of the Urana Formation

Nadda No. 1, North Renmark No. 1, Wentworth No. 1, the Numurkah Trough sequence, and Jerilderie No. 1 form a roughly continuous sequence spanning the time during which the Stage 2 microflora changed to Stage 3 (Fig. 16). The amount of ice-rafted detritus in North Renmark No. 1 and Wentworth No. 1 — the two younger Stage 2 sequences — is less than in Nadda No. 1. This, taken with the facies change associated with the microfloral change in the Numurkah Trough, suggests that glacial ice retreated from the southern edge of the Murray Basin area just before the arrival of the Stage 3 microflora. This change has also been recorded in outcrops of the Cape Jervis beds in South Australia (Foster, 1974) and in Late Palaeozoic sections in Tasmania (Kemp, 1978).

The trend to lesser amounts of ice-rafted detritus continues in Jerilderie No. 1, with 350 m of paratillite (facies D_1) passing vertically into mudstones with a much smaller ice-rafted component (facies M_1). The sequence then becomes sandier, with a microfauna that suggests a brackish or turbid environment (Harris & McGowran, 1971). The shape of the S.P. curve (Fig. 14) may represent a regressive sequence (cf. Davies, 1980) which, taken with the microfauna, suggests that this part of the Jerilderie No. 1 sequence may be deltaic. The plume of fresh, turbid water from a delta would cause the restricted microfauna, and slumping of the delta-front sediments might explain the beds of diamictite (facies D_2). Thus, the Urana Formation in Jerilderie No. 1 reflects a gradual reduction in the amount of floating ice and, hence, an improvement in the climate.

Conclusions

The Urana Formation beneath the Murray Basin consists of glaciomarine sediments deposited in a series of small intracratonic basins during the Late Palaeozoic glaciation of southeastern Australia. The most common facies present are paratillite and mudstone with an ice-rafted component of coarse clasts. Siltstones deposited by density currents, mudflow diamictites, and sandstones and conglomerates deposited by various types of currents are also present, and subglacial tillites may be present on the margins of some infrabasins. Microfloral assemblages and facies sequences indicate that deposition of the Urana Formation spanned the period of final waning of the glaciation.

References

Anderson, J.B., Kurtz, D.D., & Domack, E.W., & Balshaw, K.M., 1980 — Glacial marine sediments of the Antarctic continental shelf. *Journal of Geology,* 88, 399-414.

Archbold, N.W., 1982 — Correlation of the Early Permian faunas of Gondwana: implications for the Gondwana Carboniferous-Permian boundary. *Journal of the Geological Society of Australia,* 29, 267-276.

Banerjee, I., & McDonald, B.C., 1975 — Nature of esker sedimentation. *In* Jopling, A.V., & McDonald, B.C., (editors), Glaciofluvial and glaciolacustrine sedimentation. *Society of Economic Paleontologists and Mineralogists, Special Publication,* 23, 132-154.

Boulton, G.S., & Deynoux, M., 1981 — Sedimentation in glacial environments. *Precambrian Research,* 15, 397-422.

Bowen, R.L., & Thomas, G.A., 1976 — Permian. *In* Douglas, J.G. & Ferguson, J.A., (editors), Geology of Victoria. *Geological Society of Australia, Special Publication,* 5, 125-141.

Boyd, B., & Heibler, H.H., 1967 — A.O.G. Tararra No. 1 well, New South Wales, well completion report. *Bureau of Mineral Resources, Australia, Petroleum, Search Subsidy Acts File* 66/4238 (unpublished).

Campe, B., & Cundill, J., 1965 — Mid-eastern Oil N.L. Blantyre No. 1 well completion report. *Bureau of Mineral Resources, Australia, Petroleum Search Subsidy Acts File* 64/4131 (unpublished).

Carey, S.W., & Ahmad, N., 1961 — Glacial marine sedimentation. *In* Raasch, G.O., (editor), Geology of the Arctic. *University of Toronto Press, Toronto, Ontario.* 865-894.

Clarke, D.L., Whitman, R.R., Morgan, K.A., & Mackey, S.D., 1980 — Stratigraphy and glacial-marine sediments of the Amerasian Basin, central Arctic Ocean. *Geological Society of America, Special Paper,* 181.

Craig, M.A., & Brown, M.C., 1984 — Permian glacial pavements and ice movement near Moyhu, north-east Victoria. *Australian Journal of Earth Sciences,* 31, 439-444.

Crowell, J.C., & Frakes, L.A., 1971a — Late Palaeozoic glaciation of Australia. *Journal of the Geological Society of Australia,* 17, 115-155.

Crowell, J.C., & Frakes, L.A., 1971b — Late Palaeozoic glaciation: Part IV, Australia. *Geological Society of America Bulletin,* 82, 2515-2540.

Davies, D.K., 1980 — Sandstone reservoirs — their genesis, diagenesis and diagnosis for successful exploration and development. *Petroleum Exploration Society of Australia, Distinguished Lecturer Series,* June 1980, Course Notes.

Derrington, S.S., & Anderson, J.C., 1970 — A.A.O. Nadda No. 1 well completion report. *Bureau of Mineral Resources, Australia, Petroleum Search Subsidy Acts File* 70/234 (unpublished).

Drewry, D.J., & Cooper, A.P.R., 1981 — Processes and models of Antarctic glaciomarine sedimentation. *Annals of Glaciology,* 2, 117-122.

Duff, P.McL.D., Hallam, A., & Walton, E.K., 1967 — Cyclic sedimentation. *Developments in Sedimentology,* 10, *Elsevier, Amsterdam.*

Eyles, C.H., & Eyles, N., 1983 — Sedimentation in a large lake: a reinterpretation of the late Pleistocene stratigraphy at Scarborough Bluffs, Ontario, Canada. *Geology,* 11, 146-152.

Foster, C.B., 1974 — Stratigraphy and palynology of the Permian at Waterloo Bay, Yorke Peninsular, South Australia. *Transactions of the Royal Society of South Australia,* 98, 29-42.

Gilbert, R., & Shaw, J., 1981 — Sedimentation in proglacial Sunwapta Lake, Alberta. *Canadian Journal of Earth Sciences,* 18, 81-93.

Gravenor, C.P., Von Brunn, V., & Dreimanis, A., 1984 — Nature and classification of waterlain glaciogenic sediment, exemplified by Pleistocene, Late Palaeozoic and Late Precambrian deposits. *Earth-Science Reviews,* 20, 105-166.

Harland, W.B., Herod, K.N., & Krinsley, D.H., 1966 — The definition and identification of tills and tillites. *Earth-Science Reviews,* 2, 225-256.

Harris, W.K., & McGowran, B., 1971 — Permian and reworked Devonian microfossils from the Troubridge Basin. *Geological Survey of South Australia, Quarterly Geological Notes,* 40, 5-11.

Kemp, E.M., 1978 — Palynology of the Permo-Carboniferous in Tasmania: an interim report. *Geological Survey of Tasmania, Bulletin,* 56.

Kemp, E.M., Balme, B.E., Helby, R.J., Kyle, R.A., Playford, C., & Price, P.L., 1977 — Carboniferous and Permian palynostratigraphy

in Australia and Antarctica: a review. *BMR Journal of Australian Geology & Geophysics*, 2, 177-208.

Keunen, Ph.H., 1951 — Mechanics of varve formation and the action of turbidity currents. *Geologiska Foreningens I Stockholm Forhandlingar*, 73, 69-84.

Kurtz, D.D., & Anderson, J.B., 1979 — Recognition and sedimentologic description of recent debris flow deposits from the Ross and Weddell Seas, Antarctica. *Journal of Sedimentary Petrology*, 49, 1159-1170.

Lowe, D.R., 1981 — Sediment gravity flows: II. Depositional models with special reference to the deposits of high density turbidity currents. *Journal of Sedimentary Petrology*, 52, 279-297.

Ludbrook, N.H., 1962 — Australian Oil and Gas Corporation Wentworth No. 1 well, subsurface stratigraphy and micropalaeontological study. *Geological Survey of South Australia, Palaeontological Report* No. 14/61; *Bureau of Mineral Resources, Australia, Petroleum Search Subsidy Acts File* 62/1212 (unpublished).

Ludbrook, N.H., 1963 — A.O.C. North Renmark No. 1 subsurface stratigraphy and micropalaeontology study. *Geological Survey of South Australia Palaeontological Report*, 6/63; *Bureau of Mineral Resources, Petroleum Search Subsidy Acts File* 62/1223 (unpublished).

Ludbrook, N.H., 1967 — Permian deposits of South Australia and their faunas. *Transactions of the Royal Society of South Australia*, 91, 65-92.

McLeod, M., 1977 — Palynology of Permian samples from the southeastern Murray Basin, Victoria, for Western Mining Corporation Ltd, Exploration Division — Coal. *Report by Palaeoservices, Australia* (unpublished).

McLeod, D.M., 1978 — Palynology of samples for Western Mining Corporation Ltd, Exploration Division — Coal. *Report by Palaeoservices, Australia* (unpublished).

McLeod, M., 1979 — Report of palynological investigations on twenty-two samples for Western Mining Corporation Ltd, Exploration Division — Coal. *Report by Palaeoservices, Australia* (unpublished).

Morgan, R., 1975 — Palynological examination of samples from A.O.G. Jerilderie R.D.H.1 and A.P.E. Urana R.D.H.1., eastern Murray Basin. *Geological Survey of New South Wales Report No.* GS 1975/148 (unpublished).

O'Brien, P.E., 1981 — Permian sediments beneath the Murray Basin. *Bureau of Mineral Resources, Australia, Record* 1981/60.

Overshine, A.T., 1970 — Observations of iceberg rafting in Glacier Bay, Alaska, and identification of ancient ice-rafted deposits. *Geological Society of America Bulletin*, 81, 891-894.

Stewart, J.H., & La Marche, V.C. Jr., 1967 — Erosion and deposition produced by the flood of December 1964 on Coffee Creek, Trinity County, California. *U.S. Geological Survey Professional Paper*, 422-K.

Thornton, R.C.N., 1974 — Hydrocarbon potential of the western Murray Basin and infrabasins. *Geological Survey of South Australia, Report of Investigations*, 41.

Wright, A.J., & Stuntz, J., 1963 — A.O.G. Jerilderie No. 1 well completion report. *Bureau of Mineral Resources, Australia, Petroleum Search Subsidy Acts File* 62/1216 (unpublished).

Yoo, E.K., 1982 — Geology and coal resources of the northern part of the Oaklands Basin. *Geological Survey of New South Wales, Quarterly Notes*, 15-27.

Appendix: Definition of the Urana Formation

Derivation of name. A.P.E. Urana No. 1 (lat. 35°16'33"S, long. 146°00'10"E).

Distribution. Infrabasins beneath the Murray Basin.

Type section. A.O.G. Jerilderie No. 1 from 425 m to 1312 m (lat. 35°15'S, long. 145°58'E).

Lithology. Dark grey sandy mudstones, dark grey diamictites, white to grey fine to coarse sandstone, interlaminated claystones and siltstones and pebble to boulder conglomerates.

Thickness. Up to 887 m has been encountered.

Fossils. Arenaceous and calcareous foraminifera, palynomorphs and some ostracods.

Depositional environment. Glaciomarine basin.

Relationships. Unconformable on older Palaeozoic sediments and granitic rocks, and overlain unconformably by Late Permian, Triassic, Cretaceous, and Tertiary sediments in various parts of the Murray Basin.

Structural attitude. Flat lying.

Age. Contains Stage 2 and Stage 3 microfloras of Kemp & others (1975) and, therefore, is Late Carboniferous to Early Permian.

Correlations. Correlates with other Late Palaeozoic glacial sequences in eastern Australia such as those in central Victoria, the Cape Jervis beds of the Troubridge Basin, the Merrimelia Formation in the Cooper Basin and the lower part of the Parmeener Supergroup in Tasmania.

BMR Journal of Australian Geology & Geophysics, 10, 65-76
©Commonwealth of Australia 1986

A new late Pleistocene diprotodontid (Marsupialia) from Pureni, Southern Highlands Province, Papua New Guinea

T.F. Flannery[1] & M. Plane[2]

A new zygomaturine diprotodontid, *Hulitherium tomasettii* gen. et sp. nov., from 38 000-year-old swamp sediments at Pureni, Southern Highlands Province, Papua New Guinea is the largest mammal yet known from the Quaternary of New Guinea. Possibly the sister taxon to species of *Zygomaturus,* the new genus is represented by a partial skull and parts of the postcranial skeleton. Estimated to have weighed 75-200 kg, *H. tomasettii* was probably a browser. Its hindlimb morphology suggests that it had a greater joint mobility than is known in any other diprotodontid, and this in turn hints that it was probably not graviportal.

Introduction

The Pleistocene vertebrate fauna of New Guinea is only slowly becoming known. The first extinct late Pleistocene taxa (3 new macropodid species) from New Guinea were described by Flannery & others (1983). However, Holocene *Thylacinus* remains had been reported earlier (Van Deusen, 1963). Flannery & others (1983) have also reported on the existence of taxonomically unallocated diprotodontid postcranial remains and an I_1 fragment from Nombe rockshelter.

Three diprotodontid species have previously been described from New Guinea: *Nototherium watutense* Anderson, 1937, *Kolopsis rotundus* Plane, 1967, and *Kolopsoides cultridens* Plane, 1967. These taxa, however, are known only from the Pliocene Otibanda Formation of centralstern Papua New Guinea. Pleistocene diprotodontids have until now remained virtually unknown.

Here we describe a new zygomaturine diprotodontid, *Hulitherium tomasettii,* from late Pleistocene swamp deposits at Pureni, Southern Highlands Province, Papua New Guinea. We suggest that it represents a new genus, and speculate on its lifestyle.

Discovery of the fauna

In 1967, improvements were made to the Pureni Mission airstrip: it was lengthened and widened to comply with regulations and improve safety. During excavation of a bank on the southwestern side of the airstrip, a section was exposed, 15-20 m long and up to 3.8 m high. At the base of this excavation a layer rich in bones and plant material was uncovered. The local Huli tribesmen who were employed using hand tools were greatly excited and frightened by the discovery, bones always being associated with ancestors. A certain amount of damage was caused by the poking and prodding of these 'tabu' objects with shovels and digging sticks before the local priest, the late Father Bernard Tomasetti, realised the scientific worth of the material and salvaged most of it.

In 1969, Williams and Plane investigated the Quaternary stratigraphy of the area and made field studies of the Pureni and other sites (Williams & others, 1972). Further vertebrate and plant fossil material was collected and an auger hole was sunk on the Pureni vertebrate site (Fig. 1).

In addition to the remains of *Hulitherium tomasettii,* the Pureni local fauna includes a taxonomically unallocated right dentary fragment of a murid with I_1 and M_2 (this specimen is, however, phenetically similar to *Rattus* and *Melomys* species), a partial cranium of *Phalanger carmelitae,* and limb bones of a small cassowary (T. Rich, personal communication).

Quaternary stratigraphy

From a Quaternary perspective the basement rocks in the Pureni area are a thick sequence (at least 2000 m) of marine limestone, with interbedded siltstone, thin-bedded soft mudstone and siltstone, and subordinate calcareous sandstone of late Oligocene to Pliocene age. (Llewellyn & Zehnder, 1955; Williams & others, 1972).

In the mid Pleistocene these marine sediments were intruded and overlain by lavas which also dammed and partly filled the former valley of the Tagari River. McDougall (in Williams & other, 1972) obtained relatively good concordance for three whole-rock dates for the lavas of Mt Iumu (Fig. 1) at about 850 000 year B.P. Subsequent volcanic episodes draped the lavas and earlier sediments with mid-Pleistocene to Holocene pyroclastic rocks and their weathering products. The source of these agglomerates, fine ash, and sediments of pyroclastic origin is thought to be Mount Rentoul and Mount Sisa. Organic layers are interbedded with these rocks, indicating lengthy quiescent periods between volcanic episodes, and Doma Peaks, which local folklore suggests may have erupted in known memory, is not extinct.

Holocene swamp deposits at Haibuga (Fig. 1), at Tarifuga and Mogorofuga to the northwest of Pureni, and Wabafuga to the west are the most recent deposits in the area, and comprise peat, clay, and ash bands.

Haibuga basin stratigraphy and palaeoecology

The surface exposures at Pureni and at Telabo footbridge were mapped in detail (Williams & others, 1972) and both sections were traced subsurface by augering. Although these sites are nearly 2 km apart, accurate barometer readings, close agreement of the sediment types and ^{14}C dates, and their deposition in the same small sedimentary basin lend confidence to the correlation of the sections, which is the basis for the Quaternary stratigraphy of the fossiliferous rocks of the Haibuga basin.

We are fortunate in that both sections contain good pollen spectra and, from these samples, Powell (in Williams & others, 1972) outlined a rough sequence of events that enables us to put *Hulitherium tomasettii* in its vegetative and climatic context:

'Locally, conditions changed from open water with marginal conifers to grass-swamp surrounded by conifers and to bog forest on the site itself. Regionally, conditions ameliorated

authors listed alphabetically
[1]The Australian Museum, 6-8 College St., Sydney, N.S.W. 2000
[2]Division of Continental Geology, Bureau of Mineral Resources, GPO Box 378, Canberra, ACT

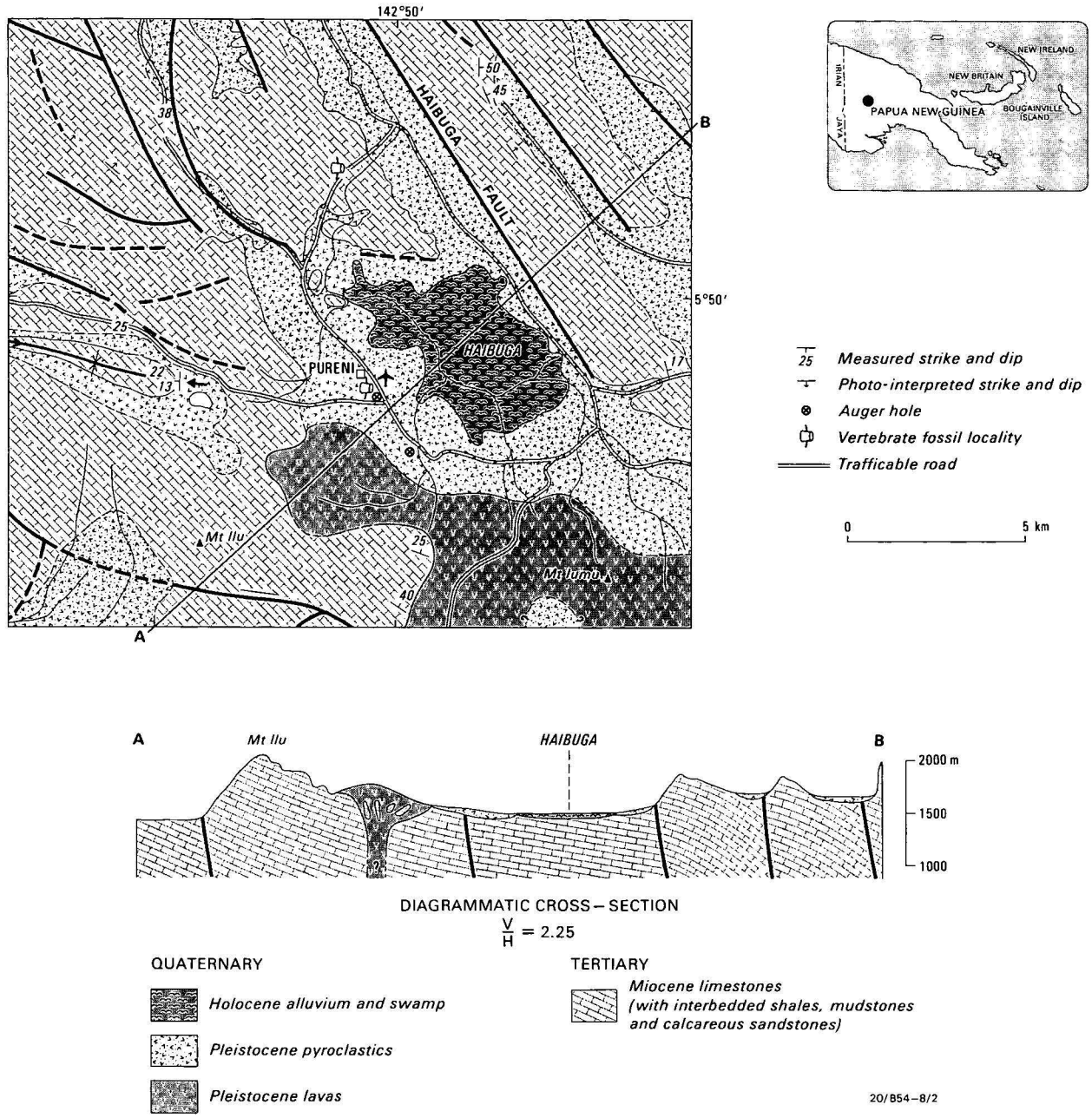

Figure 1. Geology of Pureni area, Papua New Guinea.
Modified from Williams & others (1972).

from rather cool with mixed forest dominant and subalpine grassland nearby, to mild with beech forest dominant on the slopes and mixed forest and subalpine grassland further away, and to relatively warm with oak forest and oak-beech forest dominant. In all cases, however, the extrapolated environment was colder than that experienced at the present time in this area.'

Systematic palaeontology

Diprotodontidae Gill, 1872

Zygomaturinae Stirton, Woodburne & Plane, 1967

Hulitherium gen. nov.

Derivation of generic name. Named for the Huli people of the Pureni area to honor their discovery of the animal.

Genotypic species. *Hulitherium tomasettii*

Generic diagnosis. *Hulitherium tomasetti* is a zygomaturine diprotodontid that can be distinguished from other members of its subfamily in the following ways. It is unique among close relatives in that the palate is deeply arched and the capitulum of the femur is placed directly above its shaft. It possesses high-vaulted frontals that are otherwise seen only in the species of *Plaisiodon* and *Zygomaturus,* and a reduced paracrista on M_2 and an anterodorsally directed maxillary-premaxillary suture, features otherwise seen only in the species of *Zygomaturus.* It differs from the species of *Kolopsoides* and *Kolopsis* in having a lower posterointernal cusp on P_3.

Further, it differs from *Raemeotherium yatkolai* in being much larger, in having less-rectangular molars and less-crenulate molar enamel. It differs from *Kolopsoides cultridens* in possessing a double-rooted rather than triple-rooted P^3, less-developed cristids obliqua on lower molars, and squarer molars; and from *Plaisiodon centralis* in having

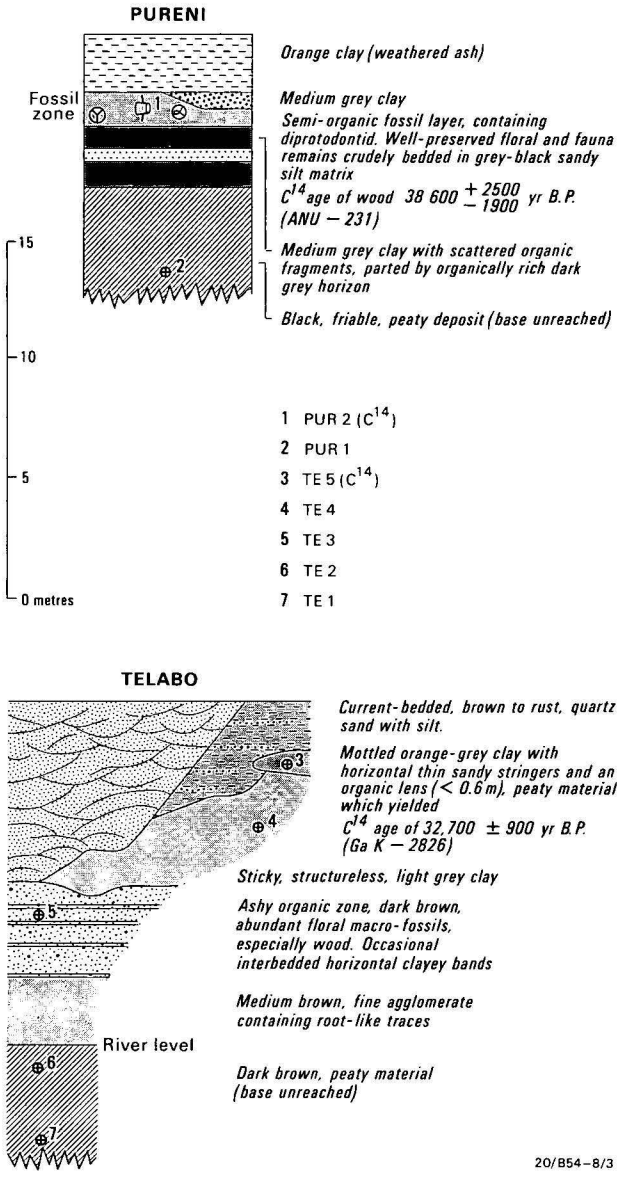

Figure 2. Auger section, Pureni vertebrate site.

broader nasals, and less-developed parastyles and metastyles on upper molars.

Hulitherium tomasettii differs from *Zygomaturus keani* and *Z. gilli* in being smaller, in having the cristids obliqua of M_{3-5} less-developed, and (from *Z. keani* only) in having better developed parastyles and metastyles on M^{2-5}. It further differs from *Z. gilli* in having the cristids obliqua of M_{2-5} less developed, and in having the paracone and metacone of P^3 closer bucally.

Hulitherium tomasettii differs from *Zygomaturus trilobus* in having premaxillae that are not laterally expanded at the nares, the frontal bulge rising at a less acute angle from the nasals, the palate between the upper incisors less deeply excavated, a better developed groove at the palate mid- line, and in having the paracone and metacone of P^3 closer at their buccal margin.

Hulitherium tomasettii, gen. nov. et sp. nov. (Figs. 3–7, Table 1)

Holotype. CPC 25718; a partial skeleton, including a partial cranium that is almost complete anterior to the frontal-parietal contact. A fragment of the enamel cap of a left P^3, nearly complete M^3s and M^4s, and fragments of M^5s, posterior fragments of the right and left dentaries, including most of the left angle, a fragment of a right P_3, and broken enamel caps of left and right M_{2-5} are preserved. The right M_5 fits perfectly into the posterior alveolus of the right dentary fragment.

Postcranial remains consist of: the left side of the atlas and the centrum of a cervical vertebra; the right humerus, which is almost complete, lacking only a central section of the shaft; a distal fragment of the left humerus; the left femur, represented by the proximal end, preserved as far distally as the termination of the lateral rugose area, an extension of the greater trochanter; the proximal and distal ends of the right femur; the right tibia, with only the distal end missing; and fragments of a radius (distal end) and fibula.

Type locality. Excavated bank on southwestern side of Pureni Mission airstrip, Wabag 1:250 000 Sheet area 5°50'S, 142°49'E, Southern Highlands District, Papua New Guinea.

Age. Late Pleistocene: a ^{14}C determination on a log in the bed that contained the diprotodontid remains gave an age of 38 600 ± 2500 years B.P.; sample ANU-231 (Williams & others, 1972).

Etymology. Named specifically for the late Father Bernard Tomasetti, a man of learning and culture, who ensured not only that the remains were preserved, but that they were brought to the attention of appropriate workers.

Specific diagnosis. The generic diagnosis will serve as that for the species until further species are recognised.

Description. Dentition: P^3. A small fragment of the buccal face of the P^3 is preserved. It includes the posterobuccal portion of the paracone and the anterobuccal portion of the metacone. The paracone and metacone apparently formed a single crest buccally, and are only separated by a shallow, ill-defined depression.

M^2. The M^2 is not represented by any certainly identifiable fragments.

Table 1. Measurements (mm) of the holotype of *Hulitherium tomasettii.*

Length of I^1 alveolus	19.3
Length of I^2 alveolus	10.2
Length of I^3 alveolus	10.0
Length of P^3-M^5 alveoli	110.9
Length of P^3-I^3 diastemal length	37.6
Length of right M^3	24.8
Length of right M^4	28.0
Length of right M_3	24.8
Length of left M_4	27.9
Anterior width of left M_4	20.2
Posterior width of left M_4	19.1
Length of right M_5	29.3
Anterior width of right M_5	21.4
Posterior width of right M_5	~20.3
Width of palate at anterior of P^3	38.7
Width of palate at anterior of M^2	41.0
Height of rostrum at anterior of M^2	54.1
Minimum interorbital width	41.0
Width of proximal epiphysis of humerus	69.0
Length of proximal epiphysis of humerus	60.0
Width of distal epiphysis of humerus	94.8
Diameter of head of femur	45.6
Maximum width of shaft of femur	75.6
Maximum depth of shaft of femus	32.0
Width of femur across distal condyles	73.0
Width of femur proximal epiphysis of tibia	63.8
Length of femur proximal epiphysis of tibia	55.6

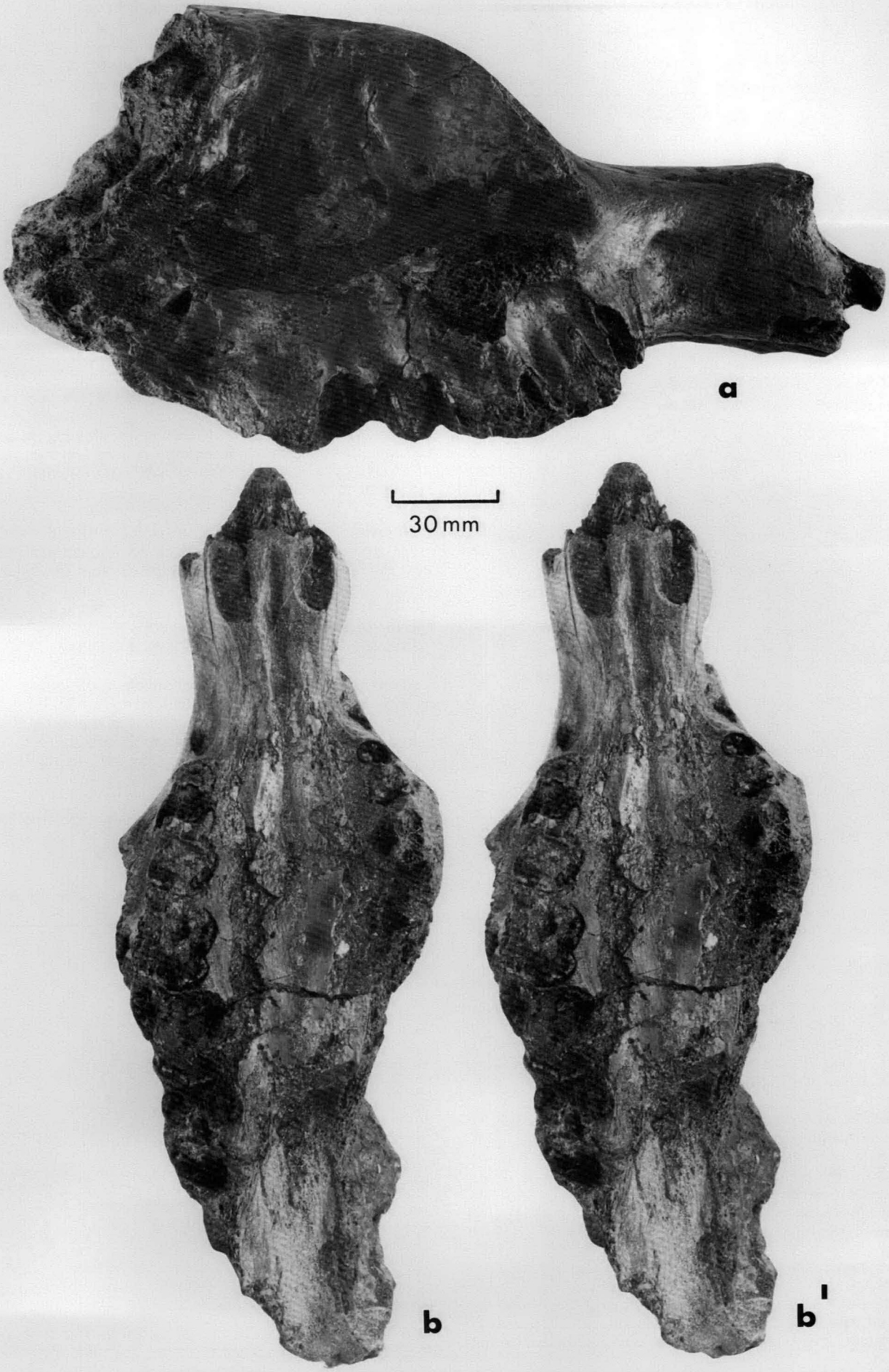
a
30 mm
b
b'

Figure 4. Stereo dorsal view of cranium of *Hulitherium tomasettii* gen. et sp. nov.

M^3. The M^3 is represented by a right enamel cap, lacking only the buccal part of the hypoloph and the posterobuccal portion of the protoloph, and fragments of a left enamel cap. The enamel of the anterior face of the protoloph is crenulated to a greater degree than other parts of the crown. The anterior cingulum is broad and terminates lingually against the anterolingual flank of the protocone. On the buccal edge of the anterior cingulum a prominent parastyle is present, which is connected to the base of the paracone by a slight ridge. A basal cingulum is present in the lingual end of the interloph valley, which extends between the posterolingual base of the protocone and the anterolingual base of the hypocone. The posterior cingulum is narrower than the anterior cingulum. It commences at the posterolingual face of the hypocone, and continues to the posterobuccal corner of the tooth, where the crown is broken away. The posterior cingulum does not appear to have extended beyond the point of breakage. A prominent metastyle (which is smaller than the parastyle) is present near the posterobuccal corner of the tooth. It is connected to the base of the metacone by a small crest. A rounded midlink extends basally from the apex of the protocone and terminates in the interloph valley. There is no trace of a midlink on the anterior face of the hypoloph.

M^4. Both partial M^4s lack the buccal end of the protoloph, the posterobuccal face of the protoloph, and the lingual corner of the hypoloph. The M^4 differs from M^3 in the following ways. It is less worn and larger, and the parastyle and metastyle are reduced in size. In addition the anterobuccal portion of the M^4 (an area not preserved on M^3) possesses a slight cuspule placed basal and slightly lingual to the apex of the metacone in the interloph valley. This structure may be a remnant of a premetacrista.

M^5. Only fragments of M^5 remain. A portion of the anterior face of the right protoloph indicates that M^5 was not fully erupted and that the parastyle was slightly smaller than that of M^4.

Figure 3. a, lateral view, and b–b′; stereo occlusal view of partial cranium of holotype of *Hulitherium tomasetti* gen. et sp. nov.

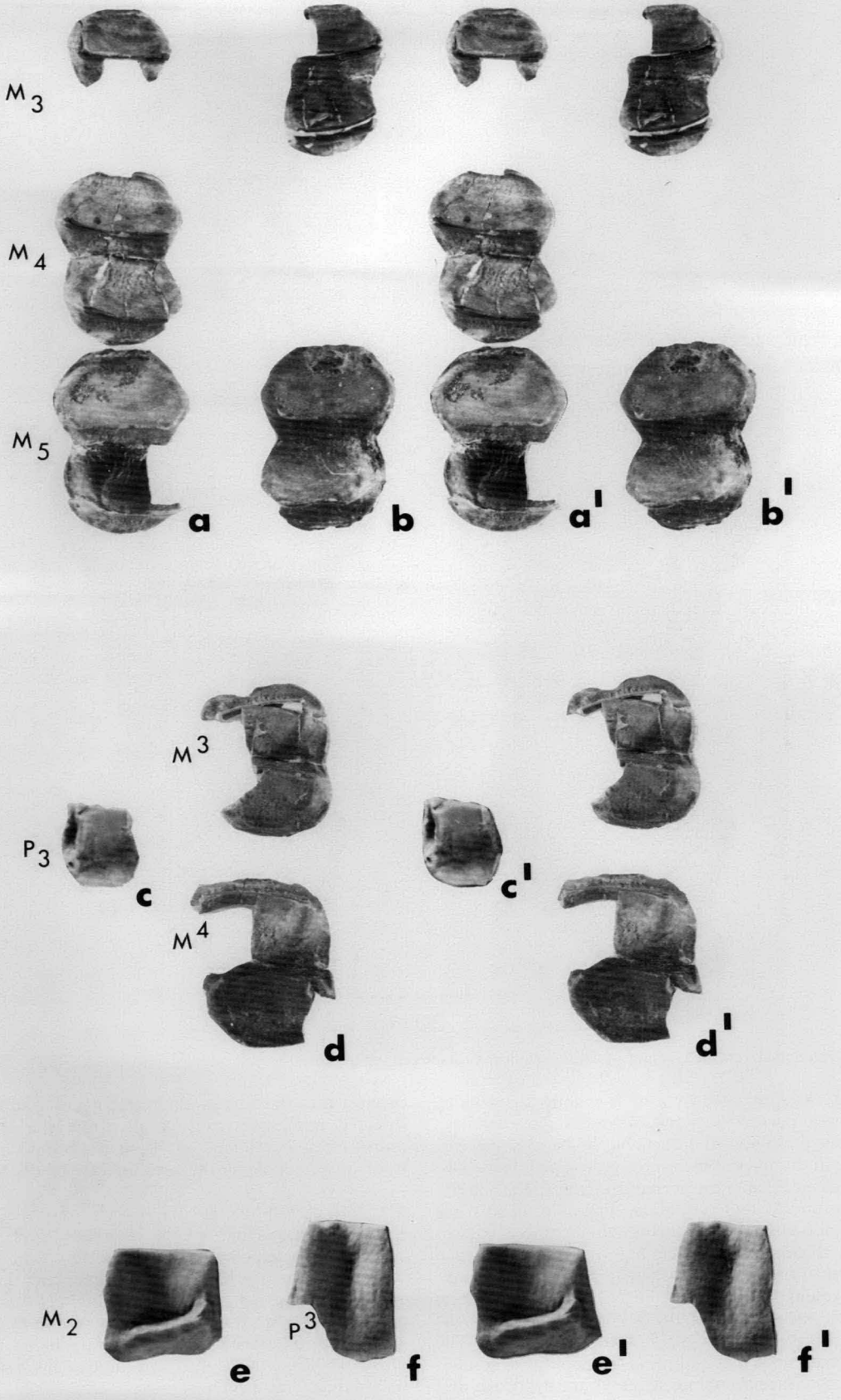

Figure 5. Holotype of *Hulitherium tomasettii* gen. et sp. nov.
a-a', stereo occlusal view of partial left M_{3-5}, xl; b-b', stereo occlusal view of right M_3 and M_5, xl; c-c', stereo occlusal view of posterointernal corner of right P_3, x2; d-d', stereo occlusal view of partial right M^{3-4}, xl; e-e', stereo anterior view of anterior face of protolophid left M_2, x2; f-f', stereo view of central portion of buccal face of right P^3, x2.

P_3. A small fragment represents the posterolingual portion of a left P_3. A small posterobasal cusp is united with a larger posterobuccal cusp by a ridge. A horizontal crest with a well-developed facet extends anteriorly from near the posterobuccal crest. A small fossette is enclosed behind the ridge joining the two posterior cusps.

M_2. A fragment of the anterior face of the protolophid and a portion of the anterobuccal face of the hypolophid, both from the left M_2 are preserved. The anterior cingulum is confined to an area lingual to the paracristid. It is highest buccally, and slopes basally towards the anterobuccal margin of the tooth, becoming narrower as it descends. It terminates near the base of the metaconid. The paracristid is very poorly developed relative to that of other zygomaturines, forming a rounded crest that descends from the apex of the protoconid. The anterobuccal face of the hypoconid shows that a moderately well-developed cristid obliqua was present, which ascended to about half the height of the hypoconid.

M_3. Fragments of the left and right M_3 are enough to reconstruct an almost complete (composite) enamel cap. The anterior cingulum extends across the central portion of the anterior face of the protolophid, but terminates before reaching the buccal or lingual margin of the tooth. It is narrower than the posterior cingulum, and no evidence of buccal or lingual basal cingula is preserved. The posterior cingulum is highest in the centre, sloping basally, buccally, and lingually, and not quite reaching the buccal and lingual margins of the tooth. The cristid obliqua is extremely poorly defined. It originates at the apex of the worn hypoconid, and terminates at the base of the interloph valley, about one-third of the distance from the buccal margin of the tooth. A slight bulge at the apex of the protoconid suggests the presence of a paracrista, and a similar feature at the apex of the entoconid suggests the presence of preentocrista.

M_4. The left M_4 is preserved as an almost complete enamel cap. The right M_4 is represented by fragments only. It differs from M_3 in being markedly larger and less worn, the anterior cingulum is less-developed, and the enamel is slightly more crenulate in appearance.

M_5. Both left and right M_5s are preserved almost complete, both lacking only the lingual corner of the entoconid. They differ from M_4 in the following ways: both are unworn and apparently were not fully erupted; the anterior cingulum is less-developed, and the cristid obliqua terminates further buccally in the interloph valley; the hypolophid is markedly narrower than the protolophid.

The skull. Both zygomatic arches, the posterior face of the cranium, the basicranial region, part of the left maxilla and parts of the nasals are missing. The alveoli for I^{1-3} indicate that I^1 was much larger than I^{2-3}, and that I^3 was larger than I^2. The alveoli for P^3 also indicate that this tooth was double-rooted. The palate between the cheektooth rows is deeply arched, an unusual feature among diprotodontids. It is flat near the midline, but rises sharply towards the cheektooth rows. It thus forms a flat-topped arch shape in cross section. The palate is non-fenestrate and narrows anteriorly. Anterior to P^3 the palate narrows sharply, but broadens slightly as it approaches the incisor region. A deep sulcus separates the left and right sides of the palate anterior to the premolars.

The rostrum is markedly narrow, and subovate in cross section. It does not broaden appreciably anteriorly, as is the case in *Zygomaturus trilobus*. The premaxillaries lack the anterolateral expansions seen in *Z. trilobus*. The premaxillary/maxillary sutures on the sides of the skull slope anterodorsally. The nasals are broadest posteriorly, and the nasal-frontal suture is almost linear, and is transversely oriented, being situated at the base of the frontal bulge.

The infraorbital canal opens onto the facial region dorsal to and anterior of the P^3. The nasal septum is broken away, but it seems unlikely from what remains that it would have been as large as in *Z. trilobus*.

The frontals rise sharply from the plane of the nasals, and are dished mesially, the frontal depression being parallel with the midline of the skull. The orbits are situated low on the skull, their ventral rims being about 3 cm dorsal to the P^3 alveolus. A very low saggital crest is formed on the frontals dorsal to the posterior end of the cheektooth row.

Only posterior fragments of the left and right dentaries remain. The left dentary fragment is almost complete posterior to M_5, but lacks much of the ascending ramus and condyle. The angle of the dentary is extremely broad, and the pterygoids were thus probably massive. A well-developed ridge is present on the ventral edge of the buccal area of masseter attachment. The horizontal ramus of the dentary is relatively shallow, being about 57 mm deep below M_5.

Postcranial skeleton: Atlas. The left side is preserved. The ventral portion was incomplete, as in all other marsupials. This element appears to have been surprisingly slightly built relative to the size of the skull. The cranial condyle articulation is antero-posteriorly short and tall relative to that of many marsupials (eg. vombatids, macropodoids).

Cervical vertebra. The centrum of a cervical vertebra is preserved. It is anteroposteriorly very short (16 mm), and all processes are broken away. However, the shortness of the centrum indicates that the neck of *H. tomsettii* was short.

Humerus. The right humerus lacks only a central portion of the shaft, and thus the proximal and distal parts can no longer be joined. The proximal articular surface appears to have allowed a considerable degree of movement. There is approximately 180° of articular surface in an anteroposterior direction, but much less laterally. The pectoral ridge is well developed, terminating proximally in the ectotuberosity, which stands slightly above the proximal articular surface. The deltoid crest and tuberosity for insertion of the *Latissimus dorsi* and *Teres major* are not preserved, if they were ever present.

The middle portion of the shaft is extremely narrow and delicate (being 32 mm wide at its narrowest) and is slightly anteroposteriorly compressed (being 23 mm deep at the narrowest point). An entepicondylar tubercle is small. The distal epiphysis is similar to that seen in macropodoids, with the lateral and medial condyles having arcuate articular surfaces that span about 180° of arc.

Radius. The distal fragment of a radius is preserved. However, it lacks an epiphysis and little of its original morphology is discernible.

Femur. The distal and proximal fragments of the femur can no longer be joined, as a segment from the middle of the shaft is missing. The proximal femur fragment exhibits some highly unusual features. The head of the femur is positioned directly above the mesial edge of the shaft, and projects prominently above the rest of the bone. The head is hemispherical, and the articular surface (when entire) probably consisted of approximately two-thirds of a sphere.

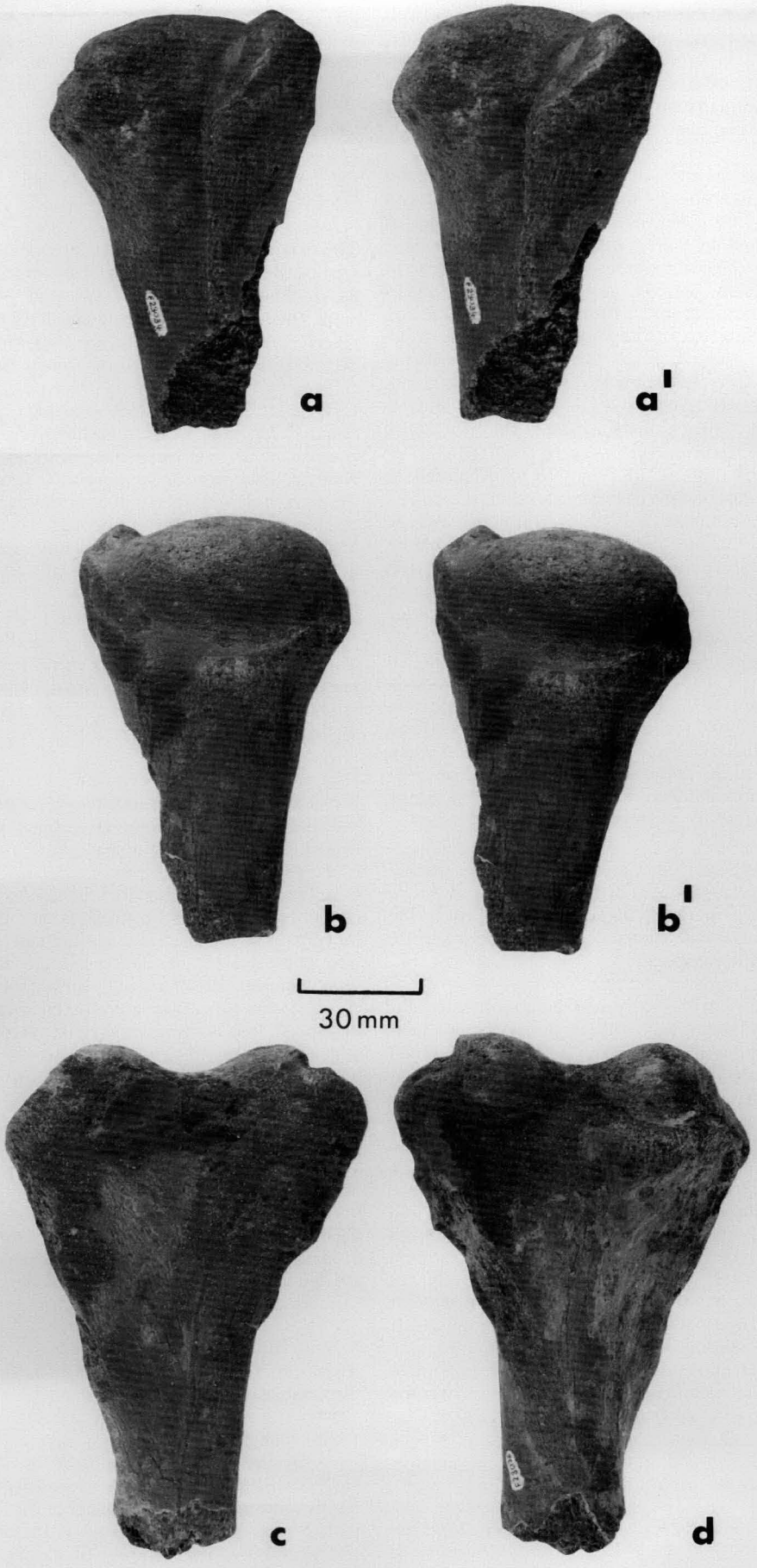
a
a'
b
b'
30 mm
c
d

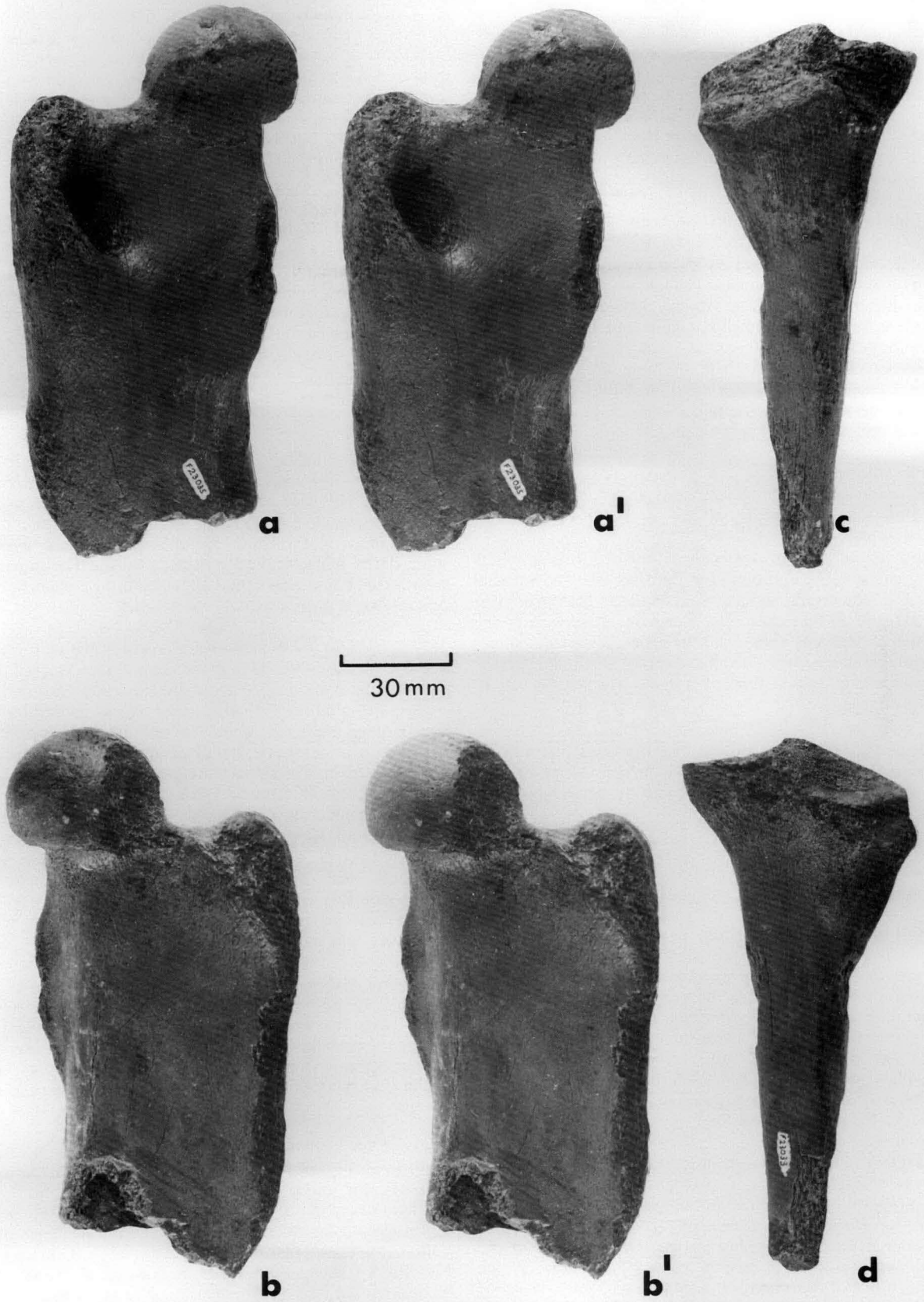

Figure 7. a–a', stereo view of posterior face, and b–b', anterior face of proximal left femur fragment; c, anterior face, and d, posterior face of right tibia of *Hulitherium tomasettii* gen. et sp. nov.

Figure 6. a–a', stereo view of anterior face, and b–b', posterior face of right proximal humerus fragment; c, posterior face, and d, anterior face of distal right humerus fragment of *Hulitherium tomasettii* gen. et sp. nov.

The neck is short but narrow, and the globular head forms a prominent bulge. The greater trochanter projects anteriorly, and thus there is a concavity on the shaft distal to it. The muscle insertion tract that runs along the lateral edge of the bone distal to the greater trochanter is very extensive, extending 130 mm along the shaft. The trochanteric fossa is shallow and subovate. The lesser trochanter is prominent and placed on the posteromedial margin of the bone. The shaft of the femur is markedly compressed anteroposteriorly, being 55 mm broad, but only 19 mm deep at the point where the lateral muscle insertion tract terminates.

The distal femur fragment is broken away approximately 50 mm proximal to the condyles. The lateral condyle is broader than the medial one. The conical process of the medial condyle forms a marked prominence. Much of the rest of the morphology of this fragment is obscured by abrasion and adhering matrix. A fragment of bone situated near the dorsolateral part of the distal end of the humerus (and joined to it by encrusting matrix) may represent the remains of a lateral sesamoid.

Tibia. The tibia is gracile, and broken away at its distal end. It appears, however, that it lacks only its distal epiphysis and a small portion of shaft.

The external condylar depression of the proximal epiphysis is a concave facet and longer than broad. The internal condylar depression, however, is more planar and slopes away posteriorly and mesially. The non-articular surface of the proximal epiphysis anterior to the articular surfaces slopes steeply away anteriorly. The proximal tibial-fibular facet is almost planar and is subovate in shape. The shaft is oval in cross section.

Fibula. The fragment tentatively identified as part of a fibula preserves almost no external bone surface. However, it is flattened and expands anteroposteriorly at one end (probably the proximal end).

Discussion

Relationships. *Hulitherium tomasettii* is clearly a zygomaturine diprotodontan most closely similar to the species of *Plaisiodon* and *Zygomaturus*. A unique feature it shares with these taxa is the presence of highly vaulted frontals. Furthermore, *Hulitherium tomasettii* shares some unique features with the species of *Zygomaturus*, including (1) the presence of an anterodorsally directed maxillary/premaxillary suture; (2) having the palatine surface of the rostrum extremely 'pinched in'; and (3) having a very reduced paracristid on M_2.

Apart from *Zygomaturus trilobus*, the previously described species of *Zygomaturus* are extremely poorly known, and it is not possible to determine in many cases if the condition seen in *Hulitherium tomasettii* is shared with other zygomaturines. This applies particularly to aspects of the skull and postcranial morphology. Thus, although the relationship of *Hulitherium tomasettii* to some species of *Zygomaturus* is unknown, we place it in its own genus for the following reasons.

1 — In many features, *Hulitherium tomasettii* is more plesiomorphic than *Z. trilobus*. Thus, it seems possible that *Hulitherium tomasettii* may be the sister taxon of the species of *Zygomaturus* if other forms are similar to *Z. trilobus*, (as they appear to be on cranial morphology).

2 — the postcranial morphology of *Hulitherium tomasettii* is markedly different from that of *Z. trilobus*, indicating an apparently long period of specialisation in *H. tomasettii*. It thus appears unlikely that *H. tomasettii* is simply a dwarf, rainforest-dwelling form of *Zygomaturus* that developed during the Pleistocene in New Guinea. Rather, it seems more likely that *H. tomasetti* diverged from the species of *Zygomaturus* long before, in the late Tertiary.

Functional morphology and habitat. Some aspects of the morphology of *Hulitherium tomasettii* are highly unusual. These include the highly arched palate and the morphology of the proximal end of the femur. The presence of the highly arched palate in *H. tomasettii* is unique among diprotodontans. However, a similar condition exists in other mammals, and Nowak & Paradiso (1983) have noted that the palate of the sloth bear (*Ursus ursinus*) is highly arched. This adaptation, plus a gap between the front incisors, allows the bear to feed on termites, which make up the major portion of its diet.

We have been unable to find close analogues among living mammals to the hind limb morphology of *Hulitherium tomasettii*. The head of the femur clearly would allow for a great degree of movement to take place. The functional significance of the shaft of the femur being placed immediately below the head remains unknown. The humerus-ulnar articulation also would allow for a far greater degree of mobility than in other diprotodontids.

38 000 years ago the Pureni area was colder than at present, and the vegetation fossilised at the site is more typical of that found today at altitudes of about 2100 m. Thus, *Hulitherium tomasettii* would have inhabited cool, mossy upland forest. This kind of habitat is occupied elsewhere in the world by large herbivores in the 60–200 kg weight range, including the giant panda in China, mountain gorilla in Africa, and spectacled bear in South America. It is possible that *H. tomasettii* represents a marsupial ecologically equivalent to these placental species. Certainly the greater limb mobility suggested for *H. tomasettii* indicates that the species was probably not graviportal, as were other known diprotodontids. The bear-like or panda-like posture of *H. tomasettii* in our reconstruction is certainly possible, given these data and the femur/humerus morphology.

Extinction. *Hulitherium tomasettii* is the largest mammal yet known from the late Pleistocene of New Guinea. Compared with similarly proportioned placentals, *Hulitherium tomasettii* probably weighed between 75 and 200 kg. Its habitat apparently included mid-montane rainforests very similar to relict stands that survive in the Pureni area to the present.

There is no evidence of a human presence in the late Pleistocene fossiliferous sediments at Pureni. At Nombe rockshelter in Simbu Province (6°08'S, 145°10'E), however, a fragmentary I^1 and some postcranial remains of a diprotodontid are associated with abundant evidence of a human presence (Flannery & others, 1983; Gillieson & Mountain, 1983). Radiocarbon dating of flowstones associated with the Nombe fossils gave ages ranging from 24 000 to 14 000 years B.P. (Gillieson & Mountain, 1983). Unfortunately, there are few elements in common between the Pureni and Nombe diprotodontids. However, a partial humerus and almost complete tibia from Nombe are superficially similar to those of *Hulitherium tomasettii*, but come from a slightly smaller but less gracile animal. Here, then, is evidence that *Hulitherium*-like diprotodontids co-existed with humans in the highlands of New Guinea and,

Figure 8. Artist's reconstruction of *Hulitherium tomasettii*.
Reproduced by permission of the artist, Peter Schouten.

given the lack of evidence for massive environmental change, it may well be that human predation was a factor in the extinction of these fascinating diprotodontids.

Summary

Hulitherium tomasettii is a zygomaturine diprotodontan, as yet known only from a partial skull and parts of the postcranial skeleton from 38 000-year-old swamp deposits at Pureni, Southern Highland Province, Papua New Guinea. The morphology of the femur and humerus suggest that the limbs were highly mobile relative to those of other diprotodontids. *Hulitherium tomasettii* was a browser, and inhabited montane rainforest. Man may have contributed to its extinction.

Acknowledgements

We acknowledge the late Father Bernard Tomasettii and his successor at Pureni Mission, Father Bill Trauba for their great help to the authors during their visits to the Pureni site. Kate Lowe of the Australian Museum and Richard Brown of the BMR produced the photographic plates. We are most grateful for the wonderful reconstruction that Peter Schouten has done of *Hulitherium* and thank him for permission to reproduce it.

References

Flannery, T.F., Mountain, M.J., & Aplin, K., 1983 — Quaternary kangaroos (Macropodidae; Marsupialia) from Nombe rock shelter, Papua New Guinea, with comments on the nature of megafaunal extinction in the New Guinea highlands. *Proceedings of the Linnaean Society of New South Wales,* 107(2), 75-98.

Gillieson, D., & Mountain, M.J., 1983 — Environmental history of Nombe rock shelter, Papua New Guinea highlands. *Archaeology in Oceania,* 18, 53-62.

Nowak, R.M., & Paradiso, J.L., 1983 — Walker's mammals of the world. *John Hopkins University Press, Baltimore.*

Van Deusen, H.M., 1963 — First New Guinea record of *Thylacinus. Journal of Mammalogy,* 44, 279-280.

Williams, P.W., McDougall, I., & Powell, J.M., 1972 — Aspects of the Quaternary geology of the Tari-Koroba area, Papua. *Journal of the Geological Society of Australia,* 18, 333-347.

BMR Journal of Australian Geology & Geophysics, 10, 77-83

©Commonwealth of Australia 1986

The elusive Cook volcano and other submarine forearc volcanoes in the Solomon Islands

N.F. Exon[1] & R.W. Johnson[2]

Submarine volcanoes reported from the forearc region of the New Georgia Group are anomalously close to the line of northeastwards subduction of the Woodlark Basin. Kavachi is a basalt-andesite volcano that rises nearly 1000 m above the sea floor south of Vangunu. It is frequently active and sometimes builds subaerially. A seamount 9 km northeast of Kavachi may also be a youthful volcano. Kana Keoki volcano, southwest of Rendova, is andesite to rhyolite in composition. It has not been recorded in eruption, and rises to within 700 m of sea level from a base at around 2500 m. Activity ascribed to Cook submarine 'volcano' west of Rendova was reported for 1963-4, and a shoal was reported to have been found by leadline sounding, but no volcano was found by detailed bathymetric surveys in 1979 and 1981. The activity probably consisted largely of hydrothermal blow-outs from a sea-floor vent (or vents) 1300 m below sea level, rather than from a volcano. Another submarine volcano has been reported to lie 25 km west of Kavachi, and southeast of Tetepare, but no sign of it was seen on a bathymetric profile run through this location. The New Georgia Group forearc region is very poorly surveyed bathymetrically. A single swathe-mapping sonar survey would show how many submarine volcanoes are present in the region and where they are located, prior to further sampling.

Introduction

Five submarine volcanoes have been reported from the forearc of the Solomon Islands (Fig.1): Kavachi volcano south of Vangunu (Johnson & Tuni, in press), a seamount 9 km northeast of Kavachi (Okrugin, 1985), Cook volcano — postulated from activity sighted in 1963 (Grover, 1968), Kana Keoki volcano (Taylor & Exon, in press), and a volcano shown west of Kavachi on Admiralty Chart 3995. The evidence for the existence of all five volcanoes and the nature of the better known ones are discussed below. Our aim is to encourage further sea-floor studies in the western Solomon Islands by drawing attention to the results of three recent bathymetric surveys of the area, two of which also used seismic reflection profiling, and by querying the existence of 'Cook submarine volcano' on the basis of results from two of the surveys (Exon, 1981; Okrugin, 1985). We define a submarine volcano as a recognisably volcanic constructional feature on the sea floor; a sea-floor vent without peripherally distributed volcanic rocks would not, according to our definition, be a volcano.

The reported submarine volcanic centres are all in or near the narrow (less than about 50 km wide) forearc area between the New Georgia Group of volcanic islands (part of the Solomon island arc) and the northeastern margin of the Woodlark Basin, an area of active sea-floor spreading (Taylor & Exon, in press). The Pliocene to Recent New Georgia Group volcanoes are of arc-trench type, but all are less than 80 km from where subduction of the Woodlark Basin, including its active ridge, is believed to be taking place northeastwards beneath the New Georgia Group. In other words, the 'arc-trench gap' in this area is considerably less than the usual width of 100-150 km in other island arcs. The submarine volcanoes are even closer to the presumed line of subduction: Kavachi volcano, for example, is only 30 km away (Fig.1).

Techniques for investigating the geology of submarine volcanoes have improved in recent years, particularly through the development of sea-floor scanning sonar systems, such as SeaMARC II (Hussong & Fryer, 1983), and the use of research submersibles such as Alvin. There is considerable scope for future investigations of this type in the island-arc and marginal-basin areas of the southwest Pacific, because little is known about the sea-floor volcanoes, despite their being potential sites for exhalative mineral deposits. Some of the volcanoes also have a potential for the generation of hazardous tsunamis, and for this reason also warrant investigation.

[1] Division of Marine Geosciences & Petroleum Geology, Bureau of Mineral Resources, GPO Box 378, Canberra, ACT 2601

[2] Division of Petrology & Geochemistry, BMR

Kavachi volcano

Kavachi and Cook are both listed as submarine volcanoes in the *Catalogue of the Active Volcanoes of the World* (Fisher, 1957), as well as in the Smithsonian Institution volcano data file (Simkin & others, 1981). Kavachi is indisputably a volcano (Johnson & Tuni, in press), but the identification of Cook as such is equivocal.

Kavachi is a roughly conical, generally submarine mountain. It has slopes up to 25° that rise from water depths of about 900 m in the north, and from considerably greater depths in the southwest. A bathymetric map of Kavachi has been prepared by Taylor (in press), using data from a May-June 1982 cruise by the R/V *Kana Keoki* and from the January-February 1981 R/V *Machias* survey. However, the crater area of Kavachi evidently changed its form between the two cruises, possibly owing to slumping. The crater rim in 1982 was a little less than 300 m below sea level, and had an arcuate form open to the south, but was only 60 m deep when sounded during the *Machias* cruise.

A 1979 cruise of R/V *Vulcanolog* (Okrugin, 1985) located the active vent of Kavachi at 8°59.4'S, 157°59.3'E and identified three other seamounts in an east-northeast-trending line north of Kavachi (Fig. 2). The largest of the three is the one in the south-southwest, 7 km northwest of Kavachi, which is capped by corals, whereas the east-northeastern seamount, 9 km northeast of Kavachi, appears to be a recently active volcano (Okrugin, 1985). Both porphyritic and aphyric, youthful, volcanic rocks have been dredged from the northeastern seamount.

Kavachi has built up above sea level at least seven times since 1950, forming islands that existed for a few days up to several weeks, before being removed by wave action, slumping, and explosive activity. Its existence and volcanic activity were first reported in late 1950 (Grover, 1955a,b), after which reports came to light of activity in 1939 and 1942. Johnson & Tuni (in press) have described reported eruptions between 1950 and 1982. Explosive activity is mostly in the form of dome-shaped upheavals, fountains, and jets of sea water, which include differing proportions of entrained rocks; shallow-water

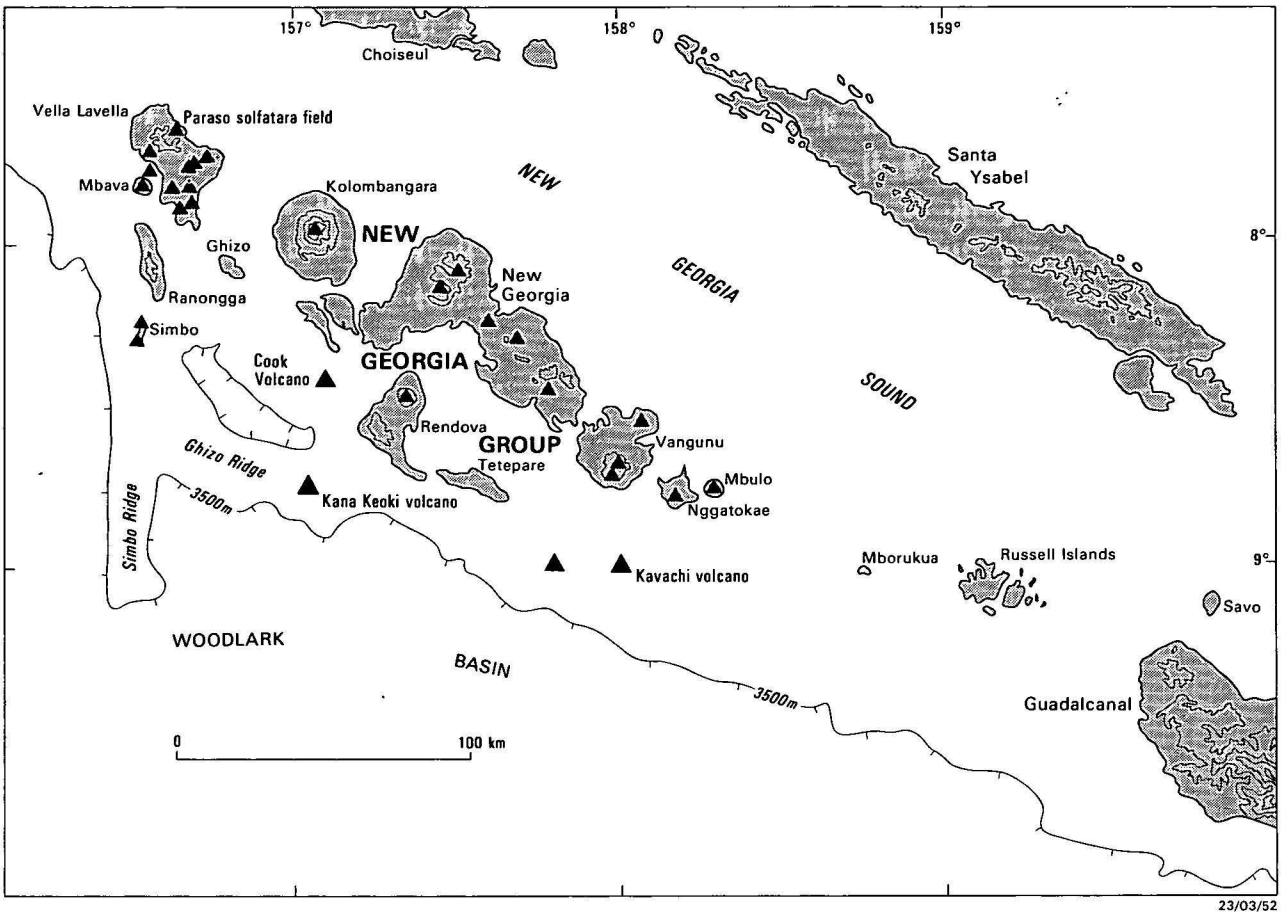

Figure 1. Western Solomon Islands, showing reported locations (large filled triangles) of Cook, Kana Keoki, and Kavachi submarine volcanoes, and an unnamed submarine volcano west of Kavachi located from Admiralty Chart 3995.
Small filled triangles represent volcanic centres of the New Georgia Group.

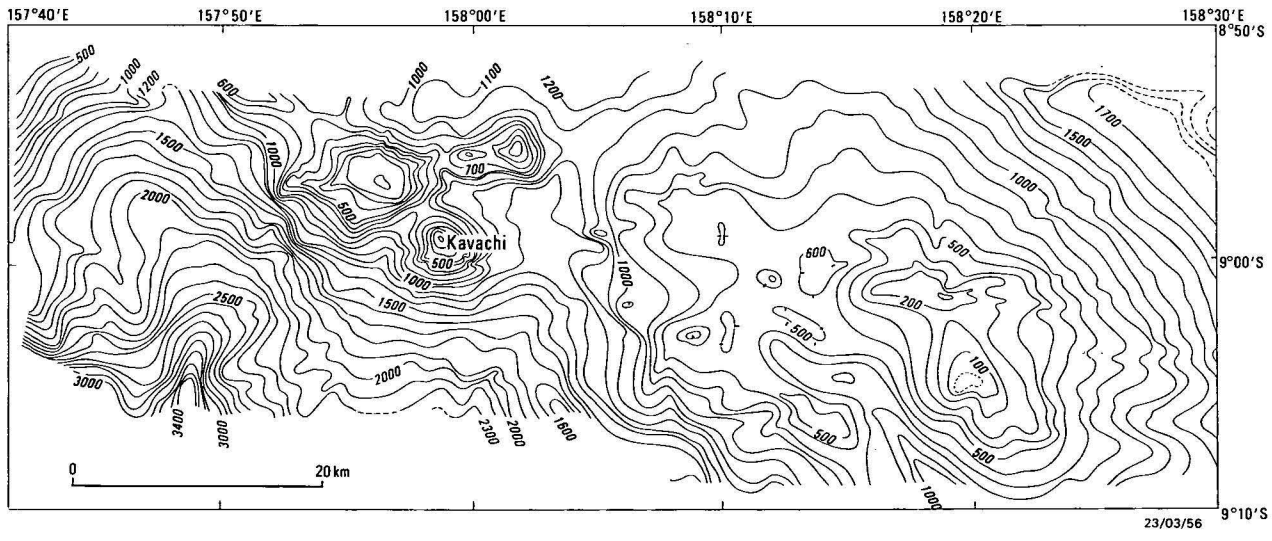

Figure 2. Isobath map of the Kavachi area produced from detailed survey by R/V *Vulcanolog* in 1979 (after Okrugin, 1985).
1450 km of data were used in this compilation; the average line spacing was 3 km, but was much less over Kavachi and the three seamounts to the north.

phreatomagmatic activity also takes place. Subaerial ash and scoria eruptions have been reported, and subaerial lava flows have formed on occasions. Dredge hauls obtained by the *Kana Keoki* (RD 34 and 35) consist largely of tholeiitic basalt and low-silica andesite including agglomerate (Johnson & others, in press; cf. Okrugin, 1985).

Cook volcano

First reports

The commander of the survey vessel HMS *Cook* reported an uncharted shoal and submarine disturbance on 14 December 1963, while his vessel was leaving the strait between

Rendova and the New Georgia Group islands (Grover, 1968). The shoal was about 6.7 miles away from Munda Point, and its position was fixed by radar at 8°24.9'S, 157°06'E (Fig. 1; point A of Fig. 3). Grover (1968, p. 121), who had just left the vessel, reported that the commander had 'discovered a submarine volcano which was probably at the very commencement of its "initial penetration" activity. It was described as solfataric in nature . . . Owing to darkness and a time schedule it was not possible to investigate the area further on this occasion'. These brief remarks represent the only published description known to us of the disturbance. Grover's term 'initial penetration' means that he considered the activity to represent the first volcanic eruption at that site (J.C. Grover, personal communication, 1985), and the term 'solfataric' meant that the commander detected a sulphuretted smell (R. Morris, personal communication, 1985). The depth of the summit of Cook volcano is given as 36 m on Admiralty Chart 3995. Grover (1968, p. 121) continued: 'Some local residents of many years standing were prepared to have their doubts about this submarine volcano that had never before been observed by anyone travelling in the area'.

Further light was shed on the HMS *Cook* sighting by a letter from the British Hydrographic Office, sent to us in May 1985. The present Hydrographer of the Navy, Rear Admiral R. Morris, was navigator of HMS *Cook* in 1963 and remembers the Cook volcano discovery well. All *Cook*'s echo-sounders had been destroyed in a grounding in Fiji, but a small acoustic device — a 'submarine sentry' — had been streamed to provide some indication of shoals. At 2325 (local time) on 14 December 1963 the sentry tripped, and the ship was stopped while soundings were taken with a hand lead, which appeared to indicate shallow bottom. The ship was in apparently shallow water for 35 minutes. The smell of sulphur was strong and unmistakable, but 'no stones or dust were seen'.

Grover (1968) reported that on 3 January 1964, 20 days after the submarine disturbance, a strong shallow ('33 km') earthquake took place in the same vicinity; its epicentre was later located by the United States Coast and Geodetic Survey at 8.2°S, 157.1°E. Grover took this event as 'forceful confirmation' of the existence of a submarine volcano, which he named 'Cook'. Seismologist C. Blot (quoted in Grover, 1968) added his support, maintaining that the earthquake was one of a series in depth-time-distance relationship that had led to the 'eruption' observed from on board the *Cook*.

Another submarine disturbance took place south of Vona Vona and west of Rendova on 25 May 1964 (Grover, 1968, pp. 121-3). Two young Solomon Islanders were travelling in their outboard-powered dugout canoe from the Vona Vona Lagoon eastward to Munda at about 1300 hours in calm seas when they saw a large 'mountain of black water' with 'smoke' issuing from its summit rise from the sea and fall back. They heard no sound above the noise of their outboard, and reported the dome-shaped mass of water to be 'as large as an island' and the steam emission to rise 'very much higher'. The islanders had described what mariners had reported when

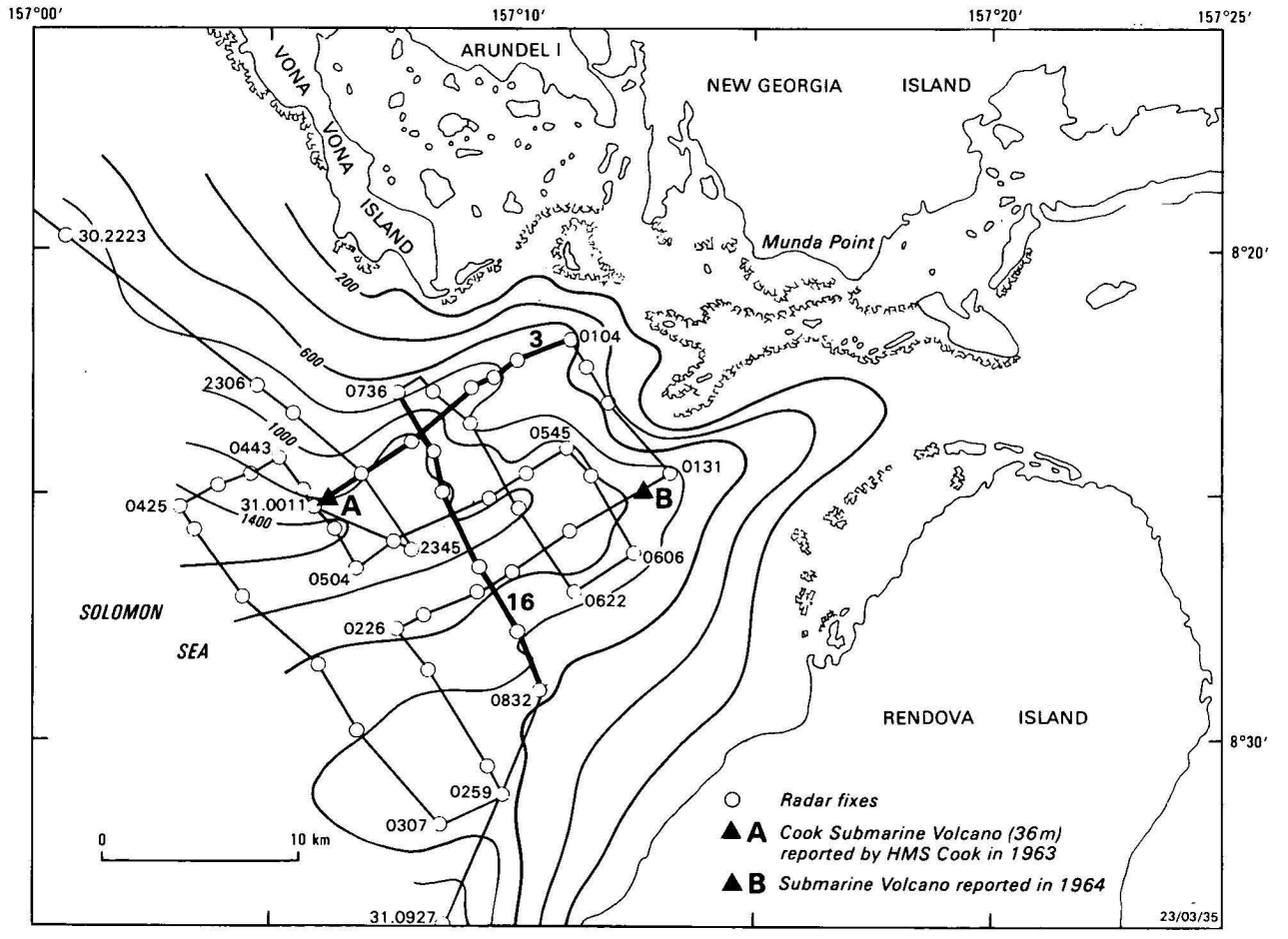

Figure 3. Isobath map produced from detailed survey of R/V *Machias* (Exon, 1981) covering the reported locations of Cook submarine volcano. Numbers such as 31.0011 represent GMT day and hour for radar fixes. Note two reported locations for Cook submarine volcano and lack of bathymetric evidence for its existence.

observing eruptions at Kavachi volcano to the east. Grover (1968) calculated that 'as they were distant four or five miles, sitting at water level, the eruption of water must have been much greater than 100 feet in height'. This report could refer to either, or neither, of locations A and B on Figure 3.

Grover also reported that 'Sea muddied with ejectamenta' was seen by Frank Wickham during a launch crossing between Munda and Rendova. Furthermore, on 11 and 12 June, Mr. Kitchener Wheatley on Hombu Island, one of the coral islets of the Munda Barrier Reef, twice heard distant thuds together with a strong vibration of the atmosphere. On 13 June, Mr Frank Wickham reported a sharp 2 second earth tremor from Kenelo Plantation on Rendova, and the next day observed 'steam rising from the sea directly opposite Munda Bar'.

Grover reported further that large specimens of fresh floating black pumice were subsequently found on the beach near Munda. They lacked phenocrysts, and consisted entirely of a brownish black isotropic glass, highly vesicular, with a chilled exterior. No reports of eruptions were received after 13 June 1964.

Grover (1968, table on p. 121) placed the May 1964 disturbance at exactly the same position as the December 1963 'eruption', presumably by inference. However, separate positions for the 1963 and 1964 locations are plotted on Admiralty Chart 3995: one is at the 1963 site (point A of Fig. 3) located by the *Cook;* the other is 15 km to the east (point B of Fig. 3). The information for the 1964 position presumably derives from Mr Wickham's observation of the disturbance 'directly off Munda Bar'.

Machias survey 1981

A bathymetric survey of the area around the supposed Cook submarine volcano was undertaken in 1981 by the Committee for Coordination of Joint Prospecting for Mineral Resources in South Pacific Offshore Areas (CCOP/SOPAC), using R.V. *Machias,* at the request of the Solomon Islands Geological Division and as part of a research cruise designed to help assess offshore mineral resources. The aim was to locate the volcano and to sample it in search of hydrothermal minerals. The following is an extract from the unpublished cruise report by Exon (1981, pp. 4-5):

'Nine hours were spent in search for Cook Submarine Volcano, using the location given by HMS *Cook* . . . as a starting point. Altogether about 65 nautical miles of echo sounding was carried out, on a grid averaging 1.5 miles in spacing. This showed that the sea bed was very rough, with little sediment cover. A profile was also run along the true bearing of 241° from Munda Point quoted by HMS *Cook* as defining the position of the volcano. The survey concentrated on the area between the volcano's position as reported by HMS *Cook,* and another position shown on Admiralty Chart 3995 at roughly 8°24'S, 157°12.5'E. This chart shows the water depth at the Cook volcano as 36 metres. Our survey showed that water depths were generally between 1000 and 1500 metres near the charted position of the volcano'. Thus, the inferred volcano would have to be at least 1000 m high; assuming its slopes were as steep as 30°, its diameter would be 4 km at a water depth of 1200 m. A volcano of this size could not have been missed by the survey.

A bathymetric map of the area surveyed by the *Machias* was prepared by us (Fig. 3) in 1984. There is no indication of a conspicuous submarine volcano in the survey area. The sea bed appears to have formed by tectonic, erosional, and sedimentological processes, rather than by volcanic constructional processes. Slopes are generally about 5-10°, much less steep than those at Kavachi. The main feature of the map is a submarine canyon beginning in Blanche Channel between Munda Point and Rendova, descending westward, and passing just south of the HMS *Cook* location (point A).

Two bathymetric profiles from the *Machias* survey are shown in Figure 4. Line 3 of the survey (Figs 3 & 4A) runs from near Munda Point on the 241° bearing given by HMS *Cook* to Point A, the point at which the Admiralty plotted the location of Cook volcano. The apparent slope of the sea bed west- southwestward along the line is about 5°; the true slope to the south is perhaps 10° (Fig. 3). Clearly, there is no large volcanic cone on the line.

Line 16 (Figs. 3 & 4B) cuts both Line 3 and the canyon axis at right angles, about 5 km east of Point A. Again, the sea bed falls steadily toward the canyon, and there is no sign of a volcanic cone. The apparent slope of the sea bed on line 16 is about 5°, but the true average slope down from Vona Vona is about 10°; that from Rendova is somewhat less.

The 1979 cruise of R/V *Vulcanolog* (Okrugin, 1985) included a rather more detailed survey of the area around Cook volcano, and a bathymetric map, very similar to that from the *Machias* survey, was produced. This map, based on a one mile grid, extends farther west than does Figure 3 and shows that the submarine canyon does not extend beyond the 1400 m isobath. No evidence for a submarine cone is seen. Seismic profiles were also obtained, and the upper part of the sequence was described as consisting generally of an 'acoustically impenetrable, and structurally heterogeneous, series of rocks' (Okrugin, 1985, page 3). Unconsolidated sediments were confined to two small depressions on the slope down to the canyon from Rendova. Geological sampling at five sites in the survey area revealed that pumice is widespread.

Discussion

The evidence for the present-day existence of the elusive Cook submarine volcano is poor. Reports of both the 1963 and 1964 disturbances are tantalisingly brief and do not correspond to those of ash or pumice-bearing volcanic eruption plumes, though they could represent ejections and doming of sea water accompanying volcanic activity of phreatic origin. The source of the 'fresh floating black pumice' on the beach near Munda is uncertain. Kavachi had been active in January 1964, when a red glow, believed to be incandescent lava, could be seen at night (Grover 1968), so Kavachi might have been the source of the pumice seen at Munda the following June. However, Kavachi magmas are conspicuously porphyritic, whereas the Munda pumice was 'distinguished by a complete lack of phenocrysts' (Grover, 1968). The aphyric pumice need not have originated from either Cook or Kavachi, but may have come from some other as yet unknown source, for example the seamount 9 km northeast of Kavachi or perhaps even from outside the New Georgia Group area.

The evidence of a 36 m shoal gathered by HMS *Cook* and shown on Chart 3995, is not as strong as it appears. Firstly, hydrothermal venting was clearly taking place, as the smell of sulphur was strong, and therefore a turbulent column of gas and water, like that commonly present at Kavachi, was probably present in the vicinity. This column could have triggered the 'submarine sentry'. Secondly, associated turbulence may have affected the leadline sounding, giving an erroneous impression of shallow bottom. This possibility is increased because the sailors on board *Cook* were not expert at hand sounding (R. Morris, personal communication, 1985).

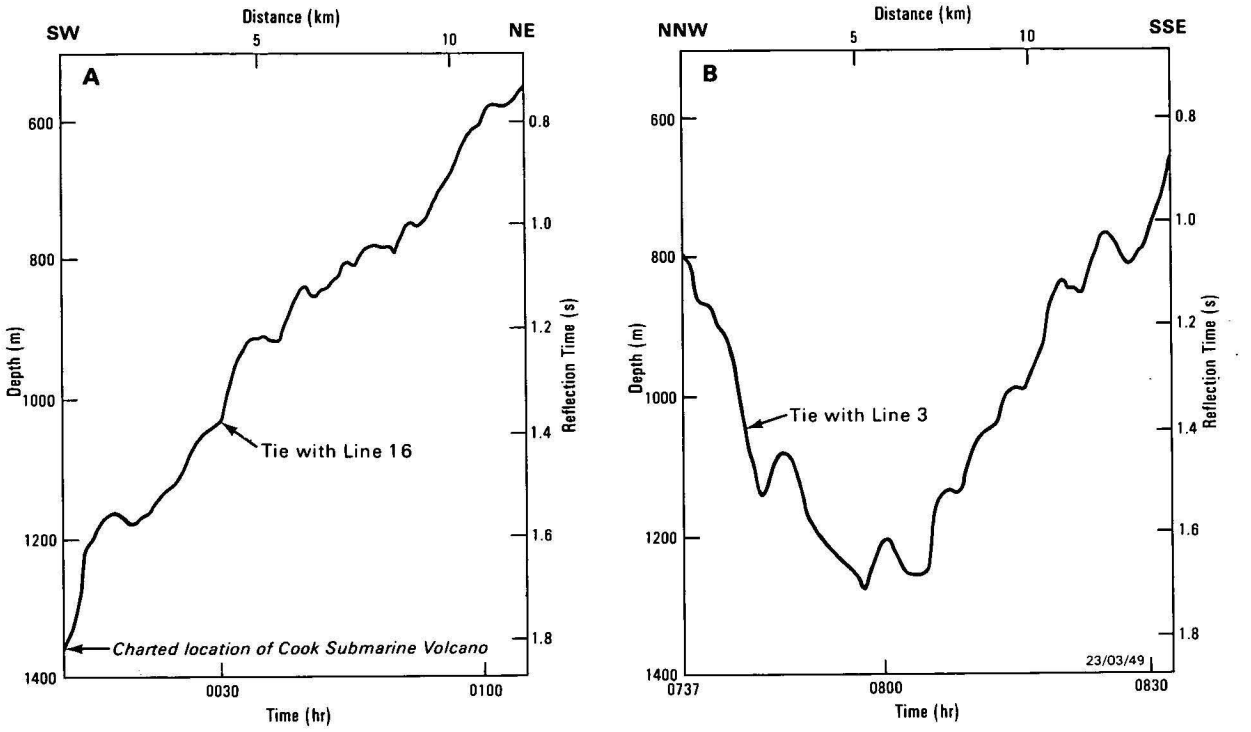

Figure 4. Two bathymetric profiles from 1981 *Machias* survey.
A — Line 3, running southwestward from Munda Point along 241°, on which HMS *Cook* recorded the existence of Cook submarine volcano. Location now lies at 1370 m, despite Admiralty Chart water depth of 36 m. Average apparent slope 5°.
B — Line 16, running southeastward from Vona Vona Island and showing canyon at 1300 m that runs westward just south of HMS *Cook*'s location of Cook submarine volcano. Average apparent slope is 5°. Locations in Fig. 3, vertical exaggeration about 20.

The location of the 'shoal' could hardly lie outside the *Machias* and *Vulcanolog* echo-sounding grids, because HMS *Cook* fixed its position by radar. It is conceivable, but highly unlikely, that a volcano did indeed rise 1200 m above the sea floor in 1963, but had disappeared before the *Vulcanolog* survey 16 years later. This would have needed a remarkable combination of mass wasting of gravitationally unstable slopes and undercutting by the canyon nearby.

Another point suggestive of Cook volcano never existing is that nothing was reported until *Cook*'s discovery in December 1963. It is most improbable that a large volcanic cone could form so close to sea level and to nearby land without local inhabitants having noticed volcanic activity. Indeed, even after the sighting, during the six months when activity was noted, there was no report of pyroclastic outbursts like those at Kavachi, suggesting that activity was relatively subdued.

We are convinced that the activity relating to Cook 'volcano' came from a deep-water vent or vents, largely in the form of hydrothermal blowout of groundwater and sea-floor sediments from a volcanically heated geothermal area. Blowout in some instances may have been caused by release of pressure during seismic activity.

Kana Keoki volcano

A seamount discovered southwest of Rendova Island during the 1982 cruise of R/V *Kana Keoki* (Taylor & Exon, in press) rises to a summit at about 700 m, from the sea floor 2500 m below sea level. It lies at 8°47'S and 156°43'E on the east-west-trending Ghizo Ridge, which may be a short segment of the Woodlark Basin spreading axis (Taylor, in press). The seamount is shown on several echo-sounder profiles as a steep-sided cone, which, like Kavachi, has slopes of about 25°. One such profile is illustrated in Figure 5.

The southeastern flank of the seamount was dredged (RD 33) by the *Kana Keoki* (Taylor & Exon, in press) and a large

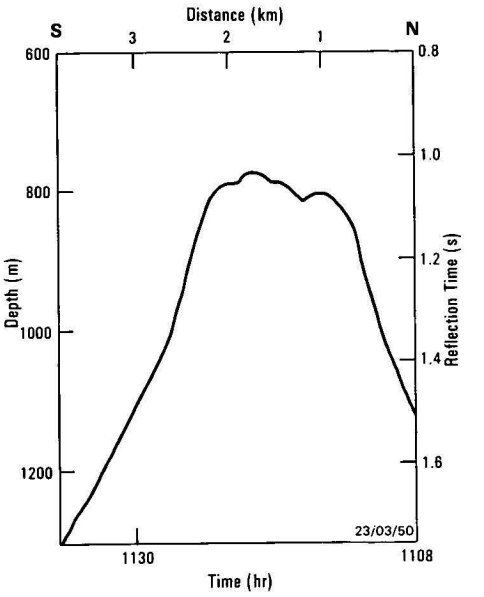

Figure 5. Bathymetric profile 6A of 3 June 1982 from *Kana Keoki* survey (Taylor & Exon, in press).
Line runs southward across location of Kana Keoki volcano shown in Figure 1. Vertical exaggeration about 8. The volcano is a cone that rises almost 2000 m above the surrounding sea floor, and from which dacite, rhyolite, and andesite rocks have been dredged. Maximum slope about 25°.

haul of volcanic rocks was recovered from 1550-1250 m. The rocks recovered from the slope are variably vesicular dark glassy andesites and dacites, and those from the upper slope are mostly gray pumice (Johnson & others, in press). Both the bathymetric and petrological observations are a clear indication that the seamount is a volcano, which may or may not be active at present.

Reported volcano west of Kavachi

A submarine volcano is shown on Admiralty Chart 3995 at 9°S, 157°48'E, about 25 km west of Kavachi (Fig.1). The *Machias* 1981 survey (Exon, 1981) attempted to find the volcano on an east-west line along 9°S. No bathymetric high was found at the charted position, but one was found about 10 km to the west-northwest. An echo-sounder profile across the high (Fig. 6) shows it to rise to within 700 m of the surface, from a base at around 2500 m. The high is also seen on several other profiles in the vicinity, which means it is probably part of a southward-trending ridge originating on Tetepare, rather than a volcano. Isobaths on the map of the Kavachi area (Fig. 2) produced by Okrugin (1985), and extending as far west as 157°40'E, are consistent with this interpretation. The slopes shown on the echo-sounder profile are less than 10° — that is, much lower than at Kavachi.

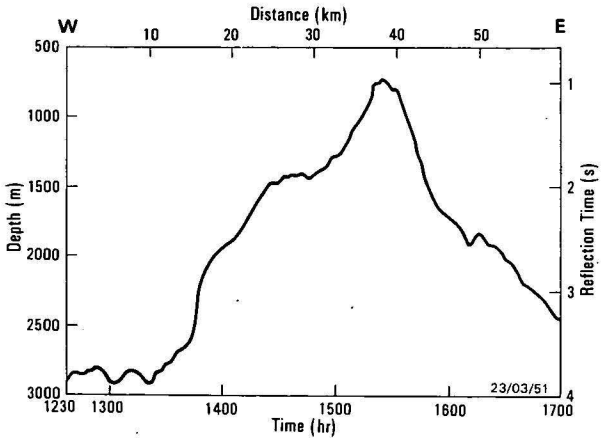

Figure 6. Bathymetric profile from 1981 *Machias* survey, running eastward along the 9°S parallel, near location of unnamed volcano west of Kavachi volcano, shown in Figure 1.

Recorded on Day 31 (GMT). Vertical exaggeration about 15. Slopes do not exceed 10°, and the rise to 750 m appears to be part of a non-volcanic ridge extending southward from Tetepare.

Discussion and conclusions

Four submarine forearc volcanoes were originally reported from the New Georgia area, but only two — Kavachi and Kana Keoki — have been confirmed to be large volcanic cones. However, other forearc volcanoes are known to be present in the area (Okrugin, 1985), and there may be more, given the generally widely spaced bathymetric grid in the region.

Kavachi and Kana Keoki are cones built at their angle of rest of about 25°. Kavachi consists of alkali-poor tholeiitic basalt and low-SiO_2 andesite, whereas Kana Keoki is made up of dacite, rhyolite, and low-SiO_2 andesite. The chemical characteristics of rocks from both volcanoes are much like those of normal island-arc rocks, despite the unusual tectonic setting of both eruptive centres (Johnson & others, in press).

There is eye-witness evidence of submarine disturbances at the location of Cook 'volcano' in 1963 and 1964 (Grover, 1968), but the precise location of some of the disturbances is uncertain. The disturbances consisted largely of ejections and doming of seawater, and there is no clear evidence of the ejection of volcanic rocks. There have been no further reports of activity, and in 1979 and 1981 R/V *Vulcanolog* and R/V *Machias* failed to locate any volcanic buildup whatsoever in the area where the volcano was reported to have been in 1963-64. The water depth in 1981 was more than 1300 m at the location provided by HMS *Cook*. Cook 'volcano' was apparently only a deepwater vent or vents, meaning that the 36 m water depth was erroneous. Alternatively, but very improbably, there has been a vast amount of submarine mass wasting since 1964.

We have no evidence to corroborate the existence of the volcano plotted west of Kavachi and southeast of Tetepare on Admiralty Chart 3995 and in Figure 1. The high 10 km west of the plotted location appears to be simply an offshore extension of Tetepare.

This fascinating forearc region is clearly very imperfectly surveyed. A single swathe-mapping sonar survey of the region would resolve many of the problems regarding the number and location of volcanoes, and provide ideal site information for future sampling by surface vessels or submersibles*.

Acknowledgements

Most of the data on which this paper is based come from the CCOP/SOPAC *Machias* cruise of 1981 and the Tripartite *Kana Keoki* cruise of 1982. We are most grateful to CCOP/SOPAC, Suva, for the use of the *Machias* data, the Tripartite group (Australia, New Zealand, and the United States of America) for the use of the *Kana Keoki* data, and the Institute of Volcanology at Petropavlovsk-Kamchatsky for the use of the *Volcanolog* data.

Special thanks are due to the Hawaii Institute of Geophysics, who made the *Kana Keoki* available for the Tripartite cruise, to their Sharon Warlop, who digitised the *Machias* Cook volcano cruise data, and to M. Marlow (USGS) and D.E. Mackenzie (BMR) for reviewing the paper. We are also most grateful for the assistance provided by Mr J.C. Grover, former Director of the British Solomon Islands Geological Survey, and B.E. Skittrall and Rear Admiral R. Morris of the British Hydrographic Office for their help in answering our questions about Cook volcano.

References

Exon, N.F., 1981 — Solomon Islands offshore survey: phosphate and metalliferous sediments, Cruise SI-81(2). *Committee for Coordination of Joint Prospecting for Mineral Resources in South Pacific Offshore Areas (CCOP/SOPAC) Cruise Report* 50 (unpublished).

Fisher, N.H., 1957 — Catalogue of the active volcanoes of the world, Part 5, Melanesia. *International Association of Volcanology, Naples.*

Grover, J.C., 1955a — Geology, mineral deposits and prospects of mining development in the British Solomon Islands Protectorate. *Interim Geological Survey of the British Solomon Islands Memoir* 1.

* Footnote added at proof stage.

In December 1985, at our instigation, the R/V *Moana Wave* ran two SeaMARC II sidescan sonar swathes across HMS *Cook*'s location for the Cook volcano. The tracks ran north-northeastward and westward, and the swathe width was nearly 10 km. *Moana Wave*'s co-chief scientist, Dr. Keith Crook (Australian National University), has stated there was no sign of a volcano, its reported location being covered by recent sediment. Several small westerly trending scarps exist between the 'volcano' site and the canyon to the south, and one of these may have been the site of the reported venting.

Grover, J.C., 1955b — The submarine volcano in the western Solomons. *Transactions of the British Solomon Islands Society for the Advancement of Science and Industry,* 2, 13-17.

Grover, J.C., 1968 — Submarine volcanoes and oceanographic observations in the New Georgia Group, 1963-64. *British Solomon Islands Geological Record,* 3 — 1963-67 *Report* 96, 116-125.

Hussong, D.M., & Fryer, P., 1983 — Back-arc seamounts and the SeaMARC II seafloor mapping system. *Transactions of the American Geophysical Union (EOS),* 64, 627-632.

Johnson, R.W., Jaques, A.L., Langmuir C.H., Perfit, M.R., Staudigel, H., Dunkley, P.N., Chappell, B.W., Taylor, S.R., & Baekisapa, M., in press — Ridge subduction and forearc volcanism: petrology and geochemistry of dredge rock samples from the western Solomon arc and Woodlark Basin. *Circum-Pacific Council for Energy and Mineral Resources, Earth Science Series.*

Johnson, R.W., & Tuni, D., in press — Kavachi, an active forearc volcano in the western Solomon Islands: reported eruptions between 1950 and 1982. *Circum-Pacific Council for Energy and Mineral Resources, Earth Science Series.*

Okrugin, V.M., 1985 — Information note on the results of the 7th cruise of the R/V 'Vulcanolog' in the vicinity of the Solomon Islands. *Solomon Islands Geological Division File Report.* (unpublished).

Simkin, T., Siebert, L., McClelland, L., Bridge, D., Newhall, C., & Latter, J.H., 1981 — Volcanoes of the world. *Hutchinson Ross, Stroudsberg.*

Taylor, B., in press — A geophysical survey of the Woodlark-Solomons region. *Circum Pacific Council for Energy & Mineral Resources, Earth Science Series.*

Taylor, B., & Exon, N.F., in press — Seafloor spreading, ridge subduction, volcanism and sedimentation in the offshore Woodlark-Solomons region. *Circum Pacific Council for Energy & Mineral Resources, Earth Science Series.*

BMR Journal of Australian Geology & Geophysics, 10, 85-87

©Commonwealth of Australia 1986

Migration of deep-water seismic data

S.P. Kravis[1]

Seismic data recorded in deep water have several features that make them very well suited to migration by the use of a simple, constant velocity algorithm. A case is made for such migrations to be applied routinely to deep-water data.

Introduction

Deep-water areas, from the point of view of a seismic survey, are defined as areas in which the water depth is more than a few times greater than the active length of the seismic cable. Data collected from such areas have the following characteristics: 1) Stacking velocities close to the water propagation velocity; 2) small values of normal moveout; 3) only very small changes in the stacked section with different stacking velocities; 4) prominent diffractions from any irregularities, owing to the large Fresnel zone at large reflector distances.

The small values of moveout give a large dip bandwidth to the stack response: dipping events will have stacking velocities close to the stacking velocities of horizontal events. This feature would not normally be considered advantageous, as stacking-velocity discrimination is an important method of suppressing events such as water-bottom multiples, diffractions, and coherent noise. However, for deep-water data, the first water-bottom multiple usually appears at a time beyond the penetration time of the seismic source or even beyond the end time of the data trace, so its suppression is less important than in shallow water. Whilst suppression of diffraction events by stacking may give sections a less confusing appearance by weakening the steeply dipping 'wings' of the diffraction hyperbolae, the correct procedure for removing their effect is migration.

In order for migration to work successfully, two criteria must be fulfilled: the effective propagation velocity in the medium in which the diffractions are occurring must be known, and the diffractions themselves must be faithfully recorded without spatial aliasing. Deep-water data satisfy both these criteria very well, as water occupies most of the propagation path, thus giving a constant, known propagation velocity, and the diffractions are faithfully recorded, owing to the large dip bandwidth of the stack response. Spatial aliasing may be controlled by restricting the temporal bandwidth of the data, if necessary.

As the effective propagation velocity is close to the constant velocity of sound through the water layer, a constant velocity migration method may be used, provided the reflections are not at such a depth below the water bottom that the propagation path is no longer mainly through water. The F-K domain method described by Stolt (1978) is thus applicable. Its benefits include speed of operation and good performance in correctly migrating steeply dipping events (Chun, 1981).

Berkhout (1980) identified several parameters that limit the lateral resolution obtainable with migration in the practical situation. The finite aperture available means that part of the diffraction energy will not be recorded, and thus cannot be collapsed back to its point of origin. A rule of thumb is to allow a length at each end of the line, equal to the water depth, to accommodate diffractions from points at the end of the region of interest. Lynn & Deregowski (1981) made a similar observation on the need for long lead-ins to record steeply dipping, deep events. Similarly, the trace length should be long enough to allow recording of the diffraction arrivals until they become submerged in noise.

Long source or detector arrays result in the suppression of the wings of the diffraction hyperbolae, owing to their high angle of incidence, and this also leads to loss of resolution. For data with low penetration, which often consist almost entirely of diffractions, any amplitude-correction process should be carried out after migration. If applied beforehand it will tend to boost the amplitude of the diffraction wings, resulting in a higher noise level after migration is applied.

Synthetic and real data studies

The effect of increasing dip bandwidth with reflector depth is shown in Figures 1 and 2. Figure 1 shows a 12-fold stack of some synthetic CDP gathers over point diffractors at depths of 1, 2, 3, and 4 km, in a medium with a constant propagation velocity of 1500 m/s. Trace offsets vary between 470 m and 1670 m. The data set was calculated for a CDP spacing of 50 m, for 140 positions centred on the point directly above the diffractors.

The increase in dip bandwidth with diffractor depth is clearly shown by the attenuation of the wings of the diffractions from shallower depths, compared to the deeper ones.

Figure 2 shows the results of F-K migration on the data shown in Figure 1. In all cases, there has been a substantial collapse of the diffractions, but the resolution may be seen to be diminishing as the depth to the diffractor decreases, owing to the attenuation of the steeply dipping diffraction wings.

Figures 3a and 3b show 6-fold stacked data, recorded by BMR in the Prydz Bay area of Antarctica, before and after migration. The water depth in this area is about 2500 m, and with a streamer length of only 300 m, the 'deep water' condition is well satisfied. The source used was a single air gun of 7.64 L capacity, fitted with a wave-shape kit. The data were recorded and processed at a 2 ms sample period up to the migration stage, when they were resampled at 4 ms. The CDP spacing was 25 m. The Stolt migration algorithm was used, and processing performed on the BMR in-house seismic-processing system, SPOCK (Brassil & others, in press). A constant velocity of 1500 m/s was used for the migration.

It may be seen (Fig. 3) that the diffractions from the faults visible in the section have been very successfully collapsed, so that the fault planes are much more clearly visible. Note in particular the effect of migration on the fault shadow zone between 4.0 s and 4.2 s on traces 55 to 65. The shadow disappears completely on migration, leaving the fault sharply imaged. It should be noted that a constant velocity, or indeed

[1] Division of Marine Geosciences & Petroleum Geology,
Bureau of Mineral Resources
GPO Box 378
Canberra, ACT 2601

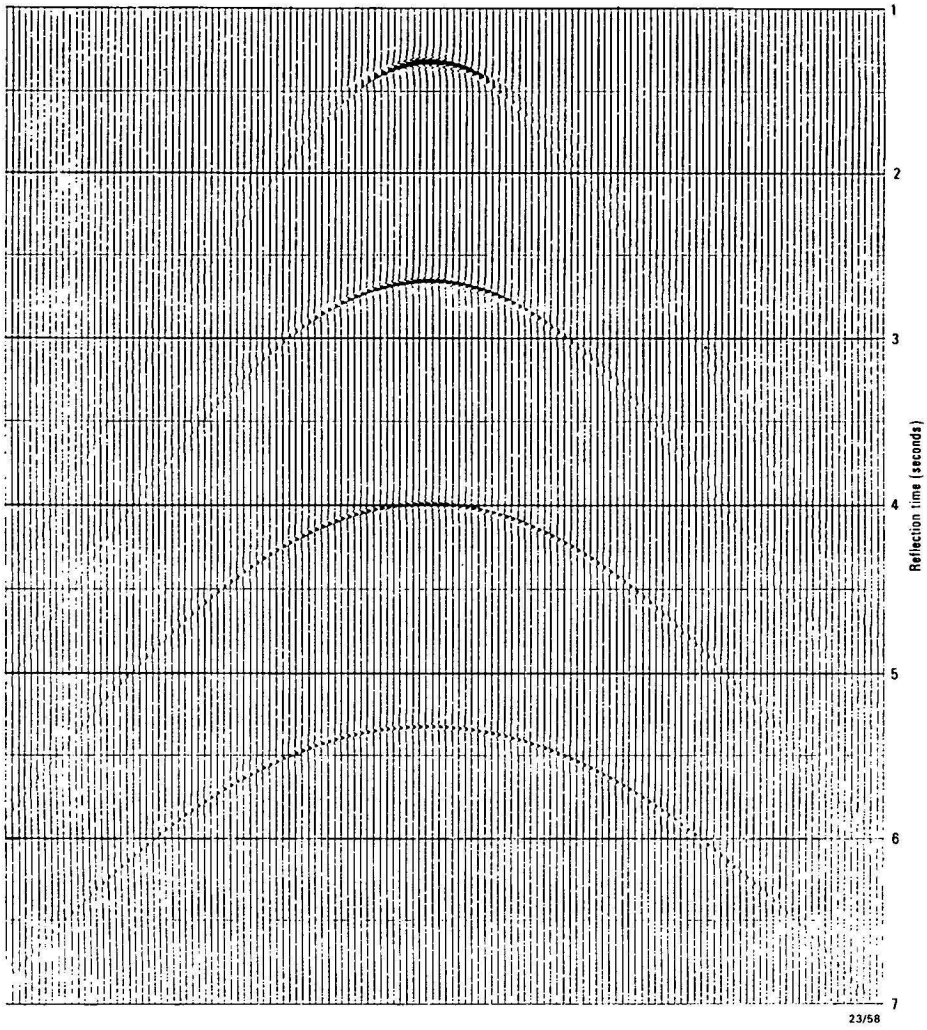

Figure 1. Stack of synthetic 12-fold CDP gathers over point diffractors at 1,2,3 and 4 km depth in a medium of constant velocity, 1500 m/s.
Note the attenuation of the wings of the diffraction hyperbolae from shallower diffractions.

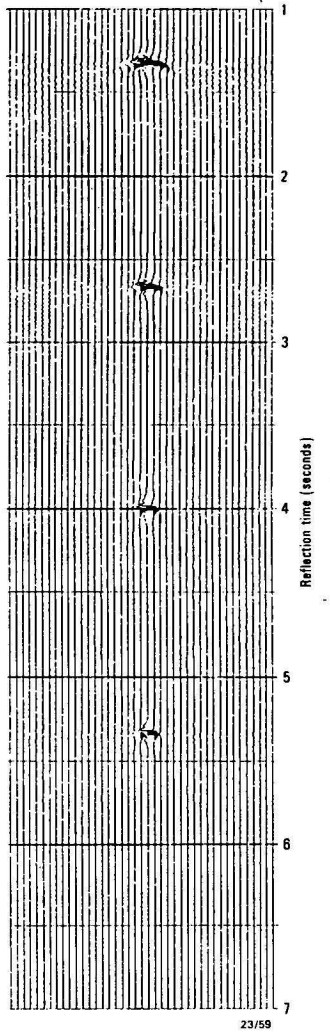

Figure 2. F-K migration of data shown in Figure 1.
The shallower diffractors can be seen to be less resolved than the deeper ones.

any non-recursive form of migration, will misplace reflectors in the presence of large lateral velocity variations (Berkhout, 1984).

The migrated section may be said to interpret itself, at least so far as the location of faults is concerned. Although the example (Fig. 3) shows stacked data, similar gains in clarity would be obtained for single-channel data showing prominent diffractions.

For water depths over 5 km, diffractions from water-bottom irregularities may cover several hundred traces. In these circumstances, the variation in CDP spacing caused by changes in ship speed may have a significant effect on the migration velocity, as the parameter in F-K migration is actually the velocity divided by the trace spacing. Hence, a 10 per cent change in ship speed will cause a change of similar magnitude in the correct migration velocity. For this reason, tests for the correct migration velocity should be done along the line to account for any possible variation in ship speed.

Conclusions

Diffractions on seismic sections are commonly regarded as obscuring the 'true' seismic reflections. But, for deep-water data, they carry important structural information and, unless they are recorded faithfully, degradation of the final migrated section may result. Because of the lack of lateral velocity variation, deep-water data are intrinsically suited to the use of fast, non-recursive migration methods, such as F-K or Kirchoff migration. The efficiency of such algorithms allows the routine migration of deep-water data, and the knowledge of the correct migration velocity allows confident interpretation of the results.

Acknowledgements

I thank Howard Stagg and other participants in the 1981 BMR Antarctic survey for collecting the data used in the example, and Peter Mora for providing the core of the Stolt migration algorithm.

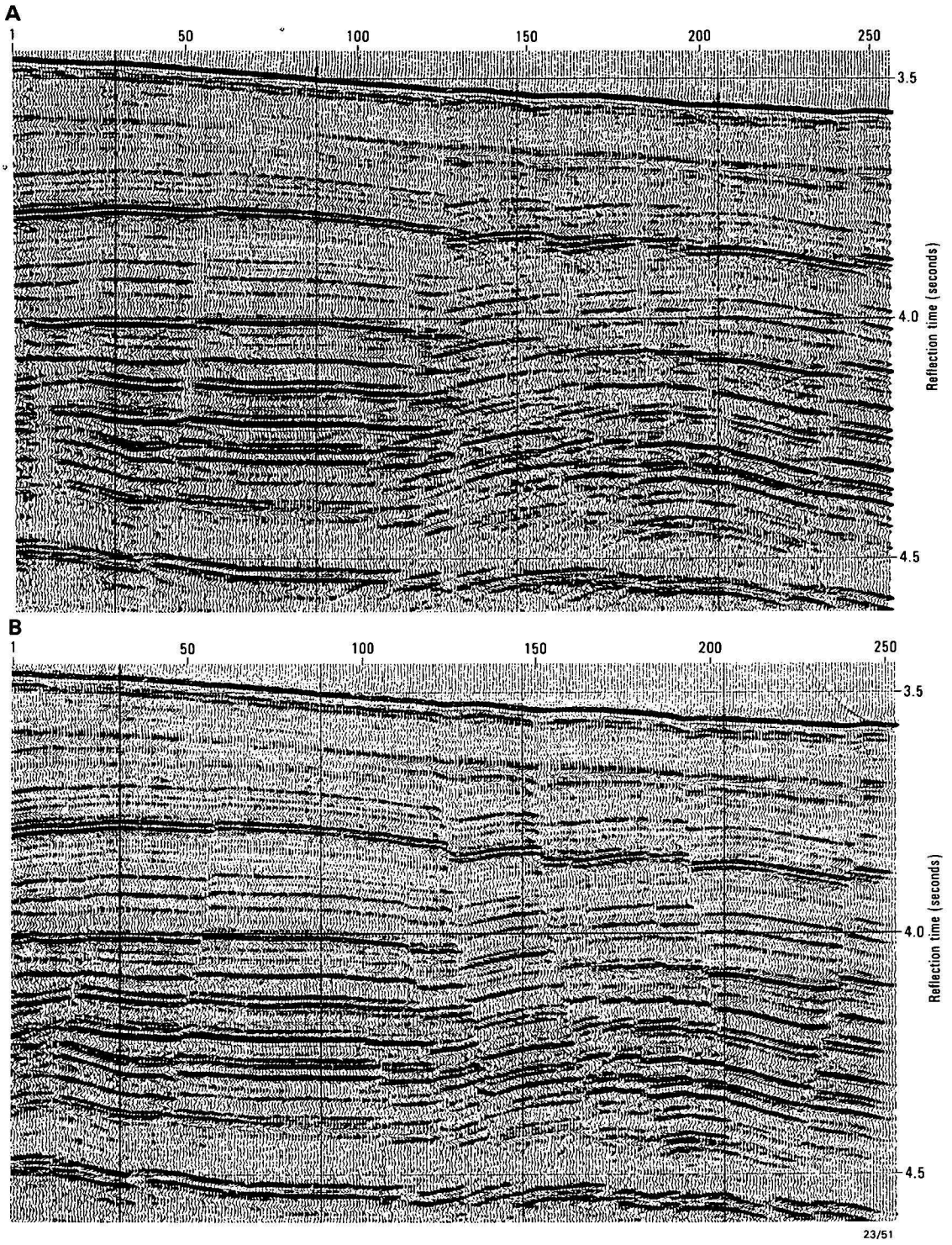

Figure 3. A — Stacked data before migration. Note the confused area suggestive of faulting in the right hand half of the section. **B — Stacked data after constant velocity F–K migration.** The faulting is now extremely clear.

References

Berkhout, A.J., 1980 — Fundamentals of seismic migration. *Elsevier, Amsterdam.*

Berkhout, A.J., 1984 — Seismic migration: imaging of acoustic energy by wavefield extrapolation: practical aspects. *Elsevier, Amsterdam.*

Brassil, F.M., Kravis, S.P., & Allen, L.J., in press — BMR seismic processing system, SPOCK, reference manual. *Bureau of Mineral Resources, Australia, Report* 255.

Chun, J.H., & Jacewitz, C.A., 1981 — Fundamentals of frequency domain migration. *Geophysics,* 46, 717-733.

Lynn, H.B., & Deregowski, S., 1981 — Dip limitations on migrated sections as a function of line length and recording time. *Geophysics,* 46, 1392-1397.

Stolt, R.H., 1978 — Migration by Fourier transform. *Geophysics,* 43, 23-48.

CONTENTS

R38 614(5) Cat. No. 85 1234 9